A SIMULATION FRAMEWORK FOR EVALUATION OF REAL-TIME ELECTRIC VEHICLE (EV) CHARGING CONTROL STRATEGY AND INVESTIGATION OF ITS INTERACTION WITH V2G-BASED FREQUENCY REGULATION

A Dissertation
Presented to
The Academic Faculty

by

Joosung Kang

In Partial Fulfillment
of the Requirements for the Degree
Doctor of Philosophy in the
School of Aerospace Engineering

Georgia Institute of Technology
May 2017

A SIMULATION FRAMEWORK FOR EVALUATION OF REAL-TIME ELECTRIC VEHICLE (EV) CHARGING CONTROL STRATEGY AND INVESTIGATION OF ITS INTERACTION WITH V2G-BASED FREQUENCY REGULATION

Approved by:

Prof. Dimitri N. Mavris, Advisor
School of Aerospace Engineering
Georgia Institute of Technology

Dr. Scott J. Duncan
School of Aerospace Engineering
Georgia Institute of Technology

Prof. Daniel P. Schrage
School of Aerospace Engineering
Georgia Institute of Technology

Ken Caird
GE Energy

Prof. Jechiel Jagoda
School of Aerospace Engineering
Georgia Institute of Technology

Date Approved: 5 April 2017

"Life is like riding a bicycle. To keep your balance, you must keep moving."

Albert Einstein

To my family

ACKNOWLEDGEMENTS

First, I would like to express my sincere gratitude to my advisor Prof. Mavris for the continuous support of my Ph.D. study and for his motivation and immense knowledge. His guidance helped me in all the time of research and writing of this thesis. I could not have imagined having a better advisor and mentor for my Ph.D. study.

Besides my advisor, I would like to thank the rest of my thesis committee: Prof. Schrage, Prof. Jagoda, Dr. Duncan, and Mr. Caird, for their insightful comments and encouragement, but also for the hard questions which helped me to widen my research from various perspectives. Especially I would like to thank Dr. Duncan again for the immeasurable amount of support and guidance. He has spent a considerable amount of time and efforts to make my ideas more constructive and concrete, and has supported all of my research works.

My sincere thanks goes to my team members. I could not have completed this work without their consideration and understanding. A very special gratitude also goes out to my company for letting me have the opportunity and providing the funding for the work.

And finally, last but not the least, I would like to thank my family: my parents and to my brother and sister for supporting me spiritually throughout writing this thesis and my life. My precious son, Minhyeok, who complains that he has no choice but to be a second Ph.D. in my family... I'm sorry for that. My lovely wife, Suyeon, you're everything to me.

South Korea, April 2017

TABLE OF CONTENTS

ACKNOWLEDGEMENTS . . . . . **v**

LIST OF TABLES . . . . . **x**

LIST OF FIGURES . . . . . **xii**

LIST OF SYMBOLS OR ABBREVIATIONS . . . . . **xviii**

SUMMARY . . . . . **xxii**

I INTRODUCTION **1**

1.1 Motivation 1

1.1.1 Need for Electric Vehicles 1

1.1.2 Technical Challenges of Integration of EVs 6

1.2 Research Statement 9

1.2.1 Research Objective 10

1.2.2 Thesis Organization 10

II LITERATURE REVIEW **12**

2.1 Operational Management and Control Strategies Regarding EV Charging 12

2.1.1 Centralized/Coordinated EV Charging Control Strategies . . 12

2.1.2 Decentralized EV Charging Control Strategies 45

2.1.3 Scheduling Techniques for Electric Power Systems 59

2.2 EV Potential to Participate in the Provision of Power System Services 65

2.3 Summary of Literature Review 72

2.3.1 Synthesis of Literature Review 72

2.3.2 Observations and Technical Gaps 78

III RESEARCH QUESTIONS AND HYPOTHESES **81**

3.1 Real-time Scheduling Techniques for EV Charging Control 81

3.1.1 EV Charging Control System as a Real-time System 84

3.1.2 Real-time Scheduling Algorithms for EV Charging Control . 90
3.1.3 Charging Rates Control for Maximum Energy Utilization . . 93
3.2 V2G-based Ancillary Services within Real-time EV Charging Control Framework 99
3.2.1 Integration of V2G-based Frequency Regulation into Real-time EV Charging Control 101
3.2.2 Statistical Reference EV Power Demand Estimation 105
IV THEORETICAL FOUNDATIONS 112
4.1 EV Charging Control Problems 112
4.2 Real-time Scheduling Techniques 117
4.2.1 Real-time Systems 117
4.2.2 Taxonomy of Real-time Scheduling Algorithms 119
4.2.3 Real-time Scheduling Algorithms for Uniprocessor Systems . 123
4.2.4 Real-time Scheduling Algorithms for Multiprocessor Systems 126
4.3 Frequency Regulation and Vehicle-to-Grid (V2G) Technologies . . . 134
4.3.1 Frequency Regulation 134
4.3.2 Vehicle-to-Grid (V2G) Concept 138
4.3.3 V2G-based Frequency Regulation 141
V TECHNICAL APPROACHES 146
5.1 System Model of EV Charging Control System 147
5.2 Object-oriented Programming (OOP) Model for EV Charging Control System 150
5.2.1 EV Class 151
5.2.2 Finite State Machine for EV Class 152
5.2.3 Scheduler Class 155
5.2.4 Message Protocols between EVs and Scheduler 158
5.2.5 Overall OOP Model for EV Charging Control System 162
5.3 Real-time Scheduling for EV Charging 165
5.3.1 Reference EV Power Demand Estimation 165

5.3.2 Determination of the Number of Processing Queues and Charging Rates . . . 174
5.3.3 Electricity Prices for V2G-based Frequency Regulation and EV Charging . . . 178
5.3.4 Real-time Scheduling Algorithms and Dynamic Priority . . . 179
5.3.5 Effects of Charging Rates Control on Real-time EV Charging Control . . . 182
5.4 Real-time EV Charging Scheduling in Support of V2G-based Frequency Regulation . . . 184
5.4.1 V2G-based Frequency Regulation within Real-time EV Charging Control . . . 184
5.4.2 Effects of V2G-based Frequency Regulation on Real-time EV Charging Control . . . 186
5.5 Simulation Framework for Real-time EV Charging Control . . . 188
VI SIMULATION STUDIES . . . 190
6.1 Preparation of Dataset and Benchmark System . . . 190
6.1.1 Baseload Profiles and EV Charging Profiles . . . 191
6.1.2 Implementation of a Benchmark System and Substantiation of Its Technical Gaps . . . 195
6.2 Applicability of Real-time Scheduling Techniques to EV Charging Control . . . 201
6.2.1 (HYP I-1) Verification of Real-time EV Charging Control . . . 201
6.2.2 (HYP I-2) Evaluation of Real-time Scheduling Algorithms for EV Charging . . . 209
6.2.3 (HYP I-3) Effects of Charging Rates Control on Real-time EV Charging . . . 211
6.2.4 (HYP I) Real-time Charging Control Strategy vs. Valley-filling Control Strategy . . . 215
6.3 Real-time EV Charging Control Strategy in Support of V2G-based Frequency Regulation . . . 224
6.3.1 (HYP II-1) Incorporation of V2G-based Frequency Regulation into Real-time EV Charging . . . 224
6.3.2 (HYP II-2) Evaluation of the Impacts of V2G-based FR on Real-time EV Charging . . . 229

VII CONCLUSION **242**

7.1 Recapitulation of the Thesis 242

7.2 Contributions and Recommendations 244

7.3 Q & A from the Thesis Defense 248

7.4 Concluding Remarks 256

REFERENCES **258**

VITA **266**

LIST OF TABLES

1 Vehicle efficiency by fuel type 3

2 Scenarios description 23

3 Demand Response (DR) strategy by load type 31

4 Time of use pricing strategy 42

5 Analogy between real-time computing systems and cyber-physical energy systems 64

6 System timing characteristics 86

7 EV charging modes 92

8 Mapping research questions to hypotheses and tasks 110

8 Summary of EV charging schemes 113

9 Examples of soft, firm, and hard real-time systems 118

10 Task set for the example of RM scheduling algorithm 124

11 Task set for the example of EDF scheduling algorithm 125

12 Task set for the example of global EDF scheduling algorithm 128

13 Class definition for the example of next-fit algorithm for RM scheduling algorithm 129

14 Task set for the example of next-fit algorithm for RM scheduling algorithm 130

15 Task assignments for the example of next-fit algorithm for RM scheduling algorithm 131

16 Task assignments for the example of first-fit algorithm 132

17 Definitions of key ancillary services 135

18 Characteristics of regulation and load following 137

19 State definition for EV objects 152

20 State transition table for EV objects 154

21 Message protocol for EV objects 159

22 Message protocol for scheduler object 161

23 EV charging parameter settings for simulation studies 192

24 Quantitative comparison of real-time scheduling algorithms 210
25 Performance measures for different charging rates 212
26 Summary of real-time charging scheme performance with load fluctuation 220
27 Summary of Monte Carlo simulation on effects of load fluctuation . . 221
28 Summary of Monte Carlo simulation runs on a set of load profiles . . 223
29 Summary of Monte Carlo simulation runs on a set of EV profiles . . . 223
30 Summary of Monte Carlo simulation runs on V2G-based FR without timing buffer 233
31 Summary of Monte Carlo simulation runs on V2G-based FR with timing buffer 239
32 Summary of hypotheses testing and findings 240
32 List of bread-and-butter references 245

LIST OF FIGURES

1	Comparison of electric vehicles and gasoline-powered vehicles	2
2	U.S. carbon dioxide emissions and liquids fuel consumption	3
3	U.S. nonhydropower renewable electricity generation, 1990-2035	4
4	New and upcoming electric vehicles	6
5	U.S. market share and fleet composition of electric vehicles	7
6	Technical potential of the current power grid	8
7	Thesis structure overview	11
8	Load profiles with EV charging of 10% penetration level	13
9	Load profiles with EV charging of 20% penetration level	14
10	Power demand for different charging control schemes with 2 million EVs	15
11	Effects of optimal dispatch of PHEV charging demand	16
12	1999 CAISO system daily load curves for different charging scenarios	18
13	Load profiles for uncontrolled evening charging scheme	19
14	Load profiles for uncontrolled twice per day charging scheme	20
15	Load profiles for delayed nighttime charging scheme	20
16	Load profiles for optimal charging scheme	20
17	Voltage level for different charging strategies	23
18	Efficiency of a typical distribution transformer against load	24
19	Load profiles for two charging schemes	25
20	Load profiles for two quick charging schemes	25
21	Load profiles for staggered normal/quick charging schemes	26
22	Household load control with PHEV quick charging scheme	27
23	Demand per 11kV/400V substation for typical winter/summer days	28
24	Aggregated charging profiles using normal and quick charge strategies	30
25	Household load profiles with PHEVs	30
26	TOU rates from the chosen utilities	31

27 Summer load profiles with low PHEV penetration 31
28 Summer load profiles with high PHEV penetration 32
29 Winter load profiles with low PHEV penetration 32
30 Winter load profiles with high PHEV penetration 32
31 EV power consumption and load profiles for the dumb charging with 10% penetration of EVs 34
32 EV power consumption and load profiles for different charging strategies 35
33 Load profiles for different charging algorithms 37
34 Load profiles and peak substation loading for 80% PEV penetration with Level 1 charging 43
35 Optimal charging strategies using Nash Certainty Equivalence 47
36 Converged Nash equilibrium with $\delta = 0.015$ 51
37 Sufficient condition on tracking parameter δ for convergence 51
38 Optimal decentralized charging (ODC) algorithm 52
39 Optimality comparison 56
40 Optimality of the online algorithm for different plug-in times 57
41 Measurements of consumed power in an apartment 64
42 Simulation results of the optimal V2G aggregator 68
43 V2G control based on frequency deviation and SOC balance 69
44 Overview of literature on smart EV charging systems 73
45 Schematic representation of a generic real-time system 85
46 System model of an EV charging system as a real-time system 86
47 Operating scenario for the proposed real-time EV charging system . . 87
48 Overview of real-time scheduling for EV charging control 88
49 Underutilization of processing queues 94
50 Possible EV charging modes 103
51 Concept of timing buffer for V2G-based frequency regulation 108
52 Concept and technical potential of “valley-filling” approach 114
53 Spectrum of real-time systems 117

54 A schematic block diagram of a real-time system 119
55 Classification of real-time scheduling algorithms 120
56 Real-time scheduling algorithms for multiprocessor systems 122
57 Example of RM scheduling algorithm 124
58 Example of EDF scheduling algorithm 125
59 Example of global EDF scheduling algorithm 128
60 An example of frequency regulation 136
61 Frequency drop 137
62 Frequency deviation due to load change 138
63 Basic concept of vehicle-to-grid 140
64 Weighting functions on SOC for V2G-based frequency regulation . . . 144
65 Revisit of real-time scheduling algorithm for EV charging control . . . 146
66 Interpretation of EV charging as a real-time system 147
67 Queue structures for real-time scheduling algorithms 149
68 Anatomy of EV class 151
69 State transition diagram for EV objects 153
70 Anatomy of scheduler class 156
71 Example of the information contained in queues 157
72 Message format of an EV charging station to scheduler 159
73 Message format from scheduler to EV objects 160
74 Overall structure of the OOP model for EV charging system 163
75 Flowchart for real-time EV charging algorithm 164
76 Concept of charging packets 166
77 Reference EV power demand estimation 168
78 Relationship between charging packets and energy queue length . . . 169
79 Construction of a quadratic Bézier curve 173
80 Reference EV power demand estimation using Bézier curve 173
81 Energy overutilization resulting from being charged at the maximum charging rate 175

82 Energy underutilization due to energy queue length 175
83 Investigation process of real-time scheduling algorithms 181
84 Experimental setting for testing Hypothesis I-3 183
85 Overview of verification of V2G-based frequency regulation 184
86 Frequency regulation in CAISO 185
87 Desirability for frequency regulation against SOC 186
88 Schematic overview of testing Hypothesis II-2 187
89 Front-end graphical user interface of simulation framework 189
90 Baseload profile 191
91 An example of EV charging profile 193
92 Timing characteristics of the exemplary EV profile 194
93 Verification of the implemented benchmark system 196
94 Load profile of valley-filling strategy with load fluctuation 197
95 Number of EVs being charged of valley-filling strategy with load fluctuation 198
96 State-of-charge (SOC) of valley-filling strategy with load fluctuation . 199
97 Valley-filling strategy with different EV profiles and timing constraints 200
98 Load profiles of valley-filling and real-time charging by global EDF with no timing constraints 202
99 Number of EVs being charged and charging rate of valley-filling and real-time charging by global EDF with no timing constraints 203
100 Load profile of valley-filling and real-time charging by global EDF with timing constraints 204
101 Number of EVs being charged of valley-filling and real-time charging by global EDF with timing constraints 205
102 State-of-charge (SOC) of valley-filling and real-time charging by global EDF with timing constraints 205
103 Number of EVs being charged (global EDF) 206
104 Duration plugged in vs. duration being charged without preemption . 207
105 Duration plugged in vs. duration being charged with preemption . . . 208
106 Effects of charging rate on load profile with global EDF 213

107 Effects of charging rate on state-of-charge (SOC) with global EDF . . 214
108 Load profiles of valley-filling and real-time with load fluctuation . . . 216
109 Number of EVs being charged of valley-filling and real-time with load fluctuation 216
110 State-of-charge (SOC) of valley-filling and real-time with load fluctuation 217
111 Load profile of real-time charging scheme with load fluctuation 217
112 Number of EVs per mode without and with load fluctuation 218
113 Load prediction error and available power with load fluctuation . . . 219
114 Number of EVs missing deadlines without and with load fluctuation . 219
115 State-of-charge (SOC) of real-time charging scheme with load fluctuation 220
116 Monte Carlo simulation of number of EVs missing deadlines with load fluctuation 221
117 Overview of sensitivity analysis 222
118 Load profiles without and with V2G-based FR 225
119 Total number of EVs being charged without and with V2G-based FR 226
120 State-of-charge (SOC) without and with V2G-based FR 227
121 Number of EVs per mode without and with V2G-based FR 227
122 V2G power without and with V2G-based FR 228
123 State-of-charge (SOC) of EVs with mode 4 without and with V2G-based FR 228
124 Monte Carlo simulations on the number of EVs missing deadlines with 100 sets of load profiles 230
125 Monte Carlo simulations on averaged plug-out SOC with 100 sets of load profiles 230
126 Monte Carlo simulations on the number of EVs missing deadlines with 100 sets of EV profiles 231
127 Monte Carlo simulations on averaged plug-out SOC with 100 sets of EV profiles 231
128 Load profiles without and with timing buffer for V2G-based FR . . . 234
129 State-of-charge (SOC) without and with timing buffer for V2G-based FR 235

130 Monte Carlo simulations on the number of EVs missing deadlines for timing buffered V2G-based FR with 100 sets of load profiles 236

131 Monte Carlo simulations on averaged plug-out SOC for timing buffered V2G-based FR with 100 sets of load profiles 236

132 Monte Carlo simulations on the number of EVs missing deadlines for timing buffered V2G-based FR with 100 sets of EV profiles 237

133 Monte Carlo simulations on averaged plug-out SOC for timing buffered V2G-based FR with 100 sets of EV profiles 237

134 Schematic overview of EV charging system with HEMS 247

135 Proposed real-time scheduling algorithm for EV charging 252

LIST OF SYMBOLS OR ABBREVIATIONS

β_n	Battery capacity of the n-th EV.
Δt	Duration of each time slot.
η	Charging efficiency.
γ_n	Urgency of the n-th EV.
$\mu_{f_{\mathsf{SOC}}}$	Averaged plug-out state-of-charge (SOC).
$\mu_{i_{\mathsf{SOC}}}$	Averaged plug-in state-of-charge (SOC).
$\sigma_{t_{\mathsf{plugin}}}$	Standard deviation of plug-in time.
$\sigma_{t_{\mathsf{plugout}}}$	Standard deviation of plug-out time.
τ_i	Real-time task.
P	Processing queue.
W	Waiting queue.
a_i	Arrival time.
d_i	Deadline.
E_{a}	Energy available.
E_{c}	Energy consumed by EVs.
e_i	Execution time.
E_n	Energy queue length of the n-th EV.
$m(t)$	Number of EVs plugged in at time t.
n_{PQ}	Number of charging stations activated.
n_{rem}	Number of remaining time slots.
n_{req_i}	Number of time slots for i-th EV to be fully charged.
p	Pointer for processing queue.
p_i	Period.
P_{base}	Aggregated non-EV base demand.
P_{ref}	Reference total demand.

$r(t)$	Charging rate at time t.
r_{max}	Maximum charging rate.
$r_{\mathsf{opt}}(t)$	Optimized charging rate at time t.
s_{plugin}	State-of-charge at plug-in time.
s_{plugout}	State-of-charge at plug-out time.
s_n	State-of-charge of the n-th EV.
t_{plugin}	Plug-in time.
t_{plugout}	Plug-out time.
$U(t)$	Energy utilization at time t.
w	Pointer for waiting queue.
n_{EVsInPQ}	Number of EVs in processing queues.
P_{a}	Available Power.
A/S	Ancillary Services.
ABM&S	Agent-based Modeling and Simulation.
AGC	Automatic Generation Control.
AMI	Advanced Metering Infrastructure.
AWGN	Additive White Gaussian Noise.
BEV	Battery Electric Vehicle.
CAISO	California Independent System Operator.
CPES	Cyber-physical Energy System.
DER	Distributed Energy Resource.
DR	Demand Response.
DSO	Distribution System Operator.
EDF	Earliest Deadline First.
EES	Electric Energy Storage.
EIA	U.S. Energy Information Administration.
EV	Electric Vehicle.

EVSE Electric Vehicle Supply Equipment.

FAB Focused Addressing and Bidding.

FCFS First Come, First Served.

FERC Federal Energy Regulatory Commission.

G2V Grid-to-Vehicle.

GA Genetic Algorithm.

GEV Grid-enabled Vehicle.

GUI Graphical User Interface.

GW Gigawatt.

HEMS Home Energy Management System.

ICE Internal Combustion Engine.

ISO Independent System Operator.

kW Kilowatt.

LDV Light-duty Vehicle.

LFC Load Frequency Control.

LLF Least Laxity First.

MISO Midwest Independent System Operator.

MPC Model Predictive Control.

MSS Maximum Sensitivities Selection.

NCE Nash Certainty Equivalence.

NREL National Renewable Energy Laboratory.

ODC Optimal Decentralized Charging.

OOP Object-oriented Programming.

ORNL Oak Ridge National Laboratory.

PEV Plug-in Electric Vehicle.

PHEV Plug-in Hybrid Electric Vehicle.

PLC Power Line Communication or Carrier.

RES Renewable Eneregy Source.

RFB Requests For Bids.

RHC Receding Horizon Control.

RM Rate Monotonic.

RM-FFDU Rate Monotonic First-Fit Decreasing Utilization.

RMA Rate Monotonic Analysis.

RTPS Real-time Physical System.

SCE Southern California Edison.

SJF Shortest Job First.

SOC State-of-Charge.

SoS System of Systems.

TOU Time-of-Use.

V2G Vehicle-to-Grid.

WCETA Worst Case Execution Time Analysis.

SUMMARY

An electric vehicle (EV) is powered by an electric motor rather than a gasoline engine. EVs provide significant potential for increasing energy efficiency in transportation, reducing greenhouse gas emissions, and relieving reliance on foreign oil. In addition to the economical and environmental benefits, the large-scale adoption of EVs presents an opportunity to provide electric energy storage (EES)-based ancillary services for smoothing the natural intermittency of renewable energy sources (RES) and ensuring grid-wide frequency stability as large-scale renewable energy sources (RES) are integrated into the power grid.

However, the potential benefits of EVs come with a multitude of challenges including those in the integration into the electric power grid. The charging of EVs has an impact on the distribution grid because they consume a large amount of electrical energy and this demand of electrical power can lead to extra large and undesirable peaks in the electrical consumption. Many simulation-based studies have suggested that, if no regulation on EV charging is implemented, even a 10% penetration of EVs may cause unacceptable variation in voltage profiles. It was shown, however, that adopting "smart" charging strategies for the high penetration of EVs can alleviate some of the integration challenges and defer infrastructure investment needed otherwise.

Among a variety of EV charging strategies, the decentralized "valley-filling" approach, which minimizes the total load variance, is the most popularly researched, and many of its variations have been proposed for different objectives. It was shown that the valley-filling charging strategy is the most versatile for a given daily load profile prediction in that it achieves the maximum load factor and simultaneously minimizes

the daily operating costs of utilities. However, the decentralized valley-filling charging strategy has a number of technical limitations: it generates a charging schedule through a day-ahead negotiation process between a utility and EVs; it is very sensitive to the accuracy of the prediction of non-EV power demand; and it also requires simultaneous participation of all EVs in the negotiation process, with exact knowledge of EV charging profiles. Moreover, the valley-filling charging strategy does not take into account EV owners' charging requirements such as desired departure state-of-charge (SOC) and plug-out time.

It is observed that the technical limitations of the valley-filling EV charging strategy can be tackled by applying real-time scheduling techniques, which have been widely researched and applied to a variety of real-time systems, where timing constraints are as important as the correctness of system outputs. In this research, a real-time scheduling algorithm for an EV charging system, which enables EV charging to be controlled in real time without exact knowledge of EV charging profiles as well as to satisfy EV owners' preferences, is proposed, and its technical feasibility and capability to fill the technical gaps of the valley-filling charging strategy are evaluated. In addition, a methodology for incorporating V2G-based frequency regulation into the real-time EV charging system is presented, and their interactions are investigated. Furthermore, a simulation framework for developing the real-time EV charging algorithm with V2G-based frequency regulation incorporated is presented.

CHAPTER I

INTRODUCTION

1.1 Motivation

1.1.1 Need for Electric Vehicles

An electric vehicle (EV) is powered by an electric motor rather than a gasoline engine [29]. EVs use energy stored in rechargeable batteries. Unlike a hybrid car, which is fueled by gasoline and also uses a battery, which is continuously recharged with power from the internal combustion engine and regenerative braking rather than from the electric grid, and an electric motor to improve efficiency, EVs are powered by electricity from the electric grid or a battery with chemical energy stored in [29].

Based upon how their batteries are recharged, EVs can be categorized into several groups: battery electric vehicles (BEVs), plug-in electric vehicles (PEVs), and plug-in hybrid electric vehicles (PHEVs). A BEV uses chemical energy stored in rechargeable battery packs as its only source for driving, and does not have an internal combustion engine (ICE) at all. A PEV is any electric vehicle with rechargeable battery packs that can be charged from the electric grid, and the electricity stored in batteries is used for driving the wheels. PEVs are also sometimes referred to as grid-enabled vehicles (GEVs), and they do not have an internal combustion engine, either. A PHEV is a hybrid electric vehicle with rechargeable battery packs that can be restored to full charge by connecting a plug to an external electric power source. PHEVs share the characteristics of both a conventional hybrid electric vehicle and an all-electric vehicle. Since the impacts of a large population of EVs on the electric grid and their interactions with the grid will be investigated in this research, PEVs and PHEVs will be only considered, and the terminology "EV" will be used as a collective name for

PEVs and PHEVs, unless otherwise stated.

EVs have not been widely adopted because of its limited driving range and long recharging time [29]. However, as battery technology improves, in other words, the amount of energy storage in a battery increases and the related costs are reduced simultaneously, major automakers are expected to begin introducing a new generation of EVs [29]. EVs provide significant potential for increasing energy efficiency in transportation, reducing greenhouse gas emissions, and relieving reliance on foreign oil [12]. Figure 1 compares EVs with internal combustion engine (ICE) vehicles, i.e., gasoline-powered vehicles. According to [80], EVs convert about 59-62% of the electrical energy from the grid to power at the wheels while gasoline-powered vehicles only convert about 17-21% of the energy stored in gasoline. Also, it is demonstrated that an EV requires the energy equivalent of about 0.89 gallons of gas to go 100 miles, or about 112 miles per gallon equivalent (refer to Table 1 for details) [79].

The Environmental Protection Agency's 2011 U.S. Greenhouse Gas Inventory Report estimates that the transportation sector accounted for more than 31 percent of annual greenhouse gas emissions in 2009 [85], and most of the growth in CO_2 emissions is accounted for by the electricity generation and transportation (see Figure 2(a)).

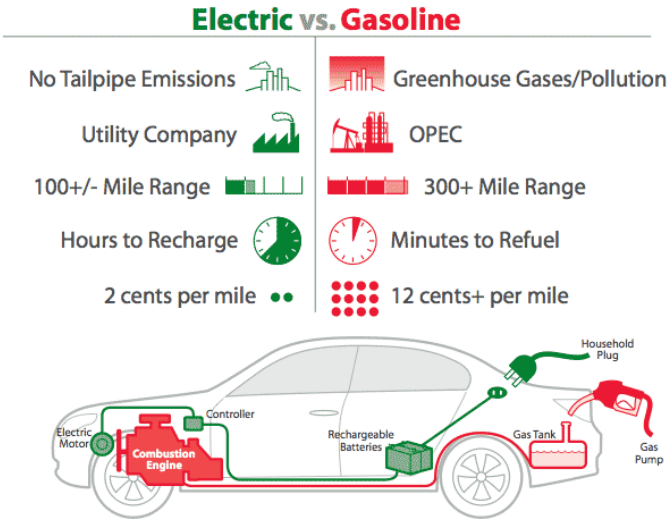

Figure 1: Comparison of electric vehicles and gasoline-powered vehicles [29].

Table 1: Vehicle efficiency by fuel type [79].

Technology	Source fuel	Well-to-station efficiency	Vehicle mileage	Vehicle efficiency	Well-to-wheel efficiency
Tesla electric	Natural gas	52.5%	110 Wh/km	2.18 km/MJ	1.14 km/MJ
Hybrid (gas/electric)	Crude oil	81.7%	55 mpg	0.68 km/MJ	0.556 km/MJ
Commuter car (gas)	Crude oil	81.7%	51 mpg	0.63 km/MJ	0.478 km/MJ
Sports car (gas)	Crude oil	81.7%	20 mpg	0.24 km/MJ	0.202 km/MJ

Although power plants use various types of fuel to generate electricity, EVs emit about 50 percent fewer greenhouse gases compared with conventional vehicles. Even PHEVs powered by older coal plants emit approximately 25 percent fewer greenhouse gases, and can achieve a 66 percent reduction in emissions if charged with electricity from zero emission power plants [13]. An EV recharged from the U.S. electric power grid emits about 115 grams of CO_2 per kilometer driven (6.5 oz CO_2/mile), whereas

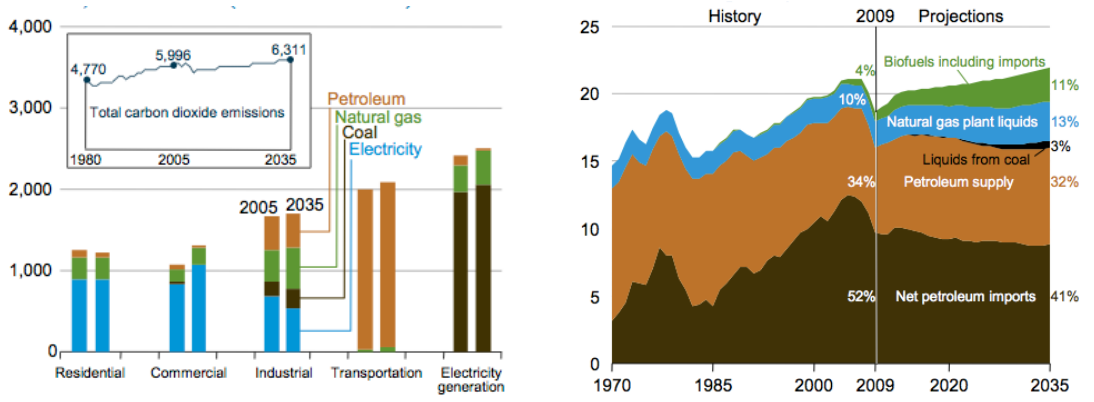

(a) U.S. carbon dioxide emissions by sector fuel, 2005 and 2035 (million metric tons)

(b) U.S. liquids fuel consumption, 1970-2035 (million barrels per day)

Figure 2: U.S. carbon dioxide emissions and liquids fuel consumption [83].

a conventional vehicle emits 250 grams of CO_2 per kilometer (14 oz CO_2/mile), most of which are from its tailpipe, and some of which are from the production and distribution of gasoline [39]. Therefore, broad adoption of EVs will dramatically lower emissions from the transportation sector [85]. In the United States, 84 percent of cars, trucks, ships, and planes depend on oil. In 2009, the U.S. imported 11.7 million barrels of crude oil and refined petroleum products per day, which is about 52% of the petroleum the U.S. consumes (see Figure 2(b)) [83, 84]. To ensure stability in the world oil markets, American troops are deployed on oil-security missions, costing U.S. taxpayers $67 billion to $83 billion a year, according to [68]. The United States also faces increased competition for oil from developing nations. According to the U.S. Energy Information Administration (EIA), developing nations will account for 85 percent of new energy demand through 2035 [82]. Furthermore, since electricity generation from renewable sources grows by 72 percent, raising its share of total generation from 11 percent in 2009 to 14 percent in 2035 (see Figure 3) [83], electricity can be an alternative sources of fuel for U.S. vehicle fleet to avoid economic impacts and security effects of dependence on foreign oil that is getting scarce and more expensive.

In addition to the economical and environmental benefits, there are many technical

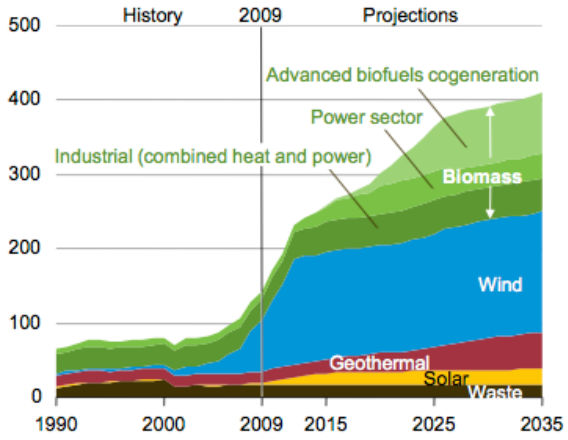

Figure 3: U.S. nonhydropower renewable electricity generation, 1990-2035 (billion kilowatts per year) [83].

benefits that are expected by deploying a large number of EVs. The most promising, but least proven, providers of ancillary services are electric energy storage (EES) technologies such as flywheels and advanced batteries, which store and release electric energy on demand and are prized for their fidelity and rapid response functionality [44]. However, high costs associated with the operation of EES assets have prevented their deployment at a meaningful scale. The large-scale adoption of EVs presents an opportunity to overcome this barrier. With recent advancements in demand response, vehicle-to-grid (V2G), and battery technologies, many researches have suggested that networks of aggregated EVs could provide EES-based ancillary services at a competitive price. According to [16], an average private vehicle remains parked 90% of the time to realize that parked EVs could soon constitute a massive amount of persistent stored energy connected to the grid. This is potentially very attractive to utilities that can utilize such grid-connected storage devices as an alternative ancillary service resource [66] for regulating voltage profiles, ride-through support for fault protection, and even compensating fluctuating renewable energy generation [51].

1.1.2 Technical Challenges of Integration of EVs

Currently, several types of EVs are either already in the U.S. market or about to enter, and the electrification of transportation is at the forefront of many research and development agendas (see Figure 4). According to [83], the maximum market penetration of EVs is estimated to be about 70 percent under the baseline oil price scenario and almost 90 percent of light-duty vehicle (LDV)[1] market under the high oil price scenario (see Figure 5). Therefore, the potential benefits of EVs described in the previous section come with a multitude of challenges including those in the integration into the electric power grid. The charging of EVs has an impact on

[1]The light-duty vehicle classification includes cars, light trucks, SUVs, minivans, and trucks with gross vehicle weight less than 8,500 pounds.

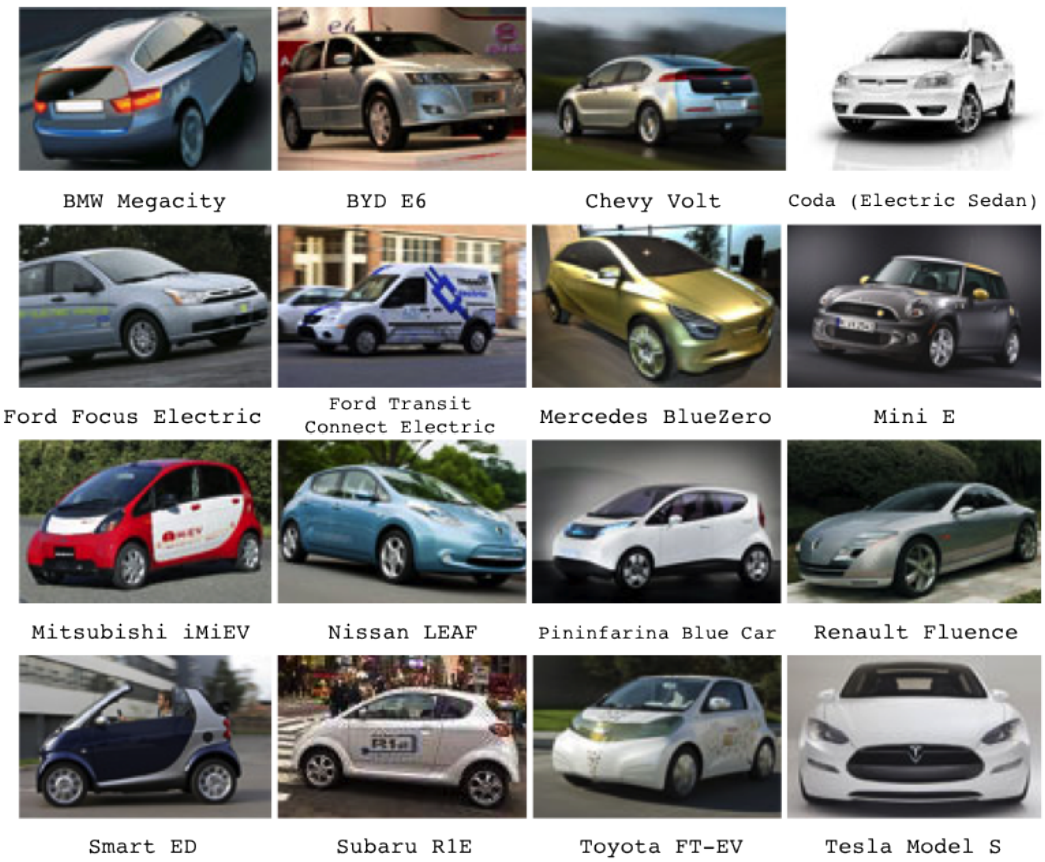

Figure 4: New and upcoming electric vehicles [29].

the distribution grid because they consume a large amount of electrical energy and this demand of electrical power can lead to extra large and undesirable peaks in the electrical consumption [6]. It also increases the demand side uncertainties, and presumably reduces the distribution circuit and transformer lifespan [69]. Moreover, power losses and voltage variations become more likely [5]. The simulation-based study in [52] suggests that, if no regulation on EV charging is implemented, even a 10% penetration of EVs may cause unacceptable variation in voltage profiles.

Depending on when and where they are plugged in, EVs could cause local or regional constraints on the grid. They could require the addition of new electric generation and transmission capacity and increase the utilization of existing capacity [24]. A study by National Renewable Energy Laboratory (NREL) shows that large PHEV penetration would place increased pressure on peaking units with an uncontrolled charging strategy [63]. Researches from Oak Ridge National Laboratory (ORNL) indicates that most regions would need to build additional generation capacity to meet the added demand when charging PHEVs in the evening [24].

However, the U.S. electric power infrastructure is a strategic national assets that is underutilized most of the time [36]. With the proper changes in the operational paradigm, it could generate and deliver the necessary energy to fuel the majority of the U.S. light-duty vehicle (LDV) fleet. If electric vehicles are properly charged, especially during off-peak periods, the technical potential of the current grid is to

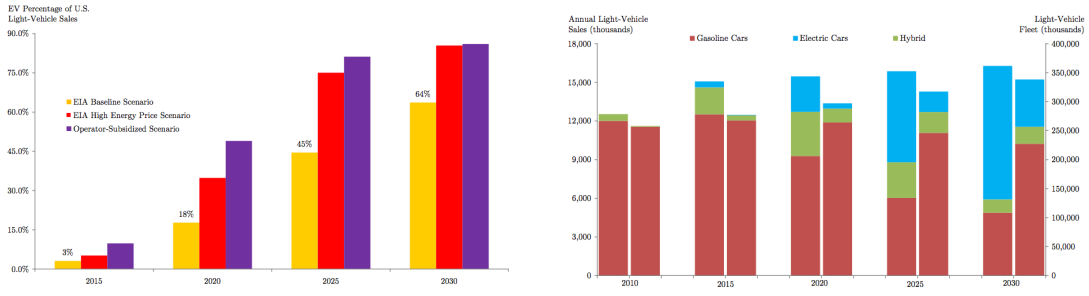

(a) market share of electric vehicles (b) light-vehicle sales and fleet composition

Figure 5: U.S. market share and fleet composition of electric vehicles [2].

cover 73 percent of light-duty vehicles, which has an estimated gasoline displacement potential of 6.5 million barrels of oil equivalent per day, or approximately 52 percent of the nation's oil imports (see Figure 6) [64]. The general expectation has been that the grid will not be greatly affected by the use of EVs because the recharging will occur during off-peak hours, or the number of vehicles will grow slowly enough so that capacity planning will respond adequately [24]. However, this expectation does not consider that EV owners will control the timing of recharging, and their inclination will be to plug in when convenient, rather than when utilities would prefer.

Many studies demonstrate that adopting "smart" charging strategies can mitigate some of the integration challenges, defer infrastructure investment needed otherwise, and even stabilize the grid [19]. For example, scheduling EV charging so that aggregated EV load fills the overnight valley in demand may reduce daily cycling of power plants and operational costs of electricity utilities [9]. From EV owners' point of view, the batteries of the EVs have to be charged overnight so that the owners can drive off in the morning with a fully-charged batteries. This also gives opportunities for intelligent or smart charging control.

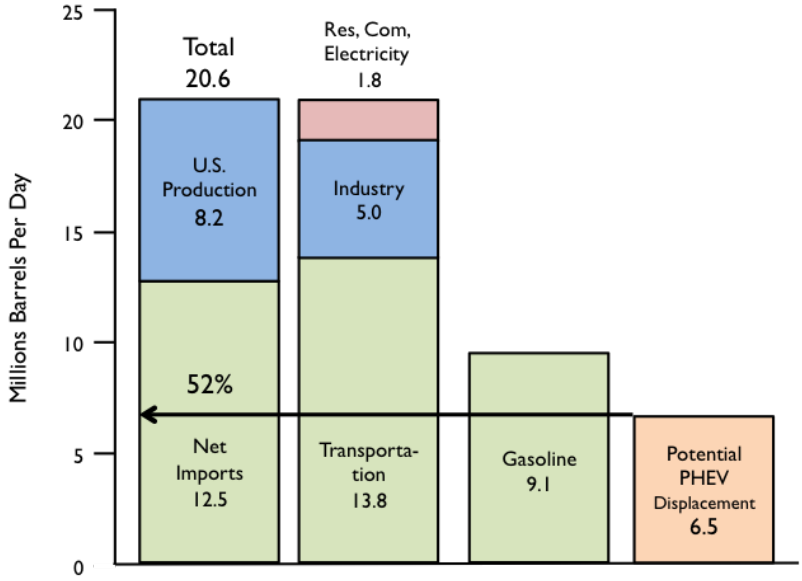

Figure 6: Technical potential of the current power grid (Source: R. Pratt, *et al.* [64]).

In summary, a large deployment of EVs will involve the following technical challenges [52]:

- evaluation of the impacts that battery charging have in system operations;
- identification of adequate operational management and control strategies regarding batteries' charging periods;
- identification of the best strategies to be adopted in order to use preferentially renewable energy sources (RES) to charge EVs; and
- assessment of the EV potential to participate in the provision of power systems services, including reserves provision and power delivery, within a vehicle-to-grid (V2G) concept.

All the aforementioned technical challenges except for the third one will be addressed in this research.

1.2 Research Statement

As addressed in §1.1, the potential benefits of the integration of EVs into the power grid come with unavoidable technical challenges. It is shown, however, that "adopting smart charging strategies for the high penetration of EVs can alleviate some of the integration challenges and defer infrastructure investment needed otherwise" [19]. Also, EVs will play an important role as energy storage devices for smoothing the natural intermittency of renewable energy sources (RES) and ensuring grid-wide frequency stability as large-scale renewable energy sources (RES) are integrated into the power grid [62]. In this context, a "smart" charging strategy must take into account possible vehicle-to-grid (V2G) applications along with vehicle charging to fully utilize the potential benefits of a high penetration level of EVs. Furthermore, timing constraints must be considered since it is highly likely that EV owners will control the timing of recharging their vehicles rather than utilities. Therefore, a "smart" EV

charging system is required to be developed such that it cannot only facilitate V2G applications but also satisfy EV owners' charging requirements.

1.2.1 Research Objective

The purpose of this research is to develop a framework for designing a "*smart*" or "*intelligent*" *EV charging control system* that cannot only mitigate the impacts of the high penetration of EVs on the grid without reinforcement of the infrastructure but also facilitate V2G-based applications. For the sake of the development of an EV charging control system, existing technical approaches will be investigated and compared with the proposed EV charging control system. As discussed in the previous paragraph, EV owners' charging requirements as well as possible V2G-based applications are also considered within the development framework of the EV charging control system.

1.2.2 Thesis Organization

The technical challenges related to EVs and the need for this research have been outlined in this chapter. Chapter II addresses previous efforts in the literature relevant to the topic of this research. In Chapter III, research questions and related hypotheses are presented. A theoretical foundation is given to assist in facilitating the course of the thesis in Chapter IV, followed by detailed information on the simulation model and implementation of the proposed design methodology in Chapter V. Chapter VI presents and explores a set of simulation studies as a proof of concept. Finally, a brief recapitulation of the research and proposed future work are addressed in Chapter VII. The overall structure of this thesis is provided in Figure 7, where the interdependency and flow amongst chapters and sections are described to help readers understand the work presented in this thesis.

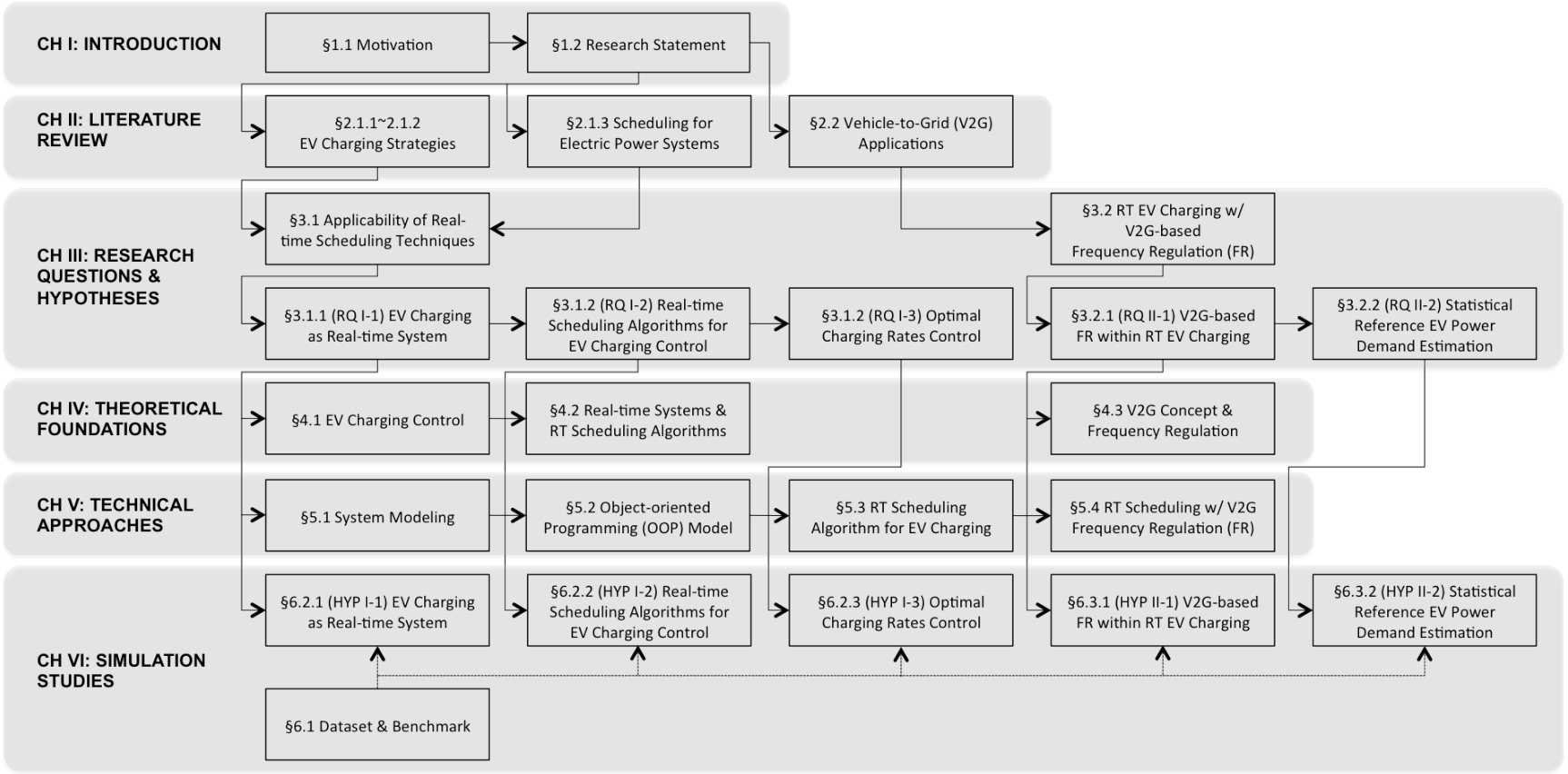

Figure 7: Thesis structure overview.

CHAPTER II

LITERATURE REVIEW

This chapter reviews key topics related to the focus of the research and the technical challenges mentioned in Chapter I. In order to identify technical limitations or gaps leading to formulating the real-time EV charging control problem, a variety of EV charging control strategies, which have been previously proposed to aim at minimizing the impacts of EV integration on the electric power grid, are reviewed in the first section, followed by the review of attempts to applying scheduling techniques to electric power systems. The next section addresses the previous efforts regarding the vehicle-to-grid (V2G) concept, which is one of technical potentials of high penetration of EVs and is expected to have some interactions with EV charging control so that it must be considered when an EV charging control strategy is developed. Finally, the last section of this chapter summarizes the literature review and presents the observations from the review of the literature.

2.1 Operational Management and Control Strategies Regarding EV Charging

2.1.1 Centralized/Coordinated EV Charging Control Strategies

The likely impacts of the introduction of EVs on the existing power distribution were evaluated in [67]. In order to evaluate the impacts, the authors assumed that the charging would be occurred during overnight off-peak hours of 8:00 pm to 8:00 am, and they performed two case studies for 10% and 20% EV penetration levels. For the case of the 10% penetration level, the new load caused by EV charging is comfortably absorbed by total area loads without any adverse effect on the distribution system,

and in fact it appears to improve the system performance since EV charging load fills up some portion of the off-peak valley without increasing the peak load in total load curves as illustrated in Figure 8(a). However, if the residential load is considered separately, the new peak is higher than the peak load without EV charging load, as depicted in Figure 8(b), which requires the distribution system to be upgraded to accommodate the additional charging load. Thus, at the residential distribution system, EV charging load, even at a low penetration level of 10%, may not be absorbed without any adverse effect on the distribution system, suggesting that a *charging strategy* and *proper economic incentives* may be required to alleviate the adverse effects by distributing charging load during the off-peak hours, even at low levels of EV penetration. Needless to say, the EV penetration level of 20% introduces a significantly higher new peak, and the system cannot absorb EV loads of above 20% penetration level unless a *strict control over temporal distribution of EV charging* is implemented (see Figure 9). The case studies revealed several important issues regarding the impacts that EV charging may have on the distribution system. First, it is not desirable to have only sufficient generation capacity during off-peak hours to ensure the system performance and reliability since EV loads can introduce an additional peak load or near-peak load in early off-peak periods. Secondly, a typical distribution system may not be able to supply EV loads of beyond 20% penetration

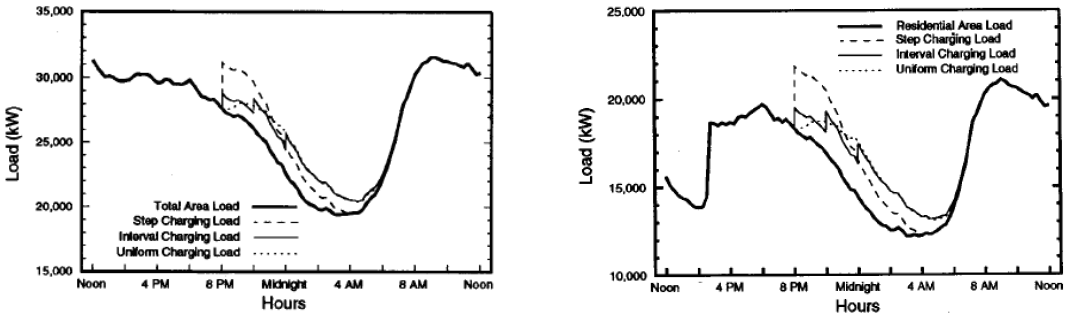

(a) total area (b) residential area

Figure 8: Load profiles with EV charging of 10% penetration level [67].

level unless charging load is properly managed.

Ford summarized previous studies on the potential impacts of EVs on the Southern California Edison (SCE) System, and investigated how two widely defined charging control schemes affect load shapes and efficiency of operations [17]. The study confirmed that EVs can improve load shapes and efficiency of operations, and claimed that the *management of EV loads* is needed even if the daytime charging is minimal and EV charging may otherwise lead to secondary peaks, as claimed in [67]. To avoid undesirable secondary peaks due to EV charging, the author proposed a load management strategy with different electric rates for different charging periods, which can discourage EV owners from initiating the nighttime charging until later in the evening. The author examined two widely defined charging control schemes in the Southern California Edison studies: blind control and smart control. In the blind control where only one-way communication exists, the utility sends signals to EVs to initiate charging while not receiving any information from EVs. Since the controller does not know how long EVs need to be charged, it sends the signals out early in the evening in order to ensure that all EVs are fully charged in time when EV owners leave for work, which prevents EV load from being filled in the early morning hours as depicted in Figure 10(a). For the smart control system, it is assumed that two-way communication is established between the controller and EV chargers. The

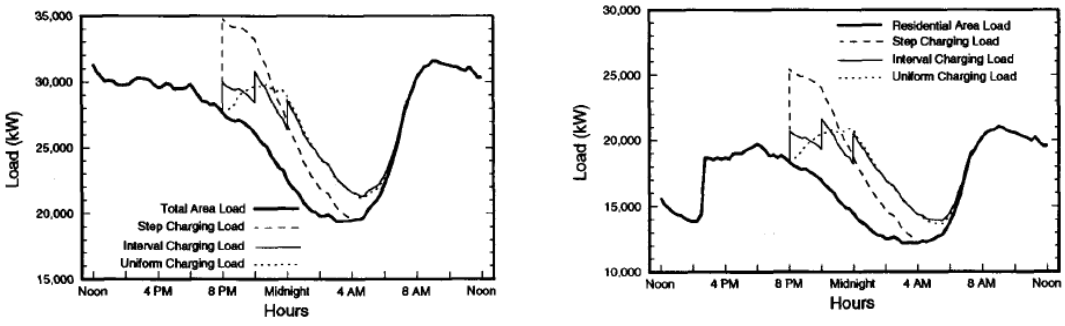

(a) total area (b) residential area

Figure 9: Load profiles with EV charging load of 20% penetration level [67].

utility sends signals to initiate charging, and the status of EVs can be monitored by the controller. Figure 10(b) illustrates that the load shape, obtained by applying the smart control, shows an improvement over the one by the blind control in that it fills in the valley from around midnight and early in the morning. It was concluded that, if advanced batteries are utilized and *EV charging is properly controlled*, the Edison's power system would be able to accommodate a large number of EVs. Furthermore, it was also demonstrated that, from the system operations perspective, around 90% of the electricity required to charge EVs would come from natural gas fired units, which in turn leads to a significant reduction in tailpipe emission, and higher costs to operate the SCE system would be outweighed by the increase in electricity sales, caused by EV charging.

Denholm and Short evaluated the effects of optimal PHEV charging on the grid, under the assumption that utilities have a direct or an indirect control authority on when charging takes place while providing customers with the possibly lowest cost of driving energy [9]. With direct control, it is assumed that a utility would send a signal to an individual vehicle or a group of vehicles to allow to start charging, similarly with the one in [17]. An indirect control, on the other hand, would have each vehicle responding intelligently to real-time price signals or some other price schedule to buy

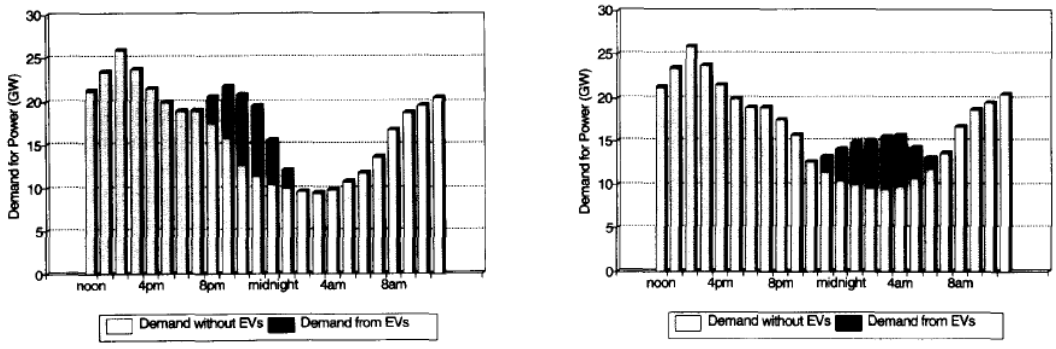

(a) blind control (b) smart control

Figure 10: Power demand for different charging control schemes with 2 million EVs [17].

or sell electricity at an appropriate time. In either control scheme, vehicles would be effectively dispatched to provide the most economic charging and discharging to consumers. It was shown through simulation studies that low-cost off-peak electricity would accommodate up to 50% of the vehicle fleet with no additional electric generation capacity *under optimal dispatch rules* and the assumption that PHEVs derive 40% of their miles from electricity. It was also shown that, while increasing total electrical energy consumption – but without requiring additional generation capacity – the optimal dispatch of the additional PHEV demand would increase the load factor of baseload power plants (Figure 11(a)) and substantially decrease the daily cycling of power plants (Figure 11(b)), both of which can be translated into lower operational costs. It appears that PHEVs are much better *suited for short-term ancillary services such as regulation and spinning reserve* and a large fleet of PHEVs could possibly replace a fraction of conventional low-capacity generation used for periods of extreme demand or system emergencies. In conclusion, the authors indicated that current electric power systems have large amount of underutilized capacity, which could potentially offer electricity to PHEVs, provided utilities have some control over when charging occurs, and they also claimed that an *optimal dispatch for PHEVs charging* and their *ability to provide power to the grid* could significantly increase the utilization of power systems.

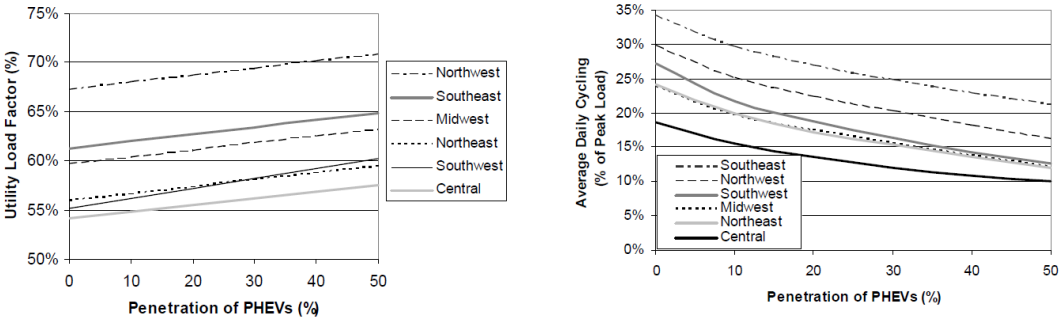

(a) utility load factor

(b) average daily cycling

Figure 11: Effects of optimal dispatch of PHEV charging demand [9].

Lemoine *et al.* studied how many PHEVs could be served by the California Independent System Operator (CAISO) without additional generation/transmission infrastructure by investigating the cost per mile of all-electric operation and how real-time electricity pricing affects the charging behaviors of PHEVs [43]. However, although there has been considerable interest in the use of PHEVs, especially to provide energy or energy services to the electric grid, the authors did not consider this application, and also ignored distribution-level constraints on the quantity and pattern of PHEV charging. The study suggested that, if most PHEVs are charged after the time of peak electricity demand, millions of PHEVs could be economically deployed in California without requiring new generation capacity even with modest gasoline prices and real-time electricity pricing, and that the number of PHEVs as well as their charging patterns would strongly influence the power grid. In addition, the paper showed that the state's PHEV fleet size is not likely to reach into millions within the current electricity sector planning cycle. The authors indicated that, although the real-time electricity pricing would encourage PHEV owners to charge their vehicles at night, they might choose to charge even during peak hours unless real-time price for PHEV charging is sufficiently cheap compared with gasoline price, and, therefore, if peak-hour charging is undesirable, it is needed to *implement new pricing structures* or *technical means to coordinate PHEV charging* and electric power system operations. For this reason, the authors analyzed three different charging scenarios to see the impact of PHEV charging on the grid: optimal charging, evening charging, and twice per day charging. In the optimal charging scenario, it is assumed that PHEV charging can be perfectly allocated by charging vehicles during periods of lowest demand and by allowing vehicles to charge with interruptions so that the system load curve is flattened as much as possible (see Figure 12(a)). In this best case, PHEVs would not require additional generation, transmission, or distribution since generators currently shut off at night might pick up PHEV charging demand. In

the evening charging scenario, the authors assumed that PHEVs begin charging when the owners return home from work between 6:00 pm and 8:00 pm and each PHEV charges for 4 continuous hours. As shown in Figure 12(b), 5 million PHEVs would call for more generation capacity since the peak load grows by 4 GW, or 12%. The twice per day charging scenario assumed that those same evening-charging cars are plugged in and charged again in the morning when the owners arrive at work between 8:00 am and 9:00 am with drained batteries. In this scenario, adding more than 5 million PHEVs creates a very different load shape with two peaks per day, implying additional electricity generation, but 1 million compact cars still do not affect the system's peak load, as illustrated in Figure 12(c) The analysis showed that, as long as on-peak charging is avoided, the CAISO may be able to accommodate 1 million PHEVs before new generation or transmission investments are required, but, if PHEV fleets grow to several million vehicles and charging is not optimally timed, new investments would be required. The authors concluded that, without *special PHEV pricing structures or charging control*, adopting a large number of PHEVs could raise system peaks, which depends upon the *timing of the system peak* and the *as-yet-unknown charging behaviors of PHEV owners*, and suggested, as a future research, the investigation on how consumers who would buy PHEVs will tend to operate their cars so that effective technologies and efficient tariff can be devised, tested, and implemented in order to allow possible large-scale PHEV deployment.

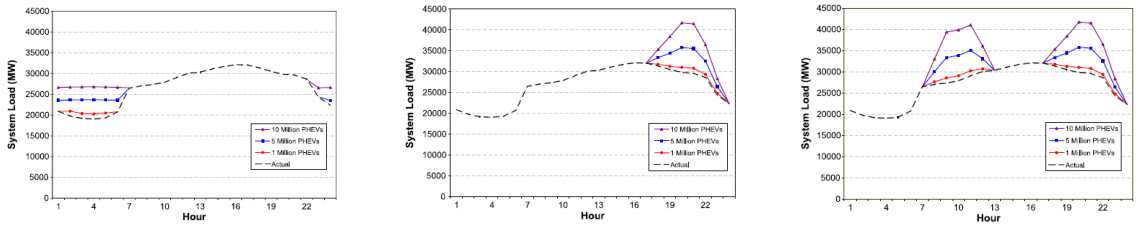

(a) optimal charging (b) evening charging (c) twice per day charging

Figure 12: 1999 CAISO system daily load curves for different charging scenarios [43].

Letendre and Watts assessed the effect, greenhouse gas (GHG) emissions, and end-user costs of large number of PHEVs on the electric grid in the state of Vermont, which is a small power system with peak demand of approximately 1 GW, in terms of PHEV penetration levels, i.e., 50,000 PHEVs (about 9% of the total light duty vehicle LDV) fleet), 100,000 PHEVs (approximately 17% of LDVs), and 200,000 PHEVs (more than 35% of the total LDV fleet) [45]. In order to examine the impact of PHEVs, considered are four different charging scenarios: 1) an uncontrolled evening charging, 2) an uncontrolled twice per day charging, 3) a delayed nighttime charging, and 4) an optimal nighttime charging with smart grid technology. In the uncontrolled evening charging scenario, one-third of PHEVs start charging at 6:00 pm, and, even at a low PHEV penetration level of 50,000 vehicles, the demand for PHEV charging could add to the system peak demand as illustrated in Figure 13. For the uncontrolled twice per day charging, a second peak demand would be added during daytime hours, from 8:00 am to 2:00 pm as shown in Figure 14. However, the delayed nighttime charging scheme could accommodate 100,000 PHEVs without adding to system peak demand, indicating that it would not be required to build additional generation and transmission, as depicted in Figures 15. Furthermore, the optimal charging scheme, in which vehicles are charged in a pattern that increases utility load factors by charging during the periods of lowest demand, could allow 200,000 PHEVs, or approximately one-third of Vermont LDVs, to fully charge daily from the grid without adding to

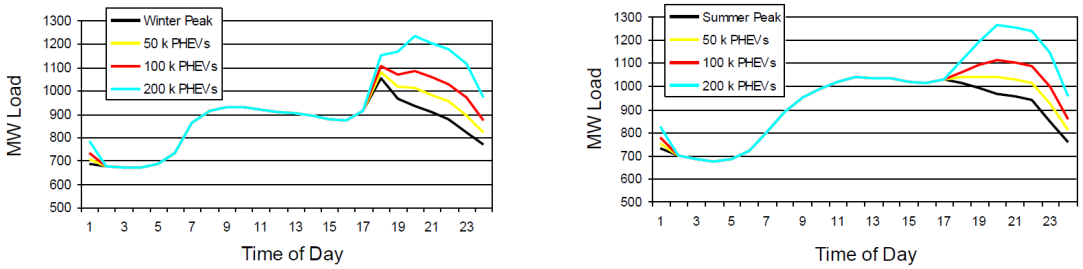

(a) typical winter day (b) typical summer day

Figure 13: Load profiles for uncontrolled evening charging scheme [45].

system level peak demand (see Figure 16). The conclusion of this paper is that a large fleet of PHEVs could be accommodated in Vermont's power grid without the need to build additional generation, transmission, or distribution infrastructure if either *financial incentives for off-peak charging* or *direct control of PHEV charging* is properly utilized. For future study, the authors suggested the *impact assessment of PHEVs with vehicle-to-grid (V2G) capability*, using PHEVs as load leveling devices, and the investigation of the potential benefits of V2G technology.

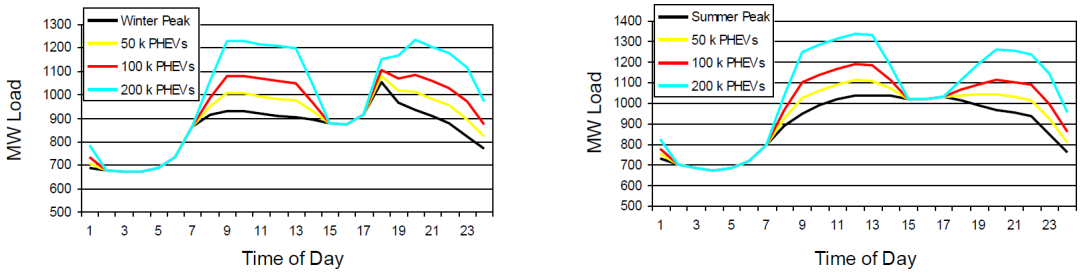

(a) typical winter day (b) typical summer day

Figure 14: Load profiles for uncontrolled twice per day charging scheme [45].

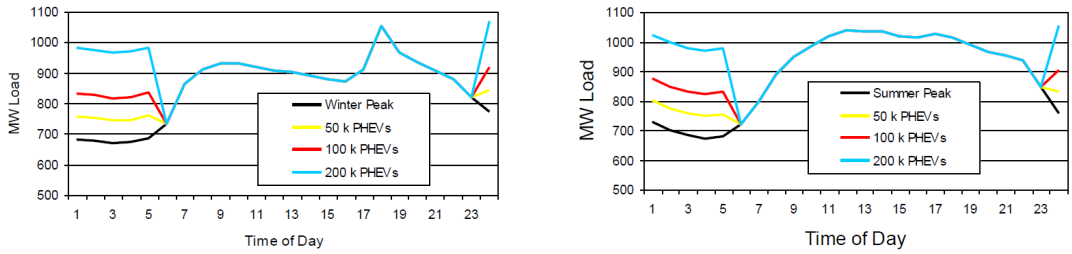

(a) typical winter day (b) typical summer day

Figure 15: Load profiles for delayed nighttime charging scheme [45].

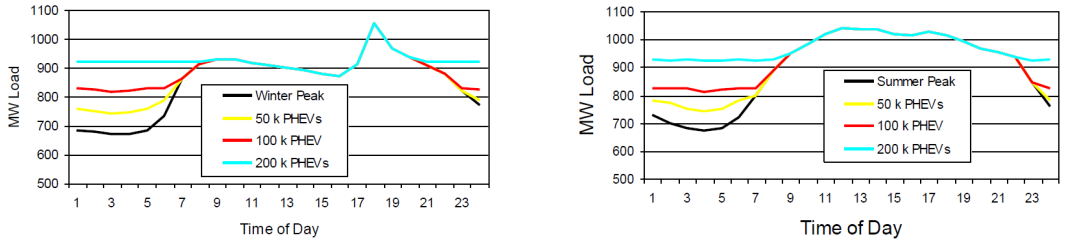

(a) typical winter day (b) typical summer day

Figure 16: Load profiles for optimal charging scheme [45].

Lopes *et al.* investigated the impact of massive integration of EVs in a representative medium-voltage electricity distribution network, installed in residential areas in Portugal, in terms of different integration level of EVs and different charging methods to identify solutions to accommodate a large population of EVs in electricity grids, and try to minimize the need for reinforcements or changes in the existing electrical power infrastructures [53]. They suggested three EV charging management methods: dumb charging, dual tariff policy, and smart charging. In the dumb charging approach, they assumed that EV owners are completely free to plug in their vehicles and start charging whenever they want. According to the authors, it is important to investigate the dumb charging approach since it provides a measure for the assessment of the effectiveness of the other management methods even though it cannot be described as a charging control strategy. The charging control strategy utilizing a dual tariff policy intends to simulate a situation in which electricity is less expensive during some specific hours of a day, and they investigated the effect of electricity price on EV charging. They supposed that the economic incentive is enough to make 25% of EV owners shift their charging to the cheaper period, i.e., off-peak periods, rather than start charging their cars immediately after EVs are connected to the grid. For the smart charging strategy, they considered a hierarchical control structure, which continuously monitors all the elements connected to the grid and determines when EVs start charging. This type of charging management strategy tries to utilize resources available at each moment efficiently. In order to determine the charging period, they proposed an optimization approach that maximizes the integration level of EVs, as follows:

$$\text{maximize} \quad \text{EV integration} \tag{2.1}$$

subject to

$$V_i^{\min} \leq V_i \leq V_i^{\max}, \quad i \in [1,\, l] \tag{2.2a}$$

$$S_j \leq S_j^{\max}, \quad j \in [1,\, m] \tag{2.2b}$$

$$E_{k,\,\Delta t}^{\mathrm{EV}} = E_{k,\,\Delta t}^{\mathrm{EV\ required}}, \quad k \in [1,\, n] \tag{2.2c}$$

where

l	is the number of buses;
m	is the number of branches;
n	is the number of EVs;
V_i	is the voltage at bus i;
$V_i^{\min}$ / $V_i^{\max}$	are the minimum/maximum allowable voltages at bus i;
S_j	is the apparent power flowing at branch j;
$S_j^{\max}$	is the maximum allowable apparent power flow at branch j;
$E_{k,\,\Delta t}^{\mathrm{EV}}$	is the battery energy level of the EV k at the end of the connection period Δt;
$E_{k,\,\Delta t}^{\mathrm{EV\ required}}$	is the required battery energy level for EV k at the end of the connection period Δt.

The optimization is performed iteratively by increasing the number of EVs in a stepwise manner until it violates the constraints imposed on the optimization problem. They performed simulation studies for five different scenarios with the same number of vehicles, as summarized in Table 2. According to the results of power flow analysis in terms of voltage deviations, branches' congestion level, power losses, and load profiles, it was concluded that the grid could handle 10% penetration level of EVs without changes in or reinforcements on the electricity network if a dumb charging approach is used, as shown in Figure 17. Figure 17 also shows that two other approaches – dual tariff policy and smart charging – can be implemented to allow the

Table 2: Scenarios description [53].

Scenario no.	0	1	2	3	4
No. of vehicles	12744	12744	12744	12744	12744
EVs %	0%	5%	10%	14%	52%
Hybrid share	-	70%	40%	30%	10%
Medium EV share	-	15%	30%	35%	45%
Large EV share	-	15%	30%	35%	45%
Energry consumption for the selected day (MWh)	277.1	283.2	294.0	301.7	388.1

integration of higher share of EVs while avoiding capital expenditures by the utility in network reinforcements. The simple dual tariff policy is proved to be more effective than the dumb charging approach, increasing the integration capability of the grid up to 14%. Further, this paper proved that the smart charging approach is the most effective charging strategy in that it could increase the EV deployment capability of the grid to 52% by solving a simple set of rules, i.e., the optimization problem.

While most of the previously published studies related to PHEVs focused on the

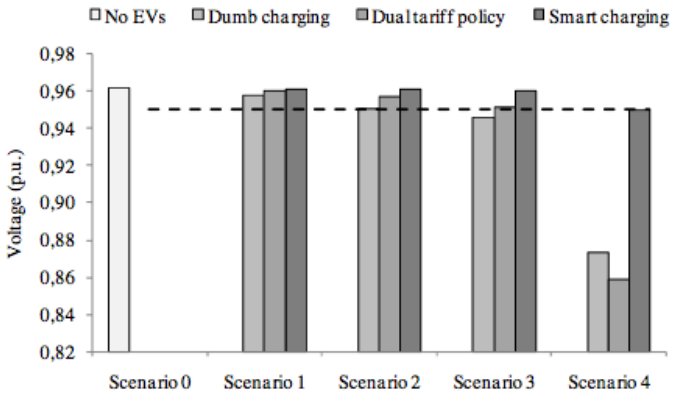

Figure 17: Voltage level for different charging strategies [53].

potential impacts of PHEVs at the generation level, Shao *et al.* examined the adaptability of the residential distribution network to support PHEVs, and evaluated the impact of charging PHEVs on a distribution transformer under two different charging scenarios, that is, normal charging and quick charging strategies [71]. A typical 25 kVA distribution transformer, generally serving four to seven houses in a neighborhood, was considered, and a distribution network having five houses with two PHEVs, which represents the penetration level of about 9%, was evaluated. Without PHEVs, the hourly residential load curve, derived from the RELOAD database, has the peak load of about 14 kW in winter and 13 kW in summer around 6:00 pm, and the distribution transformer is lightly loaded at about 35% on average, i.e., at the highest efficiency, and about 52-57% at the peak (see Figure 18). The normal charging scenario with all PHEVs starting charging at 6:00 pm demonstrates the worst case that all PHEVs come home with the minimum SOC and start charging at the same time, leading to the increase in the maximum transformer load levels by 68% in winter and 52% in summer (Figure 19(a)). If all PHEVs are charged during off-peak hours (10:00 pm to 11:00 am for summer; 9:00 pm to 7:00 am and 11:00 am to 5:00 pm for winter) under the normal charging scenario, new load peaks are created at the start of off-peak hours in both summer and winter load profiles (Figure 19(b)). The new peaks are a little higher than the case without PHEVs, i.e., 58% in winter and

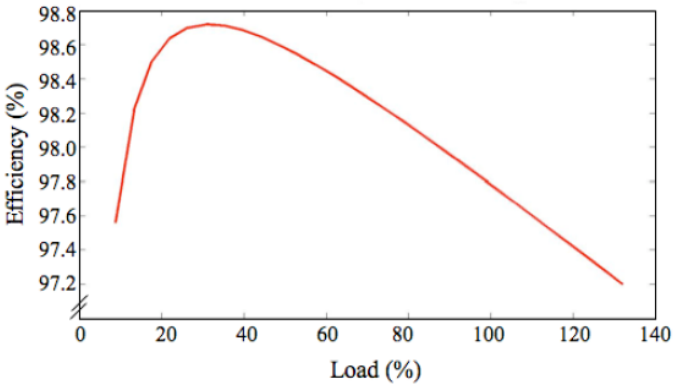

Figure 18: Efficiency of a typical distribution transformer against load [71].

52% in summer, implying that transformer efficiency during off-peak hours is slightly increased since charging PHEVs during off-peak hours will increase transformer loading level close to 35%, which yields the maximum transformer efficiency. The authors also evaluated the quick charging scenarios, in which a PHEV draws power from a 240V/30A outlet. It is illustrated that quick charging starting at 6:00 pm will lead to the transformer overload, i.e., increase in the peak load by 103% in winter and 98% in summer, thus reducing the transformer efficiency by at least 1% (Figure 20(a)). The quick charging during off-peak hours causes a new peak load, a little less than the quick charging starting at 6:00 pm case, but leads to a significant issue on the distribution network (Figure 20(b)). In order to mitigate the adverse effects caused

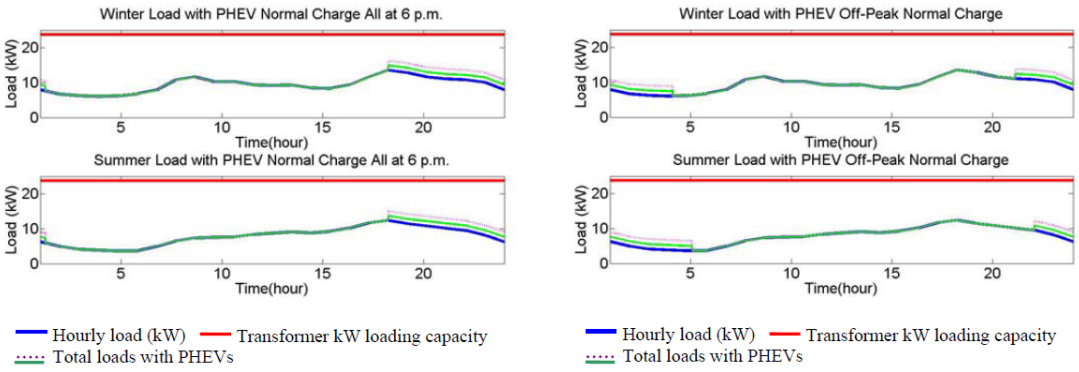

(a) normal charging scheme all at 6:00 pm (b) off-peak normal charging scheme

Figure 19: Load profiles for two charging schemes [71].

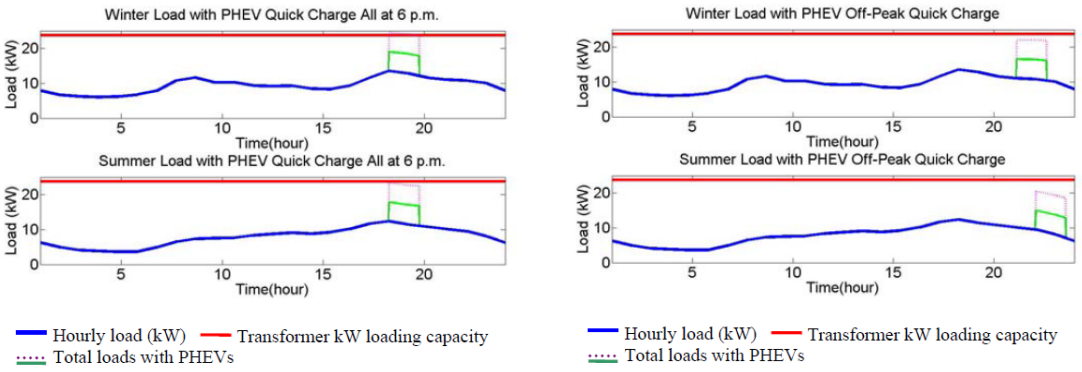

(a) quick charging scheme all at 6:00 pm (b) off-peak quick charging scheme

Figure 20: Load profiles for two quick charging schemes [71].

by a large fleet of PHEVs, the authors proposed demand management, which can be accomplished by 1) staggering PHEV charging time or 2) performing household load control, rather than installing additional transformer capacity. The proposed demand management requires advanced metering infrastructure (AMI), together with a PHEV control unit and remote switches, which controls the On/Off status of PHEV outlets and household loads. The staggered charging time implies that PHEVs are allowed to be charged only when the current load, seen by the distribution transformer, is less than a specified value, e.g., its original peak load. It is shown that the stagger control can reduce the peak load caused by charging PHEV and smooth the load, thus mitigating the additional peak issue, as illustrated in Figure 21, when compared with Figures 19 and 20. For the household load control, non-critical loads (e.g., water heaters or clothes dryers) can be shed or deferred when PHEVs are being charged, and it is shown that the household load control can also alleviate the new peak loads, resulting in peak increase to about 15 kW, which is less than the quick charging scenario without household load management, as shown in Figure 22. In contrast to the staggered charging control, the household load control does not require PHEV owners to wait longer for their vehicles to be charged; however, the household load control requires to be done without the notice of PHEV owners or the utility would

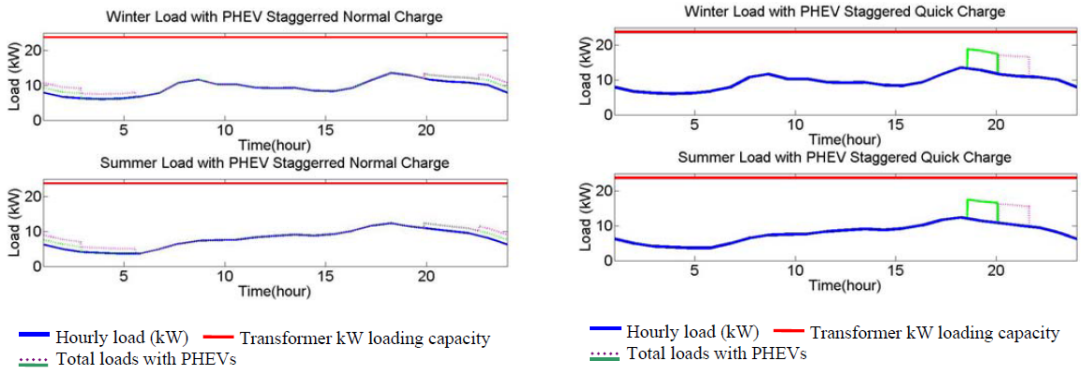

(a) staggered normal charging scheme (b) staggered quick charging scheme

Figure 21: Load profiles for staggered normal/quick charging schemes [71].

provide incentives to PHEV owners who are willing to let their non-critical loads be controlled. This work makes a contribution in the sense that it examined the impact of PHEV charging on a residential distribution network and considered both charging control and household load management to mitigate the impact of PHEVs on the distribution transformer. However, the proposed charging control does not take into account PHEV owners charging preferences, and the impact of only a small number of PHEVs is evaluated. For future research, the authors suggested the exploration of the impact of a large-scale PHEV penetration on electricity infrastructure, esp. at the distribution level.

According to [65], EVs can be considered as active loads, increasing the demand during being charged, and as distributed generators when being discharged, and their impacts on the grid are expected to be significant due to their high energy capacity and mass deployment of EVs in the future. The authors investigated the effects of EV deployment on existing distribution networks in terms of 1) load profile and uncontrolled peak demand, 2) change in voltage levels and violation of statutory limits, and 3) voltage imbalance, the last two of which are out of the scope of this thesis and will not be described here. The authors also considered three charging

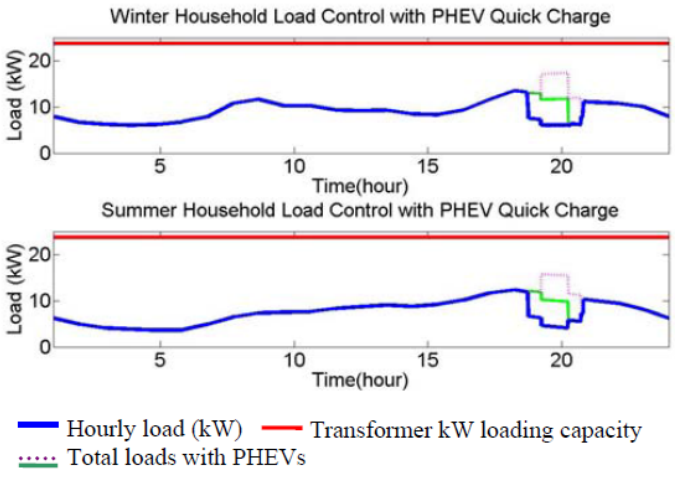

Figure 22: Household load control with PHEV quick charging scheme [71].

scenarios, i.e., uncontrolled charging, off-peak charging, and phased charging, which is considered smart charging, for three different penetration levels of EVs: 10%, 20%, and 30%. For the uncontrolled charging, EV owners are assumed to start charging their cars as soon as they get home from work, at approximately 6:00 pm, resulting in an even larger peak at the early evening on a winter day, as shown in Figure 23(a). The off-peak charging assumed that EVs charging are scheduled to start charging at 1:00 am and remain until 7:00 am, and Figure 23(b) shows the improvement to the load curve compared with the uncontrolled charging case even though there is an additional peak after midnight and a dip at around 7:00 am. The phased charging leads to a more uniform load profile, as shown in Figure 23(c), by splitting the total charging load into four schedules. The same scenarios with the three penetration

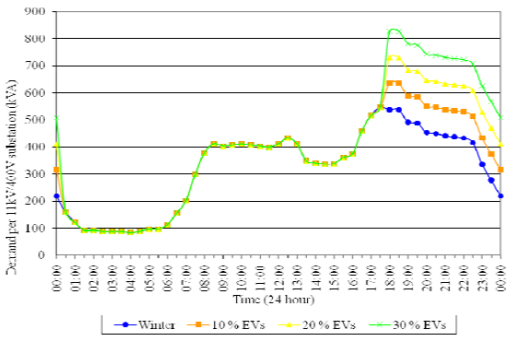

(a) uncontrolled charging for a typical winter day

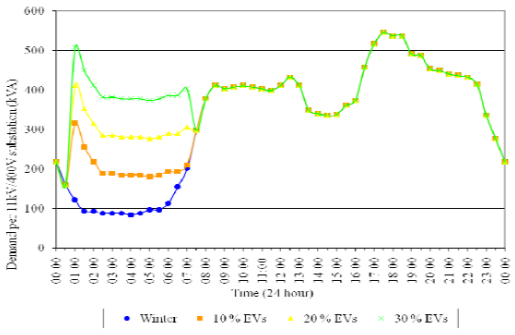

(b) off-peak charging for a typical winter day

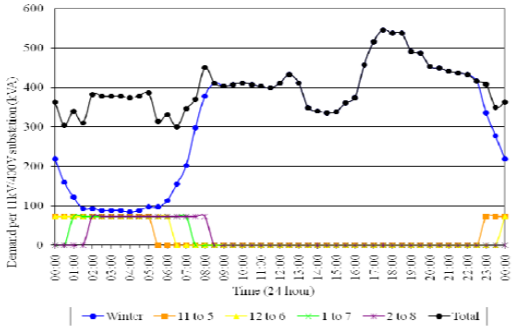

(c) phased charging for a typical winter day

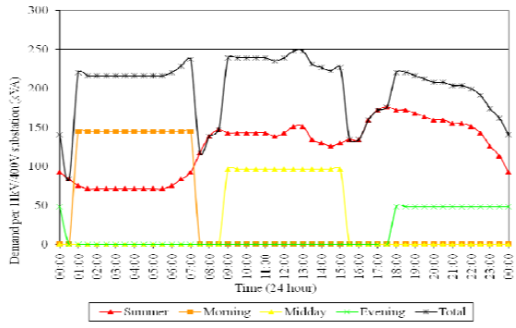

(d) three charging scenarios for a typical summer day

Figure 23: Demand per 11kV/400V substation for typical winter/summer days [65].

level were applied for a typical summer day, and it was shown that the charging scheduling requirements for summer are somewhat different from ones for winter, as charging during the early morning hours would result in a peak demand at this period as shown in Figure 23(d). The investigation presented in this paper showed that the deployment of large-scale EVs could result in mismatching between supply and demand and violation of statutory voltage limits and, under certain operating conditions, they may also lead to power quality problems and voltage imbalance. It was concluded that *a "smart" charging control* or *incentives for EV owners* would need to be introduced to minimize or even eliminate the effects of EVs on the network, i.e., distribute EV loads throughout the day, and avoid additional peak demands, and EVs could be designed to provide ancillary services with appropriate control and communication within the "smart grid" concept.

Shao *et al.* presented a demand response model for residential customers with the presence of PHEVs to assess the impacts of different time of use (TOU) pricing schemes on distribution feeder load shapes [70]. In order to generate PHEV charging demand profiles, the authors considered two charging strategies, i.e., normal charging and quick charging, and modeled PHEV arrival times (or plug-in times) using a normal probability distribution function with mean at 6:00 pm and one hour standard deviation. The normal charging is defined as the standard PHEV charging from the 110V/15A outlet, and the quick charging is assumed to be accomplished by charging from a 240V/30A outlet. Figures 24 illustrates the aggregated PHEV charging loads using both normal and quick charging strategies for the low penetration of 20% and the high penetration of 40%, respectively. The total household load profiles with PHEVs for a typical summer and winter days are depicted in Figures 25, and it can be seen that charging PHEVs significantly aggravates peak loads since, compared with flat rates, TOU rates provide more incentives for customers to shift their power demand to the less expensive hours, i.e., off-peak hours. The authors also evaluated

the impact of TOU rates on load shapes by considering two TOU pricing policies from Baltimore Gas & Electricity (BG&E) and Dominion Virginia Power (DOM). Figure 26 illustrates the TOU rates, which are considered in this paper. The authors classified nine residential customers' load types into three groups: critical, interruptible, and deferrable loads, as summarized in Table 3. Based on the total household load profiles with PHEV charging loads and the proposed DR strategies, the impacts of different pricing structures on distribution feeder load shapes were evaluated. In the summer low penetration of PHEVs (Figure 27), it can be seen that the demand response can help lower the system peak in both normal and quick charging strategies. In the high penetration scenario (Figure 28), similar results are observed. For the winter low penetration scenario (Figure 29), the demand response can help lower the system peak as in the summer load penetration scenario. However, for the high

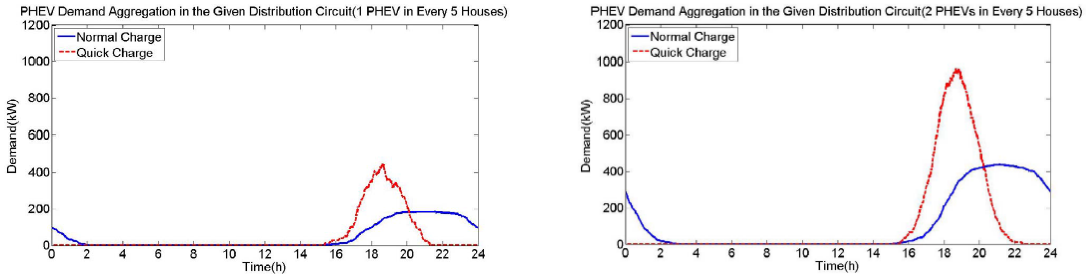

(a) 156 PHEVs (b) 312 PHEVs

Figure 24: Aggregated charging profiles using normal and quick charge strategies [70].

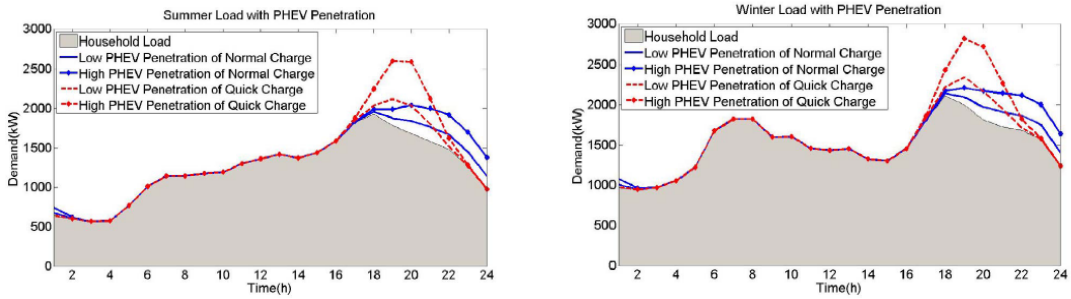

(a) summer month (b) winter month

Figure 25: Household load profiles with PHEVs [70].

Table 3: Demand Response (DR) strategy by load type [70].

Priority	Type	DR strategy
Critical loads	Refrigerator, freezer, cooking, lighting	These loads will not be shifted or shed.
Deferrable loads	Water heating, clothes drying, others, PHEV	Shut down the equipment when the price is higher than a pre-determined value, the load will be shifted to the less-expensive hours.
Interruptible loads	Space cooling/heating	From 9 am to 5 pm: turn off; from 5 pm to 9 am: adjust by 10 °F and resume after peak hours
	Optional lighting (50%)	Turn off 50% of the lighting loads when the price is higher than a pre-determined value.

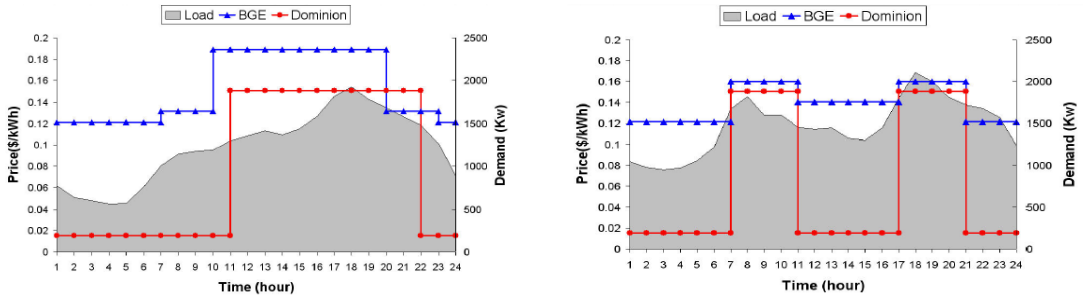

(a) summer month (b) winter month

Figure 26: TOU rates from the chosen utilities [70].

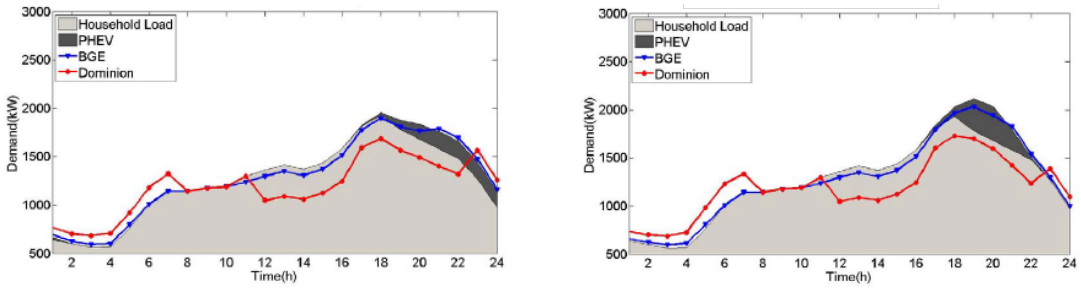

(a) normal charging (b) quick charging

Figure 27: Summer load profiles with low PHEV penetration [70].

penetration scenario with the normal charging strategy, DOM's winter TOU pricing scheme introduces a new peak (see Figure 30). The authors pointed out that the design of TOU rates is important in terms of selecting the appropriate peak/off-peak price levels and periods. It is, however, claimed that if the TOU rate for peak hours is too high, more customers are willing to shift their loads to off-peak hours, thereby creating additional peak loads. In this paper, the authors presented a demand

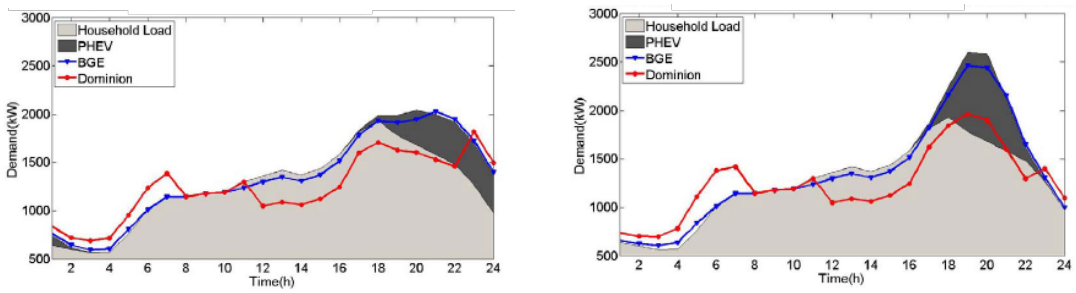

(a) normal charging (b) quick charging

Figure 28: Summer load profiles with high PHEV penetration [70].

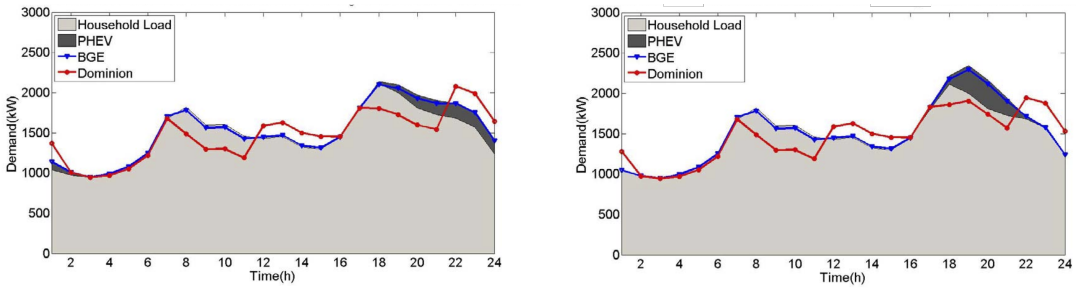

(a) normal charging (b) quick charging

Figure 29: Winter load profiles with low PHEV penetration [70].

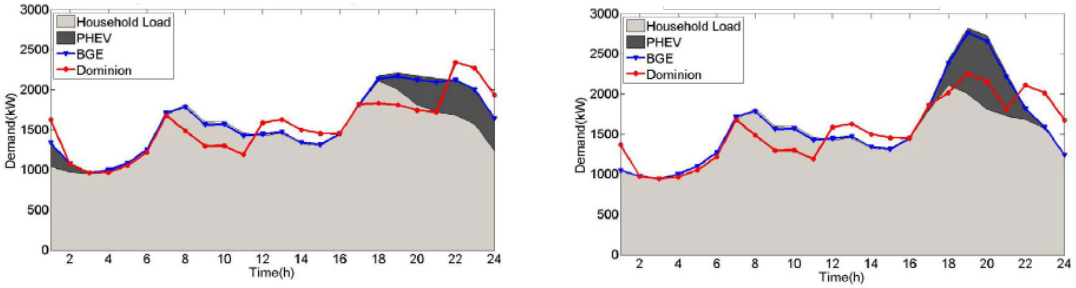

(a) normal charging (b) quick charging

Figure 30: Winter load profiles with high PHEV penetration [70].

response model and evaluated the effect of time-of-use rates on PHEV charging and system load profiles, but did not provide a specific strategy for setting the electricity price for PHEV charging. Moreover, even though the authors claimed the importance of TOU rate design for demand response (DR) and PHEV charging control, TOU pricing schemes does not seem to be effective compared with other smart PHEV charging control strategies in terms of peak loads mitigation.

Lopes *et al.* presented a conceptual framework for successful integration of electric vehicles into electric power systems, which considered two different domains: the grid technical management and the electricity market operation [52]. The authors claimed that the technical management of a large-scale deployment of EVs will require a *combination of a centralized hierarchical management and control structure and a local control located at the EV grid interface* since there will be issues, such as managing branches' congestion levels or enabling EVs to participate in the electricity markets, that cannot be solved by the simple use of smart EV grid interfacing devices, and will require a higher control level, i.e., a hierarchical, coordinated management and control structure. The maximum number of EVs that could be safely integrated into the grid was evaluated without any kind of charging control of EVs, meaning that EV owners are completely free to connect and charge their vehicles after parking, and the charging starts automatically when EVs plug in and lasts for the next few hours. They showed that the distribution network can handle up to 10% EV penetration, of which power consumption and load profile are shown in Figure 31, respectively, without changes in the usual electricity grid operation and planning procedures, indicating that grid restrictions may limit the growth of EV penetration, if no additional measures are adopted. Additionally, the increase in load consumption at peak hours, due to the presence of EVs, will require generation levels to increase, leading to a subsequent increase on electricity prices. The authors indicated that different approaches need to be adopted to deal with this problem, allowing a higher level of integration of

EVs while avoiding capital expenditures by the utility in network reinforcements. By analyzing the impacts of a large population of EVs on the distribution network, they realized that grid restrictions may limit the growth of EV penetration if there is no changes in the usual electricity grid operation and planning procedures, and, in order to allow a higher share of EV integration without capital expenditures in network reinforcements, the authors proposed and tested two solutions to deal with this problem: a simple dual tariff system and a more complex approach, based on a smart charging mechanism, to be performed by the distribution system operator (DSO). The dual tariff policy intends to simulate a situation where electricity is cheaper during some specific hours of the day. The aggregator might implement this approach by making specific dual tariff contracts with EV owners, who are willing to take advantage of cheaper electricity price periods, similarly to what already happens between electricity traders and their clients. On the other hand, the smart charging algorithm determines the amount of EV load that needs to be shifted for the safe operation of the distribution network by iteratively disconnecting a small percentage of EVs, like 2% or 5%, to reduce EV charging load and giving priority to EVs that are disconnected first from the grid when enough power for battery charging is available. The EV load profiles obtained with the two proposed algorithms during one entire

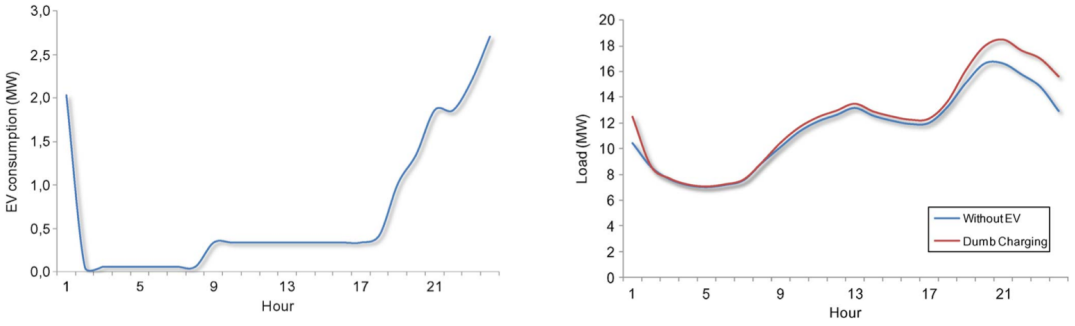

(a) EV power consumption

(b) load profile

Figure 31: EV power consumption and load profiles for the dumb charging with 10% penetration of EVs [52]

day are presented in Figure 32(a), showing that the allowable share of EVs is 14% with the dual tariff policy and 52% with the smart charging. The smart charging method provides better results by making the load distribution along the day more uniform, consequently reducing the grid's peak demand. The load profiles for 52% of EVs, i.e., the maximum percentage of conventional vehicles replaced by EVs without any reinforcement of the grid evaluated in this paper, with the two different charging strategies, compared with the case without EVs and the dumb charging approach – without charging control – are presented in Figure 32(b). With the dumb charging approach, the load in the peak hour increase by 85%, from the scenario without EVs to the scenario with 52% penetration of EVs, whereas with the dual tariff policy only by 11%. The conclusion of this work is that the *adoption of advanced centralized EV charging control strategies* will allow the integration of a larger number of EVs in the grid without the need of grid reinforcements.

In [73], the authors identified the relationship between feeder power losses, load factor, and load variance in the context of coordinated charging of PHEVs, and formulated objective functions for coordinated PHEV charging, based on load factor and variance, which in effect minimize system losses and improve voltage deviation.

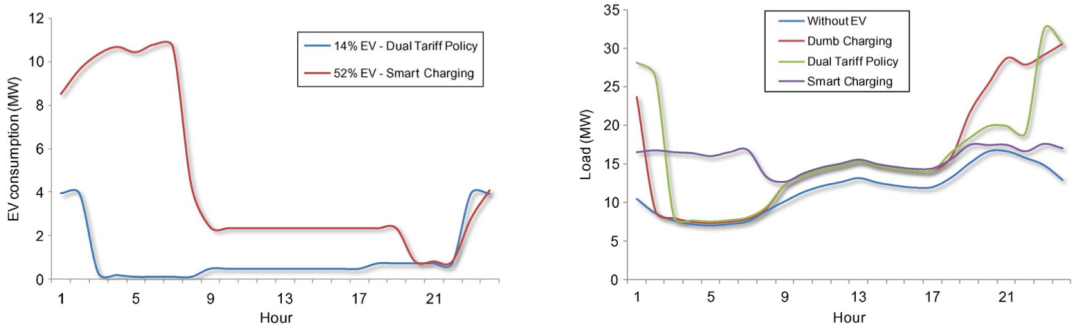

(a) EV power consumption for the dual tariff policy and for the smart charging

(b) load profile for the three charging strategies with 52% of EVs

Figure 32: EV power consumption and load profiles for different charging strategies [52].

According to the paper, the relationship between losses and load factor is that minimizing losses maximizes load factor since the maximum losses and the load factor are given by

$$\text{losses}_{\max} = kI_{\max}^2 \quad \text{and} \quad \text{load factor} = \frac{I_{\text{avg}}}{I_{\max}} \tag{2.3}$$

where k is a positive constant, $I_{\max}$, the maximum load current, and I_{avg}, the average load current, respectively. Also, they claimed that, since the system current at a specific time, I_t, and the load variance seen by the substation, σ_I^2, are related to each other as

$$\mu_{I^2} = \mu_I^2 + \sigma_I^2 \tag{2.4}$$

and μ_i is constant, minimizing the load variance, σ_I^2, minimizes the losses, $\text{losses}_{\text{total}} = \mu_{I^2} R$. Finally, it was argued that, since the load factor is maximized when $I_{\text{avg}} = I_{\max}$ from Equation (2.3), maximizing the load factor is equivalent to minimizing the load variance σ_I^2 according to Equation (2.4). Base upon the analysis results for the relationship between feeder power losses, load factor, and load variance, they formulated three optimization objectives for coordinated PHEV charging: minimizing losses, maximizing load factor, and minimizing load variance. They performed simulations on the proposed objective functions with two test systems, and compared their average losses and PHEV load profiles for different penetration levels of PHEVs. Load profiles for the different charging algorithms are illustrated in Figure 33. The authors showed through simulation studies that the uncoordinated charging significantly adds to the peak load in all cases, and minimizing the load variance produces almost same load profiles as minimizing power losses as they proved analytically. However, maximizing the load factor does not minimize the load variance or power losses, and shows different load profiles. The authors concluded that minimizing losses maximizes the load factor and minimizing load variance minimizes losses exactly under the assumption that the distribution system of interest is a single feeder from the substation

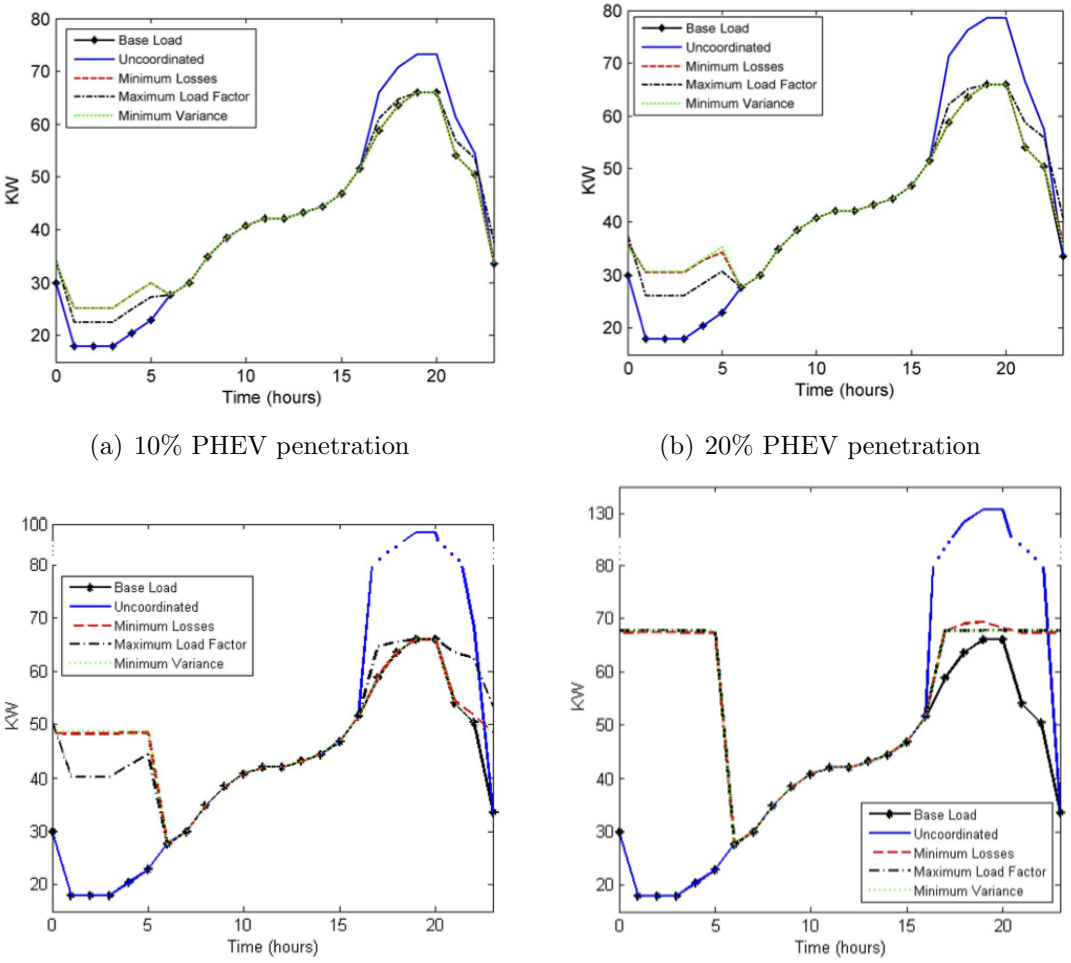

(a) 10% PHEV penetration

(b) 20% PHEV penetration

(c) 50% PHEV penetration

(d) 100% PHEV penetration

Figure 33: Load profiles for different charging algorithms [73].

with all loads connected at the end. It was also indicated that the load variance minimization is more versatile than minimizing losses since it produces result in a fraction of time, important for real-time dispatch of PHEVs.

The paper by Deilami *et al.* proposed a real-time load management algorithm to coordinate multiple PEVs charging while mitigating its impact on the reliability, security, and performance of the distribution grid [8]. Since conventional optimization techniques such as genetic algorithm (GA) are not computationally efficient for real-time applications with short time steps (e.g., 5 minutes), the proposed coordination algorithm employs the maximum sensitivities selection (MSS) optimization approach for real-time charging coordination, in which the sensitivities of system losses due to each node with PEVs are computed and nodes with lowest sensitivities are first allocated for charging to minimize the impacts of PEV charging on system losses. The proposed PEV charging coordination problem is based on real-time cost minimization, and improves voltage profile while considering charging time zones designated by PEV owners. The objective function as defined by

$$\text{minimize } F_{\text{cost}} = \sum_{\Delta t} K_E P_{\Delta t}^{\text{total loss}} + \sum_{\Delta t} K_{\Delta t,G} P_{\Delta t}^{\text{total demand}}, \tag{2.5}$$

where Δt is the time interval, K_E, the cost per MWh of losses, and $K_{\Delta t,G}$, the cost per MWh of generation at time interval Δt based on the variable price of purchasing or producing the energy, can be interpreted as the minimization of total cost of purchasing or producing the energy for charging PEVs (the first term) plus the associated grid energy losses (the second term). The cost of purchasing or producing the energy for charging PEVs can be minimized by defining time zones to minimize a utility's generation costs during on-peak hours, and there are three different charging time zones considered in this work: 18:00 to 22:00, 22:00 to 01:00, and 01:00 to 08:00. The optimization problem is solved by minimizing system losses at each time interval and incorporating time-varying energy prices along with PEV owners preferred charging time zones. The proposed coordination algorithm is a centralized

charging control scheme in that it decides which PEVs will be charged at what time, thereby PEV charging control is scheduled automatically without any interactions with PEV owners except for the indication of their preferred time zones for charging. The contribution of this paper is that it proposed an algorithm, which is solved by minimizing the cost for purchasing or producing electricity while maintaining voltage profiles within generation limits, capable of real-time coordination of randomly arriving and departing PEVs based on PEV owners' charging time zone priorities. In addition, it demonstrated that the proposed pricing and time-zone priority scheme for PEV charging is feasible and works effectively with the charging coordination, and showed that the smart load management is beneficial in reducing overall system overloads and power peaks. However, in order to apply the MSS technique, the proposed algorithm is required to perform power flow analysis first, which needs a sophisticated power flow model with high computational costs and might not be run in real time (e.g., every 5 minute) as the complexity of the distribution grid to be coordinated increases.

A possible solution for EV smart charging with the consideration of EVs as controllable loads was investigated under electricity market in [40]. However, even though EV smart charging is considered within electricity market, the functionality of the aggregator of EVs for providing regulation services is not discussed in this paper. In the paper, centralized control architecture was presumed, in which an aggregator directly generates charging profiles of all EVs and coordinates their charging/discharging operations. It was assumed that the aggregator does not have sufficiently large market share to affect electricity price so that most of charging takes place in the nighttime when given less expensive electricity prices. It was also assumed that the following data are available for the aggregator to generate charging profiles: predicted electricity price, future driving pattern, energy requirement during every trip, and EV status

data such as state-of-charge (SOC) of EV battery. The authors presented a mathematical formulation and a dynamic programming based algorithm for optimizing EV charging, given electricity prices and driving patterns. The total cost, f_0^U, which is to be minimized, is given by the cost of the final step, $f_N(x_N)$, plus the cost for all other steps, $v_k(x_k,\ u_k,\ k)$:

$$f_0^U(x_0) = f_N(x_N) + \sum_{k=1}^{N-1} v_k(x_k,\, u_k,\, k). \tag{2.6}$$

The optimal control strategy, $u^* = \{u_0^*,\ u_1^*,\ \ldots,\ u_{N-1}^*\}$, can be obtained using a classic dynamic programming formulation. Since the charging profiles is to be generated so as to satisfy EV owners charging requirements, i.e., the battery is fully charged before the first trip of the following morning, the cost of the final step $f_N(x_N)$ should be defined as $f_N(x_N) = 0$. The state transition models for the SOC of the battery, x_k, are given by

$$x_{k+m} = x_k - \frac{\sum_{j=1}^{m} P_{dr}(j)\Delta t}{E_{max}} \times 100\% \tag{2.7}$$

for driving mode and

$$x_{k+1} = x_k + \eta_k u_k \frac{P_{max-plug}\Delta t}{E_{max}} \times 100\% \tag{2.8}$$

for plug-in charging mode, where Δt is the time interval, $P_{dr}(j)$ denotes power required for driving, $P_{max-plug}$ is the maximum charging power, η_k, charging efficiency parameter, and u_k, charging control strategy at time k, respectively. It was shown through a case study that the smart charging strategy without provision of regulation service reduces daily electricity costs for driving, and, with the proposed smart charging, EVs are recharged during off-peak hours, where electricity price is the lowest. For future research, the authors suggested that the proposed optimization model needs to be extended to account for the provision of regulation service, different types of electric vehicles, and various driving patterns.

In [27], Hemphill presented a methodology, utilizing a series of tools, to assess the impact of PEV charging on the distribution network of a New South Wales metropolitan area in Australia. The tools, developed in this work, are 1) a modeling tool for charging energy requirements and charging availability of PEVs, 2) load profile generation tool for various charging options, and 3) cost estimation tool for charging options. The modeling tool for PEV charging energy requirements consists of three key tasks: calculating PEV load, determining PEV charging availability times, and modeling travel distances. First, the author used a simple battery charging model to calculate the time required for charging, as given by

$$T_c = \frac{dC}{r\eta P_g} \tag{2.9}$$

where d is the traveling distance, C is the battery pack capacity, r is the driving range of a PEV, η is the charging efficiency, and P_g is the power supplied by the grid. In addition, they modeled PEV availability for charging as a function of the average number of weekday travelers on roads, f_k, by combining two gamma distribution functions to characterize the data sets with time intervals 5:00 am to 2:00 pm and 3:00 pm to 12:00 am, given by

$$g(t) = \frac{k_1}{\beta_1^{\alpha_1}\Gamma(\alpha_1)} t^{\alpha_1 - 1} e^{-t/\beta_1} + \frac{k_2}{\beta_2^{\alpha_2}\Gamma(\alpha_2)} t^{\alpha_2 - 1} e^{-t/\beta_2} \tag{2.10}$$

where

$$k_1 = \frac{\sum_{k=11}^{29}(f_{k+1} - f_k)}{\sum_{k=11}^{29}(f_{k+1} - f_k) + \sum_{k=31}^{49}(f_{k+1} - f_k)} \tag{2.11a}$$

$$k_2 = 1 - k_1 \tag{2.11b}$$

and modeled PEVs' traveling distance using a log-normal distribution function,

$$f(x) = \begin{cases} \frac{1}{\sqrt{2\pi}\sigma x} e^{-[\ln(x) - \mu^2]/2\sigma^2}, & x > 0 \\ 0, & x \leq 0 \end{cases} \tag{2.12}$$

Table 4: Time of use pricing strategy [27].

Period	Time	Price	Ratio
Peak	2:00 pm to 8:00 pm	40.1 ¢/kWh	13.1%
Shoulder	8:00 pm to 10:00 pm	16.4 ¢/kWh	32.1%
Off-peak	10:00 pm to 7:00 am	9.6 ¢/kWh	54.8%

where $E(X) = e^{\mu+\frac{1}{2}\sigma^2}$ and $MODE(X) = e^{\mu-\sigma^2}$, respectively. To generate and evaluate load profiles of various charging options, an unmanaged PEV charging, a time of use metering, and two smart charging control strategies were taken into account. Similarly to other studies, the unmanaged charging allows PEV owners to start charging right after they plug in their vehicles to the outlet, i.e., the plug-in times are sampled from $g(t)$ in Equation (2.10), and PEVs' initial SOCs are calculated based on the samples from the distribution $f(t)$ in Equation (2.12). A time of use metering strategy was developed, based upon the pricing strategy, as summarized in Table 4, which assumes that PEV customers would respond to time of use pricing and start charging at the earliest possible time to gain the price incentive. For smart charging control, two scenarios are considered: 1) PEVs with the lowest SOC first for Level 1 charging (230V/15A) and 2) PEVs with the highest SOC first for Level 2 charging (230V/32A). Figure 34(a) shows PEV load profiles for various charging options, superimposed on a historical load profile, for the penetration level of 80% and Level 1 charging. It is seen that the time of use metering introduces significant new daily peak loads by encouraging PEV owners to delay charging until the shoulder or off-peak periods starts and allowing a large number of PEVs to start charging simultaneously. The results also demonstrated that the smart charging strategies prevent PEV loads from contributing to the peak demand for all penetration levels of PEVs with Level

1 charging and support penetration levels up to 80% with Level 2 charging. In addition, the author claimed that the lower SOC first is the optimal strategy for Level 1 charging and the highest SOC first for Level 2 charging. Figure 34(b) shows the peak loading for various charging schemes against the increasing level of PEV penetration for Level 1 charging. The unmanaged PEV charging causes the rating of substation to be exceeded for any penetration level, and the time of use metering is the worst for all penetration levels. Either of the smart control strategies proposed in this study can potentially avoid additional peak load due to PEV charging demand. The case studies confirmed that a relatively small penetration level of PEVs will require investment in the distribution network and that unmanaged PEV charging will potentially have a drastic impact of peak demand on distribution assets. Contrary to the conclusion in [70], it was demonstrated that a time of use metering strategy is not likely to be suitable for the management of PEV charging demand since it introduces additional peaks to demand profiles at the penetration level greater than 10%. Also, it was revealed that a smart PEV demand control strategy can be more effective for preventing PEV load from contributing to the peak demand of distribution assets,

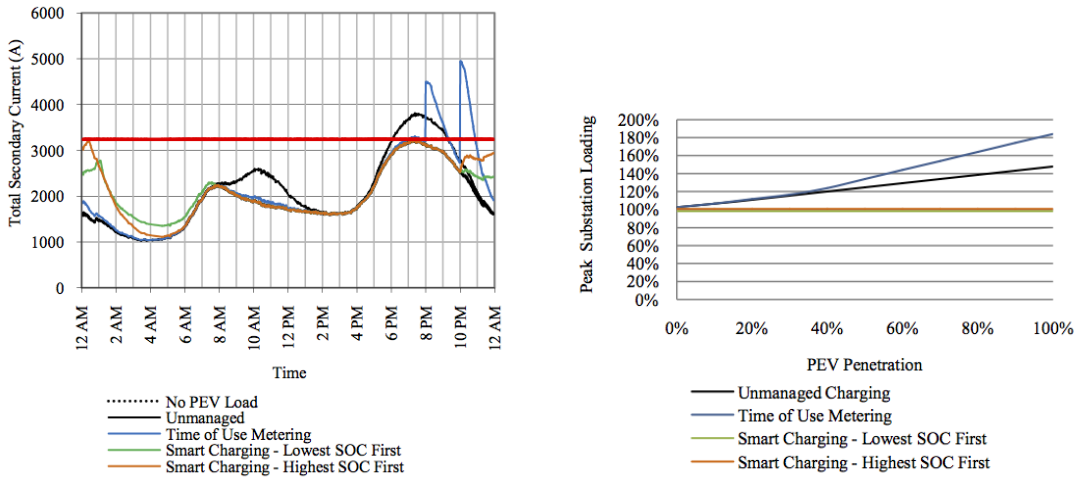

(a) load profiles

(b) peak substation loading

Figure 34: Load profiles and peak substation loading for 80% PEV penetration with Level 1 charging [27].

compared with the time of use metering strategy.

In this subsection, literature on coordinated/centralized EV charging strategies was reviewed. Most studies revealed that a large population of EVs has a significant impact on power systems and their charging must be optimally dispatched by implementing new pricing structures or technical means in order to accommodate a large number of EVs and minimize their impacts on the grid. Without special EV pricing structures or charging control, a large number of EVs could raise system peaks, depending upon the timing of the system peak and the as-yet-known charging behaviors of EV owners, and degrade the system stability and reliability. Various papers proposed EV charging control schemes such as blind control, where a utility sends a signal to an individual vehicle or a group of vehicles to allow to start charging, time-of-use (TOU), i.e., different rates for different charging periods, smart charging control, where a hierarchical control structure continuously monitors all the elements connected to the grid and determines when EVs start charging, and so forth. Several optimization problems were also proposed to determine the timing of EV charging in terms of minimizing load variance or voltage deviation, maximizing load factor, or maximizing the number of EVs that could be accommodated in the grid. Furthermore, a few papers claimed that a large fleet of EVs could possibly replace a fraction of conventional low-capacity generation, used for periods of extreme demand or system emergencies, and they are well suited for short-term ancillary services such as regulation and spinning reserve with appropriate control and communication within the smart grid concept for regulating the voltage in distribution networks and even compensating fluctuating renewable energy generation. The impact assessment of EVs with vehicle-to-grid (V2G) capability, using EVs as load leveling devices, and the investigation of the potential benefits of V2G technology were also suggested.

2.1.2 Decentralized EV Charging Control Strategies

A few studies have been conducted on decentralized EV charging control, while EV charging schemes based on a centralized structure have been consistently proposed since the mid 1990s. This subsection will review several approaches for controlling EV charging with a decentralized control structure, and address their technical limitations, which will lead to the research statement of this thesis.

In [55], the authors argued that the implementation of centralized charging control for large populations of PEVs is computationally intractable and it may also be impractical because PEV owners might not be willing to allow their utility to directly control their vehicles charging. Therefore, proposed was a decentralized charging control algorithm, in which each PEV implements a local optimal charging control, resulting in a valley-filling load curve aggregately. According to the Nash Certainty Equivalence (NCE) principle, "a collection of each PEV's local charging profile is a Nash equilibrium (NE), if each charging profile is optimal with respect to one commonly observed charging profile, and the average of local optimal charging profiles is equal to the common charging profile" [55]. Furthermore, for homogeneous PEVs, the common charging profile, i.e., the average of all PEVs charging profiles, turns out to flatten out a load profile by filling the valley(s) of the profile. The authors modeled the PEV charging dynamics as follows:

$$x_{t+1}^n = x_t^n + \frac{\alpha^n}{\beta^n} u_t^n, \qquad t = T_0, \ldots, T-1 \tag{2.13}$$

with an initial state-of-charge (SOC) of x_0^n, where $x_t^n \in [0,\, 1]$ is the SOC of the vehicle n at time t, α^n, the charging efficiency, β^n, the battery size, and $u_t^n \geq 0$, the charging rate at time t. They assumed that a PEV is fully charged at the end of the charging interval, i.e. $x_T^n = 1$, and defined the set of feasible full charging controls,

$$\mathcal{U}^n \triangleq \left\{ u^n \equiv \left(u_{T_0}^n, \ldots, u_{T-1}^n \right) ;\ \text{s.t. } u_t^n \geq 0,\, x_T^n = 1 \right\}. \tag{2.14}$$

The cost function of the proposed decentralized charging control problem is formulated as

$$J^n(\mathbf{u}) \triangleq \sum_{t=T_0}^{T-1} \left\{ p_t u_t^n + \delta \left(u_t^n - \text{avg}(\mathbf{u}_t) \right)^2 \right\}, \tag{2.15}$$

where δ is a non-negative constant, $\text{avg}(\mathbf{u}_t) = \frac{1}{N} \sum_{n=1}^{N} u_t^n$, and the price $p_t \equiv p\left(d_t + N\text{avg}(\mathbf{u}_t)\right)$ denotes the electricity price at time instant t, which is dependent on the non-PEV demand, d_t, and the total PEV power demand, $N\text{avg}(\mathbf{u}_t)$. It can be implied from Equation (2.15) that each PEV's optimal charging strategy is trying to achieve a trade-off between the total electricity cost for charging, pu^n, and the tracking cost incurred in deviating from the average charging profile of the PEV population, $(u^n - \text{avg}(\mathbf{u}))^2$, i.e., a Nash equilibrium. The NCE-based decentralized charging algorithm is implemented through a charging negotiation procedure, which takes place at some time prior to the actual charging period, as follows [55]:

(S1) The utility broadcasts the prediction of non-PEV base demand d to all the PEV agents.

(S2) Each of the PEVs proposes a charging control minimizing its charging cost with respect to a common aggregate PEV demand broadcast by the utility.

(S3) The utility collects all the individual optimal charging strategies proposed in (S2), and updates the aggregate PEV demand corresponding to the proposed charging strategies. This updated aggregate PEV demand is rebroadcast to all of the PEVs.

(S4) Repeat (S2) and (S3) until the optimal strategies proposed by the PEVs no longer change.

In order to investigate the performance of the proposed algorithm, a number of illustrative examples are simulated with a homogeneous PEV population of 1×10^7, i.e., 10% of all the vehicles in the Midwest Independent System Operator (MISO) region, and a heterogeneous population of two groups, of which size is 0.5×10^7 for each with

the same values for all charging parameters except for battery size. In Figure 35(a), it is shown that, if a PEV minimizes its charging cost regardless of other PEVs, the iterative scheduling procedure is unlikely to converge, and that, by penalizing PEVs for deviating from the average behavior of all other PEVs, the scheduling process is guaranteed to converge to a unique Nash equilibrium. Figure 35(b) and Figure 35(c) show the iterations of optimal charging profiles with a tracking-cost constant $\delta = 0.007$ and different sets of initial charging controls – the one with zero initial charging controls and the other with non-zero initial charging controls – for the homogenous case, and Figure 35(d) illustrates the convergence of charging controls for the heterogeneous case, respectively. It can be seen from these figures that the negotiation procedure converges to the unique Nash equilibrium, i.e., filling the overnight

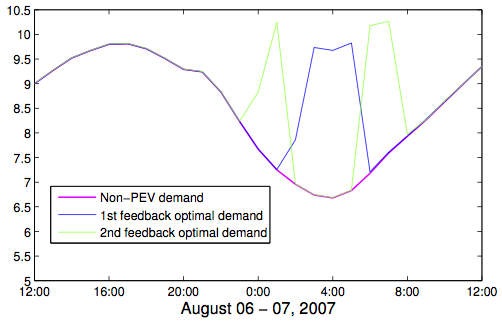

(a) optimal charging strategy for homogeneous PEVs with zero tracking cost, $\delta = 0$

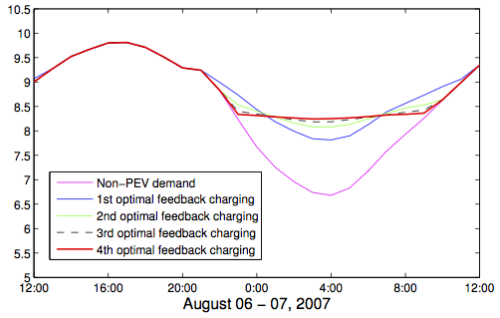

(b) converging to a Nash equilibrium (red) for homogeneous PEVs with $u_0 = 0$ and $\delta = 0.007$

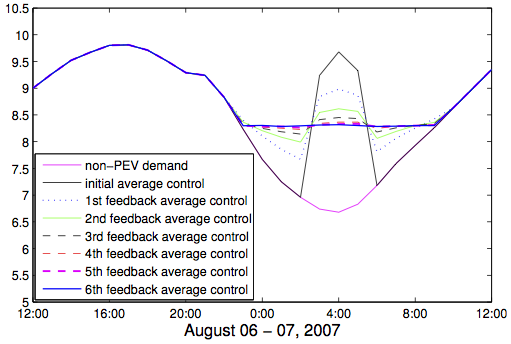

(c) converging to a Nash equilibrium (blue) for homogeneous PEVs with $u_0 \neq 0$ and $\delta = 0.007$

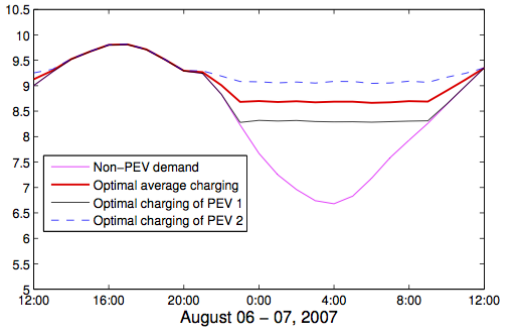

(d) converged Nash equilibrium (red) for heterogeneous PEVs with $\delta = 0.007$

Figure 35: Optimal charging strategies using Nash Certainty Equivalence [55].

demand valley, in a finite number of negotiation iterations, no mater whether or not initial charging controls are zero, or regardless of the homogeneity of the PEV population. For the homogeneous case, the converged solution optimally fills the valley, all PEVs will adopt an identical charging strategy, and the tracking cost associated with deviating from the average will be zero. On the other hand, if the PEV population is heterogeneous, the solution is a nearly valley-filling, and charging profiles for PEVs will be similar, but not identical, thereby the tracking cost will be small but not zero. It can be seen that the proposed decentralized charging control algorithm successfully achieves the social optimality, i.e., valley-filling, as the authors argued, in a decentralized manner. But the limitations of the proposed algorithm are, as the authors indicated, that the negotiation procedure must occur ahead of the actual charging period and that it is based on predictions of non-EV demand and of charging requirements of the PEV population. The conditions in negotiating charging profiles must differ from the actual charging conditions, and the non-EV demand will never exactly match the prediction. Moreover, there will be some mismatch between the PEVs participating in the prior negotiations and those being actually charged.

Ma *et al.* elaborated their decentralized optimization algorithm for PEV charging in [55], formulated as a class of finite-horizon, non-cooperative, dynamic games, to find the PEV charging profile that minimizes individual charging costs, and suggested and proved a sufficient condition for the uniqueness and convergence of its solution that guarantees the social optimality, so called "valley-filling" [54]. In this formulation, PEVs are coupled through a common price signal, determined by the average charging profiles of all PEVs, through which each PEV effectively interacts with the rest of PEVs in the population. The authors claimed that, "as the population size increases, the influence of each individual PEV on the average charging profile becomes negligible." The remaining part of this paragraph quotes Ma *et al.*'s work in [55] frequently, including the explanation of the problem formulation and a theorem

for a sufficient condition on the uniqueness and convergence of Nash equilibrium. They used the same charging dynamics model as in Equation (2.13), and defined the feasible charging control u^n for PEV n as:

$$\mathcal{U}^n \triangleq \left\{ u^n \equiv \left(u^n_{T_0}, \ldots, u^n_{T-1} \right) ; \text{ s.t. } u^n_t \geq 0,\, x^n_T = 1 \right\}. \tag{2.16}$$

The cost function of the proposed decentralized charging control problem is formulated as

$$J^n(\mathbf{u}) \triangleq \sum_{t=0}^{T-1} \left\{ p(r_t) u^n_t + \delta \left(u^n_t - \text{avg}(\mathbf{u}_t) \right)^2 \right\}, \tag{2.17}$$

where $r_t \equiv \frac{d_t + \text{avg}(\mathbf{u}_t)}{c}$, and the tracking parameter δ is a non-negative constant, which is very similar to Equation (2.15) except that Equation (2.17) assumes an electricity price function, $p(\cdot)$, to be dependent on the ratio of the total aggregated demand in the grid and the generation capacity, defined by

$$p(\cdot) \equiv p\left(\frac{D_t + \sum_{n=1}^{N} u^n_t}{C} \right) = p\left(\frac{d_t + \text{avg}(\mathbf{u}_t)}{c} \right) \tag{2.18}$$

where D_t is the aggregate non-PEV base demand at time instant t, C, the grid generation capacity, N, the PEV population size, and a positive constant $c = C/N$. The optimization algorithm computes a day-ahead charging schedule, i.e., prior to the actual charging periods, based on predictions of load profiles, and simply flattens the load at a certain point in the distribution network. In this work, the authors presented a theorem for a sufficient condition on the uniqueness and convergence of Nash equilibrium as follows [54]:

Theorem 1 *(A sufficient condition on the uniqueness and convergence of Nash equilibrium) Assume the retail price $p(r)$ is continuously differentiable and increasing on r, such that*

$$\sup_{r \in [r_{min},\, 1]} \frac{dp}{dr} < 2 \inf_{r \in [r_{min},\, 1]} \frac{dp}{dr}, \tag{2.19}$$

and the tracking parameter δ satisfies

$$\frac{1}{2c}\sup_{r\in[r_{min},\,1]}\frac{dp}{dr}\leq\delta\leq\frac{a}{c}\inf_{r\in[r_{min},\,1]}\frac{dp}{dr}, \tag{2.20}$$

for some a, with $\frac{1}{2}<a<1$. Then the system converges to a unique Nash equilibrium for the decentralized charging problem.

Assumed that the minimum ratio between the total demand and the generation capacity, $r_{\min}$, is approximately 0.6, the decentralized negotiation procedure is guaranteed to converge to a unique Nash equilibrium from Theorem 1 if the tracking parameter δ satisfies

$$\frac{1}{2c}\sup_{r\in[r_{\min},\,1]}\frac{dp}{dr}=0.015\leq\delta\leq\frac{a}{c}\inf_{r\in[r_{\min},\,1]}\frac{dp}{dr}=0.018a, \tag{2.21}$$

for some a with $\frac{1}{2}<a<1$, i.e., $0.015\leq\delta\leq0.018$. The authors presented a number of numerical examples with a PEV population of 1×10^7, which is approximately 30% of all the vehicles in the Midwest Independent System Operator (MISO) region, to explore the convergence properties and valley-filling performance of the proposed decentralized charging control process. In the case of homogeneous PEV populations, where all PEVs have the same initial state-of-charge (SOC) and an identical charging efficiency, the Nash equilibrium coincides with the valley-filling strategy as illustrated in Figure 35(b). Figure 36(a) shows that charging profiles of PEVs are getting converged to an equilibrium since the conditions in Theorem 1 are sufficient to ensure that a Nash equilibrium obtained by the decentralized optimization process is unique and charging profiles of each PEV converges to that equilibrium, and the tracking parameter $\delta=0.015$ satisfies the conditions. For the heterogeneous case, where half of the PEVs have a battery of 20kWh and the other half have a 10kWh battery, the optimal charging profile obtained by the algorithm is shown in Figure 36(b) to converge to the unique Nash equilibrium under the assumption that there is an infinite population of PEVs, even though the proposed algorithm does not guarantee fair allocation of available power to PEVs. It is also seen from Figure 37 that the conditions

from Theorem 1 are not necessary to ensure the uniqueness and convergence of Nash equilibrium. The convergent process in Figure 37(a) is obtained with $\delta = 0.007$, not satisfying the conditions specified in Theorem 1, and converges to the same Nash equilibrium as in Figure 36(a). However, if the tracking parameter δ is negligible to some extent, for example, $\delta = 0.003$, then the process would not converge to an equilibrium, as depicted in Figure 37(b). The contribution of this paper is that it established a sufficient condition under which the system converges to a unique Nash equilibrium, and that it proposed a decentralized optimization problem for generating an optimal charging strategy, of which optimality is, however, guaranteed only for homogeneous cases, where all EVs plug at the same time with the same charging finish time and need to consume the same amount of energy at the same maximum

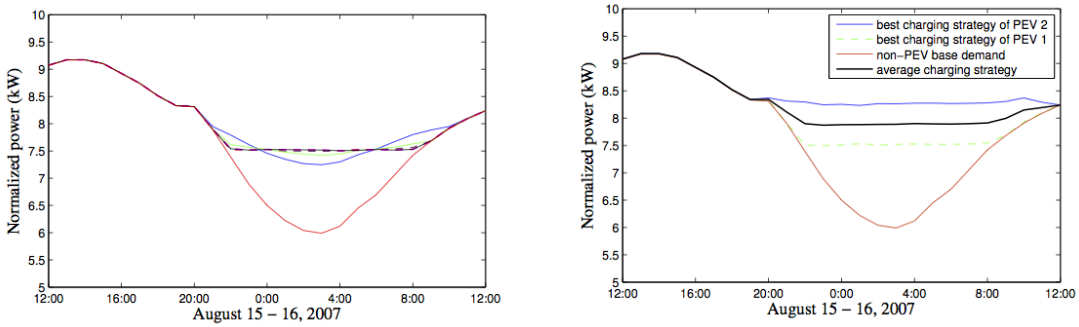

(a) homogeneous PEV population (b) heterogeneous PEV population

Figure 36: Converged Nash equilibrium with $\delta = 0.015$ [54].

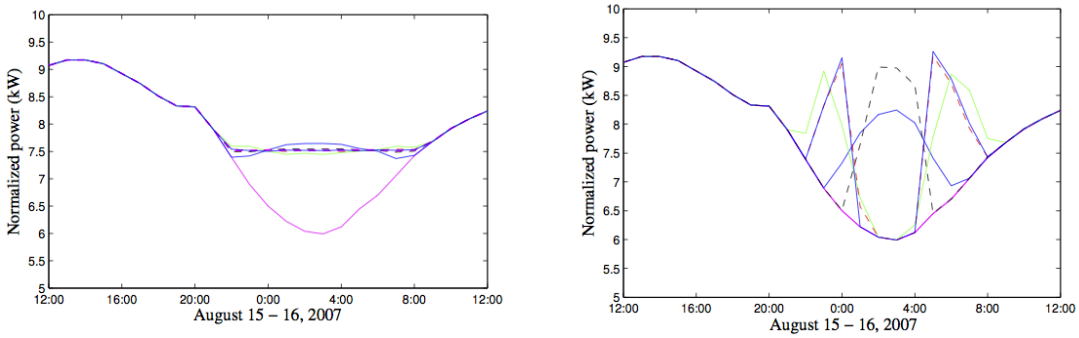

(a) $\delta = 0.007$ (b) $\delta = 0.003$

Figure 37: Sufficient condition on tracking parameter δ for convergence [54].

charging rate.

In [20], the authors proposed a decentralized EV charging scheduling algorithm, exploiting EV charging demand as deferrable loads to fill the valleys in electric load profiles. By decentralized, the authors meant that EVs choose their own charging profiles, instead of being determined by a centralized controller or an aggregator. The authors considered a scenario where a utility negotiates with N EVs to schedule their charging profiles over T time slots of length ΔT in the future with the assumptions that all EVs are available when an optimal charging profile is determined, EVs are charged at a fixed rate, and the charging process cannot be interrupted. The utility is also assumed to precisely predict the inelastic baseload profile (aggregate non-EV load), and attempts to flattening the total load profile (baseload plus aggregate EV load) by shaping the aggregate EV load. The schematic view of the proposed scheduling algorithm and a valley-filling load profile generated by the algorithm are presented in Figure 38. (In the remaining part of this paragraph, the details of Gan *et al.*'s work in [20] are frequently quoted since their formulation will be used as a benchmark to evaluate the proposed real-time EV charging control strategy.) Let $D(t)$ denote the baseload at time slot t, $r_n(t)$ denote the charging rate of EV n at time slot t, and $r_n := (r_n(1), \ldots, r_n(T))$ denote the charging profile of EV n for

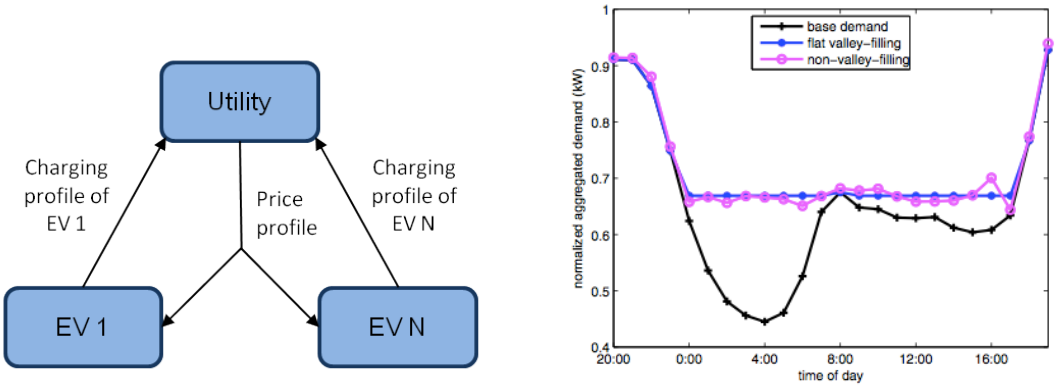

(a) schematic view of information flows

(b) valley-filling load profile

Figure 38: Optimal decentralized charging (ODC) algorithm [19].

$t \in \mathcal{T} := \{1, \ldots, T\}$ and $n \in \mathcal{N} := \{1, \ldots, N\}$. Let $r := (r_1, \ldots, r_N)$ denote the charging profile of all EVs. The intent of flattening the total load profile is captured by minimizing

$$L(r) = L(r_1, \ldots, r_N) := \sum_{t \in \mathcal{T}} U\left(D(t) + \sum_{n \in \mathcal{N}} r_n(t)\right) \tag{2.22}$$

where $U : \mathbb{R} \to \mathbb{R}$ is strictly convex, and the charging rate, $r_n(t)$, is defined by

$$0 \leq r_n(t) \leq \bar{r}_n(t), \quad t \in \mathcal{T}, \quad n \in \mathcal{N} \tag{2.23}$$

and $\bar{r}_n(t)$ is the maximum charging rate of EV n at time slot t. The charging dynamics of EV n, a constraint that it needs to reach its final state-of-charge (SOC) by its deadline, is given by

$$\eta_n \sum_{t \in \mathcal{T}} r_n(t) \Delta T = B_n \left(s_n(T) - s_n(0)\right), \quad n \in \mathcal{N}, \tag{2.24}$$

and can be re-expressed in

$$R_n := \sum_{t=1}^{T} r_n(t) = B_n \left(s_n(T) - s_n(0)\right) / \left(\eta_n \Delta T\right), \quad n \in \mathcal{N}, \tag{2.25}$$

where B_n denotes its battery capacity, $s_n(0)$ and $s_n(T)$ denote initial and final SOCs, respectively, η_n for charging efficiency, and R_n, the sum of charging rates over the time period of T. Using the equations aforementioned, the authors made the following definition for their EV charging control scheme.

[**Definition**] Let $U : \mathbb{R} \to \mathbb{R}$ be strictly convex. A charging profile $r = (r_1, \ldots, r_N)$ is

1) *feasible*, if it satisfies the constraints given in Equations (2.23) and (2.25);

2) *optimal*, if it solves the optimal decentralized charging (ODC) problem

$$\underset{r_1, \ldots, r_N}{\text{minimize}} \ \sum_{t \in \mathcal{T}} U\left(D(t) + \sum_{n \in \mathcal{N}} r_n(t)\right) \tag{2.26}$$

such that

$$0 \leq r_n(t) \leq \bar{r}_n(t), \quad t \in \mathcal{T}, \quad n \in \mathcal{N} \tag{2.27a}$$

$$\sum_{t \in \mathcal{T}} r_n(t) = R_n, \quad n \in \mathcal{N} \tag{2.27b}$$

3) *valley-filling*, if it is feasible, and there exists $A \in \mathbb{R}$ such that

$$\sum_{n \in \mathcal{N}} r_n(t) = [A - D(t)]^+, \quad t \in \mathcal{T} \tag{2.28}$$

If the objective is to track a given load profile G rather than to flatten the total load profile, the objective function in Problem ODC can be modified as

$$\sum_{t \in \mathcal{T}} \left(\sum_{n \in \mathcal{N}} r_n(t) - G(t) \right)^2. \tag{2.29}$$

Based upon these assumptions, they formulated an EV charging scheduling problem as a discrete optimization problem, of which objective, as shown in Equation (2.26), is to minimize the total load variance, if $U(x) = x^2$, resulting in a flat valley-filling. Based on the formulated optimization problem, two decentralized algorithms to solve the optimization problem for computing optimal charging profiles were proposed: a synchronous algorithm and an asynchronous algorithm. The synchronous algorithm requires all EVs to make their own charging profiles at the same time with up-to-date information, meaning that all EVs are available for negotiation at the beginning of the planning horizon, while EVs are allowed to make decisions at different times using possibly outdated information with bounded delays in the asynchronous algorithm. In both algorithms, each EV optimizes its own charging profile based on the optimization problem, given by

$$\underset{r_n \in \mathcal{F}_n}{\text{minimize}} \ \left\{ \left\langle p^{k-a_n(k)}, \, r_n \right\rangle + \frac{1}{2} \| r_n - r_n^k \|^2 \right\}, \tag{2.30}$$

where $\mathcal{F}_n$ denotes a set of feasible charging profiles for EV n, and r_n^k denotes the charging profile of EV n at the kth iteration, with a control signal, i.e., electricity price, $p^{k-a_n(k)}$, broadcast by a utility company. Note that the delay $a_n(k)$ is zero for the synchronous algorithm, but is a delay for the asynchronous algorithm, implying that EV n does not determine its charging profile at every iteration. Similarly to other decentralized charging control algorithms, electricity price, seen by all EVs, is

Algorithm 1 Pseudocode of optimal decentralized charging (ODC) [20].

Input: Scheduling horizon $\mathcal{T}$. The utility knows the base load profile D and the number N of EVs. Each EV $n \in \mathcal{N}$ knows its charging rate sum R_n and charging profile upper bound $\bar{r}_n$, therefore the set $\mathcal{F}_n$ of its feasible charging profiles.
Output: Charging profile $r = (r_1, \ldots, r_N)$

Pick a parameter γ satisfying $0 < \gamma < 1/(N\beta)$

i) Initialize the charging profile r^0 as

$$r_n^0(t) := 0, \quad t \in \mathcal{T}, \quad n \in \mathcal{N}$$

Set $k \leftarrow 0$, repeat step (ii)-(iv).

ii) The utility calculates the control signal p^k as

$$p^k(t) := \gamma U' \left(D(t) + \sum_{n \in \mathcal{N}} r_n^k(t) \right), \quad t \in \mathcal{T}$$

and broadcasts the control signal p^k to all EVs.

iii) Each EV $n \in \mathcal{N}$ calculates a new charging profile r_n^{k+1} by solving

$$\min \left\langle p^k, r_n \right\rangle + \frac{1}{2} \left|\left| r_n - r_n^k \right|\right|^2 \quad \text{s.t.} \quad r_n \in \mathcal{F}_n$$

and reports r_n^{k+1} to the utility.

iv) Set $k \leftarrow k + 1$, go to step (ii).

assumed to be a function of the total demand on the grid, which is the summation of the inelastic non-EV base demand together with the aggregated charging demand of the whole population of EVs. The electricity price is set to be higher for time slots with higher total demand to give EVs the incentive to shift their energy consumption to slots with lower total demand. Through iterative negotiation processes, which take place prior to the actual charging interval, all EVs' charging profiles converge to an optimal charging profile that is as flat as it can possibly be. The decentralized scheduling algorithm for solving the problem given by Equation (2.26) is presented in Algorithm 1, which is called the optimal decentralized charging (ODC) algorithm.

For case studies, the authors used the same baseload profile, i.e., non-EV demand,

and EV charging parameters used in [54] to evaluate the optimality of their algorithms by comparing the algorithm in [54], which does not guarantee the optimality for non-homogeneous scenarios, in which maximum charging rate and charging capacity are not necessarily the same for all EVs and EVs may plug in at different times with different deadlines. Figure 39 show the optimality of the proposed algorithm, compared with the one in [54]. Figure 39(a), for the homogeneous case, where all EVs have the same maximum charging rate and charging capacity along with the same plug-in time and deadline, demonstrates that both algorithms converge to a flat charging profile although the proposed algorithm converges within a single iteration while the algorithm in [54] takes several iterations to converge. Figures 39(b) and

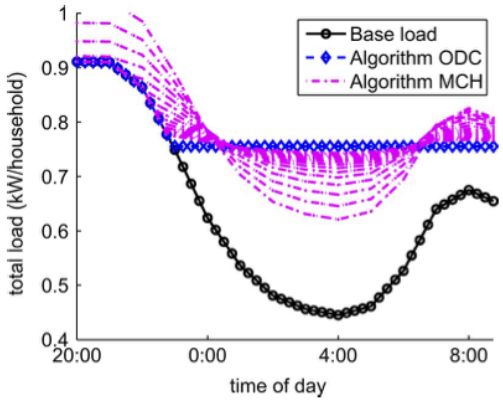

(a) homogeneous case

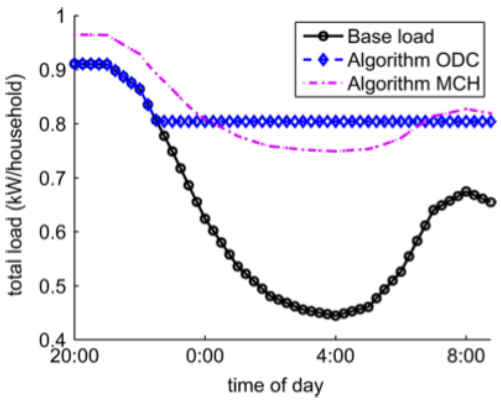

(b) non-homogeneous case with different charging capacity

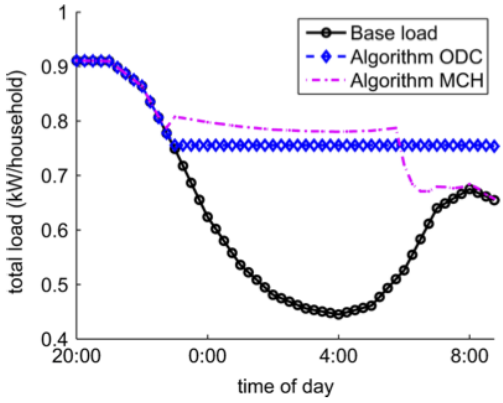

(c) heterogeneous case with different plug-in times & deadlines

Figure 39: Optimality comparison [20].

39(c) indicate that the proposed algorithm does guarantee the optimality even for non-homogeneous cases, while the algorithm in [54] does not straightforwardly extend to non-homogeneous cases. The author also, to derive a more realistic model, proposed an online algorithm, which incorporates EVs when they are available for negotiation, e.g., when they are plugged in for charging. For 20 EVs out of 100 houses, with the same deadline and charging capacity of 10 kWh, participating in negotiation for charging scheduling, simulation results show as illustrated in Figure 40 that the proposed online algorithm performs well even with increasing uncertainty in arrival time, but tends to deviate more from the optimal charging profile as arrival

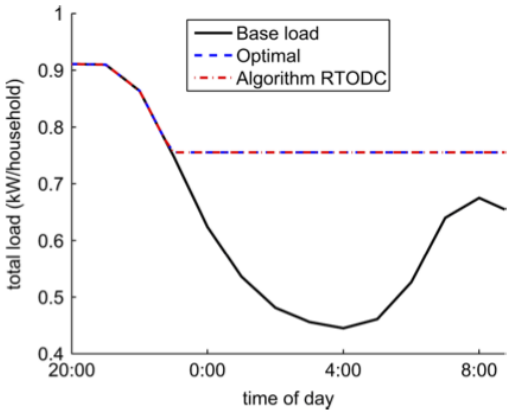

(a) plugged in uniformly between 20:00 and 23:00

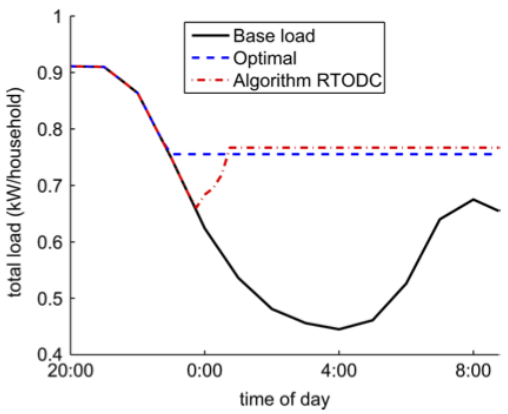

(b) plugged in uniformly between 20:00 and 01:00

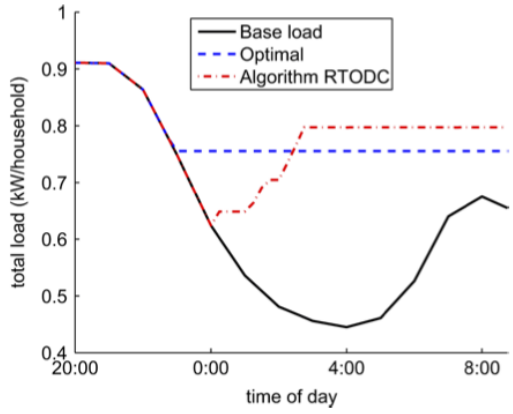

(c) plugged in uniformly between 20:00 and 03:00

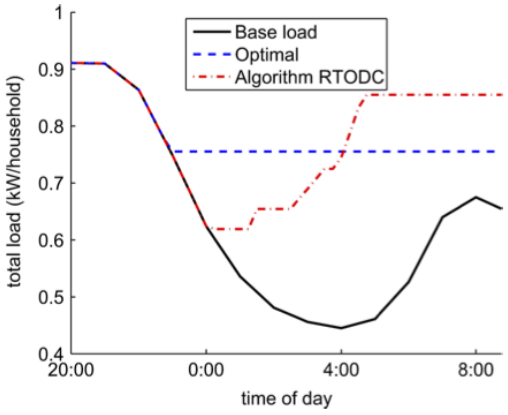

(d) plugged in uniformly between 20:00 and 05:00

Figure 40: Optimality of the online algorithm for different plug-in times [20].

uncertainty increases. The contribution of this work is that the proposed algorithm can define an optimal charging profile of EVs explicitly, as the authors claimed, by generalizing the implicit definition in [54], and that it reformulated the decentralized charging control algorithm to allow tracking of system variations as suggested in [54]. Also, the study proposed a decentralized charging strategy that guarantees the optimality in both homogeneous and non-homogeneous cases. The proposed online scheduling algorithm is more likely to be implemented, if a utility is willing to mitigate the impact of EV charging on the gird, since EV fleet will be non-homogeneous, that is, EVs will have different plug-in times/deadlines and different charging capacities, which are, however, difficult to predict. However, it is obvious that the proposed online algorithm would deviate more from the optimal charging profile for more realistic situations, where the charging process can be interrupted and the usage of renewable energy resources gets increasing more and more. Furthermore, it is difficult to accurately predict the future demand from non-EV loads, the number of EVs being charged at each time slot, and their initial states of charge. Required is, therefore, a new approach for computing an optimal charging profile, which can take into account all the stochastic behaviors of EV charging and thus provide a robust, optimal charging profile.

In this subsection, attempts at controlling EV charging in a decentralized manner were reviewed. Compared with centralized EV charging schemes, relatively a small number of studies have been done on decentralized schemes, but their technical approaches for controlling EV charging are similar to ones based on a centralized control structure: minimizing the total load variance, i.e., filling the valley(s) in the baseload profile (aggregated non-EV demand). The decentralized EV charging control algorithms, based on an optimization problem to minimize the load variance, were proposed under some assumptions that are quite different from the reality. In order to develop an algorithm to tackle their practical limitations, it is more desirable

to control EV charging in real time so that it can satisfy EV owners' charging preferences, which is somewhat random, and utilize the economic and technical benefits that a large population of EVs can provide. In the following subsection, studies on the application of real-time scheduling techniques to electric power systems will be addressed.

2.1.3 Scheduling Techniques for Electric Power Systems

As reviewed in §2.1.1 and §2.1.2, the common technical limitations of existing EV charging strategies result from the following facts:

- All of them are based on accurate day-ahead prediction of load profiles.
- They do not take account of EV owners' charging requirements and preferences.
- They are required to have the information of EV charging profiles before they are plugged in.
- They do not take into account the initial and departure states-of-charge.

However, in reality, the predicted load profiles almost always do not match the actual load profiles, and satisfying EV owners' charging preferences/requirements are more important than those of any organizing entities. Also, it is not practical that coordinating entities know EV charging profiles before they start charging. In order to cope with these technical limitations, EV charging control must be done in real time rather than ahead of time, and, thus, real-time scheduling[1] techniques might be utilized. A very few papers regarding the application of real-time scheduling techniques to electric power systems have been published. In this subsection, literature related to the application of real-time scheduling techniques to electric power systems is reviewed.

[1] "Real-time scheduling allows managing the execution of tasks on processors under timing constraints. In more general terms, real-time scheduling can be seen as the discipline of allocating resources over time to a set of time-consuming tasks, so that given timing constraints are satisfied" [14].

Facchinetti *et al.* proposed a method for applying real-time scheduling techniques to balance the power usage of electric loads in cyber-physical energy systems [14]. The authors claimed that "it is the first attempt of using real-time scheduling techniques to organize the activation of electric loads in a cyber-physical energy system." They presented "a methodology for modeling a power system as periodic activities that can be scheduled by adapting traditional real-time scheduling algorithms" such as Rate Monotonic (RM) and partitioning scheduling algorithm. (The remaining part of this paragraph is excerpted from Facchinetti *et al.*'s paper [14], since it could help readers grasp the idea on how real-time scheduling techniques can be applied to electric power systems more accurately.) Consider a system composed of a set $\Lambda = \{\lambda_1, \ldots, \lambda_n\}$ of n independent electric loads that request to be turned on and off (or activated/deactivated), depending on their specific timing requirements. At time $r_{i,j}$ happens the j-th request for activating the i-th load λ_i that is modeled by the tuple (T_i, C_i, P_i), where

- T_i is the minimum separation between two consecutive requests of activation $r_{i,j}$, $r_{i,j+1}$. Hence,

$$\forall \lambda_i, \forall j \quad r_{i,j+1} \geq r_{i,j} + T_i \tag{2.31}$$

- C_i is the longest time the load λ_i can be active between two consecutive requests;
- P_i is the nominal power consumed by the load λ_i during its active time.

Then, the utilization of λ_i is defined as $U_i = C_i/T_i$, and the total utilization of Λ is $U = \sum_{i=1}^{n} U_i$. The load activity is controlled by a *load scheduler* that decides when each load is activated/deactivated. In other words, the scheduler assigns to each load λ_i a schedule that is modeled by the function $s_i(t)$

$$s_i(t) = \begin{cases} 1 & \text{if } \lambda_i \text{ is active at } t \\ 0 & \text{otherwise} \end{cases} \tag{2.32}$$

The schedule of loads is then given by $\mathcal{S} = \{s_1, \ldots, s_n\}$, and a schedule $\mathcal{S}$ is said to be *valid* if it assigns to each load λ_i an amount of activity time equal or larger than C_i between two consecutive requests:

$$\forall \lambda_i, \forall j \quad \int_{r_{i,j}}^{r_{i,j+1}} s_i(t)dt \geq C_i. \tag{2.33}$$

For a given schedule $\mathcal{S}$, the actual power consumed by the load λ_i at time t is

$$p_i(t) = P_i s_i(t), \tag{2.34}$$

and the overall actual power consumption $p(t)$ at time t is then given by

$$p(t) = \sum_{i=1}^{n} p_i(t). \tag{2.35}$$

The *peak load* can be defined as $P = \max_{t \geq 0} p(t)$. Given these hypotheses, the authors proposed to use classic real-time scheduling algorithms such as Rate Monotonic (RM) or Earliest Deadline First (EDF) to schedule the loads in Λ. Specifically, each load can be considered as a task with computation time C_i and period (equal to the deadline) T_i. For example, when $U \leq 1$, the EDF scheduling algorithm can build a schedule $\mathcal{S}$ with the minimum possible peak power, that is, $P = \max_i P_i$. However, if $U > 1$, some loads must be contemporarily activated, leading to a possibly larger peak power consumption P. Hence, the authors suggested to partition the load set Λ into m disjoint sets Λ_j, $j = 1, \ldots, m$, that is called *scheduling groups*. Scheduling groups are determined such that their total utilization, defined as

$$U(\Lambda_j) = \sum_{\lambda_i \in \Lambda_j} U_i, \tag{2.36}$$

is smaller than or equal to 1 so that the EDF or RM can find a valid schedule within each scheduling group. The problem of partitioning the set of loads can be formulated as a *level packing* problem. In level packing, a strip must accommodate a set of rectangles such that the total height is minimized. The peculiarity of level packing is that rectangles are partitioned in horizontal levels of decreasing height

from the bottom to the top. In each level, items are packed from left to right by decreasing height, similarly to the arrangement of books within a bookshelf. Each load is modeled as a rectangle whose height corresponds to the power consumption p_i and width is determined by its utilization u_i. Without loss of generality, all loads are assumed to be sorted by decreasing power, namely $p_i \geq p_j \Leftrightarrow i \leq j$. A set of n variables $y_i \in \{0, 1\}$ defines level initialization. There is one such variable for each load, being $y_i = 1$ if an item i initializes level i, $y_i = 0$ otherwise. A level is labeled by the index of the item initializing it. The variables $x_{i,j}$ with $i \in \{1, \ldots, n-1\}$ and $j > i$ define the packing of the item j when it does not initialize a level. The value $x_{i,j}$ is set to 1 if the item j is packed in the level i, $x_{i,j} = 0$ otherwise. Then, the optimization problem can be formulated as minimizing the sum of the peak powers on each group, that is,

$$\text{minimize} \sum_{i=1}^{n} p_i \, y_i \tag{2.37}$$

subject to

$$y_i + \sum_{i=1}^{j-1} x_{i,j} = 1, \quad \forall j = 1, \ldots, n \tag{2.38}$$

and

$$\sum_{j=i+1}^{n} u_j x_{i,j} \leq (W - u_i) y_i, \quad \forall i = 1, \ldots, n-1 \tag{2.39}$$

where W is defined to be equal to the utilization upper bound that guarantees the schedulability of a load set. For example, if EDF with implicit deadlines is used, then W is set to 1. The authors introduced a heuristic algorithm to address the problem of generating scheduling groups. Algorithm 2 shows the pseudocode of the proposed algorithm, called the RM-FFDU (Rate Monotonic First-Fit Decreasing Utilization) partitioning scheme for scheduling fixed priority real-time tasks on a multiprocessor system [60], where bin-packing techniques are used to allocate tasks on processors (Facchinetti *et al.* [14]). In this paper, a methodology for modeling electric loads

Algorithm 2 Pseudocode of the load balancing heuristic [14].

```
1: sort Λ in decreasing order of power
2: λ_1 ... λ_m are the scheduling groups
3: m = 1 is the initial number of scheduling groups
4: for all λ_i ∈ Λ do
5:     for j = 1 to m do
6:         if λ_j is schedulable in Λ_j then
7:             add λ_j to Λ_j
8:             goto end-loop
9:         end if
10:    end for
11:    create a new schedule group Λ_{m+1}
12:    add λ_i to Λ_{m+1}
13:    m = m + 1
14:    :end-loop
15: end for
```

as periodic activities that can be scheduled by traditional real-time scheduling algorithms is presented. However, this methodology is not intended to be used for event-driven, or aperiodic, load activations. Also, it is assumed that there are no interactions among loads when an optimal scheduling strategy is developed. Moreover, the proposed algorithm tries to minimize the total power usage of electric loads rather than make it constant during the period of scheduling, which an algorithm for EV charging must do in order to minimize the total load variance, i.e., achieve a flat load profile by filling its valley(s).

Vedova *et al.* proposed the application of real-time physical systems (RTPS) as a novel approach, which is based on real-time scheduling techniques, to model the physical process of cyber-physical energy systems (CPES) [87]. Therefore, the physical process is modeled in terms of real-time parameters and timing constraints, so that real-time scheduling algorithms can be applied to manage the timely allocation of resources, i.e., electric power. Table 5 summarizes the analogy between real-time computing systems and energy systems based on real-time parameters. The approach

Table 5: Analogy between real-time computing systems and cyber-physical energy systems [87].

Features	Real-time computing systems	Cyber-physical energy systems
Domain	Computing systems	Energy systems
Resource	Task	Load
C_i	Execution time	Activation time
T_i	Period	Period
D_i	Deadline	Deadline
$s(t)$	Schedule	Switching signal
Objective	Consumed energy	Peak power

is to exploit the periodic task model, widely studied in real-time systems, to represent electric loads as periodically triggered activities, and the goal is to reduce the peak load of power consumption. An example of schedule of real-time periodic tasks is given in Figure 41. Figure 41(a) depicts the normal power consumption of some electric loads, both measured power and contributions of specific loads. Figure 41(b) shows that the application of a real-time scheduling technique to electric load activations allows to achieve a peak load reduction of 25%. Once electric loads have been modeled using real-time timing parameters, a priority-based scheduling algorithm such as Earliest Deadline First (EDF) or Rate Monotonic (RM) can be applied

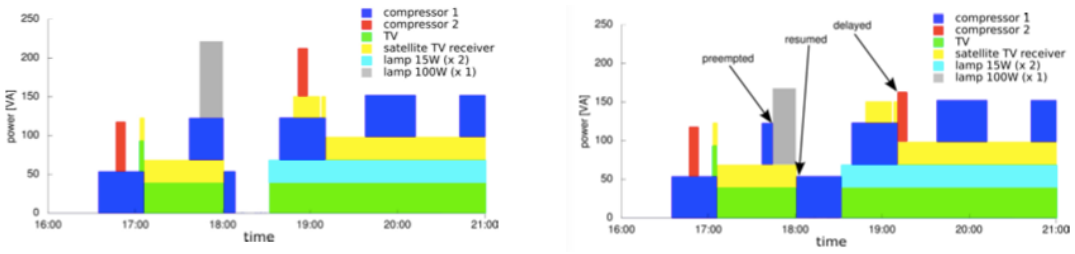

(a) normal power consumption (b) real-time scheduling

Figure 41: Measurements of consumed power in an apartment [87].

to selectively activate/deactivate electric devices. The two algorithms are known to be optimal for uniprocessor systems with full preemption and can be suitably applied only when the total utilization does not exceed an upper bound that guarantees their optimality. Also, multiple simultaneous activations of electric loads can be managed by partitioning the set of loads as in [14] that translates the scheduling problem of a multiprocessor into the scheduling problem of multiple uniprocessors, to which aforementioned, well-known scheduling algorithms, EDF or RM can be applied. The approach fosters the possibility to use real-time scheduling techniques to model energy systems in order to achieve its predictable timing behaviors. However, the approach is limited to periodic tasks with fixed priorities and repetitive rates. Also, it is assumed that power consumptions of each load are invariant.

2.2 EV Potential to Participate in the Provision of Power System Services

As described in Chapter 1, one of the potential benefits that a large population of EVs can provide is that EVs can generate or store electricity when parked, and, with appropriate connections and controls, they can feed power to the grid, which is the basic concept of "vehicle-to-grid" power or V2G power. According to Kempton and Tomić, there would be conflicts between vehicle owners and the grid operator: the vehicle owners need enough energy stored in their vehicles for driving and also want to sell some electricity to the grid for economic benefits, while the grid operator needs power generation to be turned on and off whenever it wants at precise times [34]. In order to resolve these potential issues, they proposed three strategies for V2G: (1) add extra energy capacity to batteries of the vehicles; (2) draw V2G power from the fleet of particular vehicles, such as delivery vehicles and forklifts in a warehouse, which are typically in use from 9:00 am to 5:00 pm and could then be predictably used for V2G most or all of the remaining 16 hours of the day; and (3) use intelligent controls for

the complementary needs. They claimed that, in order to realize the full potential of V2G, we need the third strategy so that non-fleet vehicles can also participate.

The electric power system must satisfy two unique requirements: one is to maintain a near real-time balance between generation and load, and the other is to adjust generation (or load) to manage power flows through individual transmission facilities [37]. The services required to meet these requirements, called "ancillary services," are those functions performed by equipment and people that generate, control, and transmit electricity in support of the basic services of generating capacity, energy supply, and power delivery, according to the definition by the Federal Energy Regulatory Commission (FERC) [15]. It is difficult to balance generation and load instantaneously and continuously since generation and load keep fluctuating. The random turning on and off of millions of individual loads results in minute-to-minute load variability, and longer-term variability results from daily and seasonal load patterns as well as more random events like shifting weather patterns. Generators also introduce unexpected fluctuations because they do not follow their generation schedules exactly and they trip unexpectedly when their operations are beyond their range of equipment failures. Among ancillary services, regulation and load following are the two services that ensure the continuous balance between generation and load under normal conditions. They utilize on-line generation, storage, or load equipment to track the moment-to-moment fluctuations or the intra- and inter-hour changes in customer loads. The authors in [37] claimed that some storage technologies should be ideal providers of several ancillary services, including regulation, contingency reserves (spinning reserve, supplemental reserve, replacement reserve), and voltage support.

EVs are utilized only 4% of the time for transportation and are potentially available the remaining 96% of time for a secondary function [33]. With appropriate connections, they can provide power to the grid while parked, which, according to many studies, is one of promising options for quick-response, high-value electric power

services that can be used to balance constant fluctuations in load and adapt to unexpected equipment failures. However, compared with traditional, large generators, EVs have low durability and high cost per kWh of electric energy, and thus V2G power should be sold only to high-value, short-duration power markets [33]. Although there are many publications studying the economical viability of V2G technologies, a few papers dealing with technical implementation of V2G for specific ancillary services has been published. This section reviews the studies exploiting the V2G concept and identifying the most suitable one using the concept among various ancillary services.

Han *et al.* developed an optimal V2G aggregator that makes efficient use of the distributed power of EVs to produce the desired grid-scale power for frequency regulation, and focused on the individual EV charging scheduling rather than collectively organizing the EVs [26]. They proposed an optimization problem, with practical constraints such as the energy restriction of batteries, that can be solved by applying the dynamic programming algorithm to compute the optimal charging control for each vehicle. The authors claimed that charging control should be on or off at the maximum charging rate to maximize the revenue and, in the end, the charging scheduling problem is to determine the charging sequence (when to turn on the charging). The discrete form of charging dynamics used in this study is described as follows:

$$x(n+1) = KC(n) + x(n) \tag{2.40}$$

where x is the state-of-charge (SOC), n is a discrete step during the time interval $(t_1 \leq t \leq t_2)$, K is a maximum charging rate for each vehicle, and $C(n)$ is a charging control sequence, i.e., a sequence of 1's and 0's. They formulated the performance measure to maximize the revenue, which is defined as

$$M\left(t_1,\, t_2,\, C(t)\right) \triangleq \int_{t_1}^{t_2} \left[P_R(t,\, x(t)) - C(t)(P_R(t,\, x(t)) + P_C(t))\right] dt - \alpha \left(x(t_2) - x_T\right)^2 \tag{2.41}$$

and, in a discretized form,

$$M\left(k_1,\, k_2,\, C(k)\right) = \sum_{n=k_1}^{k_2-1} \left[P_R(n,\, x(n)) - C(n)(P_R(n,\, x(n)) + P_C(n))\right] - \alpha\left(x(k_2) - x_T\right)^2 \tag{2.42}$$

where P_R is the regulation price, P_C is the unit price for purchasing power from the grid, α is a weighting factor that reflects the relative importance of the desire to drive the system to the final SOC, x_T. Figure 42(a) shows a set of optimal charging control sequences derived through the simulation varying the initial SOC from 0% to 100% by 10%. According to the simulation results, all control sequences successfully transfer the SOC to 90%, the designated departure SOC, regardless of the initial SOC. In this formulation, the entire control sequence could be obtained through the dynamic programming immediately after a vehicle is plugged in as shown in Figure 42(b). In this study, an aggregator for V2G frequency regulation with the consideration of optimal charging is developed, and an optimal charging control is obtained by applying the dynamic programming. However, the study does not consider discharging EVs, i.e., selling power to the grid, and the formulated optimization problem does not deal with minimizing the impacts of EV charging on the grid.

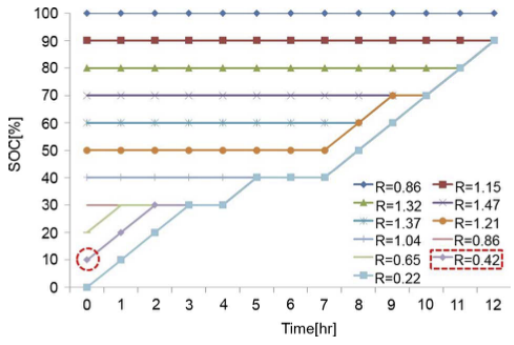

(a) optimal control sequences for each SOC with $\alpha = 0.01$

	$\alpha = 0.01$	$\alpha = 0.0005$
SOC \ HR	0 1 2 3 4 5 6 7 8 9 10 11	0 1 2 3 4 5 6 7 8 9 10 11
100	x x x x x x x x x x x x	x x x x x x x x x x x x
95	x x x x x x x x x x x x	x x x x x x x x x x x x
90	x x x x x x x x x x x x	x x x x x x x x x x x x
85	x x x x x x x x x x x x	x x x x x x x x x x x x
80	x x x x x x x x x x x o	x x x x x x x x x x x x
75	x x x x x x x x x x x o	x x x x x x x x x x x x
70	x x x x x x x x x x o o	x x x x x x x x x x o o
65	x x x x x x x x x x o o	x x x x x x x x x x o o
60	x x x x x x x x o o o o	x x x x x x x x x o o o
55	x x x x x x x x o o o o	x x x x x x x x x o o o
50	x x x x x x x o o o o o	x x x x x x x x x o o o
45	x x x x x x x o o o o o	x x x x x x x x x o o o
40	x x x x x x x o o o o o	x x x x x x x x x o o o
35	x x x x x x x o o o o o	x x x x x x x o o o o o
30	x x x x o o o o o o o o	x x x x x x x o o o o o
25	o x x o o o o o o o o o	o x x o o o x o o o o o
20	o o o o o o o o o o o o	o o o o o o x o o o o o
15	o o o o o o o o o o o o	o o o o o o x o o o o o
10	o o o o o o o o o o o o	o o o o o o o o o o o o
5	o o o o o o o o o o o o	o o o o o o o o o o o o
0	o o o o o o o o o o o o	o o o o o o o o o o o o

(b) optimal control tables. "o" means charging while "x" means idle.

Figure 42: Simulation results of the optimal V2G aggregator [26].

Ota *et al.* proposed an autonomous distributed V2G control scheme providing a distributed spinning reserve for the unexpected intermittency of the renewable energy resources (RES) with the consideration of a smart charging control of EVs, and evaluated the satisfaction of vehicle owners' convenience and the effect to the load frequency control [62]. A droop control based on the frequency deviation at plug-in terminal due to the imbalance of supply and demand of the power grid, realizing a fast and synchronized response among multiple EVs, is also proposed so that EVs' SOCs can be managed by a balance control, and the scheduled charging requests by vehicle users can be satisfied. As shown in Figure 43(a), V2G power (P_{V2G}) is controlled with droop characteristics against the frequency deviation (Δf) as follows:

$$P_{\mathrm{V2G}} = \begin{cases} K_{\mathrm{V2G}}\Delta f & \text{if } |K_{\mathrm{V2G}}\Delta f| \leq P_{\max} \\ P_{\max} & \text{if } P_{\max} < |K_{\mathrm{V2G}}\Delta f| \end{cases} \tag{2.43}$$

where maximum V2G power ($P_{\max}$) is limited by the specifications of the home outlet, and V2G gain (K_{V2G}) is determined considering a tradeoff between the effect for the load frequency control (LFC) and the fluctuation range of the batter SOC. When the SOC is near to full (empty), a high-power charging (discharging) should not be

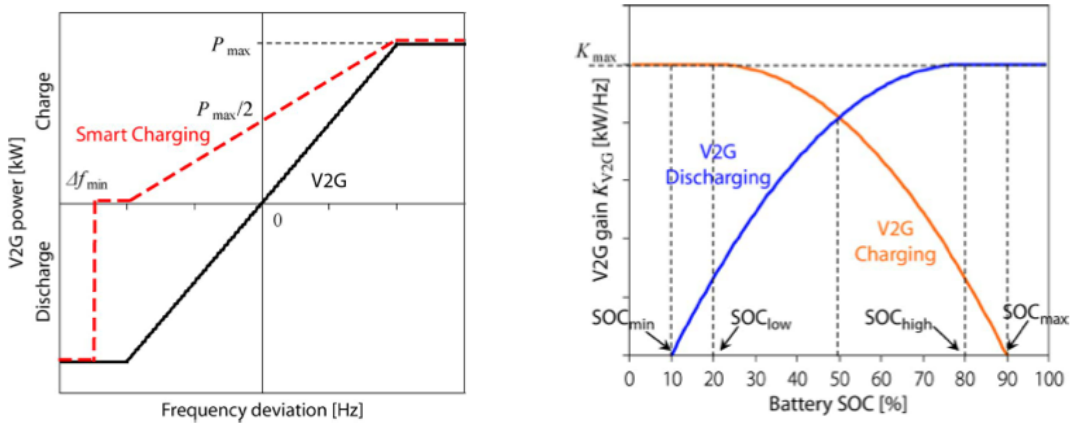

(a) V2G control with droop against frequency deviation

(b) battery SOC balance control

Figure 43: V2G control based on frequency deviation and SOC balance [62].

implemented for preventing overcharge (over discharge). Therefore, if the SOC can be accurately estimated, a balance control can be installed as follows:

$$K_{\mathrm{V2G}} = K_{\max}\left\{1 - \left(\frac{SOC - SOC_{\mathrm{low(high)}}}{SOC_{\mathrm{max(min)}} - SOC_{\mathrm{low(high)}}}\right)^2\right\}. \tag{2.44}$$

where $SOC_{\min}$, SOC_{low}, SOC_{high}, $SOC_{\max}$, and n are designed as the SOC is balanced around 50% as shown in Figure 43(b). For satisfying the scheduled charging, the V2G control is switched to a smart charging control with a charging offset of half the maximum V2G power ($P_{\max}$) and a half droop gain against the frequency deviation as follows and shown in Figure 43(a):

$$P_{\mathrm{SC}} = \begin{cases} K_{\max}/(2\Delta f) + P_{\max}/2 & \text{if } |K_{\max}\Delta f| \leq P_{\max} \\ P_{\max} & \text{if } P_{\max} < K_{\max}\Delta f \\ 0 & \text{if } K_{\max}\Delta f < P_{\max} \\ -P_{\max} & \text{if } \Delta f < \Delta f_{\min} \end{cases} \tag{2.45}$$

In this paper, a simplified battery model consisting of voltage source expressed as open circuit voltage (OCV) and internal resistance (R_{int}) is assumed, and the battery OCV is defined as the following Nernst equation:

$$OCV = V_{\mathrm{nom}} + \alpha\frac{RT}{F}\ln\left(\frac{SOC}{C_{\mathrm{nom}} - SOC}\right) \tag{2.46}$$

where V_{nom} and C_{nom} are nominal voltage and capacity, respectively. Necessary energy (E) from the current SOC(SOC_i) to the desired SOC (SOC_d) is calculated by integrating the OCV as follows:

$$E = \int_{SOC_i}^{SOC_d} OCV\, dSOC \tag{2.47}$$

During charge or discharge with current I, battery closed circuit voltage (CCV) and the V2G power (P_{V2G}) are calculated as follows:

$$CCV = OCV + R_{\mathrm{int}}I \tag{2.48}$$

$$P_{\mathrm{V2G}} = CCV \cdot I = OCV \cdot I + R_{\mathrm{int}}I^2 \tag{2.49}$$

Thus, the battery SOC is updated by the V2G power as the following differential equation:

$$\frac{dSOC}{dt} = \eta I = \eta \left(\frac{-OCV + \sqrt{OCV^2 - 4R_{\text{int}}P_{\text{V2G}}}}{2R_{\text{int}}} \right). \tag{2.50}$$

where η is the efficiency of the battery. Simulation results, not included in this thesis, indicate that frequency fluctuations caused by RES fluctuations are compensated by the proposed V2G control while the proposed smart charging control satisfies the scheduled charging by the vehicle owner. The contribution of the study is that it proposes an autonomous distributed V2G control scheme providing a distributed spinning reserves that can compensate for the unexpected intermittency of RESs. In addition, the proposed scheme is integrated with a smart charging control to satisfy the scheduled charging request by a vehicle owner. The advantages of the proposed scheme in this work is that it could be easily incorporated into automotive power electronics circuits or household charging units to facilitate plug-and-play operation. However, the study verified the capability of the proposed scheme only on the limited number of vehicles, i.e., 2 EVs and 1 PHEV, and did not consider the minimization of the impacts of EV charging on the grid.

2.3 Summary of Literature Review

2.3.1 Synthesis of Literature Review

Figure 44 presents the overview of literature relevant to smart EV charging systems, some of which have been reviewed in this chapter at some length and the others are only presented for readers' reference.

A lot of literature on the assessment of EV charging on the power gird and centralized/coordinated charging strategies have been published. Rahman and Shrestha suggested that a charging strategy, i.e., a *strict control over temporal distribution of EVs*, and proper *economic incentives* may be required to alleviate the adverse effects such as additional, undesirable peak loads by distributing charging load during off-peak hours, even at low levels of EV penetration. Ford confirmed that, without a proper management, EV charging may lead to a secondary peak. If advanced batteries are utilized and *EV charging is properly controlled*, the power system of the area of interest would be able to accommodate a large number of EVs. Denholm and Short evaluated the effects of optimal PHEV charging on the grid when a utility has a direct or an indirect control authority on EV charging while providing customers with the possibly lowest cost of driving energy. They showed through simulation studies that *low-cost off-peak electricity* would accommodate up to 50% of the vehicle fleet with no additional electric generation capacity under *optimal dispatch rule* and that PHEVs are much better suited for *short-term ancillary services such as regulation and spinning reserve*. Lemoine *et al.* studied how many PHEVs could be served by the CAISO without additional generation/transmission infrastructure, and revealed that millions of PHEVs could be economically deployed in California without requiring new generation capacity if *new pricing structures* or *technical means to coordinate PHEV charging* is implemented. Letendre and Watts assessed the effect, greenhouse gas emissions, and end-user costs of a large number of PHEVs on the electric grid in

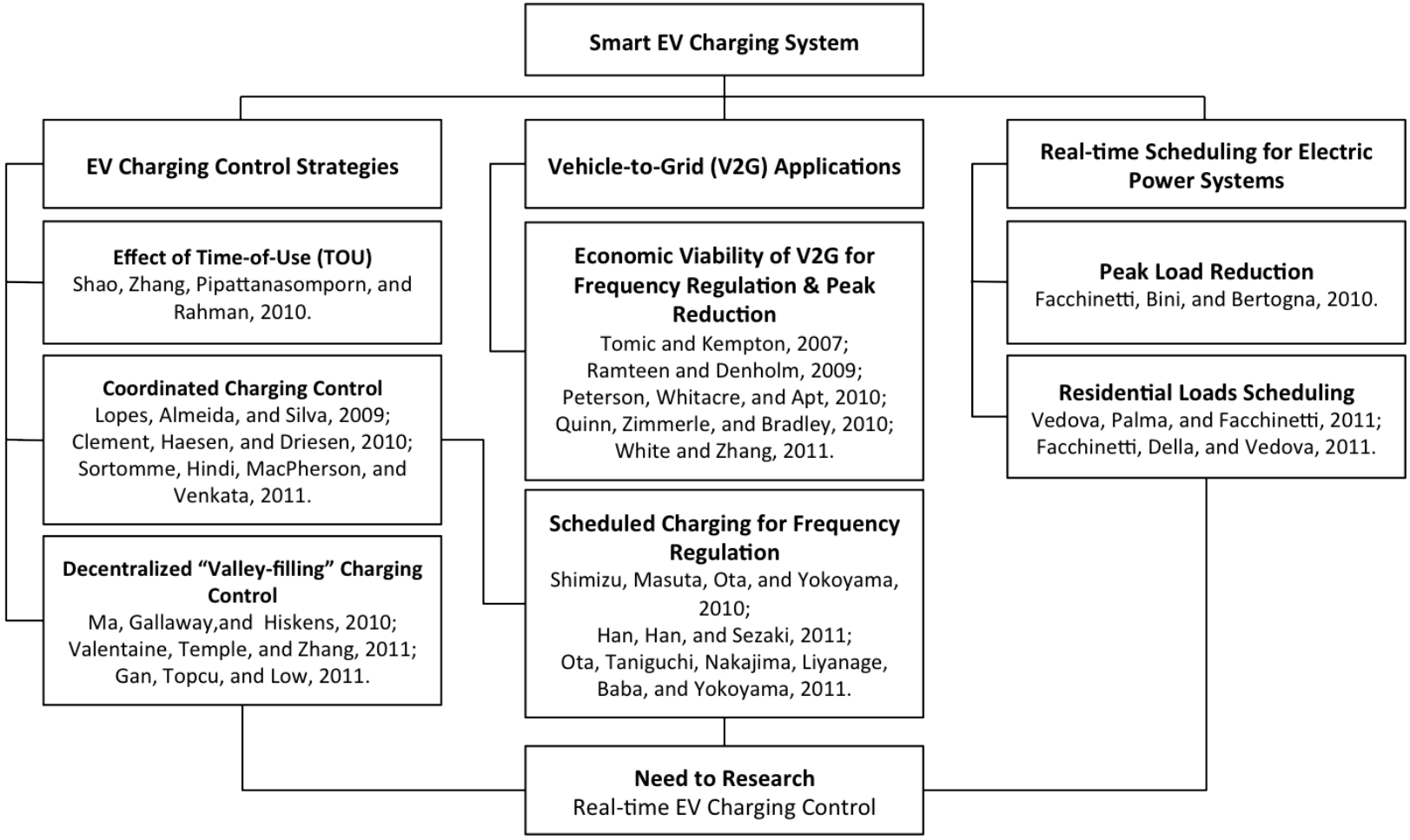

Figure 44: Overview of literature on smart EV charging systems.

the state of Vermont with four different charging scenarios considered. They concluded that a large fleet of PHEVs could be accommodated in Vermont's power gird if either *financial incentives for off-peak charging* or *direct control of PHEV charging* is properly utilized. Lopes *et al.* investigated the impact of massive integration of EVs in a representative medium-voltage electricity distribution network in residential areas in Portugal, and suggested three EV charging management methods: dumb charging, dual tariff policy, and smart charging. For the smart charging strategy, they considered a hierarchical control structure, and proposed an optimization approach that maximizes the integration level of EVs. They proved that the *smart charging approach* is the most effective strategy that could increase the EV deployment capability of the grid by solving a simple optimization problem. Shao *et al.* examined the adaptability of the residential distribution network to support PHEVs, and evaluated the impact of charging PHEVs on a distribution transformer under two different charging scenarios: normal charging and quick charging. This work makes a contribution in the sense that it considers both charging control and household load management to mitigate the impact of PHEVs. They also presented a demand response model for residential customers and explored the effect of higher price during peak hours on shifting EV load in another paper. They pointed out that the design of TOU rates is important in terms of selecting the appropriate peak/off-peak price levels and periods since too high TOU rate for peak hours would create additional peak loads during off-peak hours. Putrus *et al.* investigated the effects of EV deployment on existing distribution networks in terms of 1) load profile and uncontrolled peak demand, 2) change in voltage levels and violation of statutory limits, and 3) voltage imbalance. The authors also considered three charging scenarios: uncontrolled, off-peak, and phased charging, and concluded that a *smart charging control* or *incentives for EV owners* would need to be introduced to minimize or even eliminate the effects of EV charging on the network. Lopes *et al.* evaluated the maximum share

of electric vehicles, which can be integrated into a specific grid without violating the system's technical restrictions and complying with drivers' requests concerning the foreseen use of vehicles, and analyzed the impacts of dumb charging and smart charging. Sortomme *et al.* explored the relationship between feeder losses, load factor, and load variance in the context of coordinated PHEV charging, from which they developed three optimal charging algorithms that minimize the impacts of PHEV charging on the distribution network. These strategies require a centralized structure to collect information from all EVs and centrally optimize over their charging profiles. Deilami *et al.* proposed a real-time load management algorithm employing the maximum sensitivities selection (MSS) optimization approach to coordinate the charging of multiple PEVs, and demonstrated that the *smart load management* is beneficial in reducing overall system overloads and power peaks. Lan *et al.* investigated a possible solution for EV smart charging with the consideration of EVs as controllable loads. An aggregator directly generates charging profiles of all EVs and coordinates their charging/discharging operations. It is shown through a case study that the smart charging strategy without the provision of regulation service reduces daily electricity costs for driving, and, with the proposed smart charging, EVs are recharged during off-peak hours.

Compared with centralized/coordinated charging strategies, a relatively small number of studies dealing with decentralized charging schemes have been published. Ma *et al.* proposed a decentralized charging strategy, based on the Nash Certainty Equivalence (NCE) principle, in which individual PEV implements a local optimal charging control algorithm, resulting in a valley-filling load profile aggregately. The NCE-based decentralized charging algorithm is implemented through a charging negotiation procedure between a utility and EVs. The authors proved its optimality in terms of total load variance for the homogeneous case; however, if the PEV population is heterogeneous, the solution is a nearly valley-filling, and charging profiles

for PEVs are similar, but not identical unlike the homogeneous case. Gan *et al.* proposed another decentralized charging strategy, and they partially alleviated some of the restrictions imposed in the studies of Ma *et al.* in that they defined optimal charging profiles of EVs explicitly, and their algorithm guarantees optimality in both homogeneous and heterogeneous cases, where EVs can plug in at different times with different SOC, have different maximum charging rates. They also proposed an online scheduling algorithm that is more likely to be implemented by utilities to mitigate the impacts of EV charging on the grid.

Next, literature on applying real-time scheduling techniques to electric power systems were reviewed. Facchinetti *et al.* proposed a method for applying real-time scheduling techniques to balance the power usage of electric loads in cyber-physical energy systems. They modeled electric loads such as periodic events that can be scheduled by traditional real-time scheduling algorithms such as Earliest Deadline First (EDF) or Rate Monotonic (RM), and the problem of partitioning the set of loads is formulated as a level packing problem. Vedova *et al.* also proposed the application of real-time physical systems (RTPS) as a novel approach, which is based on real-time scheduling techniques, to model the physical process of cyber-physical energy systems (CPES). They modeled the physical process in terms of real-time parameters and timing constraints, and summarized the analogy between real-time computing systems and energy systems. The approach fosters the possibility to use real-time scheduling techniques to model energy systems in order to achieve its predictable timing behaviors.

Also, papers addressing vehicle-to-grid (V2G) applications were reviewed. Han *et al.* proposed an algorithm that enables EVs to discharge based on their state-of-charge (SOC) responding to the regulation up/down requests from an aggregator. They formulated an optimization problem to maximize the revenue, and claimed that charging control should be on or off at the maximum charging rate to maximize the

revenue. In this formulation, the entire control sequence could be obtained through the dynamic programming. Ota *et al.* presented an autonomous distributed V2G control scheme providing a distributed spinning reserve for the unexpected intermittency of the renewable energy resources (RES) with the consideration of a smart charging control of EVs, and evaluated the satisfaction of vehicle owners' convenience and the effect to the load frequency control.

In addition to literature reviewed in the previous sections, recent researches on the application of real-time scheduling techniques to EV charging were reviewed further to make extra certain that there is no published work similar to what is presented in this thesis. Subramanian *et al.* presented a model for reserve services by applying three heuristic causal scheduling policies, Earliest Deadline First (EDF), Least Laxity First (LLF), and Receding Horizon Control (RHC) in 2012 [78]. They showed that EDF is optimal unless power constraints are considered. In [47], the authors proposed two real-time price-based scheduling algorithms based on EDF and LLF for a demand side management program, which can facilitate possible penetration of renewable energy sources and better system stability. In 2015 and 2016, the authors investigated two common scheduling heuristics, EDF and LLF, and proposed a trajectory tracking algorithm based on a convex optimization model and a Model Predictive Control (MPC) for real-time scheduling of a fleet of EVs to provide V2G-based frequency regulation services [32, 89]. They claimed that the two scheduling heuristics "show several deficiencies in terms of excessive battery cycling and limited regulation capacity." Several attempts to applying real-time scheduling techniques to electric power systems have been made for evaluating V2G-based applications, but not much for EV charging itself. It seems necessary to find out more literature that can explain why real-time scheduling techniques have not been applied for controlling EV charging.

2.3.2 Observations and Technical Gaps

Among a variety of EV charging schemes, the decentralized "valley-filling" approach, which minimizes the total load variance, is the most recently and popularly researched, and many of its variations have been proposed for different objectives such as minimizing system loss or maximizing load factor. It is shown that the valley-filling charging strategy is the most versatile for a given daily load profile prediction in that it achieves the maximum load factor simultaneously and minimizes the daily operating costs of utilities [73]. However, the decentralized valley-filling charging strategy has a number of technical limitations as addressed in §2.1:

- It only deals with day-ahead negotiation of charging profiles.
- The prediction of non-EV power demand must be accurate.
- All EVs must participate in the negotiation simultaneously.
- Energy demand of EVs must be known to utilities beforehand.
- The charging requirements of EVs must not change.
- The scheme does not take into account EV owners' timing constraints.

Since an optimal EV charging profile is determined through a day-ahead negotiation based on the prediction of load profiles, its optimality is very sensitive to the accuracy of load profile prediction. However, the prediction of load profiles might not exactly match the actual load profiles. Also, it it not practical that all EVs participate in the negotiation process at the same time a day before the actual charging, and energy demand of EVs is not necessarily known to utilities beforehand. Finally, the charging requirements of EVs (e.g., plug-in/plug-out time, desired SOC, participation in V2G programs) are subject to change depending on many non-technical factors such as EV owners' charging preferences and daily driving patterns. Therefore, EV charging control must be done in real time rather than through the day-ahead negotiation process in order to tackle all the aforementioned technical limitations of

the valley-filling EV charging strategy.

It is observed that the technical limitations of the valley-filling EV charging strategy can be tackled by applying real-time scheduling techniques, which have been widely researched and applied to a variety of real-time systems, where the satisfaction of timing constraints are as important as the correctness of system outputs. There have been a few attempts to apply a real-time scheduling technique to electric power systems, most of which deal with only deterministic electric load control. The technical limitations of the proposed techniques are as follows:

- They deal with only periodic tasks (i.e., electric loads), of which periods must be known before generating schedule.
- Tasks are assumed to have pre-specified priorities and fixed processing times.
- Each electric load consumes the invariant amount of energy.

However, based on its characteristics, EV charging control must deal with event-driven (i.e., aperiodic) tasks, of which processing times and energy consumed are not invariant, which depend on plug-in/plug-out time and initial/desired SOC. Moreover, in the previous studies, the problem was formulated to minimize household power usage to shave load peak, which does not fit for the EV charging control problem, where the energy in the valley(s) of load profile should be fully utilized, not minimized. Hence, the real-time scheduling algorithms reviewed in §2.1.3 could not be applied to EV charging control problem without any modification, or a new real-time scheduling algorithm needs to be developed to be applied to the EV charging system.

Finally, one of the potential technical benefits of the high penetration of EVs is that an aggregated network of EVs can be used for ancillary service such as frequency regulation and spinning reserves to smooth out the intermittency of renewable energy sources and improve the stability of the grid. There have been many publications that investigate the economic viability of EVs as storage devices for ancillary services and propose a methodology for technical implementation of V2G applications. However,

there are a few papers dealing with both the EV charging control problem and V2G applications. Han *et al.* [25] and Ota *et al.* [62] proposed methods for V2G applications along with EV charging considered, which are verified for the limited number of EVs in the system. Therefore, it is required to develop a smart EV charging system that cannot only accommodate the high penetration of EVs but also facilitate V2G applications.

CHAPTER III

RESEARCH QUESTIONS AND HYPOTHESES

Given the discussion in Chapter 2, research questions are stated herein summarizing the issues raised. These research questions also promote the development of hypotheses that are the main thrust for this research. This chapter consists of two sections. In the first section, a methodology for investigating the applicability of real-time scheduling techniques to EV charging control and developing a real-time EV charging control strategy is discussed, and the other section describes how the proposed real-time EV charging system is augmented with consideration of integrating a vehicle-to-grid (V2G)-based application into the real-time EV charging system in order to evaluate and characterize the impacts of the V2G-based application on real-time EV charging control.

3.1 Real-time Scheduling Techniques for EV Charging Control

As discussed in §2.1.2, the *valley-filling* EV charging control strategy is claimed to be socially optimal in that it tries to minimize the impacts of EV charging on the power grid while accommodating as many EVs as possible without any further financial investment to the existing electric power infrastructure. It achieves its social optimality by trying to use up available electric energy in the valley(s) of load profiles without the consideration of EV owners' charging preferences/requirements when generating EV charging profiles through a *day-ahead* negotiation in which all EV owners are required to participate simultaneously; however, from the practical point of view, satisfying EV owners' charging preferences/requirements is as important as or might be much

more important than minimizing the impacts of EV charging on the power grid. For example, if an EV owner plug out his/her EV from the charging station at an arbitrary, pre-specified time, the valley-filling strategy might not guarantee the desired state-of-charge (SOC) that he/she specified before starting charging. Furthermore, the valley-filling strategy is not likely to guarantee its optimality either if the prediction of a baseload profile (non-EV demand) is inaccurate, if the baseload profile that is used when a set of EV charging profiles are generated is fluctuating due to some reasons, or if actual EV charging requirements (EV demand) are different from ones used for the negotiation process. Therefore, in order to make up for these technical limitations of the valley-filling strategy, an EV charging system should cope with EV owners' random charging behaviors/patterns as well as unpredictable changes in load profiles.

In conclusion, although it is quite obvious, it is desirable to substantiate the expected technical limitations of the valley-filling strategy and, if it turns out to be the case, it is necessary to develop a new EV charging control strategy to satisfy both of the two different – maybe conflicting – objectives: 1) satisfying EV owners' charging preferences/requirements and 2) minimizing the impacts of EV charging on the power grid. Then the question is how to satisfy EV owners' charging preferences/requirements as well as to make the EV charging system less sensitive to the prediction accuracy and/or fluctuation of load profiles and the changes in EV charging requirements, while still guaranteeing the optimality, i.e., minimizing the impacts of EV charging on the power grid. Accordingly, the first research question is formulated as follows:

Research Question I (Application of real-time scheduling techniques to EV charging control): *How can EV charging be controlled to satisfy EV owners' charging preferences/requirements while filling the technical gaps of the valley-filling strategy?*

This research question is directly related to filling the technical gaps of the valley-filling EV charging scheme. It is claimed in §2.3.2 that the technical limitations can be alleviated by introducing real-time scheduling techniques for controlling EV charging. This argument is made based on three reasons. First, the baseload profile (non-EV demand) is difficult to predict accurately and is likely to change in a random manner as electricity generation does, resulting from the introduction of renewable energy sources (RES) such as solar and wind. Therefore, an EV charging system should control EV charging based upon real-time demand measurements to respond quickly to the changes in load profiles. Secondly, since it is also almost impossible to force all EV owners to take part in the negotiation process at the same time to generate EV charging profiles, which is required by the valley-filling strategy, and EV owners' charging behaviors/patterns are also quite unpredictable, an EV charging system must deal with EV owners' charging preferences/requirements based on the information that EV owners provide when they plug in their cars to the charging station at home or work. Lastly, it is furthermore required to make an EV charging system guarantee the satisfaction of timing constraints, not to mention filling the battery up to the SOC that EV owners want to have when they drive off their cars. Therefore, the following hypothesis is to be investigated in response to the above research question.

Hypothesis I: *The application of real-time scheduling techniques will enable EV charging to be controlled in real time so that it can fill the technical gaps of the valley-filling charging strategy as well as achieve the social optimality of the valley-filling EV charging strategy.*

Real-time scheduling techniques have been widely researched and applied to many real-time embedded systems, where the satisfaction of timing constraints is as important as the correctness of system responses or outputs. The EV charging problem

can be interpreted as a real-time scheduling problem in that one of its objectives is to obtain a solution by which a battery is charged up to a certain level – the correctness of system responses – by the time an EV owner specifies – the satisfaction of timing constraints. Also, it is expected that the effects of inaccuracy of load profile prediction and random EV owners' charging behaviors/patterns on the optimality of the EV charging system can be mitigated by applying real-time scheduling techniques since a real-time scheduling algorithm will allow the system to be controlled based upon real-time demand measurements and the information EV owners provide when they plug their vehicles in. Accordingly, it is safely postulated that the issues described herein can be resolved by applying real-time scheduling techniques to the EV charging control problem, if possible.

3.1.1 EV Charging Control System as a Real-time System

A smart EV charging system might need to control the charging of EVs in real time to guarantee its optimality in terms of minimizing total load variance as well as to satisfy EV owners' charging preferences/requirements as reviewed in Chapter 2. Also, it is hypothesized that real-time scheduling techniques can be utilized to achieve these goals. According to [14], in order to apply a real-time scheduling technique, a system must have the features that real-time systems typically have so that its tasks (τ_i) can be mathematically represented with real-time system parameters such as period (p_i), execution time (e_i), and deadline (d_i). Therefore, the first step to develop a real-time EV charging control strategy is to see if an EV charging system can be modeled with the parameters enumerated above as a real-time system.

Research Question I-1: *How can real-time scheduling techniques be applied to EV charging control?*

As discussed above, if an EV charging system can be modeled as a real-time

system, then a real-time scheduling problem can be formulated to tackle the technical limitations of the existing EV charging control strategy, while still providing the technical/economical benefits that the valley-filling strategy can offer. In order to answer this research question, the following hypothesis is postulated:

Hypothesis I-1: *Real-time scheduling techniques can be applied to EV charging control if an EV charging system can be modeled such that its system model has all generic parameters required to apply real-time scheduling techniques.*

In general, a real-time system requires a real-time operating system that provides a real-time scheduling capability and typically consists of a *waiting queue* (or *ready queue*), a *real-time scheduler*, and *processing queues* (or *processors*) as depicted in Figure 45. Once a task or an event has arrived at the real-time system, it is first assigned to the waiting queue, where tasks are waiting to be released to the processing queue by the real-time scheduler. The real-time scheduler determines which tasks can be released to the processing queue in accordance with a specific real-time scheduling algorithm, for example, Earliest Deadline First (EDF) scheduling algorithm with static- or dynamic-priority assignment policy.

From the illustration in Figure 46, if each charging station can be viewed as a *processor* or *processing queue*, then an EV charging system can be represented as a *soft real-time system*[1] with variable number of heterogeneous, multiple processors

[1] "A soft real-time system is a real-time system in which performance is degraded but not destroyed

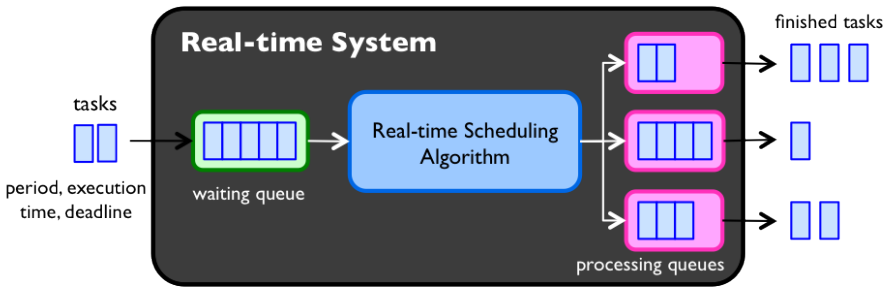

Figure 45: Schematic representation of a generic real-time system.

Table 6: System timing characteristics.

Real-time system	EV charging system
Task, τ_i	Charging an EV
Period, T_i	N/A
Execution time, C_i	Charging time
Deadline, D_i	Plug-out time

because power ratings of each charging station will be different and the number of charging stations that can be activated simultaneously will keep varying, depending on the available energy for EV charging. Also, charging an EV can be viewed as a *task* or an *event* in a real-time system, of which execution time (e_i) can be estimated based on the difference between current and desired SOC, and of which deadline (d_i) will be plug-out time (t_{plugout}). Timing characteristics of the EV charging system are summarized in Table 6. It can be seen that the task, i.e., charging an EV, has all the timing parameters required to design or apply a real-time scheduling algorithm. However, there is no parameter that can be directly related to the period (p_i) of a real-time task because charging an EV could be a periodic event, but its period

by failure to meet response-time constraints" [41].

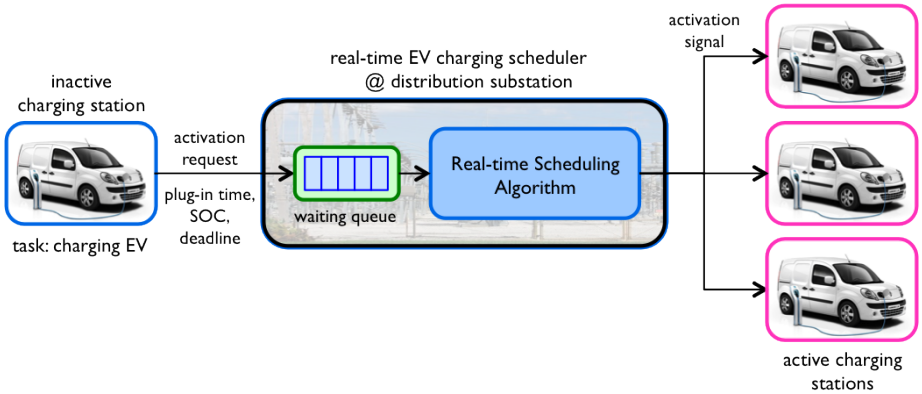

Figure 46: System model of an EV charging system as a real-time system.

may not be deterministic. Furthermore, only a daily EV charging scheduling is dealt with in this research, and the typical time interval between daily charging is 24 hours in average. Thus, the period needs not necessarily be considered in this research. Also, the priority of an EV could be assigned based on the amount of time to refill the battery up to desired SOC specified by the EV owner. As a result, it can be concluded that real-time scheduling techniques are applicable to the EV charging control problem, and, in doing so, the technical gaps of the valley-filling charging scheme can be filled, in other words, EV charging control can be done in real time.

EVs could be charged at different places such as a company's parking deck, public charging stations, or home. However, since it is not realistic to assume that EVs could be charged at any places where a standard power outlet is present, the batteries of the vehicles are assumed to be charged at home, equipped with a charger, in this research. Figure 47 illustrates the operating scenario for real-time EV charging control, proposed in this research. After coming from work, an EV owner plugs his/her car in to the charging station connected to the outlet on the wall, and sets up his/her charging preferences/requirements such as desired SOC on departure and expected plug-out time. Then, the charging station sends an activation request message containing the charging requirements to the real-time EV charging dispatch scheduler in a substation via a communication link such as Ethernet, power line communication or carrier (PLC), etc. EVs having sent activation request messages are assigned to the waiting

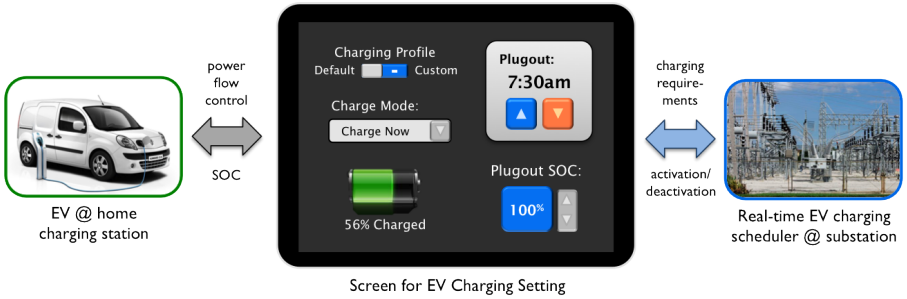

Figure 47: Operating scenario for the proposed real-time EV charging system.

queue of the real-time EV charging scheduler. Once after priorities are calculated and assigned to each charging station based on the charging requirements, the real-time EV charging scheduler determines a feasible charging schedule, and sends activation signals back to charging stations that can be assigned to a processing queue or wait signals back to charging stations that cannot be assigned to a processing queue due to their lower priorities. EVs not assigned to a processing queue are waiting to be assigned to any of available processing queues at the next scheduling iteration, typically after 15 minutes.

Figure 48 overviews the schematic representation of the proposed method of real-time EV charging control. As mentioned earlier, the EV charging system can be viewed as a soft real-time system with charging stations analogous to multiple processors, the number of which we must know to apply a real-time scheduling algorithm. Since each active charging station — a charging station activated to charge an EV — can be viewed as a processor or a processing queue, the number of charging stations that can be activated to charge EVs can be calculated by dividing the difference

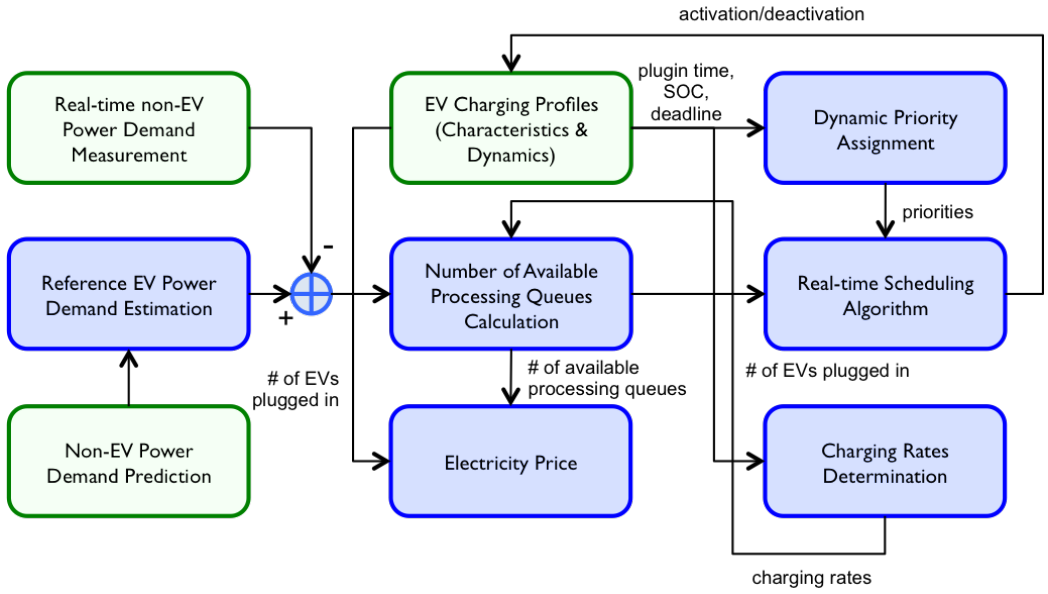

Figure 48: Overview of real-time scheduling for EV charging control.

between the reference EV power demand and real-time non-EV power demand measurements, which can be utilized to refill the batteries of EVs, by the maximum charging rate as follows:

$$n_{\mathrm{PQ}}(t) = \left(P_{\mathrm{ref}}(t) - P_{\text{non-EV}}(t)\right)/r_{\max} \tag{3.1}$$

where n_{PQ} is the number of processing queues, i.e., charging stations that can be activated simultaneously, P_{ref} is the reference EV power demand, $P_{\text{non-EV}}$ is the real-time non-EV power demand measurements, and $r_{\max}$ is the maximum charging rate.

A day-ahead generation plan, which can be established based on the prediction of non-EV power demand, can play an role as a reference EV power demand, from which the deviation will be minimized to achieve the social optimality of the valley-filling scheme. Based on the charging requirements of EV owners, the real-time scheduling algorithm assigns and updates dynamic priorities of charging stations, and determines which charging stations can be activated/deactivated. For the purpose of incorporating the V2G concept into the real-time EV charging system, the electricity prices for grid-to-vehicle (G2V) and V2G can also be taken into account. As will be discussed later, an optimization problem for charging rate control is also formulated since the assumption that an EV can be refilled only at the maximum charging rate might degrade the performance of the proposed algorithm and the longevity of the battery, and it is also impractical to increase charging current from zero to maximum ratings. The most important task when developing a real-time EV charging system is to design or choose a real-time scheduling algorithm and a dynamic-priority assignment policy for the EV charging system, which are discussed in the following section.

The proposed real-time EV charging system can be viewed as an extension of the existing valley-filling charging strategy in that it can achieve the optimality of the valley-filling charging strategy in terms of minimizing total load variance (a utility's functional requirement), but, in addition, it can also guarantee the satisfaction of

EV owners' charging preferences/requirements, i.e., *complete charging* (consumers' functional requirements) *by when they want to plug out their cars* (consumers' timing constraints). Therefore, by definition, it can be thought of as a real-time system where timing constraints as well as functional requirements must be satisfied.

3.1.2 Real-time Scheduling Algorithms for EV Charging Control

As discussed in §3.1.1, the characteristics of an EV charging system implies that it can be viewed as a soft real-time system with variable number of multiple, heterogeneous processors, or processing queues, because power ratings of each charging station might be different and the number of processing queues keeps varying based on electric power available for EV charging. In addition, the real-time scheduling for EV charging must be event-driven as well as online, and its tasks have variable processing (charging) times, and the priorities of the tasks might need to be assigned and updated dynamically based on the amount of time to refill their batteries. If it is possible to model an EV charging system as a real-time system, then the next step is to identify a real-time scheduling algorithm that can be applied to the EV charging system. Hence, the second sub research question arises as follows:

Research Question I-2: *Is there any real-time scheduling algorithm applicable to the EV charging system that can be represented as a multiprocessor system with variable number of heterogeneous processors?*

There are a number of standard scheduling algorithms such as First Come, First Served (FCFS), Shortest Job First (SJF), Earliest Deadline First (EDF), and Rate Monotonic (RM). Then, how do we select a right scheduling algorithm for EV charging control? Is there any scheduling algorithm that can be immediately applied to the problem without any modification? In fact, there is no intuitive and direct way,

based on an educated guess, to know whether or not a real-time scheduling algorithm is applicable to the scheduling problem with multiple processors. There are many approaches for simple, uniprocessor cases, such as Rate Monotonic Analysis (RMA), Worst Case Execution Time Analysis (WCETA), and system-level performance modeling analysis, which are claimed to be extremely difficult to be deployed for multiprocessor problems and in many cases impossible to configure [1]. Therefore, in order to figure out a right scheduling algorithm without a lot of efforts and time, the simplest way is to identify all real-time scheduling algorithms that seem to be applicable to EV charging, evaluate them with heuristics such as Monte Carlo simulations, and select the best one that can provide the best results in terms of performance metrics, defined for the problem of interest. As a consequence, the hypothesis that can answer the research question can be formulated as:

Hypothesis I-2: *If it can deal with all the aforementioned characteristics of the real-time EV charging system, a real-time scheduling algorithm could be applied to the real-time EV charging system, and, among those satisfying the requirements, the most suitable real-time scheduling algorithm can be determined through statistical performance evaluation.*

As will be detailed in Chapter 4, *Theoretical Foundations*, there are two categories of real-time scheduling algorithms for multiprocessor systems: partitioning algorithm and global scheduling algorithm. Algorithms that can be applied to the problem depend on both what the real-time system model of the EV charging system looks like and what real-time characteristics it has. In order to apply the two categories of algorithms to EV charging scheduling, four different EV charging modes, which might be specified by an EV owner when plugging in or might be contracted with utilities, are introduced as summarized in Table 7. EVs with charging mode 1 will start charging right after plugged in and charging requirements are specified, or right

Table 7: EV charging modes.

Mode	Description
1	charge now
2	charge when power is available
3	charge when given electricity price is less expensive
4	charge/supply (V2G)

after the charging window that is set by a utility begins. EVs with charging mode 2 will start charging when power is available after all EVs with charging mode 1 have started charging. EVs with charging mode 3 will start charging when the electricity price is less expensive than what EV owners have set or contract with utilities. EVs with charging mode 4 will draw power from the grid or supply power to the grid depending on electricity price set by owners or contract with utilities.

By introducing the different EV charging modes, either partitioning or global scheduling algorithms, or both, that is, hybrid algorithms, may be applied to the real-time EV charging system. Charging stations can be partitioned into the set of charging stations based on the charging modes of EVs plugged in to the charging stations, and priorities are assigned to charging stations within the set of a charging mode. Charging stations of a charging mode are activated based on the priorities, exclusively from the sets of other charging modes. Thus, a partitioning scheduling algorithm can be applied to the real-time EV charging system. On the other hand, a global scheduling algorithm can be applied to the real-time EV charging system as follows: a priority is assigned to each charging station based on both the amount of time to refill the battery and charging mode of the EV that is plugged in to the charging station, and the real-time scheduling algorithm allows a charging station with higher priority to be activated, no matter what charging mode it belongs to.

After identifying all scheduling algorithms applicable to the problem, they will be evaluated in terms of performance metrics and, among those, the best algorithm that has the highest guarantee ratio, defined as the ratio of the number of EVs satisfying their desired SOCs at their deadlines to the total number of EVs in the system, the largest averaged plug-out SOC over all EVs, and the least total load variance will be chosen and used for simulation studies.

3.1.3 Charging Rates Control for Maximum Energy Utilization

From the proof-of-concept simulation, which will be presented in §6.2, it is observed that all EVs are not fully charged even though, theoretically, they should be fully charged because the reference EV power demand is estimated based on the total energy required for the EVs to be fully charged. The main reason is that the end of the charging window for the reference EV power demand estimation is set to be later than plug-out times of all EVs so that the two valleys, which can be seen in typical winter load profiles, are fully filled. For another reason, it is hypothesized that EVs with lower priorities won't have enough opportunities to occupy virtual processing queues, and, as a result, fail to meet their deadlines. Therefore, in order to increase the guarantee ratio of the proposed real-time EV charging system, it is required to increase the probability that EVs with lower priorities can occupy processing queues by increasing the number of available processing queues at a given time slot, in other words, not charging EVs at the maximum charging rates.

For example, there are four EVs as illustrated in Figure 49. EV 1 has the highest priority while EV 4 has the lowest priority. The number of vertically-stacked squares represents the number of processing queues in a given time slot and the height of a square represents the maximum charging rate. It is assumed that 6 consecutive squares are required for EV 4 to be fully charged. Since the algorithm is designed to refill the battery at the maximum rate, EV 4 misses its deadline even though there

are unused processing queues. If EV 4 can be charged at the rate higher than the maximum rate, which does not make sense, then the unused processing queues can be used up and thus EV4 can be fully charged. Therefore, it can be inferred that EVs with lower priorities are more likely to occupy processing queues earlier during the charging window if the number of processing queues is increased by adjusting charging rates for a given time slot. This observation leads to the third sub research question:

Research Question I-3: *Do charging rates affect the optimality and the guarantee ratio of the real-time EV charging system, and, if so, how can they be controlled so as for its optimality and guarantee ratio to be improved?*

The proposed real-time EV charging control algorithm achieves the "*valley-filling*" by adjusting the number of EVs that can be charged simultaneously at the maximum charging rate ($r_{\max}$), calculated based on the difference between the reference power demand (P_{ref}) and the aggregated non-EV demand for a given time slot. In other words, the number of EVs that can be charged at the same time is determined so that it can maximize the energy utilization, defined as the ratio of the energy consumed by EVs to the available energy for EV charging during a time slot. However, if EVs are charged at the maximum charging rate, the number of EVs that can be charged

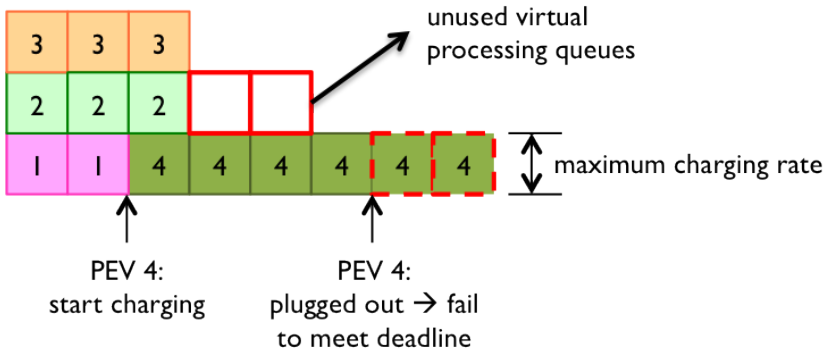

Figure 49: Underutilization of processing queues.

simultaneously is minimum, which indicates that the number of the charging stations, where EVs with lower priorities were plugged in, can be activated will be minimum. Therefore, the charging rate must be determined based on both the energy utilization and the number of EVs that can be charged at the same time to increase the guarantee ratio, and thus the following hypothesis is formulated to answer the research question:

Hypothesis I-3: *If charging rates are controlled based on both the energy utilization and the number of EVs that are charging simultaneously for a given time slot, then the performance of the real-time EV charging system will be improved.*

Let $E_{\mathrm{a}}(t)$ and $E_{\mathrm{c}}(t)$ denote the available energy for EV charging and the energy consumed by EVs at time t, respectively, defined as:

$$E_a(t) \triangleq (P_{\mathrm{ref}}(t) - P_{\mathrm{base}}(t))\Delta t \quad \text{and} \quad E_c(t) \triangleq n_{\mathrm{PQ}}(t)\frac{r(t)}{\eta}\Delta t, \tag{3.2}$$

if it is assumed that all EVs are charging at the same charging rate with the same charging efficiency, where $P_{\mathrm{ref}}(t)$ and $P_{\mathrm{base}}(t)$ are the reference power demand and the non-EV power demand at time t, respectively, $n_{\mathrm{PQ}}(t)$ is the number of charging stations activated at time t, η is the charging efficiency, $r(t)$ is the charging rate at time t, and Δt is the duration of a time slot. Then, the energy utilization at time t, $U(t)$, can be defined as:

$$U(t) \triangleq \frac{E_c(t)}{E_a(t)}, \tag{3.3}$$

where $E_a(t) \geq E_c(t)$ for all t. In order to achieve the near-optimality in terms of minimizing the total load variance, i.e., to maximize the energy utilization, an optimization problem can be formulated as:

$$\text{maximize } \frac{E_c(t)}{E_a(t)} \qquad \text{for } t = 1, \ldots, T \tag{3.4}$$

or

$$\text{minimize } \{E_a(t) - E_c(t)\}^2 \qquad \text{for } t = 1, \ldots, T \tag{3.5}$$

In accordance with Equation (3.5), if, without loss of generality, charging stations having activated by time t are indexed as 1, 2, ..., $m(t)$, then the optimization problem can be reformulated as:

$$\underset{\mathbf{r}(\cdot),\, m(t)}{\text{minimize}} \left\{ (P_{\text{ref}}(t) - P_{\text{base}}(t)) - \sum_{i=1}^{m(t)} \frac{r_i(t)}{\eta_i} \right\}^2 \qquad \text{for } t = 1, \ldots, T \tag{3.6}$$

subject to

$$0 \le r_i(\cdot) \le r_{\max}(i) \qquad \text{for } i = 1, \ldots, m(t) \tag{3.7}$$

where $\mathbf{r}(\cdot) \triangleq \{r_1(\cdot), \ldots, r_{m(t)}(\cdot)\}$, $r_i(t)$ is the charging rate of the i-th EV at time t, η_i is the charging efficiency of the i-th EV, and $m(t)$ can be seen as the number of processing queues occupied by EVs at time t. In addition, the total number of available processing queues is calculated as:

$$n_{\text{PQ}}(t) \triangleq \frac{P_{\text{ref}}(t) - P_{\text{base}}(t)}{\max(r_{\max}(n))/\max(\eta_n)} \tag{3.8}$$

for $n = 1, \ldots, N$ and $t = 1, \ldots, T$. If it is assumed that $r_n(t)$ and $\eta_n(t)$ are the same for all EVs for all t, i.e., $r(t) \triangleq r_1(t) = \cdots = r_n(t)$ and $\eta \triangleq \eta_1 = \cdots = \eta_n$, then Equations (3.6) and (3.8) can be written as:

$$\underset{r(t),\, m(t)}{\text{minimize}} \left\{ (P_{\text{ref}}(t) - P_{\text{base}}(t)) - m(t)\frac{r(t)}{\eta} \right\}^2 \qquad \text{for } t = 1, \ldots, T \tag{3.9}$$

subject to

$$0 \le r(t) \le \min_i r_{\max}(i) \qquad \text{for } i = 1, \ldots, m(t), \tag{3.10a}$$

$$n_{\text{PQ}}(t) = \frac{P_{\text{ref}}(t) - P_{\text{base}}(t)}{r_{\max}/\eta} \qquad \text{for } t = 1, \ldots, T. \tag{3.10b}$$

From Equations (3.9) and (3.10b), the optimization problem maximizing the energy utilization becomes:

$$\underset{r(t),\, m(t)}{\text{minimize}} \frac{1}{\eta} \{n_{\text{PQ}}(t) r_{\max} - m(t) r(t)\}^2 \qquad \text{for } t = 1, \ldots, T. \tag{3.11}$$

subject to

$$0 \leq r(t) \leq \min_i r_{\max}(i) \qquad \text{for } i = 1, \ldots, m(t), \tag{3.12a}$$

$$0 \leq m(t) \leq n_{\mathrm{PQ}}(t) \qquad \text{for } t = 1, \ldots, T \tag{3.12b}$$

Therefore, it is mathematically proved that the energy utilization is maximized when $r(t) = r_{\max}$ and $m(t) = n_{\mathrm{PQ}}(t)$ for all t, which indicates that charging rate should be the same with one used for calculation of $n_{\mathrm{PQ}}(t)$ and the available processing queues should be fully utilized.

Let $n_{\mathrm{rem}}(t)$ and $n_{\mathrm{req}_i}(t)$ denote the number of remaining time slots and the number of time slots necessary for the i-th EV to be fully charged at time slot t, respectively. Then, the probability that an EV would miss its deadline can be expressed as:

$$\mathrm{Prob}\{i\text{-th EV would miss its deadline}\} \triangleq \begin{cases} 0 & \text{if } n_{\mathrm{req}_i}(t) = 0 \\ n_{\mathrm{req}_i}(t)/n_{\mathrm{rem}}(t) & \text{if } 0 < n_{\mathrm{req}_i}(t) < n_{\mathrm{rem}}(t) \\ 1 & \text{if } n_{\mathrm{req}_i}(t) \geq n_{\mathrm{rem}}(t) \end{cases} \tag{3.13}$$

Hence, an optimization problem to minimize the probability of failure can be formulated as:

$$\text{minimize } \frac{\sum_{i=1}^{N} n_{\mathrm{req}_i}(t)}{n_{\mathrm{rem}}(t)} = \underset{r(t)}{\text{minimize}} \quad \frac{\sum_{n=1}^{N} E_n(t)/(\eta r(t)\Delta t)}{T - t} \tag{3.14}$$

for $t = 1, \ldots, T$. From Equation (3.14), it can be seen that the charging rate $r(t)$ must be maximum in order for the probability of failure to be minimized, which is the same as the maximum energy utilization problem.

On the other hand, since, based on the observation described previously, charging EVs at the maximum rates leads to the minimum number of EVs that can be charged at the same time, which keeps EVs with lower priorities from charging, the charging rate should be controlled so as to accommodate as many EVs as possible to provide more chance to occupy processing queues for EVs with lower priorities . Therefore,

an optimization problem maximizing the number of available processing queues (n_{PQ}) can be formulated as:

$$\underset{r(t)}{\text{maximize}} \ \frac{P_{\mathrm{ref}}(t) - P_{\mathrm{base}}(t)}{r(t)/\eta} \qquad \text{for } t = 1, \ldots, T, \tag{3.15}$$

subject to

$$0 \leq r(t) \leq \min_{i} r_{\max}(i) \qquad \text{for } i = 1, \ldots, N \tag{3.16}$$

which requires $r(t)$ to be minimized in order to obtain as many available processing queues as possible.

In consequence, Equations (3.14) and (3.15) are two conflicting objectives that the real-time EV charging system needs to accomplish simultaneously: one objective is to maximize the energy utilization, i.e., to minimize the deviation from the reference power demand (P_{ref}), by maximizing $r(t)$, and the other is to maximize the number of available processing queues, i.e., to increase the chance for EVs with lower priorities to occupy processing queues by minimizing $r(t)$. However, combining Equation (3.14) with Equation (3.15) yields a new optimization problem that satisfies both the objectives:

$$\underset{r(t)}{\text{minimize}} \quad \left\{ \omega_1 \underbrace{\left[\frac{\sum_{n=1}^{N} E_n(t)/(\eta r(t) \Delta t)}{T - t} \right]}_{\substack{\text{minimize probability of failure} \\ \Updownarrow \\ \text{maximize} \\ \text{the energy utilization}}} + \omega_2 \underbrace{\left[\frac{r(t)/\eta}{P_{\mathrm{ref}}(t) - P_{\mathrm{base}}(t)} \right]}_{\substack{\text{maximize \# of} \\ \text{processing queues}}} \right\} \tag{3.17}$$

subject to

$$0 \leq r(t) \leq \min_{i} r_{\max}(i) \qquad \text{for } i = 1, \ldots, N \tag{3.18}$$

for $t = 1, \ldots, T$, where ω_1 and ω_2 are weighting factors, and $\omega_1 + \omega_2 = 1$. Since, through Equation (3.17), $r(t)$ is determined such that it maximizes the energy utilization while maximizing the number of available processing queues, it is expected that the proposed real-time scheduling algorithm for EV charging will provide better

optimality and guarantee ratio by allowing more EVs to be charged simultaneously even though some EVs take more time to complete their charging.

3.2 V2G-based Ancillary Services within Real-time EV Charging Control Framework

As large-scale renewable energy sources (RES) are integrated in the power grid, the battery energy storage is believed to perform an important role for smoothing their natural intermittency in order to ensure grid-wide frequency stability. "An EV can be used as both a load and a generating source to balance the system frequency by charging the battery when there is too much generation in the grid and acting as a generator by discharging the battery when there is too much load in the system" [35]. In addition, a large population of EVs not only introduce a potential benefit as distributed battery energy storages but also provide plenty of time for control because they are almost plugged in to power outlets for most of the time. Therefore, vehicle-to-grid (V2G) technology, which will be detailed in §4.3.2, is expected to be one of the key technologies in the smart grid. As reviewed in §2.2, most publications on V2G technologies dealt with either the economic viability or technical implementations of the technologies, but a few made an attempt to address scheduled EV charging along with consideration of V2G-based ancillary services such as load frequency control (LFC) and spinning reserves.

However, since V2G-based services can be operated only while EVs are connected to the grid, it is highly likely that EV charging will be interrupted by V2G-based services, which means that EVs might not complete charging by their plug-out times and might not have the desired departure SOC that EV owners might specify before starting charging. Therefore, the operation of V2G-based services must be done in such a way that its impacts on EV owners' convenience is negligible, or at least minimized. In this context, the following research question arises:

Research Question II (Integration of V2G-based Ancillary Services into the Real-time EV Charging System): *How can the impacts of the operations of V2G-based services on EV charging be investigated?*

As discussed in Chapter 2 and the above, V2G-based services can be provided only when EVs are connected to the grid. EVs might be charged or in idle state, depending on the schedule generated by the real-time EV charging system. EVs in charging state will not supply power to the grid, and EVs plugged in to deactivated charging stations will not draw power from the grid. In addition, some EV owners might not want to sell power to the grid, and others might be willing to provide power to the grid. Therefore, V2G-based services are closely related to the EV charging system and EV owners' preferences. Hence, the following hypothesis is formulated to answer the question:

Hypothesis II: *If V2G-based services can be incorporated into the real-time EV charging control strategy, then the impacts of the operations of V2G-based services on EV charging can be investigated and characterized.*

The participation of EVs in the V2G ancillary market will be determined based on its charging status, i.e., active/inactive and state-of-charge (SOC). For instance, if it is plugged in and with higher SOC and it has enough time to complete charging, then an EV can sell power to the grid for up-regulation. If it is plugged in, but with lower SOC, or if there is not enough time to complete charging, it cannot sell power, but still continues charging to satisfy its charging requirements. For down-regulation, the charging rates of EVs with lower SOC can be increased depending on their current charging rates as well as power ratings of the charging station to which they are plugged in, and, in turn, the system frequency will decrease down to the nominal system frequency; however, the charging rate of an EV with higher SOC cannot be increased for down-regulation. In the similar fashion, an aggregated network of EVs

can provide V2G-based services to the grid while their charging requirement are still satisfied.

According to Kempton *et al.*, "the most economic entry for V2G-based applications is the market for ancillary services (A/S), among which frequency regulation is the most valuable market" [35]. Therefore, in this research, amongst various V2G-based ancillary services, frequency regulation is only considered to narrow down the scope of work, and it is expected that other ancillary services can be incorporated into the proposed real-time EV charging control strategy in the similar way that frequency regulation is incorporated. In the following subsections, sub research questions related to Research Question II and corresponding hypotheses regarding a methodology for incorporating V2G-based frequency regulation into the real-time EV charging system are discussed.

3.2.1 Integration of V2G-based Frequency Regulation into Real-time EV Charging Control

As issued previously, it is suspected that V2G-based applications might affect the performance of the real-time EV charging system. Accordingly, the second research question arises, and in order to answer the question, it is hypothesized that the incorporation of V2G-based services into the real-time EV charging algorithm will enable their impacts on real-time EV charging to be investigated and characterized. Therefore, the following fundamental question is required to be answered first to test Hypothesis II.

Research Question II-1: *How can V2G-based frequency regulation be incorporated within the framework of real-time EV charging control?*

Some of EV owners might want to participate in V2G-based frequency regulation, but some might not. Also, some of EV owners might be willing to take part in the program only when benefits they could get is larger than costs they might need to pay.

Furthermore, the participation in V2G-based programs could be determined by EV owners' daily preferences or contracts with utilities. In conclusion, the participation in V2G-based programs will be determined by EV owners' preferences and electricity price for frequency regulation market. In addition, charging rates of EVs will need to be determined by the type of V2G-based regulation and current SOCs of EVs, as well as the amount of energy required to stabilize the system frequency. Thus, the following hypothesis can be formulated:

Hypothesis II-1: *The introduction of different charging modes and the control of both charging rates of EVs that opt to participate in V2G-based frequency regulation and the number of EVs charging simultaneously will enable V2G-based frequency regulation to be incorporated in the real-time EV charging system.*

As explained in §3.1.2, there might be several charging options depending on EV owners' preferences. In this research, four charging modes are considered: 1) *charge now*, 2) *charge when power is available*, 3) *charge when given less expensive electricity price*, and 4) *buy(sell) power from(to) the grid (V2G)*. Figure 50 illustrates how the different charging modes can be translated in the context of the real-time EV charging system. For charging mode 1, EVs will start charging when the number of processing queues is greater than 0, that is, when power is available. EVs with charging mode 2 will initiate charging process when there are still available processing queues after some of processing queues have been assigned to all the EVs with charging mode 1. The charging of EVs with mode 3 will be activated when market electricity prices is less than the price that EV owners have set. Lastly, EVs with mode 4 will buy/sell power from/to the grid depending on real-time V2G market clearing price. EVs that participate in V2G-based programs could be identified by owner's charging preferences or contracts with utilities. Therefore, the participation in V2G-based programs can be controlled in the real-time EV charging system by introducing different charging

modes to let some portion of EVs in the system sell electricity to the grid.

By introducing different charging modes, the real-time EV charging system can include V2G-based frequency regulation in its scheduling process. For instance, if EVs need to purchase power from the grid for down-regulation, i.e., when generation exceeds load, the real-time EV charging system will increase the number of EVs that can be charged at the same time (i.e., increase $n_{\mathrm{PQ}}(t)$), encourage EVs with charging mode 3 by reducing electricity price, or increase charging rates. On the other hand, for up-regulation, when load exceeds generation, the real-time EV charging system will increase electricity price to discourage EVs to start charging, deactivate EVs with lower priorities or lower charging modes to reduce power demand due to EV charging, or decrease the number of EVs being charged at the same time based on their priorities.

Additionally, charging rates are required to be adequately sized and balanced in the long run so that the SOC of an EV opting to participate in V2G-based frequency regulation would only fluctuate around its SOC before participating in the program; it should be neither completely drained or filled. In developing the real-time scheduling algorithm for EV charging and the optimization problem for charging rates, only

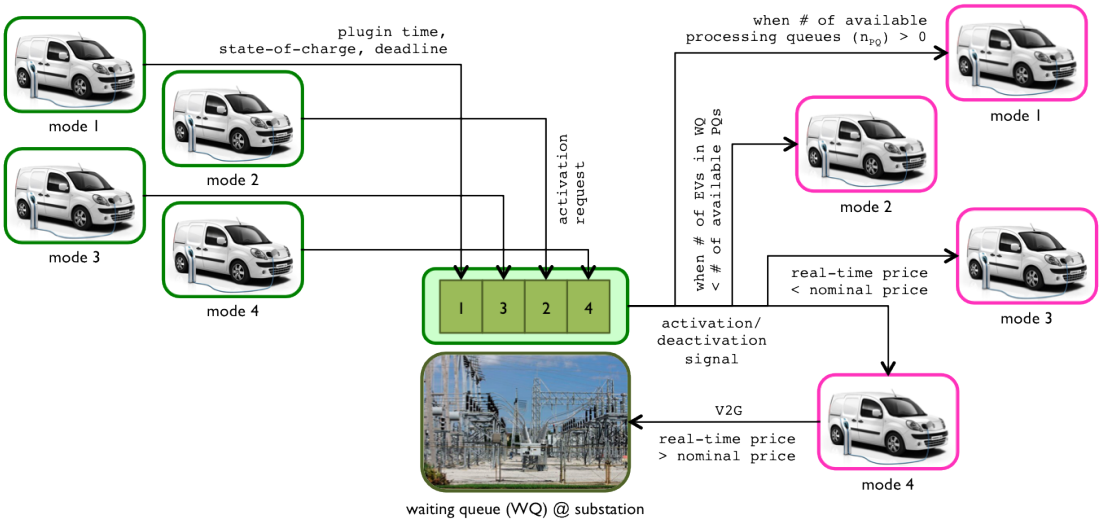

Figure 50: Possible EV charging modes.

positive charging rates, that is, drawing power from the grid, are only considered. However, it is necessary to consider negative charging rates, which represent selling power to the grid, in order to consolidate V2G-based frequency regulation into the real-time EV charging system. Therefore, the constraint for charging rates in Equation (3.17) needs to be modified to facilitate the V2G-based frequency regulation as:

$$\underset{r(t)}{\text{minimize}} \quad \left\{ \omega_1 \left[\frac{\sum_{n=1}^{N} E_n(t)/(\eta r(t) \Delta t)}{T-t} \right] + \omega_2 \left[\frac{r(t)/\eta}{P_{\text{ref}}(t) - P_{\text{base}}(t)} \right] \right\} \tag{3.19}$$

subject to

$$-\min_i r_{\max}(i) \leq r(t) \leq \min_i r_{\max}(i) \qquad \text{for } i = 1, \ldots, N \tag{3.20}$$

for $t = 1, \ldots, T$, where ω_1 and ω_2 are weighting factors, and $\omega_1 + \omega_2 = 1$. Furthermore, in order to force the SOC of an EV to fluctuate around its SOC right before participating in the program, the following constraint should also be satisfied:

$$\sum_{i=1}^{n_{\text{up}}} r_{\text{up}}(i) \approx \sum_{j=1}^{n_{\text{down}}} r_{\text{down}}(j) \tag{3.21}$$

where n_{up} and n_{down} are the number of participations for up- and down-regulation, respectively, and r_{up} and r_{down} are charging rates for up- and down-regulation, respectively.

Another factor that needs to be considered is SOCs of EVs. The key benefit we can get by introducing the real-time scheduling technique to the EV charging system is that it enables to satisfy timing constraints of EV owners while maintaining the optimality in terms of minimizing total load variance. Therefore, timing constraints must be satisfied even when V2G-based frequency regulation is contained in the real-time EV charging system. To achieve this goal, the participation in V2G-based frequency regulation must be determined based on the SOC. For example, an EV with higher SOC is more appropriate than one with lower SOC for up-regulation in that the former is more likely to arrive at the desired departure SOC than the latter

after returning from the service for a given number of time slots. For down-regulation, an EV with lower SOC needs to be charged earlier than one with higher SOC so that the overall probability of failure can be minimized. Therefore, EVs will have different desirabilities for participating in the program depending on their SOC.

As discussed above, with the appropriate control of charging rates and the determination of participation depending on SOCs, the introduction of various charging modes with the adjustment of ancillary service clearing price will enable the incorporation of V2G-based frequency regulation into the real-time EV charging system along.

3.2.2 Statistical Reference EV Power Demand Estimation

One of the technical limitations of the "valley-filling" strategy for EV charging control is that the optimality of the charging profile generated by the strategy is significantly sensitive to uncertainties such as inaccurate load prediction, unexpected load changes, or generator failures. Accordingly, an EV charging system should be capable of coping with those uncertainties in order to achieve the optimality (in terms of minimizing total load variance) that can be guaranteed only when there are no such unfavorable conditions. The real-time EV charging system has a possibility to minimize the effects of uncertainties in that it controls EV charging based on real-time measurements of power demand and generation capacity, which results in a kind of V2G-based frequency regulation that would correct the frequency deviation due to EV power demand. Even though energy flow is quite different, the total energy consumed by EV charging, however, is the same for both cases: without and with V2G-based frequency regulation. Therefore, it can be claimed that EVs opting to participate in frequency regulation might violate their timing constraints or might not arrive at the desired departure SOCs since they need to provide power to the grid during the process of charging, which implies that they would take longer time to complete

charging. Hence, the following sub research question arises:

Research Question II-2: *How can the real-time EV charging system be made to satisfy timing constraints while providing V2G-based frequency regulation?*

Since, in the proposed real-time EV charging system, the number of available processing queues is calculated as

$$n_{\mathrm{PQ}}(t) = \frac{P_{\mathrm{ref}}(t) - P_{\mathrm{base}}(t)}{r_{\mathrm{opt}}(t)} \tag{3.22}$$

where $P_{\mathrm{ref}}(t)$ and $P_{\mathrm{base}}(t)$ are the reference EV power demand and non-EV power demand at time t, respectively, and $r_{\mathrm{opt}}(t)$ is the optimized charging rate, uncertainties in the prediction of load profiles are reflected in $P_{\mathrm{base}}(t)$ and, thus, the effects of uncertainties might be minimized so that the optimality can still be maintained. Moreover, in case of generation insufficiency, where power demand is greater than the predicted or there is a generator failure, V2G-based frequency up-regulation can be operated to compensate for the lack of generation rather than simply reducing the number of EVs being activated for charging, at the expense of the degradation of guarantee ratio. As a result, a compensation for V2G-based frequency regulation is necessary to make the guarantee ratio as high as that of the case without V2G-based frequency regulation. Therefore, the following hypothesis is claimed to answer the question:

Hypothesis II-2: *If the statistics of EV charging profiles (and/or frequency regulation) is taken into account in generating charging schedules, then the real-time EV charging system can satisfy timing constraints while providing V2G-based frequency regulation.*

The proposed real-time EV charging system utilizes a reference EV power demand, which is subtracted by predicted non-EV power demand and then divided by the optimal charging rate to calculate the number of available processing queues, that is,

the number of charging stations that can be activated simultaneously (see Algorithm 4 in §5.3 on page 171). The reference EV power demand is calculated for a given exact knowledge of EV charging requirements, esp. plug-in SOC and desired plug-out SOC under the assumption that daily driving patterns and EV charging profiles are not significantly changed even if they might fluctuate from day to day. However, if V2G-based frequency regulation is contained in the real-time EV charging system, energy required to refill batteries might significantly differ from the reference EV power demand, resulting in performance degradation of the proposed charging system. Hence, the reference EV power demand needs to be adequately increased to make up for extra energy consumption due to V2G-based frequency regulation since the reference power demand is correlated with the optimality of the charging system, that is, the minimization of total load variance.

In order to offer V2G-based frequency regulation as well as to satisfy EV owners' charging requirements, it is hypothesized that the inclusion of the statistics of EV charging profiles or frequency regulation in the scheduling algorithm will help accomplish these two goals. Assumed that driving patterns and charging profiles will vary depending on day of the week, the statistics on a specific day of week such as the mean and standard deviation of plug-in/-out time and SOC, etc., can be derived from historical data. Furthermore, based on the statistics, the concept of timing buffer can be introduced to compensate for variability in plug-in/-out times and SOCs and extra energy requirement due to V2G-based frequency regulation and also to allow additional time for EVs opting to participate in V2G-based frequency regulation to complete their charging process. The timing buffer of the n-th EV ($t_{\text{buffer}}(n)$) can be calculated as (refer to Figure 51(a)):

$$t_{\text{buffer}}(n) = \sigma_{t_{\text{plugin}}}(n) + \sigma_{t_{\text{plugout}}}(n) \tag{3.23}$$

where $\sigma_{t_{\text{plugin}}}(n)$ and $\sigma_{t_{\text{plugout}}}(n)$ are the standard deviations of plug-in times and plug-out times of the n-th EV on a specific day of the week, respectively. Also, from Figure

51(b), time period allowable for charging the n-th EV should satisfy the following constraint:

$$t_{\text{plugin}}(n) \leq t \leq t_{\text{plugout}}(n) - t_{\text{buffer}}(n) \tag{3.24}$$

where $t_{\text{plugin}}(n)$ and $t_{\text{plugout}}(n)$ are plug-in/-out time of the n-th EV, respectively. Therefore, the energy queue length, redefined as energy required to fully refill the battery up to the desired plug-out SOC, of the n-th EV as in Equation (5.6) (on page 169) can be rewritten as:

$$E_n = (\mu_{f_{\text{SOC}}}(n) - \mu_{i_{\text{SOC}}}(n)) \times \beta_n + t_{\text{buffer}}(n) \times r_{\max}(n) \tag{3.25}$$

where $\mu_{i_{\text{SOC}}}$ is the averaged plug-in SOC, $\mu_{f_{\text{SOC}}}$ is the averaged plug-out SOC, β_n is the battery capacity, $r_{\max}$ is the maximum charging rate, and t_{buffer} is the timing buffer. According to Equation (3.25), the modification of the equation for energy queue length will increment total energy required to refill batteries, which cannot cover extra energy requirement for V2G-based frequency regulation but also increase the safety margin for guarantee ratio by forcing EVs to complete charging earlier than their plug-out times.

The incorporation of V2G-based frequency regulation into the real-time EV charging system may cause the degradation of guarantee ratio since the real-time scheduling of EV charging is generated using the reference EV power demand, calculated without the consideration of V2G-based frequency regulation. In order to alleviate this performance degradation of real-time EV charging, the concept of timing buffer, calculated

(a) calculation of timing buffer

(b) Timing diagram for t_{buffer}

Figure 51: Concept of timing buffer for V2G-based frequency regulation.

based on historical data of EV charging profiles, is introduced, and it increases energy required for EV charging by forcing EVs to complete charging earlier than their plug-out times, which, as a result, allows EVs to be compensated for participation in the V2G program. However, it is beyond one's grasp whether or not V2G-based frequency regulation may affect real-time EV charging. Therefore, the impacts of V2G-based frequency regulation on real-time EV charging is first investigated, and then the hypothesis will be tested to see if the concept of timing buffer can alleviate the impacts.

Table 8 overviews the entire thesis including the research statement, research questions, hypotheses, and tasks required to do for testing the hypotheses, as described in this chapter.

Table 8: Mapping research questions to hypotheses and tasks.

Research questions, hypotheses, and tasks			
Problem	The potential benefits of the integration of EVs into the power grid come with unavoidable technical challenges. It is shown, however, that adopting "smart" charging strategies for the high penetration of EVs can alleviate some of the integration challenges and defer infrastructure investment needed otherwise. Also, EVs will play an important role as energy storage devices for ensuring grid-wide frequency stability by smoothing the natural intermittency of renewable energy sources (RES). In this context, a "smart" charging strategy must take into account possible vehicle-to-grid (V2G) applications along with vehicle charging to fully utilize the potential benefits of a large-scale deployment of EVs. Furthermore, EV owners' charing preferences must be considered since it is highly likely that EV owners will control the timing of recharging their vehicles rather than utilities. Therefore, the purpose of this research is to develop a framework for designing a "smart" EV charging control system that cannot only mitigate the impacts of the high penetration of EVs on the grid without reinforcement of the infrastructure but also facilitate V2G-based applications.		
Primary	Research question I	**(Application of real-time scheduling techniques to EV charging control)** How can EV charging be controlled to satisfy EV owners' charging preferences/requirements while filling the technical gaps of the valley-filling strategy?	
	Hypothesis I	The application of real-time scheduling techniques will enable EV charging to be controlled in real time so that it can fill the technical gaps of the valley-filling charging strategy as well as achieve the social optimality of the valley-filling EV charging strategy.	
	Secondary research questions	**Secondary hypotheses**	**Tasks**
I-1	How can real-time scheduling techniques be applied to EV charging control?	Real-time scheduling techniques can be applied to EV charging control if an EV charging system can be modeled such that its system model has all generic parameters required to apply real-time scheduling techniques.	- Implementation of a benchmark system and substantiation of its technical limitations - Modeling an EV charging system as a real-time system - Implementation of a simulation framework for EV charging control using an object-oriented modeling technique - Tailoring an existing real-time scheduling algorithm and design of priority assignment policy - Verification of the applicability of real-time scheduling techniques to EV charging control

Table 8 (continued).

Research questions, hypotheses, and tasks			
I-2	Is there any real-time scheduling algorithm applicable to the EV charging system that can be represented as a multiprocessor system with variable number of heterogeneous processors?	If it can deal with all the aforementioned characteristics of the real-time EV charging system, a real-time scheduling algorithm could be applied to the real-time EV charging system, and, among those satisfying the requirements, the most suitable real-time scheduling algorithm can be determined through statistical performance evaluation.	- Survey of real-time scheduling algorithms applicable to EV charging control - Statistical evaluation of surveyed real-time scheduling algorithms
I-3	Do charging rates affect the optimality and the guarantee ratio of the real-time EV charging system, and, if so, how can they be controlled so as for its optimality and guarantee ratio to be improved?	If charging rates are controlled based on both the energy utilization and the number of EVs that are charging simultaneously for a given time slot, then the performance of the real-time EV charging system will be improved.	- Investigation of the effects of charging rates on the real-time EV charging algorithm by sweeping the charging rate from 10% to 100% of the maximum charging rate - Finding an optimal charging rate by applying a heuristic approach
Primary	Research question II	**(Integration of V2G-based ancillary services into the real-time EV charging system)** How can the impacts of the operations of V2G-based services on EV charging be investigated?	
	Hypothesis II	If V2G-based services can be incorporated into the real-time EV charging control strategy, then the impacts of the operations of V2G-based services on EV charging can be investigated and characterized.	
	Secondary research questions	**Secondary hypotheses**	**Tasks**
II-1	How can V2G-based frequency regulation (FR) be incorporated within the framework of real-time EV charging control?	The introduction of different charging modes and the control of both charging rates of EVs that opt to participate in V2G-based FR and the number of EVs charging simultaneously will enable V2G-based FR to be incorporated in the real-time EV charging system.	- Modification of the real-time EV charging algorithm to incorporate the V2G-based FR - Verification of the functionality of the algorithm to provide V2G-based FR
II-2	How can the real-time EV charging system be made to satisfy timing constraints while providing V2G-based frequency regulation?	If the statistics of EV charging profiles (and/or frequency regulation) is taken into account in generating charging schedules, then the real-time EV charging system can satisfy timing constraints while providing V2G-based frequency regulation.	- Investigation of the impacts of V2G-based FR on the charging control algorithm - Statistical evaluation of the concept of "timing buffer" for mitigating the impacts of V2G-based FR

CHAPTER IV

THEORETICAL FOUNDATIONS

The objective of this chapter is to provide necessary information to help readers to grasp the context in this thesis more easily. The chapter begins with explaining the EV charging control problem and some problem formulations that have been proposed so far to provide a solution for EV charging control. The next section introduces the real-time scheduling theory and elucidates a variety of widely-known real-time scheduling algorithms since they serve as a main thrust to this research. In the last section, a brief introduction to frequency regulation and the information on how to utilize vehicle-to-grid (V2G) technology for frequency regulation are provided.

4.1 EV Charging Control Problems

Table 8 presents a summary of all EV charging strategies that have been presented and reviewed so far. (The definition for each strategy is borrowed from Valentine *et al.*'s paper [86].) *Unregulated charging* refers to a scheme that allows an EV to start charging as soon as the owner arrive home and finishes charging when the battery becomes full or when the owner leaves home. This type of charging scheme is expected to exacerbate peak load – even create other undesirable peaks – and increase electricity price due to additional large power consumption for charging EVs. *Valley-filling* is an approach that allocates the energy required for EV charging at off-peak hours, when electricity price is relatively cheap, incurring the lowest steady-state cost, and thus fills the valley(s) of electricity demand profiles. The traditional, *flat valley-fill* approach charges EVs such that certain hours of the valley achieve a flat load. There

Table 8: Summary of EV charging schemes [86].

Charging method	Description
Unregulated	Charging begins immediately after a commuter returns home from work, incurring the highest cost.
Flat valley-fill	Charging is regulated to take place when system demand is lowest, i.e., off-peak, incurring the lowest steady-state cost.
Smooth valley-fill	A valley-fill variation with minor smoothing at the endpoints of the valley to reduce ramping cost.
Intelligent	Charging can be dispatched whenever commuters are at home to minimize total system cost from steady-state and ramping operations.

are several variations on this basic approach, including minor smoothing at the endpoints of the valley to reduce ramping costs of generators. In the *Intelligent charging* scheme, an aggregator allows EVs to charge such that total system cost from both steady-state and ramping costs can be minimized.

EVs have the valuable characteristic of being a deferrable load because their electricity demand is not constant during the course of a 24-hour period. As illustrated in Figure 52(a), the shaded area is the underutilized capacity available for charging EVs. The annual operating cost of electricity generation for utilities can potentially be greatly minimized by reducing reliance on expensive peaking plants, which generally run only when there is a high demand [9]. This can be accomplished by increasing the utilization of installed capacity, thereby spreading fixed costs over a greater quantity of electricity, i.e., filling the valley of demand profile [7]. Figure 52(b) illustrates technical potential for a 24-hour and a 12-hour night-charging period to show the impacts of a constrained charging period from a regional perspective [36]. It can be seen that a significant fraction of the regional vehicle fleet could still be supported with the existing grid infrastructure even when constraining the battery charging to

the night period.

In order to formulate a problem for EV charging, let's consider a scenario where a utility company tries to generate a schedule for charging N EVs over time period of T, which is composed of smaller time slots of Δt, typically 15 minutes or 1 hour. The utility is assumed to know the baseload (non-EV demand), which is not necessary to be precisely predicted, and is trying to flatten the total load (baseload plus aggregate EV demand) profile by scheduling the charging profiles of the EVs. On the other hand, each EV starts charging after being plugged in and is required to charge a pre-specified amount of energy by the time it is plugged out. First, the charging dynamics of an EV can be simply represented as follows:

$$s_n(t+1) = s_n(t) + \frac{\eta_n}{\beta_n} r_n(t), \qquad t = T_0, \ldots T-1 \tag{4.1}$$

where $s_n(t) \in [0, 1]$ is the state-of-charge (SOC) of the vehicle at time t with an initial condition of $s_n(T_0)$, η_n, the charging efficiency, β_n, the battery capacity, and $r_n(t) \geq 0$, charging rate at time t. In addition, T_0 is the plug-in time and T is the plug-out time, respectively. There are many other models for the charging dynamics of batteries based on their chemical characteristics; however, this research aims to investigating the system-level behavioral characteristics of EV charging control, and

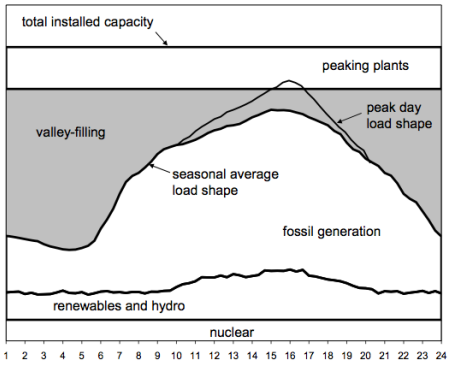

(a) concept of "valley-filling" approach

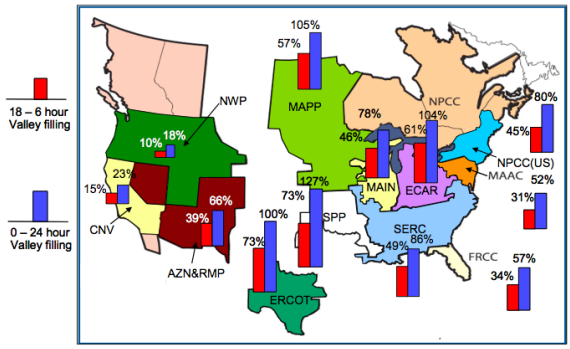

(b) regional technical potential of "valley-filling" approach

Figure 52: Concept and technical potential of "valley-filling" approach [36].

the simplest form as in Equation (4.1) is used. If the vehicle is assumed to be fully charged at the end of the charging interval, i.e., $t = T$, a set of feasible charging rates for the N EVs is defined as

$$\mathcal{R} \triangleq \{r_n \equiv (r_n(T_0), \ldots r_n(T-1)),\, n = 1, \ldots, N;\ \text{s.t. } s_n(T) = 1\} \tag{4.2}$$

The objective function for an individual EV to minimize with respect to r_n so that available energy in the valley(s) of a load profile is used up by charging EVs and every EV is fully charged at the end of its charging interval is given by

$$J(\mathcal{R}) \triangleq \sum_{t=T_0}^{T-1} U\left(d(t) + \sum_{n=1}^{N} r_n(t)\right) \tag{4.3}$$

such that

$$0 \le r_n(t) \le r_n^{\max} \tag{4.4a}$$

$$\sum_{t=T_0}^{T-1} r_n(t) = \frac{\beta_n\left(s_n(T) - s_n(T_0)\right)}{\eta_n \Delta T} \tag{4.4b}$$

where $U : \mathbb{R} \to \mathbb{R}$ is any strictly convex function, $d(t)$ denotes the non-EV demand at time t, and $r_n^{\max}$ is the maximum charging rate of the charging station to which EV n is plugged in. The constraint (4.4b), whose numerator represents the amount of energy EV n is required to charge if the charging efficiency is not considered, captures the second objective that EV n needs to reach the desired SOC $s_n(T)$ by its plug-out time T. If a feasible solution minimizing the objective function $J(\mathcal{R})$ can be obtained and there exists $A \in \mathbb{R}$ such that

$$\sum_{n=1}^{N} r_n(t) = \max\{0,\, A - d(t)\}, \quad t \in [T_0,\, T-1], \tag{4.5}$$

then the charging profile $\mathcal{R} = (r_1, \ldots, r_N)$ is *valley-filling* [20]. If the objective is to *track a given load profile* G rather than to flatten the total load profile, the objective function can be modified as [20]:

$$\sum_{t=T_0}^{T-1} \left(\sum_{n=1}^{N} r_n(t) - G(t)\right)^2 \tag{4.6}$$

There exists another type of optimization problem formulation by which *each EV minimizes its own charging cost* by adding the electricity price to the objective function as follows [55]:

$$J_n \triangleq \sum_{t=T_0}^{T-1} \left\{ p(t) r_n(t) + \delta \left[r_n(t) - \text{avg}\left(\mathbf{r}(t)\right) \right]^2 \right\}, \tag{4.7}$$

such that

$$0 \leq r_n(t) \leq r_n^{\max} \tag{4.8a}$$

$$s_n(T) = s_T(n) \tag{4.8b}$$

where $p(t) \equiv p\left(d(t) + N\text{avg}(r(t))\right)$ is the electricity price at time t, which is a function of non-EV and EV demand, δ is a positive constant – weighting factor – for two objectives, that is, minimizing charging costs and minimizing the deviation from average of other EVs' charging profiles, $\mathbf{r}(t)$ is a set of charging rates for each EV in the system at time t, which can be mathematically defined as

$$\mathbf{r}(t) \triangleq \left\{ r_1(t), r_2(t), \ldots, r_N(t) \right\}, \tag{4.9}$$

$r_n^{\max}$, the power ratings of the charging station to which the EV n is plugged in, and $s_T(n)$, the desired plug-out SOC that the owner specified before starting charging.

In summary, an EV charging control problem can be formulated to achieve a specific objective such as maximizing the revenue or the utilization of energy in the nighttime valley(s), minimizing charging costs, and so on. The solution to the EV charging control problem is a set of feasible charging profiles $\mathcal{R}$ for EVs in the system. The inputs to the problem are the day-ahead prediction or real-time measurements of baseload profile (non-EV demand), according to which generation is planned and operated, and EV charging requirements with EV owners' preferences reflected.

4.2 Real-time Scheduling Techniques

4.2.1 Real-time Systems

A real-time system is a system that must satisfy explicit (bounded) response-time constraints or risk severe consequences, including failure, where the response time is defined as the time between the presentation of a set of inputs to a system (stimulus) and the realization of the required behavior (response) [38]. There exist various other definitions for real-time systems, depending on the characteristics of the system itself, but the most common definition among them is that the system must satisfy time constraints, i.e., deadlines, in order to be correct. In other words, the logical correctness of a real-time system is based on both the correctness of the responses and their timeliness [41].

Real-time systems spans a broad spectrum from computer simulations to electronic engines as shown in Figure 53. In general, there are three types of real-time systems: soft, firm, and hard real-time systems. (Laplante's definitions in [41] are quoted for the definitions of these systems.) "A *soft real-time system* is one in which performance is degraded but not destroyed by failure to meet timing constraints." Contrarily, "a system where failure to meet timing constraints leads to complete and catastrophic system failure is called *hard real-time systems*." A *firm real-time system* can tolerate some arbitrarily small number of missed deadlines. From these definitions, it can be

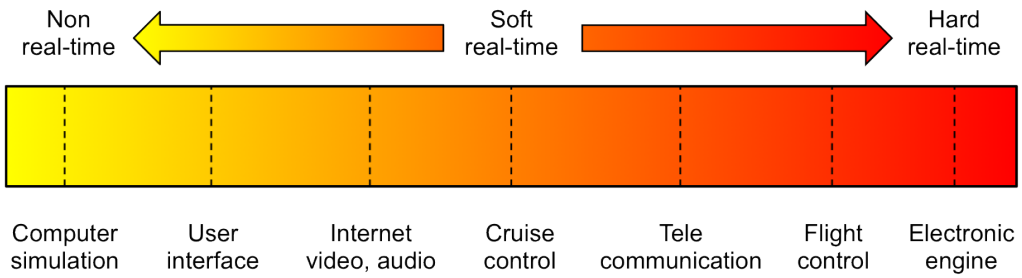

Figure 53: Spectrum of real-time systems (Source: Lee [42]).

Table 9: Examples of soft, firm, and hard real-time systems [41].

System	Real-time classification	Explanation
Automated teller machine	Soft	Missing even many deadlines will not lead to catastrophic failure, only degraded performance.
Embedded navigation controller for autonomous robot weed killer	Firm	Missing critical navigation deadlines causes the robot to veer hopelessly out of control and damage crops.
Avionics weapons delivery system in which pressing a button launches an air-to-air missile	Hard	Missing the deadline to launch the missile within a specified time after pressing the button can cause the target to be missed, which will result in catastrophe.

seen that all practical system can be represented as a soft real-time system. Table 9 gives some examples of soft, firm, and hard real-time systems.

"A real-time application is normally comprised of multiple tasks with different timing characteristics and with different levels of temporal criticality," based on which tasks can be classified [57]. First, tasks can be classified according to the predictability of their arrival. There are many tasks in real-time systems that are done repetitively and of which periods are predictable. These tasks are called *periodic* tasks, and the periodicity of them is known beforehand, and so such tasks can be prescheduled offline. In contrast, there are many other tasks that are *aperiodic*, that occur only occasionally, and aperiodic tasks with a bounded inter arrival time are called *sporadic* tasks. Real-time tasks can also be classified according to the consequences of their not being executed on time. *Critical* tasks are those whose timely execution is critical, in other words, if their deadlines are missed, catastrophic failures take place. *Noncritical* real-time (or soft real-time) tasks are, as the name implies, not critical to

the application, but it is desirable to maximize the percentages of jobs successfully executed within their deadlines..

Figure 54 shows the schematic block diagram of a real-time system in control of some process. The state of the controlled process and of the operating environment is acquired by sensors, which provide inputs to the controller, the real-time computer. There is a fixed set of tasks, the job list, that need to be assigned to processors or memories, and the question arises as to which tasks should be assigned to which processors or memories (*allocation problem*), and when and in which order, with respect to other tasks, they must start their execution (*scheduling problem*). This relates to the allocation and scheduling of tasks that can be done by a real-time scheduling algorithm and will be discussed in detail in the following subsections.

4.2.2 Taxonomy of Real-time Scheduling Algorithms

"The problem of real-time scheduling spans a broad spectrum of algorithms from simple uniprocessor to highly sophisticated multiprocessor scheduling algorithms" [57]. The goals of real-time scheduling are completing tasks within specific time constraints

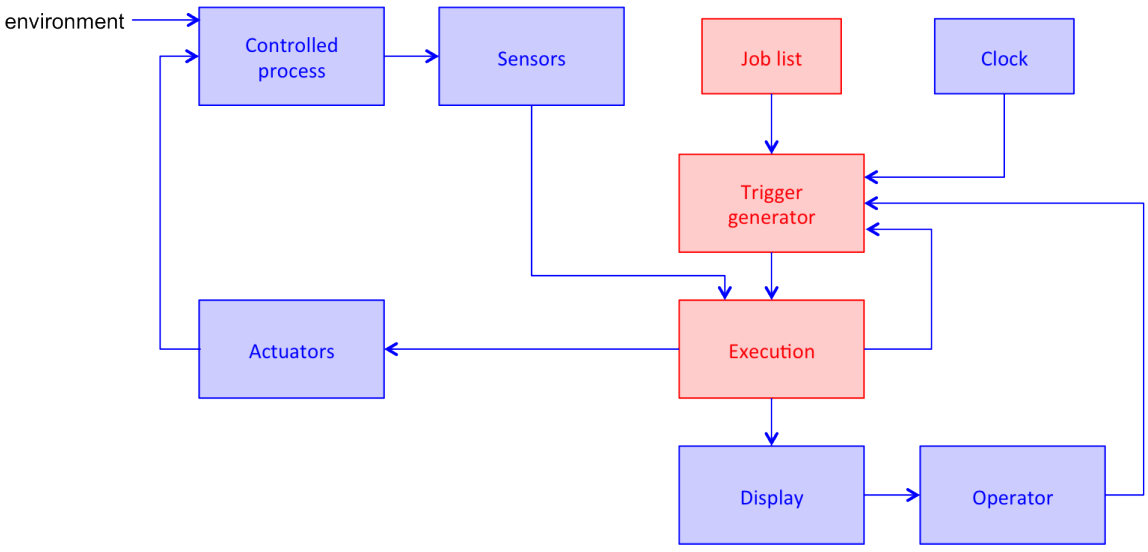

Figure 54: A schematic block diagram of a real-time system (Source: Krishna and Shin [38]).

and preventing from simultaneous access to shared resources and devices [31, 38]. Predictability and temporal correctness are the principal concerns in real-time scheduling although system resource utilization is of interest. A variety of real-time scheduling algorithms have been proposed and applied to different practical systems. However, a real-time scheduling algorithm is very problem-specific so that it is required to be tailored or even newly developed in order to be applied to a specific problem. Real-time scheduling algorithms can be categorized based on the characteristics of the systems to which they are applied. Figure 55 shows the classification of real-time scheduling algorithms.

Real-time scheduling algorithms for uniprocessor systems, that is, systems in which there is exactly one processor available and all tasks in the system are required to execute on this single processor, can be divided into two major classes:

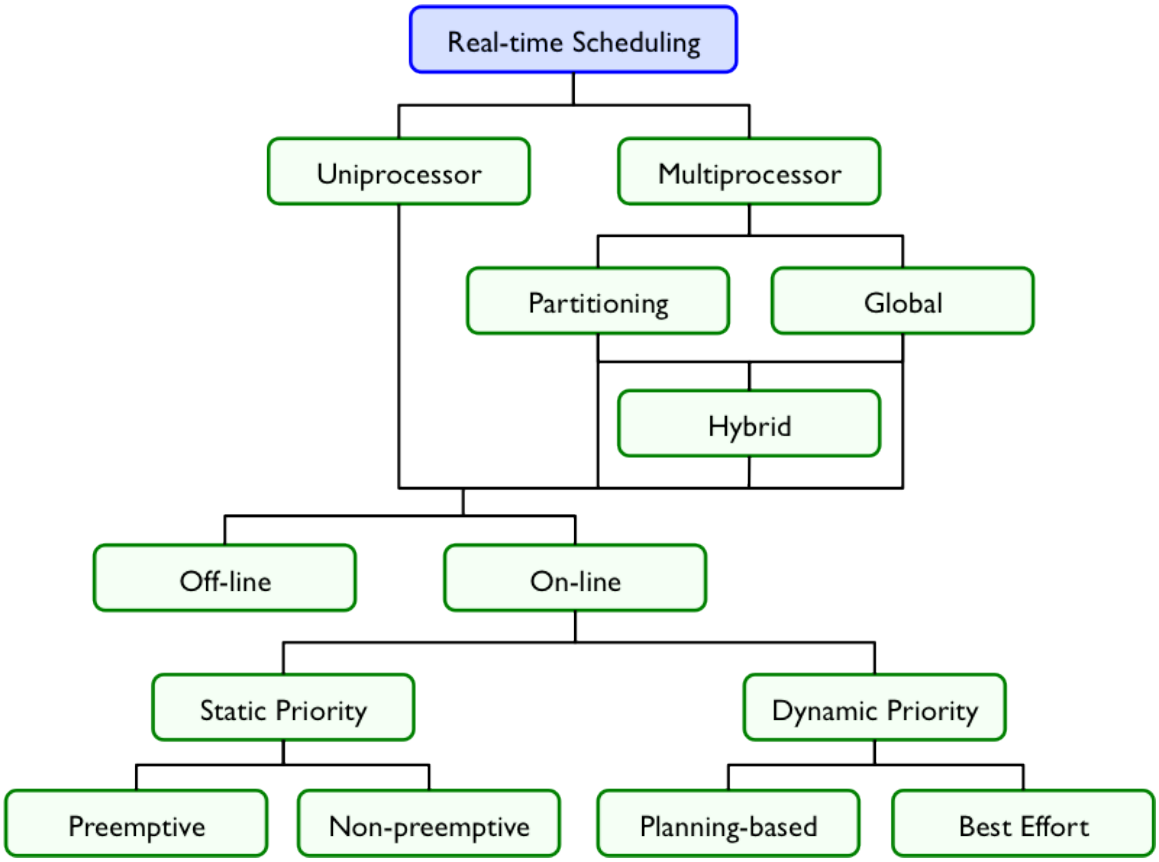

Figure 55: Classification of real-time scheduling algorithms [57].

off-line and *on-line*. On-line scheduling algorithms can be grouped into either static- or dynamic-priority based algorithms. *Static-priority* based algorithms, where the task priority does not change within a mode, are further divided into preemptive and non-preemptive algorithms, depending on whether or not a task can be preempted by another task based on their priority. A schedule is *preemptive* if tasks can be interrupted by other tasks and then resumed if there is a processor available. By contrast, once a task is processed in a *nonpreemptive* scheduling algorithm, it must be run to completion or until it gets blocked due to a resource limitation. Preemption allows for the flexibility of not committing the processor to run a task through completion once it starts executing. On the other hand, *dynamic-priority* algorithms assume that priority can change with time. The best known examples of static- and dynamic-priority algorithms are the Rate Monotonic (RM) algorithm and the Earliest Deadline First (EDF) algorithm, respectively. Dynamic-priority based algorithms can be grouped into two classes: planning based and best effort scheduling algorithms [57].

Multiprocessor scheduling algorithms are another class of real-time scheduling algorithms. Unlike uniprocessor systems, the real-time scheduling of multiprocessor systems, where several processors are available on which tasks may execute, has not been widely studied because of the complexity of the problem, and the Pfari scheduling is one of the few known optimal scheduling algorithms for multiprocessor systems [57]. The optimal assignment of tasks to multiple processors is, in almost all practical cases, an *NP*-hard[1] problem [22, 46, 58]. Therefore, the real-time scheduling of multiprocessor systems must be done with scheduling heuristics. A heuristic approach with two steps is usually adopted: a heuristic algorithm is first employed to assign tasks to processors, and then a scheduling algorithm for uniprocessor systems is used to schedule tasks on each individual processor. The problem of assigning tasks onto

[1] A decision problem Π_i is *NP*-hard if every problem in *NP* is polynomial-time reducible to Π_i [23].

a minimal number of processors has many similarities to bin-packing problems, in which items of variable sizes are packed into as few bins as possible. Therefore, many of the bin-packing heuristics are used to assign tasks onto processors. The key difference, however, is that bins in bin-packing problems have a unitary size while the size ("utilization" in the context of real-time scheduling) of a processor in a multiprocessor system varies dynamically according to some pre-defined functions, referred to as "schedulability conditions"; in other words, when a task is assigned to a processor, the real-time scheduler must make sure that the addition of the task should not jeopardize the schedulability of those tasks that have already been assigned to the processor.

Real-time scheduling algorithms for multiprocessor systems can fall into two categories: partitioning scheduling algorithms and global scheduling algorithms as illustrated in Figure 56. Partitioning scheduling algorithms partition tasks into several sets such that all tasks in a partition are assigned to the same processor. Tasks are not allowed to migrate, that is, a job that has been preempted on a particular processor is not allowed to resume execution on a different processor, hence the multiprocessor scheduling problem can be translated to many uniprocessor scheduling problems [18, 38]. The *next-fit algorithm for RM scheduling* is one of multiprocessor scheduling algorithms based on the partitioning strategy [38]. Global scheduling algorithms assign the tasks, which have arrived but not finished their execution, in one system-wide waiting queue that is shared by all processors. If, for instance, there exist m

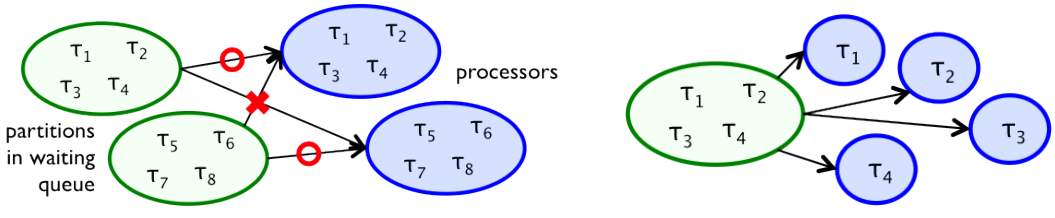

(a) partitioning scheduling algorithm (b) global scheduling algorithm

Figure 56: Real-time scheduling algorithms for multiprocessor systems.

processors, then, at every moment, the m tasks with highest priority stored in the waiting queue are selected for execution on the m processors using preemption and migration if necessary. The *focused addressing and bidding algorithm* is an example of global scheduling algorithms [38].

The following two subsections will explain a few well-known examples of real-time scheduling algorithms for uniprocessor and multiprocessor systems in depth.

4.2.3 Real-time Scheduling Algorithms for Uniprocessor Systems

4.2.3.1 Rate-monotonic (RM) Scheduling Algorithm

The Rate Monotonic (RM) scheduling algorithm is one of the most widely studied and used in practice, which is an optimal static-priority uniprocessor scheduling algorithm [38]. The task set consists of *periodic*, *preemptible* tasks whose relative deadlines are assumed to be equal to their task periods. According to [49], a task set of n tasks is schedulable under RM if

$$U = \sum_{i=1}^{n} \frac{e_i}{p_i} \leq n\left(2^{n/1} - 1\right) \tag{4.10}$$

where U is the total processor utilization of the task set, e_i and p_i are the execution time and the period of the i-th task, respectively. Task priorities are static and inversely related to their periods; if task τ_i has a smaller period than task τ_j, τ_i has higher priority than τ_j. Higher-priority tasks can preempt lower-priority tasks. Figure 57 shows an example of the rate-monotonic scheduling algorithm, excerpted from Krishna and Shin's book [38], whose task set is summarized in Table 10. Since $p_1 < p_2 < p_3$, task τ_1 has the highest priority, and every time it is released, it preempts the other tasks: for instance, at time $t = 2$, it preempts task τ_2, which is resumed at time $t = 2.5$, at which point task τ_1 is finished. Similarly, task τ_3 cannot execute when either task τ_1 or τ_2 is unfinished.

Table 10: Task set for the example of RM scheduling algorithm in Figure 57.

Task, τ_i	Arrival time, a_i	Execution time, e_i	Period, p_i
τ_1	0	0.5	2
τ_2	1	2.0	6
τ_3	3	1.75	10

4.2.3.2 Earliest Deadline First (EDF) Scheduling Algorithm

First proposed by Liu and Layland [49], EDF is one of the oldest and most well-known *dynamic-priority* scheduling algorithms; "the task priorities are not fixed but change depending on the closeness of their absolute deadline." EDF is also called the *deadline-monotonic scheduling algorithm*. The priority of each task is determined by its absolute deadline; the task with the earliest deadline will always have the highest priority. It has been proved that "EDF is an optimal uniprocessor scheduling algorithm, that is, if EDF cannot feasibly schedule a task set on a uniprocessor, there is no other scheduling algorithm that can schedule the task set" [49]. For a task set

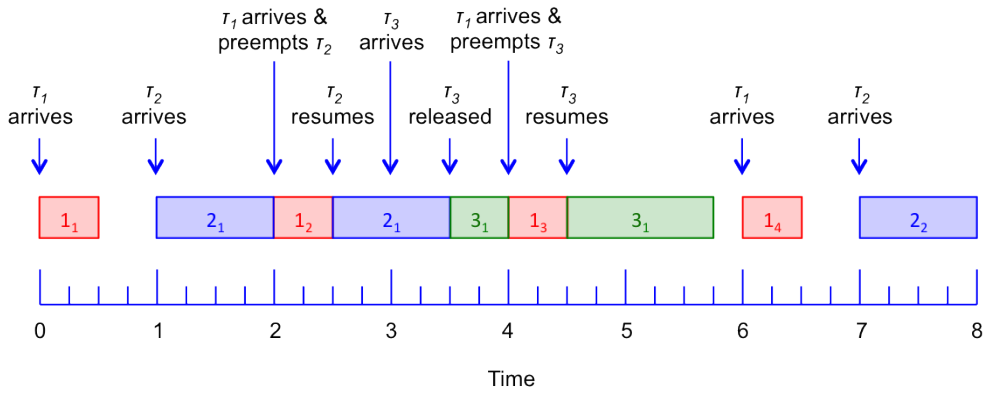

Figure 57: Example of RM scheduling algorithm (Source: Krishna and Shin [38] with modifications, K_j denotes the j-th release of task τ_K).

Table 11: Task set for the example of EDF scheduling algorithm in Figure 58.

Task, τ_i	Arrival time, a_i	Execution time, e_i	Absolute deadline, d_i
τ_1	0	5	15
τ_2	1	3	5
τ_3	2	4	10

whose n tasks are periodic and have relative deadlines equal to their periods, if

$$U = \sum_{i=1}^{n} \frac{e_i}{p_i} \leq 1, \tag{4.11}$$

where U is the total utilization of the task set, e_i and p_i are the execution time and the period of the i-th task, respectively, the task set can be feasibly scheduled on a single processor by the EDF algorithm, which is a necessary and sufficient condition for EDF to be able to schedule tasks [49]. Figure 58 contains an example of the EDF scheduling algorithm, excerpted from Krishna and Shin's book [38], whose task set consists of three aperiodic tasks, as summarized in Table 11:

When task τ_1 arrives at time $t = 0$, it is the only task waiting to execute,

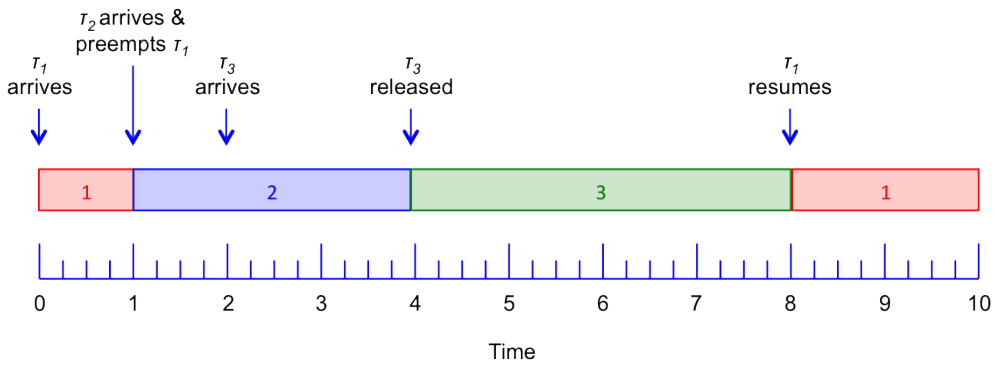

Figure 58: Example of EDF scheduling algorithm (Source: Krishna and Shin [38] with modifications).

and so starts executing immediately. Task τ_2 arrives at time $t = 1$, since $d_2 < d_1$, it has higher priority than τ_1 and preempts it. Task τ_3 arrives at time $t = 2$; however, since $d_3 > d_2$, it has lower priority than τ_2 and must wait for τ_2 to complete. When τ_2 finishes (at time $t = 4$), τ_3 is released first (since it has higher priority than τ_1). τ_3 runs until $t = 8$, at which point τ_1 can resume and run to completion.

4.2.4 Real-time Scheduling Algorithms for Multiprocessor Systems

Satisfying the deadlines of a set of real-time tasks in a multiprocessor system requires a scheduling algorithm that determines, for each task in the system, in which processor they must be executed (*allocation problem*), and when and in which order, with respect to other tasks, they must start their execution (*scheduling problem*) [91]. The allocation problem has been solved assuming a *fixed* or an *infinite* number of processors. In the *fixed* case, the objective is to find an allocation algorithm and a schedulability test to verify that a given task set is schedulable on a fixed number of processor [50]. In the *infinite* case, the problem of allocating a set of tasks is analogous to the *Bin-Packing* problem [11], in which the processor is a *bin*, whose capacity is given by the utilization bound of the processor. In the Bin-Packing problem, it is required to put n tasks with weight u_k (i.e., utilization of a task) into the minimum number of bins (i.e., processors) such that the total sum of weights of the tasks on each bin do not exceed the maximum capacity of the bin.

As described earlier, the scheduling of real-time tasks on multiprocessors can be performed under the *partitioning scheme* or under the *global scheme*. In the following paragraphs, the partitioned multiprocessor approach under RM and EDF is introduced and the best-known heuristic algorithms and different schedulability conditions are described. Also, the best-known heuristic algorithms based on the global multiprocessor approach under RM and EDF and their schedulability conditions are

introduced.

4.2.4.1 Global EDF

As previously explained, a set of independent, periodic tasks, in which the deadline of each task is equal to its period, is always successfully scheduled by EDF on a single processor if the total utilization of the tasks does not exceed 1. However, unfortunately, this optimality of EDF is not guaranteed on multiprocessor systems. The authors in [18] showed that a system of independent, periodic tasks can be scheduled successfully on m processors by EDF scheduling if

$$U = \sum_{i=1}^{n} \frac{e_i}{p_i} \leq m(1 - u_{\max}) + u_{\max} \tag{4.12}$$

where $u_{\max}$ is the maximum utilization of any individual task, that is, $u_{\max} = \max_i u(i)$. They also showed that this utilization bound is tight, in the sense that there is no utilization bound $\hat{U} > m(1 - u_{\max}) + u_{\max} + \epsilon$, where $\epsilon > 0$, for which $U \leq \hat{U}$ guarantees EDF schedulability. Also, according to [77], the authors examined the global EDF scheduling of periodic tasks on multiprocessors, and showed that any system of independent, periodic tasks for which the utilization of every individual task is at most $m/(2m - 1)$ can be scheduled successfully on m processors if

$$U \leq \frac{m^2}{2m - 1}. \tag{4.13}$$

Global EDF is an extension of EDF for multiple processors [3]. Similar to EDF, tasks are sorted in a non-decreasing order with respect to their absolute deadlines in a system-wide queue, from which the first k tasks are released to execute on the available k processors. Scheduling events occur only when new tasks are introduced or when a task completes. In order to help understand the algorithm, let's take for example a set of tasks, of which timing information is summarized in Table 12. When task τ_1 arrives, there is no tasks running, so it takes processor P_1. Similarly, task τ_2 takes processor P_2. Tasks τ_3 and τ_4 arrive at the same time, $t = 2$, but τ_4 occupies

Table 12: Task set for the example of global EDF scheduling algorithm.

Task, τ_i	Arrival time, a_i	Execution time, e_i	Absolute deadline, d_i
τ_1	0	2	5
τ_2	1	3	7
τ_3	2	2	10
τ_4	2	4	9
τ_5	3	3	12
τ_6	3	3	15
τ_7	3	4	14

the first available processor, P_3, since its absolute deadline is earlier than τ_3's, that is, it has the higher priority than τ_3. As a result, task τ_3 takes the remaining processor, P_4. The same procedure is applied to tasks τ_5, τ_6, and τ_7. Since $d_5 < d_7 < d_6$ and processor P_3 is not available when the tasks arrive, task τ_5 is assigned to processor

(a) tasks ordered by absolute deadline

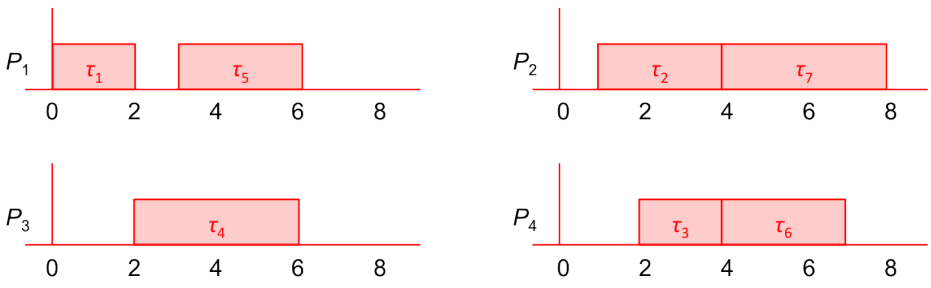

(b) processor assignment

Figure 59: Example of global EDF scheduling algorithm.

Table 13: Class definition for the example of next-fit algorithm for RM scheduling algorithm (Source: Krishna and Shin [38]).

Class	Bound
C_1	(0.41, 1]
C_2	(0.26, 0.41]
C_3	(0.19, 0.26]
C_4	(0.00, 0.19]

P_1, τ_6 to P_4, and τ_7 to P_2. Figure 59 shows the order of the tasks with respect to their absolute deadlines and the processor assignment scheduled by the global EDF algorithm.

4.2.4.2 Next-Fit Algorithm for RM Scheduling

The next-fit algorithm for RM scheduling is a utilization-based allocation heuristic that is proposed specifically to be used in conjunction with the rate-monotonic (RM) scheduling algorithm described in §4.2.3.1. The task set has the properties of RM scheduling algorithm (i.e., independence, preemptibility, and periodicity). A multiprocessor is assumed to consist of identical processors and tasks are assumed to require no resources other than processor time. Task τ_i is in class $m < M$ $(M > 3)$ if

$$2^{1/(m+1)} - 1 < \frac{e_i}{p_i} \leq 2^{1/m} - 1 \tag{4.14}$$

and in class M otherwise [38]. The set of tasks is divided into various classes based on their utilization, and a set of processors is exclusively assigned to each task class. Then, tasks are allocated, one by one, to the appropriate processor class until all the tasks have been scheduled, adding processors to classes if necessary for RM-schedulability, which is that if a set of n_m tasks in the class m is scheduled according to the rate-monotonic scheduling algorithm, then the minimum achievable utilization

Table 14: Task set for the example of next-fit algorithm for RM scheduling algorithm (Source: Krishna and Shin [38] with modifications, $u(i) = e_i/p_i$, refer to Equation (4.14) for class assignment).

	τ_1	τ_2	τ_3	τ_4	τ_5	τ_6	τ_7	τ_8	τ_9	τ_{10}
e_i	5	7	3	1	10	16	1	3	9	17
p_i	10	21	22	24	30	40	50	55	70	90
$u(i)$	0.50	0.33	0.14	0.04	0.33	0.40	0.02	0.05	0.13	0.19
Class	C_1	C_2	C_4	C_4	C_2	C_2	C_4	C_4	C_4	C_3

factor is $n_m(2^{1/n_m} - 1)$ as in Equation (4.10). The function $f(n_m) = n_m(2^{1/n_m} - 1)$ is a strictly decreasing function with regard to n_m, the number of tasks on a processor.

In order to clarify the process, let's look into an example. Suppose there are four classes ($M = 4$), whose utilization bound are summarized in Table 13, and consider the periodic task set in Table 14. Let processor P_i be reserved for tasks in class C_i, $1 \leq i \leq 4$. Since class C_1 has only one task, τ_1, of which utilization u_1 is less than 1, it is RM-schedulable, so task τ_1 is assigned to processor P_1. Similarly, task τ_2 is assigned to P_2, and τ_3 to P_4. Since $\tau_4 \in C_4$ and $u_3 + u_4 < 2(2^{1/2} - 1) = 0.83$ (refer to Equation (4.10)), $\{\tau_3, \tau_4\}$ is RM-schedulable on the same processor P_4, and, thus, task τ_4 is also assigned to processor P_4. Also, since $\tau_5 \in C_2$ and $u_2 + u_5 < 0.83$, $\{\tau_2, \tau_5\}$ is RM-schedulable, and task τ_5 is assigned to processor P_2. However, even though $\tau_6 \in C_2$, $\{\tau_2, \tau_5, \tau_6\}$ is not RM-schedulable on the same processor p_2 because $u_2 + u_5 + u_6 > 3(2^{1/3} - 1) = 0.78$, and so an additional processor P_5 is assigned to C_2 tasks and task τ_6 is assigned to processor P_5. In the same manner, $\{\tau_3, \tau_4, \tau_7\}$ is RM-schedulable on the same processor p_4 since $u_3 + u_4 + u_7 < 0.78$, so task τ_7 is assigned to processor p_4. The similar procedure can be done on tasks τ_8, τ_9, τ_{10}. The processor assignments are summarized in Table 15. With this assignment, the RM scheduling algorithm can be run on each processor.

Table 15: Task assignments for the example of next-fit algorithm for RM scheduling algorithm.

Processor	Tasks
p_1	τ_1
p_2	τ_2, τ_5
p_3	–
p_4	τ_3, τ_4, τ_7, τ_8, τ_9, τ_{10}
p_5	τ_6

4.2.4.3 Bin-packing Algorithm for Task Assignment to Processors

"The bin-packing algorithm assigns tasks to processors under the constraint that the total processor utilization must not exceed a given threshold, which is set in such a way that the uniprocessor scheduling algorithm is able to schedule the tasks assigned to each processor" [38]. Suppose that there is a set of periodic independent preemptible tasks to be assigned to a multiprocessor consisting of identical processors. The task deadlines equal their periods and tasks require no other resources than processor time. For example, so long as the sum of the utilizations of the tasks assigned to a processor is no greater than $n(2^{1/n}-1)$ (or 1) (refer to Equations (4.10) and (4.11)), the task set is RM-schedulable (or EDF-schedulable) on that processor. So, the problem reduces to making task assignments with the property that the sum of the utilizations of the tasks assigned to a processor does not exceed $n(2^{1/n}-1)$ (or 1). It is also desirable to minimize the number of processors required, which can be viewed as the famous bin-packing problem and there exist many algorithms for solving the bin-packing problem. One of the solutions for the bin-packing problem is the *first-fit decreasing algorithm*. Suppose there are n tasks to be assigned, and tasks are sorted out so that their utilizations (i.e., $u_i = e_i/p_i$, where e_i is the execution time and p_i is the period)

Table 16: Task assignments for the example of first-fit algorithm.

Step	Task τ_i	$u(i)$	Assigned to	Post-assignment U vector
1	τ_1	0.50	P_1	(0.50)
2	τ_6	0.40	P_1	(0.90)
3	τ_2	0.33	P_2	(0.90, 0.33)
4	τ_5	0.33	P_2	(0.90, 0.66)
5	τ_{10}	0.19	P_2	(0.90, 0.85)
6	τ_3	0.14	P_2	(0.90, 0.99)
7	τ_9	0.13	P_3	(0.90, 0.99, 0.13)
8	τ_8	0.05	P_3	(0.90, 0.99, 0.18)
9	τ_4	0.04	P_3	(0.90, 0.99, 0.22)
10	τ_7	0.02	P_3	(0.90, 0.99, 0.24)

are in non-increasing order. The algorithm is listed in Algorithm 3 on page 133.

To help understand the algorithm, consider the task set in Table 14, which will be assigned by applying the first-fit decreasing algorithm. The ordered list of tasks is $L = (\tau_1, \tau_6, \tau_2, \tau_5, \tau_{10}, \tau_3, \tau_9, \tau_8, \tau_4, \tau_7)$, based on their utilization. The assignment process is summarized in Table 16, where the vector $\mathbf{U} = (U_1, U_2, U_3, \ldots)$ contains the total utilization of processor P_i in U_i.

4.2.4.4 Focused Addressing and Bidding Algorithm

The focused addressing and bidding (FAB) scheduling algorithm is simple enough to be an online procedure and is used for task sets consisting of both critical and non-critical real-time tasks [38]. Based upon the partitioning strategy, the algorithm assumes that tasks arrive at the individual processors in the multiprocessor system. Once a task arrives at a processor, the processor checks if it has all resources and time to execute the task by its deadline while satisfying the deadlines of the other

Algorithm 3 Pseudocode of first-fit decreasing algorithm [38].

1: **initialize** i to 1.
2: **Set** $U(j) = 0$ for all j.
3: **while** $i \leq n$ **do**
4: **Let** $j = \min\{k|U(k) + u(i) \leq 1$.
5: **Assign** the i-th task in L to p_j.
6: $i \leftarrow i + 1$.
7: **end while**

tasks it already has. If it has resources and time, then it adds the task to its list of tasks to be executed. However, if it finds itself unable to meet the deadline or other constraints of all its tasks, then it tries to move some of its tasks onto other processors by announcing which task(s) it would like to move and waiting for the other processors to offer to take them up, which is done by the algorithm, called the FAB algorithm.

The FAB algorithm works as follows. Let's assume that there is an overloaded processor P_V that has a task to be moved to another processor to satisfy the timing constraints of the task. Each processor has a list or table containing which tasks it has already committed to run. As well, they have a table with the computational capacity of every other processor in the system. When searching for another processor on which it moves its task that cannot be executed on itself, the processor P_V checks its information on other processors, selects a processor (called the *focused processor*) P_S, which is believed to be the most likely to be able to execute the task by its deadline, and sends the task to the processor P_S. Also, processor P_V sends out requests for bids (RFB), which contain the information of the task (execution time, deadline, etc.), to other lightly loaded processors. Any processor that can successfully execute the task sends a bid to the focused processor P_S, stating how quickly it can process the task. After receiving all bids, the focused processor P_S reviews the bids to see which other processor is most likely to be able to do so, and transfers the task to that processor if the processor sending the bid can process the task better than P_S itself.

4.3 Frequency Regulation and Vehicle-to-Grid (V2G) Technologies

4.3.1 Frequency Regulation

According to the Federal Energy Regulatory Commission (FERC), ancillary services are defined as "those services necessary to support the transmission of electric power from seller to purchaser, given the obligations of control areas and transmitting utilities within those control areas, to maintain reliable operations of the interconnected transmission system" [15]. Ancillary services provide the system operators with resources required to reliably maintain the instantaneous and continuous balance between generation and load. Traditionally, ancillary services have been provided by generators; however, the integration of intermittent generation such as solar and wind and the development of smart grid technologies have prompted a shift in the equipment that can be used to provide ancillary services. Generators are manufactured in order to work best within a given frequency range, and if the system frequency goes out of bounds, they disconnect themselves to avoid damages, and blackouts can occur. To avoid this scenario, automatic regulation mechanisms using ancillary services are utilized. The network operator holds online power capacity that can be activated at any time to bring balance between generation and demand to the grid. The primary reserve such as frequency responsive spinning reserves stops the frequency drift in case of an event, e.g., a plant going down, and the secondary reserve (supplemental reserve) brings the frequency back to its nominal value. Tertiary reserve (replacement reserve) can solve longer-term (a few hours) imbalances. Key ancillary services are summarized in Table 17.

Frequency regulation and load following are the two ancillary services that are required to continuously balance generation and load under "*normal operating conditions*" [37]. Figure 60 shows an example of the morning ramp-up decomposed into base energy, load following, and regulation. The smooth load following ramp – the

Table 17: Definitions of key ancillary services [37].

Service	Service description		
	Response speed	Duration	Cycle time
Regulation	Power sources online, on automatic generation control, that can respond rapidly to system-operator requests for up and down movements; used to track the minute-to-minute fluctuations in system load and to correct for unintended fluctuations in generator output to comply with Control Performance Standards (CPSs) 1 and 2 of the North American Reliability Council (NERC 2002)		
	∼1 min	Minutes	Minutes
Spinning reserve	Power sources online, synchronized to the grid, that can increase output immediately in response to a major generator or transmission outage and can reach full output within 10 min to comply with NERC's Disturbance Control Standard (DCS)		
	Seconds to < 10 min	10 to 120 min	Days
Supplemental reserve	Same as spinning reserve, but need not respond immediately; units can be offline but still must be capable of reaching full output within the required 10 min		
	< 10 min	10 to 120 min	Days
Replacement reserve	Same as supplemental reserve, but with a 30-min response time; used to restore spinning and supplemental reserves to their pre-contingency status		
	< 30 min	2 hours	Days
Voltage control	The injection or absorption of reactive power to maintain transmission-system voltages within required ranges		
	Seconds	Seconds	Continuous

blue curve – is shown to start as a base energy of 3566 MW and rise to 4035 MW. Regulation – the dark green curve – consists of the rapid fluctuations around the underlying trend, also shown on an expanded scale to the right with a ±55 MW range – the red curve. Regulation is performed at the system level and uses on-line generators, storage, or load that is equipped with automatic generation control (AGC) and that can change quickly (MW/min) to track the constantly fluctuating load and to correct for unintended fluctuations in generation as well. This is accomplished primarily by turning large generators on and off, or ramping them up and down, some on a minute-by-minute basis, which incurs a great deal of operating cost. Like regulation, load following also uses on-line generation, storage, or load equipment that is not necessary to equip with AGC to track the intra- and inter-hour changes in customer loads. The characteristics of regulation and load following are summarized in Table 18.

In order to synchronize generation assets for electric power grid operations, the system frequency – the measure for the balance between generation and load – must be maintained within tight tolerance bounds, typically ±0.5 Hz around the nominal value, for instance 60 Hz in the U.S. A gap between power generation and demand

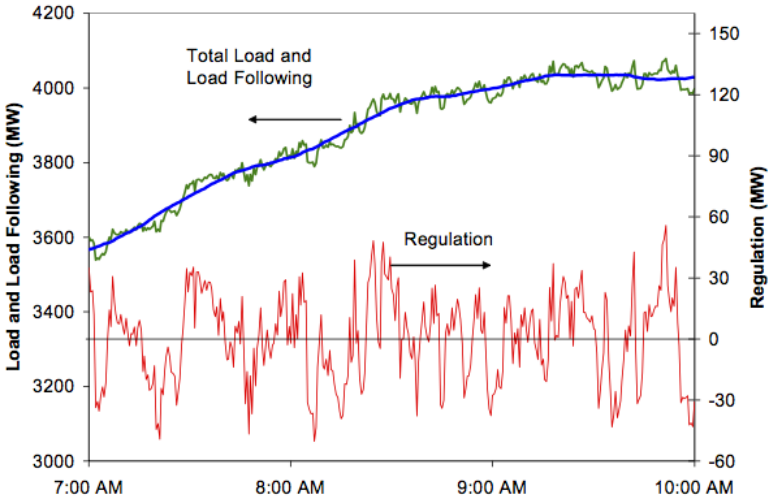

Figure 60: An example of frequency regulation [37].

Table 18: Characteristics of regulation and load following [37].

	Regulation	Load following
Patterns	Random and uncorrelated	Highly correlated
Control	Requires AGC	Can be manual
Maximum swing	Small	10–20 times regulation
Ramp rate (MW/min)	5–10 times load following	Slow
Sign changes per unit time	20–50 times load following	Few

on the grid causes the grid frequency to move away from its nominal value, which is the same everywhere on an interconnected grid, and the grid frequency must remain as close as possible from this value. For instance, if load is less than generation, then the system frequency increases, and if load exceeds generation, it decreases. Without frequency regulation, the frequency deviation from the nominal one keeps increasing or decreasing (Line 1 in Figure 61); on the other hand, the frequency regulation keeps the deviation from the nominal minimized (Line 2 Figure 61). Within a typical utility system, a 1% change in frequency will lead to a 1% change in load, as illustrated in Figure 62. If, for example, there is a 1000 MW load and frequency drops by 1% to

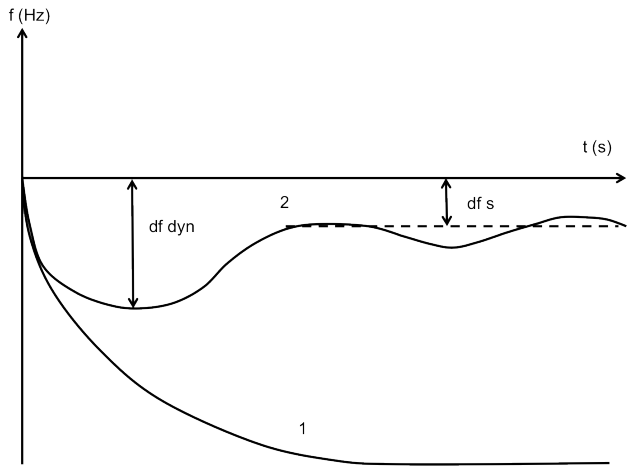

Figure 61: Frequency drop [88].

59.4 Hz, the load will also reduce by 1%, that is by about 10 MW to 990 MW.

The authors in [37] claimed that some storage technologies should be excellent regulation providers because this matches a zero net energy resource with a zero net energy service and that the quick response and precise control offered by storage is also superior to the control capabilities of many conventional generators. They also claimed that technologies capable of performing repeated high cyclic storage without degradation in their performance will be best suited for regulation.

4.3.2 Vehicle-to-Grid (V2G) Concept

The electric power grid and light vehicle fleet are exceptionally complementary as systems for managing energy and power. The power grid has essentially no storage, so it is necessary to continuously manage generation and transmission to match fluctuating customer load. By contrast, light vehicles inherently must have storage since their prime mover and fuel must be mobile, and they are designed to have large and frequent power fluctuations due to their nature of road driving. The high capital cost of large generators motivates high use (average 57% capacity factor); however, personal vehicles are cheap per unit of power and are utilized only 4% of the time for transportation, making them potentially available the remaining 96% of time for

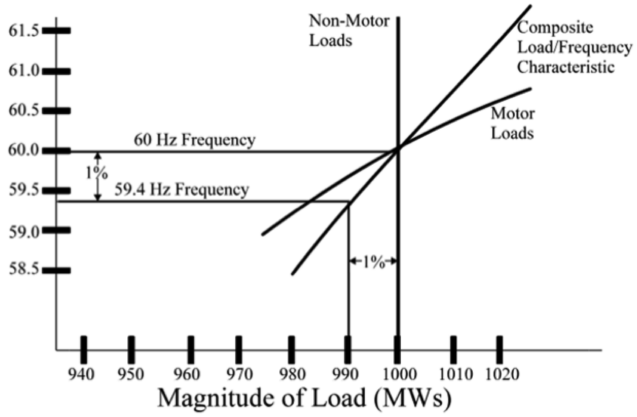

Figure 62: Frequency deviation due to load change [21].

a secondary function [33].

EVs can generate or store electricity when parked, and with appropriate connections can communicate with the power grid to sell demand response (DR) services by either selling electricity back to the grid or by adjusting their charging rates, which is called vehicle-to-grid (V2G). Figure 63 illustrates the basic concept of V2G, connections between vehicles and the electric power grid, and benefits that can be obtained by applying the V2G technology. The basic concept of V2G is that the batteries in EVs could be used to let electricity flow from vehicles to the electric distribution network and back since at any given time almost 95% of EVs are parked. Vehicles can be fully electric vehicles, hybrids, or any other vehicle with an onboard battery. V2G is classified into two categories based on the power flow direction: unidirectional V2G and bidirectional V2G. In the concept of unidirectional V2G, all legacy EVs can participate without any retrofit to the EVs themselves or substantial additional infrastructures in charging stations since they only act as controllable loads. On the other hand, bidirectional V2G enables EVs to act as both controllable loads and energy source, which is expected to generate more benefits than what they could obtain using unidirectional V2G.

In order to provide power to the grid, an EV must have three elements [34]:

(1) a connection to the grid for electrical energy flow,

(2) control or logical connection necessary for communication with the grid operator, and

(3) controls and metering on-board the vehicle.

Typically electricity flows one-way from the generators through the grid to customers. On the other hand, with the concept of V2G, electricity flows back to the grid from EVs, or with battery EVs, the flow is two-way (shown in Figure 63 as two arrowed lines). The control signal from the grid operator could be a broadcast radio signal, or through a cellular phone network, direct Internet connection, or power line carrier.

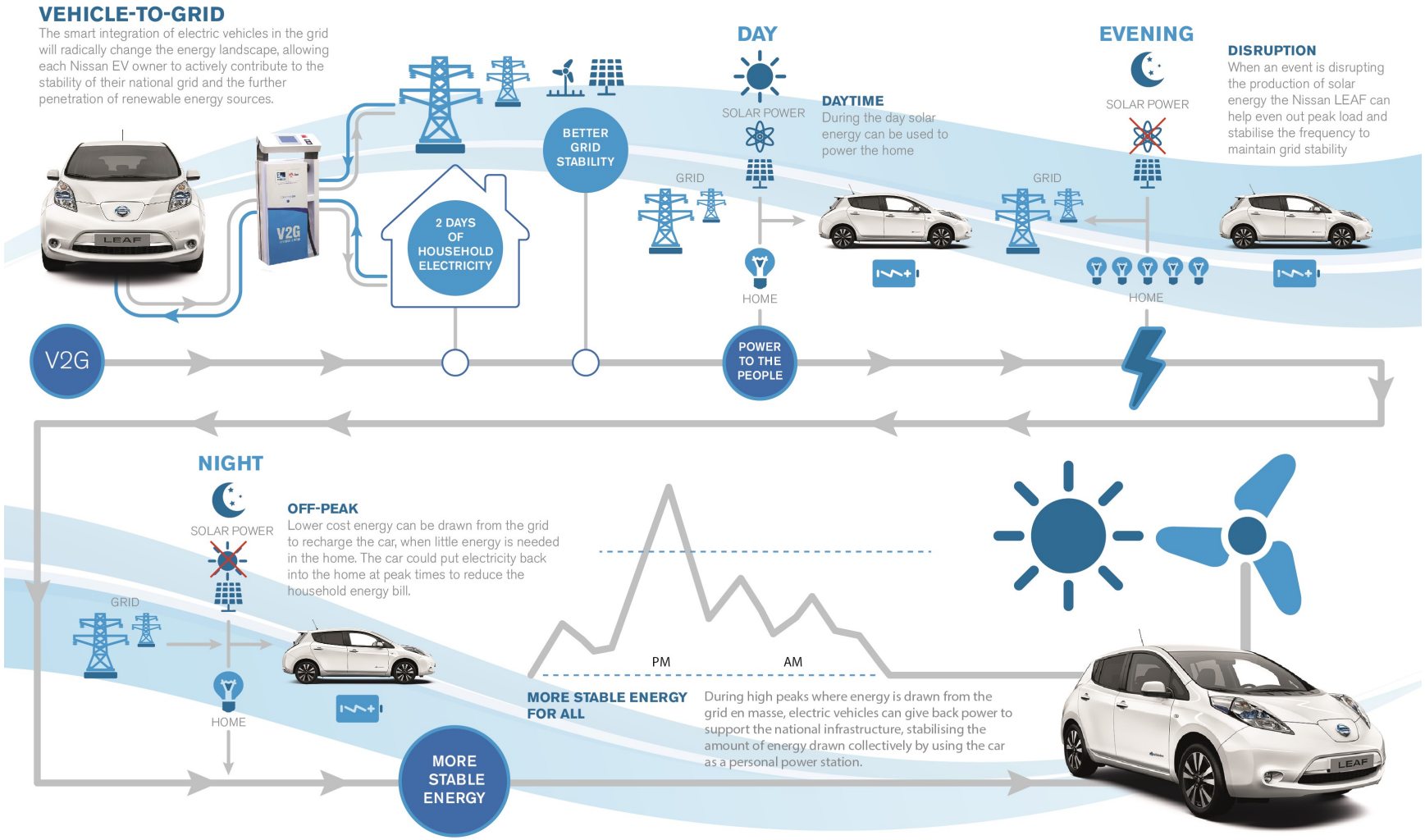

Figure 63: Basic concept of vehicle-to-grid [74].

In any case, the grid operator sends requests for participation to demand response (DR) services to a large number of EVs. The signal may go directly to each individual vehicle, or to the office of a fleet operator, which in turn controls vehicles in a single parking lot, or through a third-party aggregator of dispersed individual vehicles' power.

From EV owners' perspective, they could save money by running their home from their EV's battery during peak hours. At night time, when the grid is less strained, they charge their EV's battery and take advantage of off-peak pricing. They could also use excess power to sell back to the grid and get a discount on energy bills. Viewed from the utility's standpoint, a large population of EVs can help even out peak load and stabilize the system frequency to maintain grid stability and reliability. The concept allows EVs to provide power to the grid to help balance loads by "valley-filling" – charging at night when demand is low – and "peak shaving" – selling power back to the grid when demand is high. It also allows utilities not to build additional generation plants to meet peak demand or as an insurance against blackouts. The V2G technology can also provide utilities with new ways for ancillary services such as regulation – keeping voltage and frequency stable – and spinning reserves – meeting sudden demands or managing generator failures. Furthermore, EVs could be used to complement renewable power sources (RES) such as solar and wind power, for example, by storing excess energy during windy periods and providing power back to the grid during high demand periods, thus effectively stabilizing the intermittency of wind power.

4.3.3 V2G-based Frequency Regulation

EVs can act as both controllable loads and energy source within vehicle-to-grid (V2G) framework. There are several ways in which the energy stored in EVs might be used including [59]:

- peak shaving,
- load smoothing,
- smoothing intermittent output of renewable energy sources (RES),
- backup power supply, and
- ancillary services (e.g., voltage control, frequency regulation, etc.).

According to [59], EVs as distributed energy resources (DERs) are ideal for short duration services such as frequency regulation, load following, or spinning reserves, and for residential services such as load smoothing or peak reduction, based on their power and energy characteristics. Among those services, several recent studies, as reviewed in Chapter 2, have shown that there is potential for significant economic return for using V2G as a frequency regulation provider.

As already described in the previous section, the purpose of frequency regulation is to keep the balance between demand and supply of electricity. EVs could be used to balance generation and load in two ways:

- smooth loads, esp. residential loads, to reduce variations in loads, and
- provide regulating reserves as an aggregate energy source.

Consider a scenario where an EV provides regulation service when being plugged in but idle and is paid from the grid operator depending on the amount of energy it sends back to the grid, while it has to pay for purchasing power from the grid to charging its battery. Then, a revenue function for the EV can be defined as follows [48]:

$$R\left(T_C,\, r(t)\right) \triangleq \int_{T-T_C} P_R(t)dt - M\int_{T_C} r(t)P_C(t)dt \tag{4.15}$$

subject to

$$M\int_{T_C} r(t)dt = Q, \tag{4.16a}$$

$$0 \leq r(t) \leq 1 \tag{4.16b}$$

where T is the expected plug-in duration, T_C, the amount of time required to charge up to the desired SOC, $P_R(t)$, price for providing regulation service, $P_C(t)$, price for purchasing power from the grid, M, the maximum possible charging rate, $r(t)$, charging rate, and Q, energy required for the desired SOC. Equation (4.15) can be rewritten as

$$R\left(T_C,\, r(t)\right) = \int_T P_R(t)dt - \int_{T_C} \left[Mr(t)P_C(t) + P_R(t)\right] dt \tag{4.17}$$

In order to maximize the revenue gained by providing regulation service, the second integral term of Equation (4.17) should be minimized, and assuming that the prices are given in an hourly basis yields the second integral term in a discrete form:

$$\underset{r(k)}{\text{minimize}} \quad \sum_{k=0}^{N-1} \left[Mr(k)P_C(k) + P_R(k)\right] \tag{4.18}$$

subject to

$$M\sum_{k=0}^{N-1} r(k) = Q \quad \text{and} \quad 0 \le r(k) \le 1 \tag{4.19}$$

where N is the number of hourly timeslots in the expected plug-in duration T. Since the on/off charging control at the maximum charging rate, i.e., $r(k) = 1$, maximizes the revenue as claimed in [48], the solution to the optimization problem, Equation (4.18), is to determine the charging sequence, a sequence of 1's and 0's, rather than charging rates $r(k)$. It is also proved in §3.1.3 that the on/off charging control would maximize the utilization of the energy in the valley(s) of the load profile, resulting in "valley-filling."

In addition to maximizing the revenue, state-of-charge (SOC) is another factor to be considered when investigating the V2G-based frequency regulation since the charge and discharge are inherently disallowed at the top and bottom of the SOC, respectively. For example, from the moment the SOC of an EV reaches 100%, down-regulation, which corresponds to charging of the battery, cannot be performed since

the battery cannot be charged any more. When SOC is near the bottom, the vehicle cannot provide power to the grid for up-regulation, i.e., discharge the battery. Furthermore, EV owners want to gain economical benefits by providing the ancillary service, and also want to complete charging by when they plug out their vehicles from the charging station. Therefore, SOC should be appropriately reflected in the V2G-based frequency regulation. As shown in Figure 64, a weight function can be applied to the revenue function, Equation (4.17), in order to consider the SOC in the optimization problem. With the weight functions included, the price for regulation $P_R(t)$ in Equation (4.17) can be rewritten as follows [25]:

$$P_r\left(t, s(t)\right) = P_{UR}(t) W_U\left(s(t)\right) + P_{DR}(t) W_D\left(s(t)\right) \tag{4.20}$$

where P_{UR} and P_{DR} are the prices for up- and down-regulation, W_U and W_D are the weight functions for up- and down-regulation, and $s(t)$ is the SOC of the vehicle battery. Since the prices P_{UR} and P_{DR} are contracted on hourly basis at most energy markets, the price of regulation $P_R(t)$ could also be discretized as Equation (4.18).

In this chapter, the EV charging control problem, the main thrust of this research, is introduced, and real-time systems and scheduling algorithms for those systems are reviewed. In addition, the concept of vehicle-to-grid (V2G) technologies, one of the

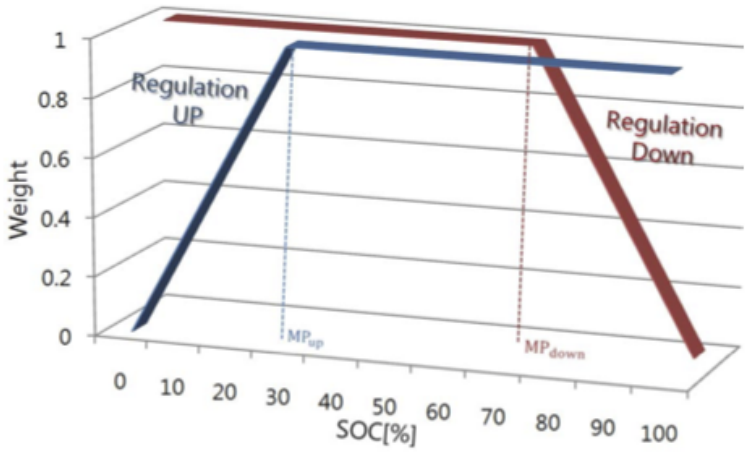

Figure 64: Weighting functions on SOC for V2G-based frequency regulation [25].

technical benefits that a large population of EVs can provide, and possible applications based on V2G technologies are addressed, and V2G-based frequency regulation, which will be integrated to the framework for real-time EV charging control, is lastly reviewed.

CHAPTER V

TECHNICAL APPROACHES

The main objective of this chapter is to explain how each component of the real-time scheduling algorithm for EV charging is implemented and how a simulation framework for evaluating the algorithm and investigating its interactions with vehicle-to-grid (V2G)-based frequency regulation is designed. In order to explain the implementation process more efficiently, the schematic overview of the real-time EV charging scheduling algorithm with subsection numbers, where the corresponding component is explained, is presented again in Figure 65. This chapter starts with the introduction of the object-oriented models for EVs and the scheduler, followed by the explanations for each component in Figure 65 and the front-end graphical user interface (GUI) of the simulation framework.

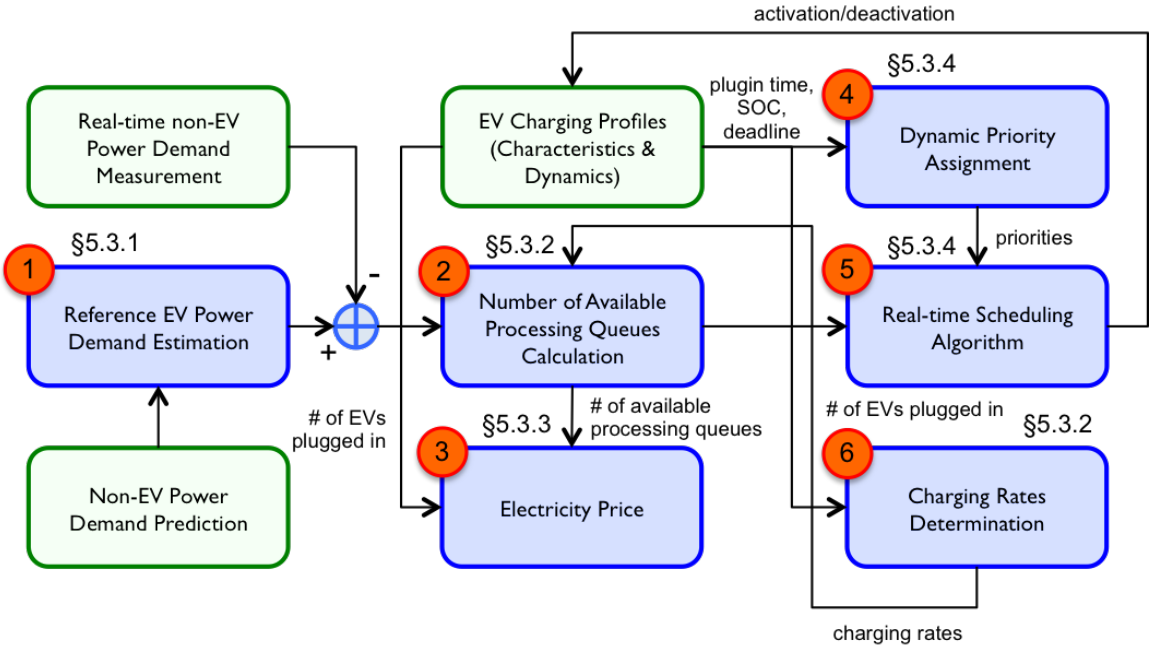

Figure 65: Revisit of real-time scheduling algorithm for EV charging control.

5.1 System Model of EV Charging Control System

As claimed in Chapter 3, an EV charging system can be modeled as a soft real-time system, where the dissatisfaction of a few of timing constraints will not result in a severe system failure. An EV charging system can be interpreted in two different ways as illustrated in Figure 66. Since available power can be viewed as processors or, conceptually, computing power of a real-time computing system, the concatenation of available power for each time slot, t_1, t_2, ..., that is, total available power for EV charging, can be regarded as the resource (i.e., computing power) of a uniprocessor in a real-time computing system, as depicted in Figure 66(a). Available power for

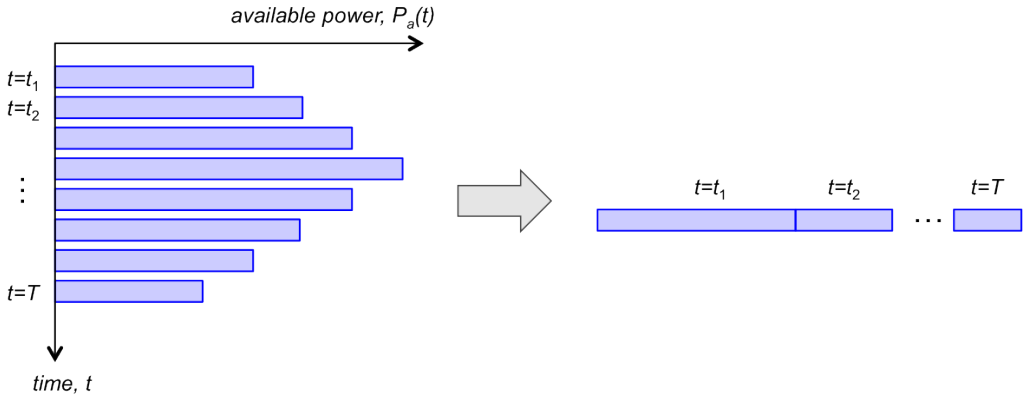

(a) interpreted as a uniprocessor

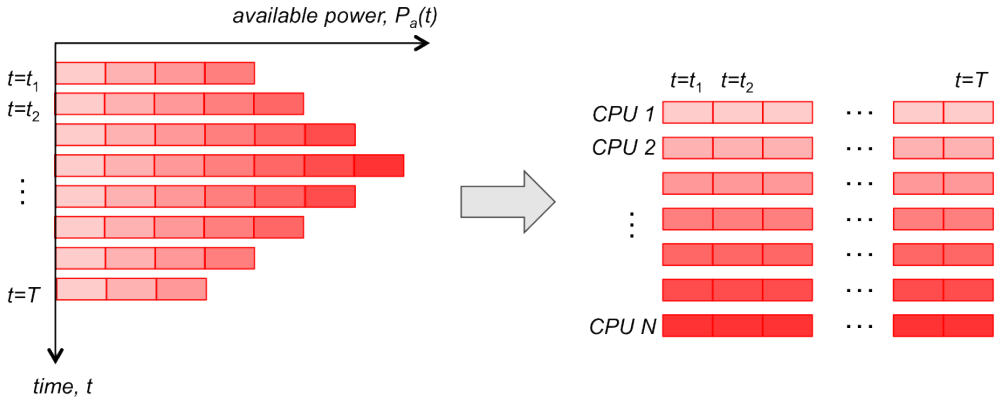

(b) interpreted as a multiprocessor

Figure 66: Interpretation of EV charging as a real-time system.

EV charging can be estimated based on the prediction of load profiles and the day-ahead generation planning, or based on real-time measurements of load and generation capacity because the scheduling of EV charging is done in real time, which will be explained in §5.3.1 in depth. On the other hand, if available power for each time slot is chopped up into small chunks of power and joined together as illustrated in Figure 66(b), the EV charging system can be modeled as a multiprocessor system with N processors or CPUs, whose availability keeps changing, depending on available power.

According to the classification of real-time scheduling algorithms (refer to Figure 55 on page 120), there are two big categories of algorithms for multiprocessor systems: global scheduling and partitioning algorithms. For global scheduling cases, all tasks are evaluated simultaneously for priority assignment; however, in partitioning algorithms, tasks are divided into groups, within which tasks are evaluated. This being interpreted in the domain of EV charging problem, for global scheduling, the real-time EV charging scheduler allows the charging station with the highest priority to be activated first, no matter what charging mode it belongs to; on the other hand, in case of partitioning algorithms, the real-time EV charging scheduler first puts together EVs with the same charging mode into groups, and evaluates EVs of the same group for assigning priorities.

For the purpose of the investigation of real-time scheduling algorithms applicable to EV charging, two different queue structures are considered. For algorithms belonging to global scheduling, all EVs are put in the same waiting queue to be evaluated for priorities, based on the "urgency" combined with charging modes, are sorted out with respect to their priorities at every time slot, and the EV with the highest priority is first released to the processing queue. For partitioning algorithms, four waiting queues and four processing queues for the four different charging modes are implemented. The size of the waiting and processing queues are determined proportional to the number of EVs with the same charging mode. EVs are assigned to one of

the waiting queues based on their charging mode, evaluated for priorities compared with the other EVs in the same waiting queue, and EVs with higher priorities are released to the corresponding processing queue. The difference between the two queue structures is illustrated in Figure 67.

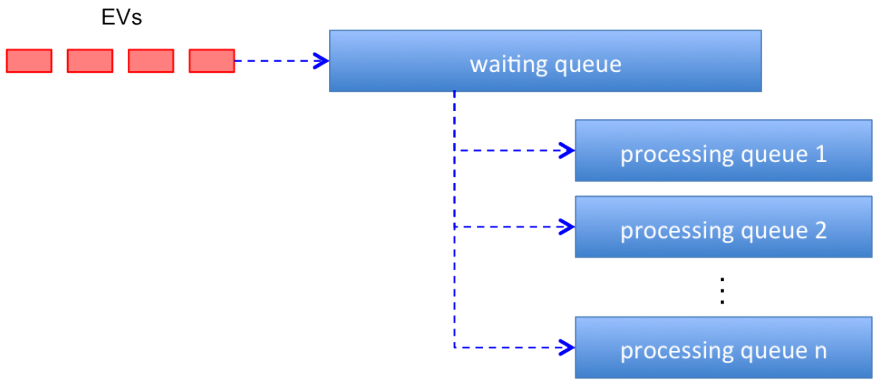

(a) global scheduling algorithms

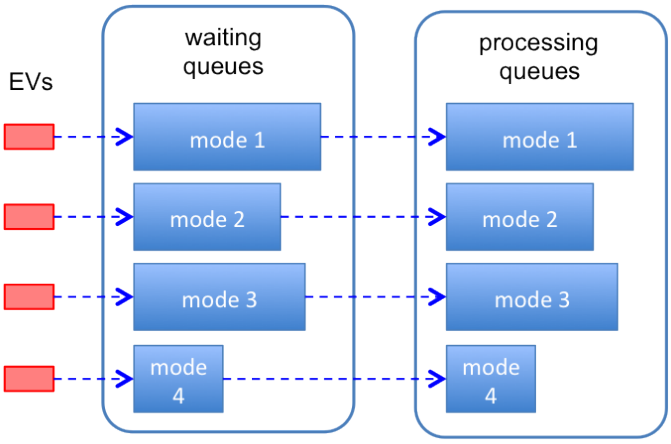

(b) partitioning algorithms

Figure 67: Queue structures for real-time scheduling algorithms.

5.2 Object-oriented Programming (OOP) Model for EV Charging Control System

A model for an EV charging system is implemented in MATLAB using its object-oriented programming capability, which will allow for an extension to a more complex environment using an agent-based modeling and simulation (ABM&S) toolkit like the Recursive Porous Agent Simulation Toolkit, commonly known as Repast. "The object-oriented programming (OOP) is a formal programming approach that combines data and associated actions (methods) into logical structures (objects), and this approach improves the ability to manage software complexity – particularly important when developing and maintaining large applications and data structures" [56]. The object-oriented programming provides a number of benefits, including [61]:

1. Modularity: The source code for an object can be written and maintained independently of other objects. Once created, an object can be easily passed around inside the system.
2. Information-hiding: By interacting only with an object's methods, the details of its internal implementation remain hidden from the outside world.
3. Code reusability: If an object already exists, the object can be used in other program. This allows for use of complex, task-specific objects, developed by experts.
4. Pluggability/debuggability: If a particular object turns out to be problematic, it can be simply removed from an application and a different object can be plugged in as its replacement.

In this section, it will be explained how to implement a model for an EV charging system using the object-oriented programming technique.

5.2.1 EV Class

The modeling of an EV charging system begins by defining a class to describe an EV in MATLAB with a class definition file as shown in Figure 68. A class is a prototype that models the states and behaviors of a real world object, and an object, created from a class, is a software bundle of related states and behaviors. The initial representation contains only charging status/requirements such as plug-in/-out time and state-of-charge (SOC), representing them as class properties. Then, methods – operations that can be carried out on objects – are added to the class definition files.

The EV class constructor creates an EV object containing related parameters (or

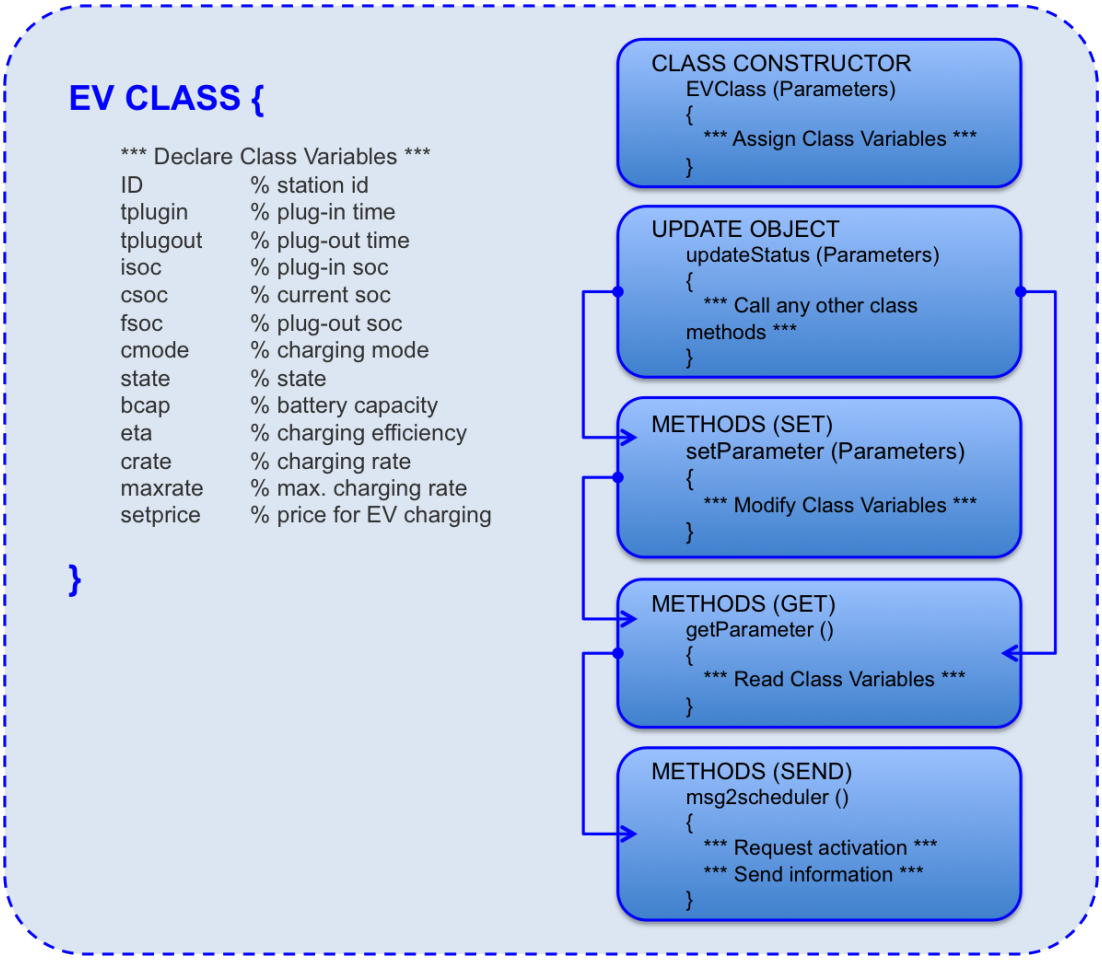

Figure 68: Anatomy of EV class.

Table 19: State definition for EV objects.

State	Description
`STATE 0`	plugged out
`STATE 1`	plugged in, but not being charged
`STATE 2`	plugged in, and being charged
`STATE 3`	completed charging

variables), and it could also be a copy constructor, which makes a clone of existing objects. In addition, two underlying methods, `getParameter()` and `setParameter()`, are implemented to allow the EV class for two basic operations on class properties, "read" and "write", respectively. The `updateStatus()` method checks whether an EV is plugged in to the system, and if so, it calculates the information such as energy queue length, current SOC, and so on, and updates the properties (i.e., class variables) of the EV object. When it updates the properties of an object, it invokes the `getParameter()` and `setParameter()` methods. Lastly, the method `msg2scheduler()`, allowing an EV object to send a request for activation as well as up-to-date information to the scheduler through a simple communication protocol, is also added. The inclusion of the `msg2scheduler()` method enables a more realistic model for the EV charging control system in that it mimics the communication between the dispatch scheduler and EVs in the real world.

5.2.2 Finite State Machine for EV Class

Objects share two characteristics: states and behaviors. Identifying states and behaviors for objects is the first step of designing a class in terms of object-oriented programming. Depending on whether it is plugged in, being charged, or completed charging, an EV object has four states, which are summarized in Table 19. `STATE 0`

represents a state in which an EV object is not plugged in yet. In `STATE 1`, the EV is plugged in, but not allowed to refill its battery yet. If, then, it is allowed to start charging, the EV switches its state to `STATE 2`. The last state identified is `STATE 3` where the EV finishes charging up to the desired plug-out SOC.

The state transition diagram for EV objects, in terms of system variables and EV object variables, is provided in Figure 69. Initially, an EV is in `STATE 0`, and it stays there during the time period of $t < t_{\text{plugin}}$ where t is the current time and t_{plugin} is the plug-in time of the EV. Once it has been plugged in to the system ($t \geq t_{\text{plugin}}$), the state of the EV is switched to `STATE 1`, in which the charging station, to which the EV is connected, sends an activation request message to the scheduler, but it does not start charging and is waiting for an activation signal from the scheduler; in other words, in terms of scheduling, the EV has been assigned to the waiting queue, but has not had a chance to be assigned to the processing queue yet. The scheduler determines if an EV can be assigned to the processing queue, i.e., start charging, depending on power available for EV charging (n_{PQ}, number of available processing queues) and

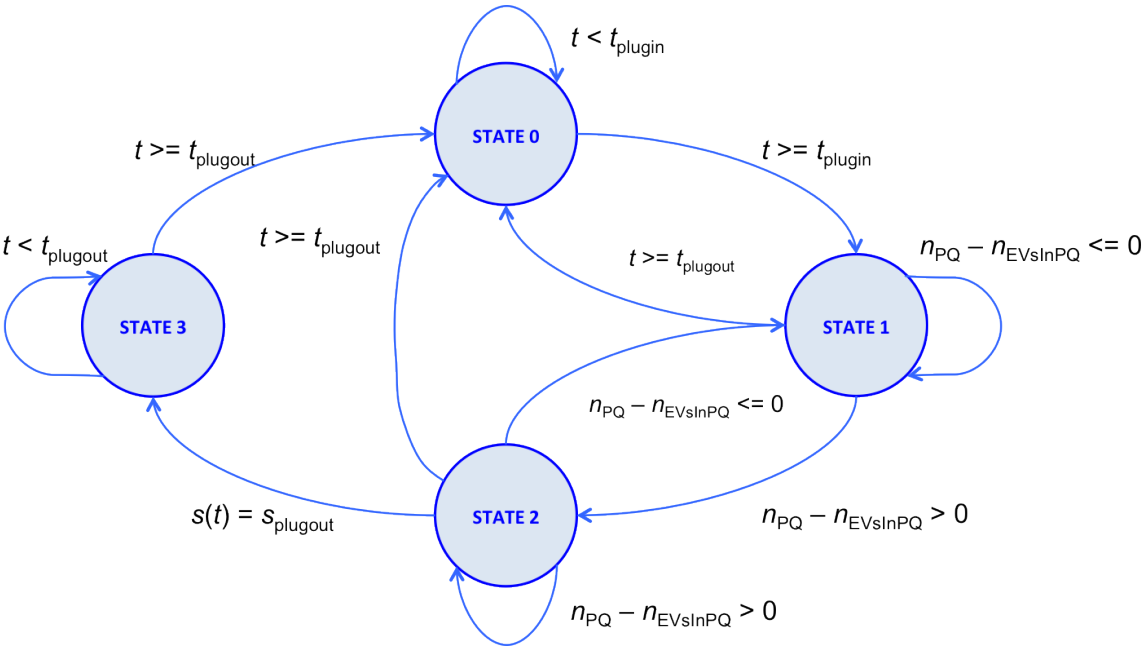

Figure 69: State transition diagram for EV objects.

Table 20: State transition table for EV objects.

Current state	Condition	Next state	Behaviors
`STATE 0`	$t < t_{\text{plugin}}$	`STATE 0`	none
	$t \geq t_{\text{plugin}}$	`STATE 1`	send a message to scheduler for activation; added to waiting queue
`STATE 1`	$t \geq t_{\text{plugout}}$	`STATE 0`	plugged out
	$n_{\text{PQ}} \leq n_{\text{EVsInPQ}}$	`STATE 1`	send a message to scheduler for status update
	$n_{\text{PQ}} > n_{\text{EVsInPQ}}$	`STATE 2`	assigned to processing queue; start charging
`STATE 2`	$t \geq t_{\text{plugin}}$	`STATE 0`	plugged out
	$n_{\text{PQ}} \leq n_{\text{EVsInPQ}}$	`STATE 1`	stop charging; moved back to waiting queue
	$n_{\text{PQ}} > n_{\text{EVsInPQ}}$	`STATE 2`	keep charging; send a message for status update
	$s(t) = s_{\text{plugout}}$	`STATE 3`	removed from processing queue
`STATE 3`	$t \geq t_{\text{plugout}}$	`STATE 0`	plugged out
	$t < t_{\text{plugout}}$	`STATE 3`	none

the utilization level of the processing queue (n_{EVsInPQ}, number of EVs in processing queues), and sends an activation signal back to the charging station. Then, the EV connected to the station gets activated, starts refilling the battery, and is switched to `STATE 2`. In `STATE 2`, the EV can possibly go to every state depending on its plug-out time (t_{plugout}) and power availability (n_{PQ} and n_{EVsInPQ}). If the current time is greater than its plug-out time, the EV goes to `STATE 0`; otherwise, it stays in `STATE 2`, i.e., keeps charging its battery when power is available ($n_{\text{PQ}} - n_{\text{EVsInPQ}} > 0$) or goes to `STATE 1`, by stopping charging when power is not available ($n_{\text{PQ}} - n_{\text{EVsInPQ}} \leq 0$) or being preempted by EVs with higher priorities. If the battery of the EV is fully

charged ($s(t) = s_{\text{plugout}}$, where $s(t)$ is the current SOC), then it switches its state to `STATE 3`. In `STATE 3`, there are only two possibilities: stays in `STATE 3` if it is not plugged out ($t < t_{\text{plugout}}$) or goes to `STATE 0` if it is plugged out ($t \geq t_{\text{plugout}}$). The state transition and behaviors of an EV object are summarized in Table 20.

5.2.3 Scheduler Class

Once the class for EV objects has been designed, the next step is to design a class for a scheduler object. First, class variables are declared, which includes two matrices for the waiting and processing queue, the number of which depends on the type of real-time scheduling algorithms (global vs. partitioning), and two scalar pointer variables for indexing the queues, one scalar variable for the number of available processing queues at a specific time, and two fractional weighting factors for dynamic priority calculation: one for the urgency (γ_n) and the other for charging mode. The structure of the scheduler class is shown in Figure 70.

In this research, two types of real-time scheduling algorithms for multiprocessor systems are considered: global scheduling algorithm and partitioning algorithm. Depending on the type of real-time scheduling algorithms applied, the structure of queue is different as depicted in Figure 67. For global scheduling algorithms, every task is waiting to be released in a system-wide waiting queue, and based on scheduling policy, it is released, i.e., assigned to an available processing queue among multiple processing queues. In a real-time computing system, the number of precessing queues or processors is typically known; however, based on the interpretation of EV charging control as a real-time multiprocessor system, it is not possible to know the number of processing queues before an actual charging schedule is generated. In the following section, the determination of the number of available processing queues will be explained in depth. On the other hand, for partitioning algorithms, multiple waiting queues, dedicated to different classes of tasks, are required, and the number of waiting queues

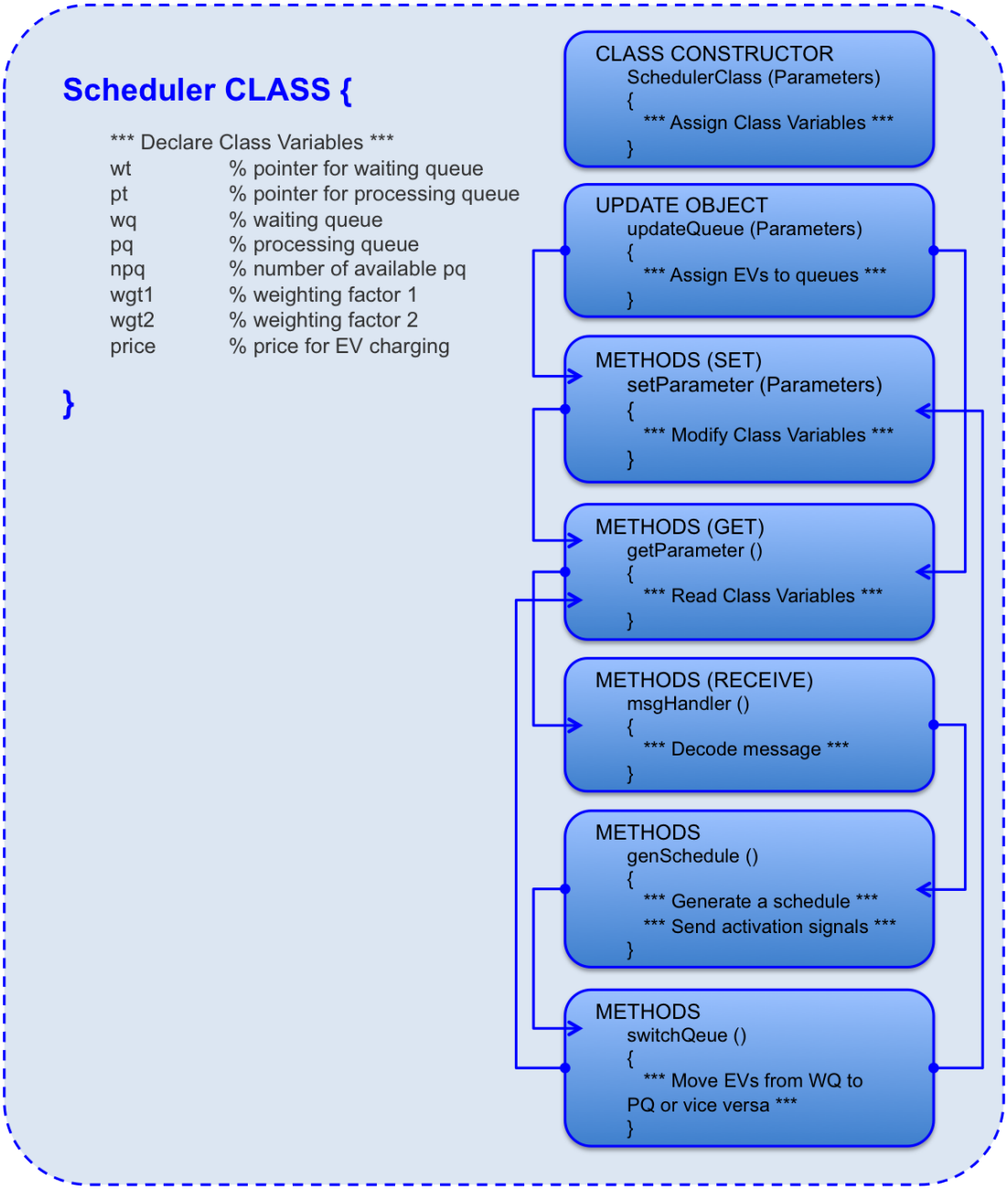

Figure 70: Anatomy of scheduler class.

is determined by the class definition of tasks, for instance, a utilization-based class definition for the next-fit algorithm for rate monotonic (RM) scheduling, introduced in §4.2.4.2.

For scheduling purposes, waiting queues (`wq`) and processing queues (`pq`) are designed to have various information such as `charging mode`, `urgency`, as illustrated in Figure 71, rather than having only `station ID` information, since, in this work, a variety of real-time scheduling algorithms and priority assignment policies are investigated to identify scheduling algorithms applicable to EV charging control and characterize the effects of priority assignment policies on scheduling performance. For global earliest deadline first (EDF), where the closeness to deadline determines priorities, information on `plug-out time` is used to determine priorities. The two parameters, `charging mode` and `urgency`, which is defined as energy required per unit time, $E_n/(t_{\text{plug out}} - t)$, where E_n is energy queue length, are also utilized to determine dynamic priorities as a variant of global EDF, and their weights are determined by the weighting factors, `wgt1` and `wgt2`. The pointers (`wt` and `pt`), also declared in the definition file of the scheduler class, are designed to point to the last EV in the queue. The number of available processing queues (`npq`), derived from available power, is also contained in the scheduler class, based on which the scheduler determines the approximate number of EVs that can be assigned to processing queues

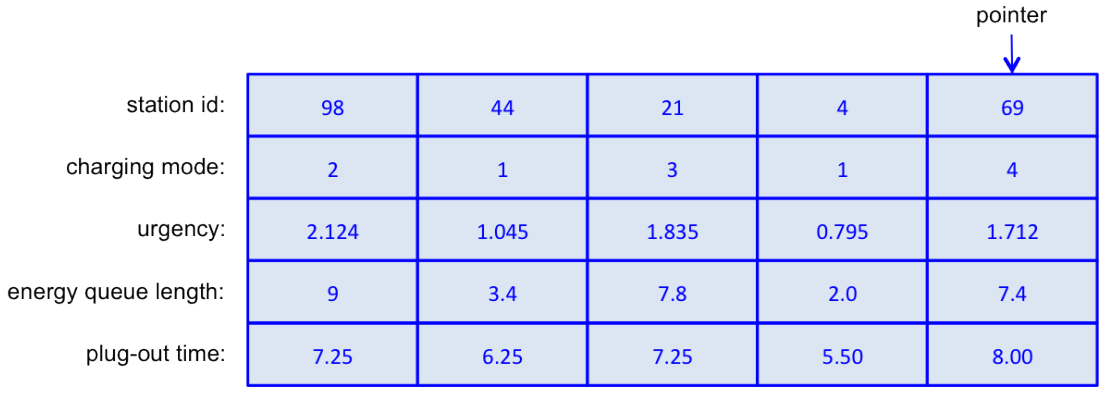

Figure 71: Example of the information contained in queues.

and their charging rates.

Similar to the EV class, the scheduler class has a class constructor for creating or cloning objects and two basic methods `getParameter()` and `setParameter()` for reading class variables from the queues or writing them to the queues, respectively. The method `msgHangler()` is, in addition, added to the class definition to decode messages sent by charging stations and to assign EVs – that have sent messages – to the waiting queue for scheduling. For the purpose of easy exchange of scheduling algorithms for the investigation of real-time scheduling algorithms, the methods `genSchedule()` and `switchQueue()` are implemented separately. The method `switchQueue()` moves EVs in the waiting queue to the processing queue when power is available or moves EVs in the processing queue back to the waiting queue when power is not available or when EVs with lower priorities are preempted by EVs with higher priorities. The method `genSchedule()` generates a schedule based on the information sent by EVs, determining which EVs can be assigned to which processing queues or which EVs should be preempted by which EVs. Once a charging schedule is determined, the method sends activation signals along with allowable charging rates back to EVs that requested activations.

5.2.4 Message Protocols between EVs and Scheduler

EV charging should be scheduled online and in real time through the interactions between EV objects and a scheduler object, which must be done via a kind of communication channel in the real world. Since it is obvious that a kind of digital communications will be used for this purpose, the communications between EV objects and the scheduler object are assumed to be done via simple digital message protocols. This kind of approach will allow further studies on the investigation of requirements of communication system supporting the EV charging system such as bandwidth, channel capacity, and so on.

Table 21: Message protocol for EV objects.

Packet	Bit length	Range
`Station ID`	8-bit	0 – 255
`EV State`	2-bit	0 – 3
`Energy Queue Length`	20-bit (5 bits for integer part, 15 bits for fractional part)	0 – 32
`Plug-out Time`	11-bit (5 bits for hour, 6 bits for minutes)	0:00 – 23:59
`Charging Mode`	2-bit	0 – 3

The message format that an EV sends to the scheduler consists of five data packets, as depicted in Figure 72, each of which contains *Station ID*, *EV State*, *Energy Queue Length*, *Plug-out Time*, and *Charging Mode*, respectively. A binary sequence containing the information sent by EVs through charging stations is composed of 43 bits, and, for expandability, each data packet is designed to have extra bits. Details such as bit length and representable range are summarized in Table 21. An 8-bit data packet is assigned for `Station ID`, and it can represent 256 EVs (or charging stations) in the grid. As previously described in §5.2.2, an EV object has four different states, which can be represented by a 2-bit binary sequence. For `Energy Queue Length`, 20 bits are assigned, of which 5 bits are for integer part and 15 bits for fractional part. For example, let's assume that an EV has a battery capacity of 16 kWh and a 15% plug-in SOC, and wants to refill its battery up to 100%, which means that its energy

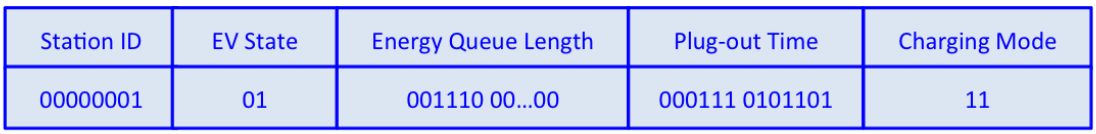

Figure 72: Message format of an EV charging station to scheduler.

queue length, i.e., energy required to refill the battery, is 13.6 kWh. Then, the energy queue length of 13.6 kWh can be encoded as a 20-bit binary sequence as follows:

$$13.6 = 2^3 + 2^2 + 2^0 + 2^{-1} + 2^{-4} + 2^{-5} + 2^{-8} + 2^{-9} + 2^{-12} + 2^{-13}$$
$$= \underbrace{01101}_{13} \quad \underbrace{100110011001100}_{0.6}$$

The same encoding policy is applied for `Plug-out Time`. The 5 bits for hour can represent 0 to 31 and the 6 bits for minutes can represent 0 to 63. Therefore, if an EV wants to complete charging by 8:30 in the morning, then the binary representation of the plug-out time is

$$8:30 \Rightarrow \underbrace{01000}_{8} + \underbrace{011110}_{30}$$

Similar to `EV State`, `Charging Mode` is also represented as a 2-bit binary sequence. A scheduler object has a function capable of translating encoded messages and the decoding process is done in the opposite direction to the encoding procedure.

On the other hand, the scheduler object broadcasts activation signals along with charging rates to EV objects, and each EV object, which has been plugged in, receives the message, extracts the information belonging to itself, and starts charging or keeps requesting an activation to the scheduler. The message format that a scheduler object broadcasts to EV objects is designed in the similar fashion with the message from EV objects to an scheduler object. An example message is depicted in Figure 73, and detailed information is summarized in Table 22. In this case, a binary sequence consists of 30 bits, of which 8 bits are for `Station ID`, 2 bits for `Activation` signals,

Station ID	00000001	00000010	...	01100100
Activation	01	00	...	01
Charging Rate	0 0011 11...00	0 0000 00...00	...	0 0011 11...00

Figure 73: Message format from scheduler to EV objects.

Table 22: Message protocol for scheduler object.

Packet	Bit length	Range
`Station ID`	8-bit	0 – 255
`Activation`	2-bit (00: deactivated, 01: activated)	0 – 3
`Charging Rate`	20-bit (1 bit for sign, 4 bits for integer part, 15 bits for fractional part)	−16 – +16

and 20 bits for `Charging Rate`. A binary sequence `00` for `Activation` indicates that an EV is not allowed for charging or is preempted by an EV with higher priority, while a sequence `01` allows an EV to start charging. As mentioned before, 20 bits are assigned for `Charging Rate`, of which 1 bit is for sign, allowing negative power flow, from EVs to grid, for the purpose of V2G-based frequency regulation, 4 bits for integer part, and 15 bits for fractional part of charging rates. The procedure to encode the `Charging Rate` packet of a message within a scheduler object is the same as described earlier for the message from EV objects to a scheduler object. Similarly, the translation of a coded message can be done as follows: let's assume that an EV receives a message from the scheduler, saying that it is allowed to start charging at a certain charging rate, encoded as `0 0011 010011001101000`. Then, the charging rate for the EV can be decoded as follows:

$$\begin{aligned} 0\ 0011\ 010011001101000 &= \underbrace{0}_{+} + \underbrace{2^1 + 2^0}_{3} + \underbrace{2^{-2} + 2^{-5} + 2^{-6} + 2^{-9} + 2^{-10} + 2^{-12}}_{0.3} \\ &= +3.3 \text{ kW} \end{aligned}$$

which means that the EV can purchase power from the grid to refill its battery. If the sign bit is set to `1`, that is, `1 0011 010011001101000`, then the charging rate is decoded as −3.3 kW, indicating that the EV is required to sell power to the grid, if

possible.

Introduced in this subsection are two simple message protocols for 1) request for activation of charging stations to the scheduler and 2) broadcast of activation signals and charging rates of the scheduler to charging stations. The protocols are implemented in such a way that they can be utilized for further analysis on the scalability of the simulation framework and communication system capability, e.g., channel bandwidth, channel capacity, and so on.

5.2.5 Overall OOP Model for EV Charging Control System

Figure 74 overviews the overall OOP model for an EV charging system. It is assumed that the measurements of power consumption are acquired by a utility and are provided to the scheduler object. Hence, the function generating load profiles is contained in the module `UTILITY`. Furthermore, it is also assumed that the utility performs the estimation of EV power consumption and provides the information to the scheduler object to calculate available power for EV charging at a specific time instant. The flowchart in Figure 75 illustrates the order of the process and information flow of scheduling EV charging. At first, EV objects are created by calling the class constructor and initialized based on EV profiles provided by a user. At the same time a scheduler object is created and initialized by receiving a predicted load profile, which is provided by the `Utility` module.

Once it has been plugged in ($t \leq t_{\text{plugin}}$), an EV starts sending a message via the message protocol, as introduced in §5.2.4, to request the activation of the charging station to which it has been plugged in, and, after that, keeps sending a message to let the scheduler know its current status, based upon which the scheduler can generate a charging schedule. The scheduler object decodes messages from EV objects, and determines which EVs can be assigned to the processing queues or should remain in the waiting queue. After determining EVs assignable to the processing queues, the

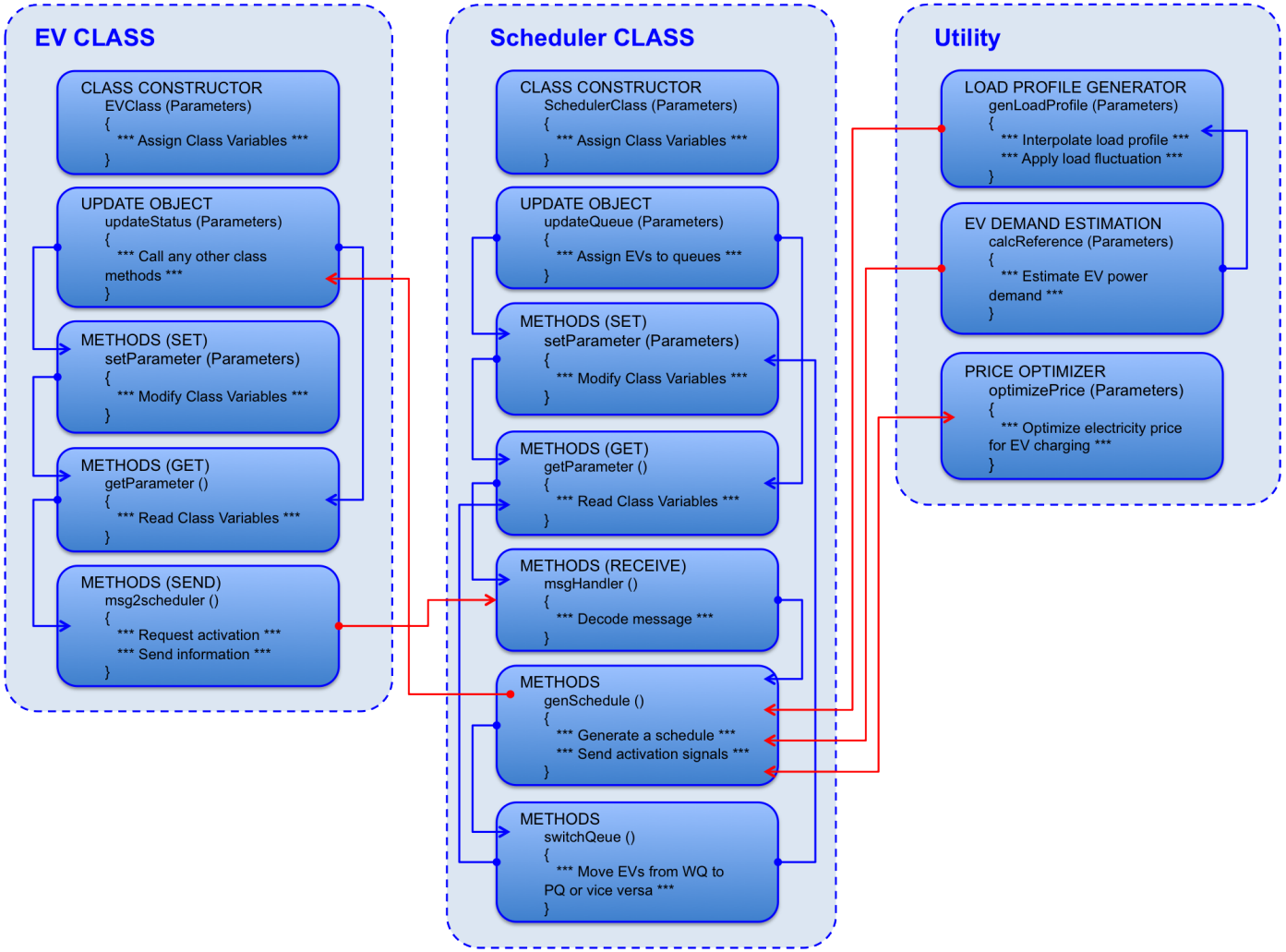

Figure 74: Overall structure of the OOP model for EV charging system.

scheduler generates a charging schedule in accordance with a scheduling policy, and broadcasts activation signals along with charging rates back to EV objects. Based on the message containing activation and charging rate information, the EV updates its status such as energy queue length and SOC. If the EV has completed charging, the scheduler deactivates the charging station based on the EV's energy queue length or SOC information, and the charging station stops sending a message to the scheduler. If not, the EV keeps sending a message to the scheduler to update the information on the waiting queue or processing queue and obtain a chance to recharge its battery.

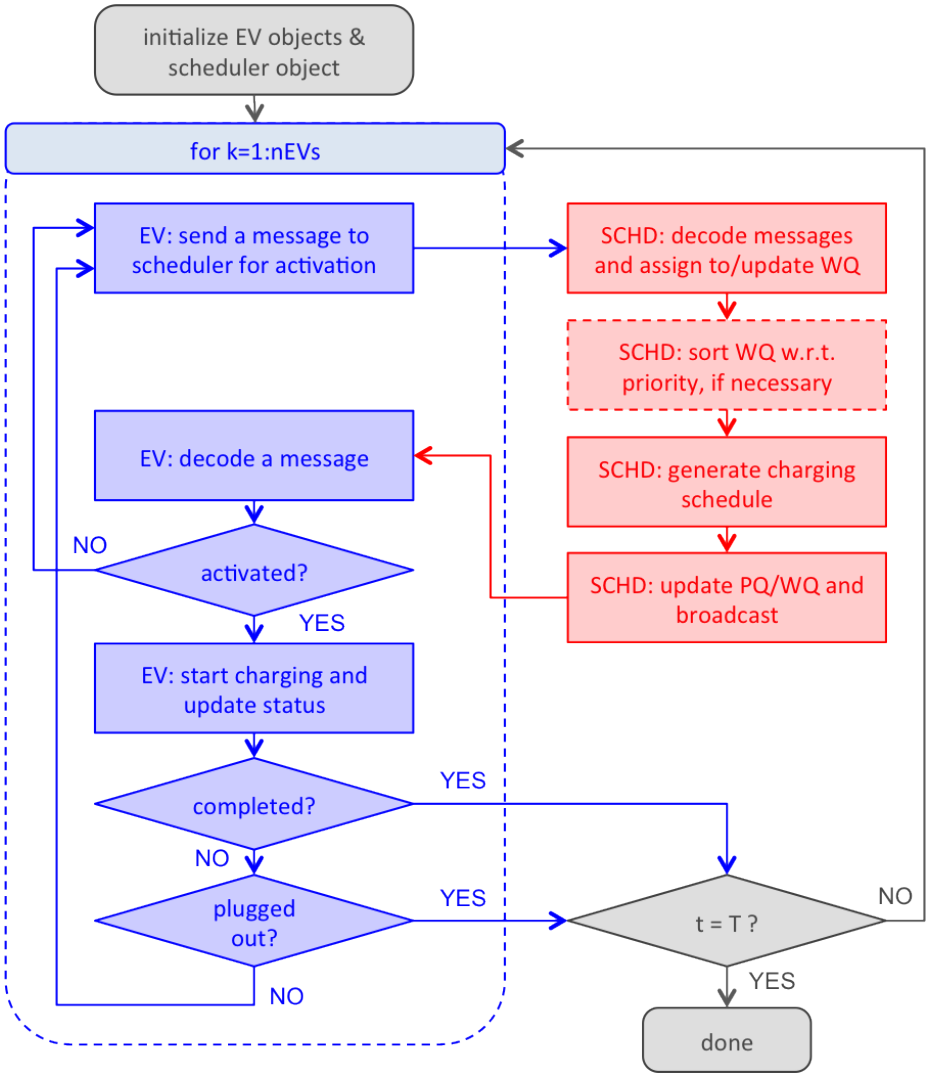

Figure 75: Flowchart for real-time EV charging algorithm.

5.3 Real-time Scheduling for EV Charging

In this section, details on the implementation of the blocks in Figure 65 are described, and the order of the explanation follows the numbers on each block.

5.3.1 Reference EV Power Demand Estimation

Basically, a real-time scheduler allocates a limited resource of processors, i.e., computing power, to different tasks, of which requirements may be conflicting with each other, in such a way that their timing constraints as well as functional requirements can be satisfied. In a typical real-time computing system, the number of processors or the amount of computing power is known before an actual scheduling process is carried out. Therefore, as well for the real-time EV charging system, it is important to know the charging capability of the system. In this research, since, contrasted with the day-ahead valley-filling scheme, the number of EVs that can be charged at the same time is controlled to achieve a flat load curve with EV owners' charging requirements satisfied, the number of processing queues must be known before a charging schedule is generated. For this reason, available power is discretized into small energy packets, called *charging packets*, as illustrated in Figure 76, whose duration is Δt and amplitude is $r_{\max}$. The number of charging packets at a time instant can be translated into the number of processing queues, denoted by n_{PQ}, which is equal to the number of EVs being charged simultaneously. However, in case of real-time EV charging, available power would keep varying, and thus the number of processing queues is not invariant. Consequently, the number of available processing queues is required to be expressed as a function of time, and can be estimated by dividing available power at a time instant ($P_{\mathrm{a}}(\mathrm{t})$) by a maximum charging rate ($r_{\max}$) for homogeneous cases, where all charging stations have the same power ratings as follows:

$$n_{\mathrm{PQ}}(t) = \left\lceil \frac{P_a(t)}{r_{\max}} \right\rceil \tag{5.1}$$

(However, this approach is not applicable to heterogeneous cases where all charging stations might not have the same power ratings, and thus another approach for heterogeneous cases will be explained later.) As a result, available power is required to be estimated in order to calculate the number of available processing queues. In this subsection, it is explained how to estimate available power (P_{a}), followed by the explanation of the determination of the number of available processing queues (n_{PQ}) for heterogeneous cases in the following subsection.

In order to determine the number of available processing queues at a time instant, it is required to estimate the amount of power available for EV charging as previously explained. Available power can be estimated by taking the difference between generation capacity and non-EV power consumption at a specific time instant. Since a utility makes a plan of generation based on predicted load profiles, the utility's cost running generation plants can be minimized if actual power consumption is forced not to be deviated from the generation plan a lot. Hence, it is desirable to design an EV charging system such that total power consumption follows the generation plan as possible as it can. For this reason, the reference EV power demand hereafter

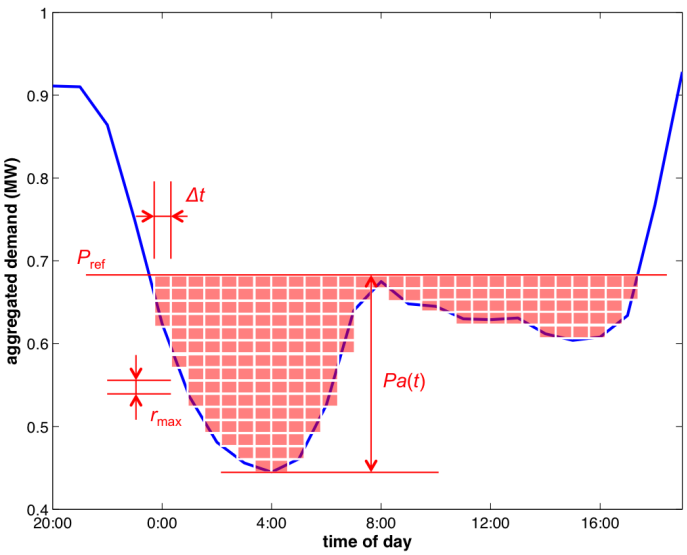

Figure 76: Concept of charging packets.

refers to the day-ahead generation plan. For the purpose of estimating a reference EV power demand, the optimal decentralized charging (ODC) algorithm presented in [19] can be used (refer to Algorithm 1 on page 55); however, from the simulation point of view, as the penetration level of EVs increases, the algorithm becomes more computationally expensive, because the number of nonlinear optimization problems to be solved increases, and, moreover, it does not take into account timing constraints when generating a day-ahead planning. So the optimization problem for the valley-filling as in Equation (2.26) is reformulated as Equation (5.2) so that a day-ahead generation planning can be done very quickly, and, thus, the simulation runtime is significantly reduced:

$$\underset{P_{\text{ref}}(\cdot)}{\text{minimize}} \left(\sum_{t=1}^{T} (P_{\text{ref}}(t) - P_{\text{base}}(t)) \times (\Delta t/\eta) - \sum_{n=1}^{N} E_n \right)^2 \tag{5.2}$$

where P_{ref} is an optimal reference total demand, P_{base} is the aggregated non-EV demand, η is the charging efficiency, Δt is the duration of each time slot, and E_n is the energy queue length of the n-th EV, defined as $E_n = (s_{\text{plugout}}(n) - s_n(t)) \times \beta_n$, s_{plugout}, s_n and β_n are the plug-out SOC, the SOC at time t, and the battery capacity of the n-th EV, respectively. Equation (5.2) can be interpreted as follows: find a P_{ref} such that it minimizes the difference between energy available for EV charging and energy required for EV charging. The ODC algorithm tries to find an optimal charging rate that minimizes the total load variance while the reformulated optimization problem minimizes the total load variance with respect to the reference total demand. Hence, Equation (5.2) solves only one optimization problem rather than solves n optimization problems until the algorithm converges to a solution as in the ODC algorithm [19]. However, this formulation does not take into account EV owners' timing constraints when finding an optimum reference EV power demand in terms of minimizing total load variance, which might cause any of timing constraints not to be satisfied. If timing constraints are available before the scheduler generates a charging schedule,

then this drawback can be alleviated. Since it is reasonable to assume that almost all EVs wanting to recharge are plugged in before midnight, the real-time EV charging scheduler might be able to have information on plug-out times of almost all EVs, and then let T_{plugout} denote the plug-out time of the last EV that will be plugged out from the system such as:

$$T_{\text{plugout}} = \max_{n} \; t_{\text{plugout}}(n), \qquad n = 1, 2, \ldots, N \tag{5.3}$$

where $t_{\text{plugout}}(n)$ is the plug-out time of the n-th EV, and N, the total number of EVs in the system. Hence, Equation (5.2) can be re-expressed as

$$\underset{P_{\text{ref}}(\cdot)}{\text{minimize}} \left(\sum_{t=1}^{T_{\text{plugout}}} \left(P_{\text{ref}}(t) - P_{\text{base}}(t)\right) \times (\Delta t/\eta) - \sum_{n=1}^{N} E_n \right)^2 . \tag{5.4}$$

The graphical difference between solutions for reference EV power demand provided by Equations (5.2) and (5.4) is illustrated in Figure 77.

In order to solve the optimization problem in Equation (5.4), the binary search algorithm is utilized. Since, in contrast to real-time computing systems, available power for EV charging is discretized into many charging packets, if, for simplicity, it is assumed that the scheduler allows an EV to be charged only at the maximum charging rate in a time slot, the energy required to refill the battery of the n-th EV,

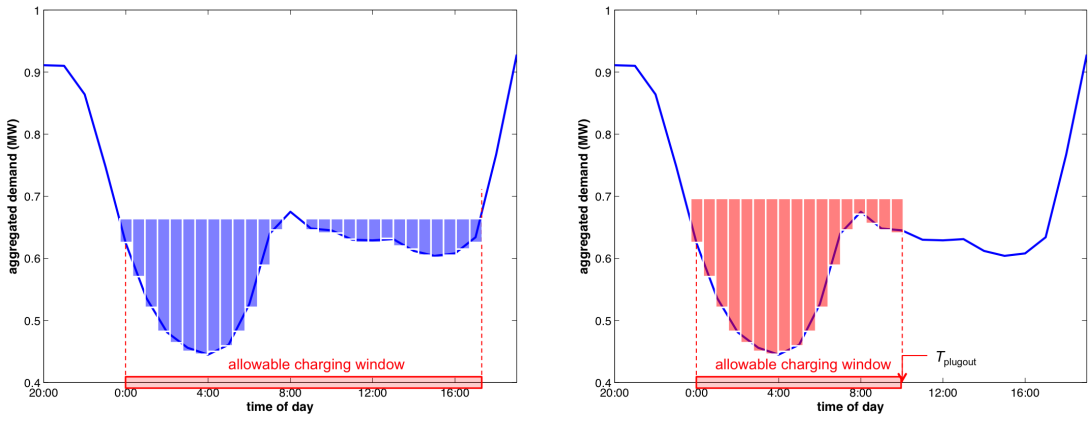

(a) estimated by Equation (5.2) (b) estimated by Equation (5.4)

Figure 77: Reference EV power demand estimation.

i.e., energy queue length, can be expressed as

$$E_n = \eta_n r_{\max}(n) \Delta t k(n) \tag{5.5}$$

where η_n is the charging efficiency, $r_{\max}$, the maximum charging rate, Δt, the duration of a time slot, and k, the total number of charging packets required to refill the battery up to s_{plugout}, whose duration is Δt and amplitude is $r_{\max}$ as depicted in Figure 76. To clarify this relationship, take an example as shown in Figure 78, in which there is an EV that has a 100% charging efficiency, its initial plug-in SOC is 20%, and wants to charge up to 10 kWh. If it can be charged only at the maximum charging rate, 2 kW, and a charging schedule is generated at every 30 minutes, then the duration and the amplitude of a charging packet is 0.5-hour and 2 kW, respectively. Therefore, to recharge its battery up to 10 kWh, it must be assigned $k_n = 8$ charging packets, taking 4 hours to refill the battery. Furthermore, since, as previously assumed, the scheduler has the charging information of the EVs, E_n can be calculated as follows:

$$E_n = \{s_{\text{plugout}}(n) - s_{\text{plugin}}(n)\} \times \beta_n, \tag{5.6}$$

where $s_{\text{plugin}}(n)$ and $s_{\text{plugout}}(n)$ are the plug-in and plug-out SOCs, and β_n, the battery capacity of the n-th EV, respectively. Therefore, the number of charging packets required for the n-th EV to be recharged can be obtained as

$$k(n) = \left\lceil \frac{E_n}{\eta_n r_{\max}(n) \Delta t} \right\rceil = \left\lceil \frac{\{s_{\text{plugout}}(n) - s_{\text{plugin}}(n)\} \beta_n}{\eta_n r_{\max}(n) \Delta t} \right\rceil, \tag{5.7}$$

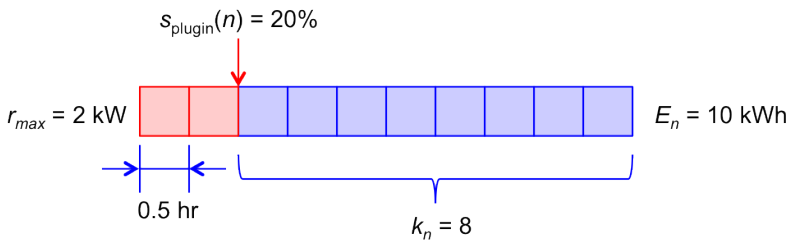

Figure 78: Relationship between charging packets and energy queue length.

where $\lceil x \rceil = \{n \in \mathbb{Z} | n \geq x\}$, and, in consequence, the total number of charging packets for the N EVs is

$$K = \sum_{n=1}^{N} k(n) = \sum_{n=1}^{N} \left\lceil \frac{\{s_{\text{plugout}}(n) - s_{\text{plugin}}(n)\}\,\beta_n}{\eta_n r_{\max}(n) \Delta t} \right\rceil. \tag{5.8}$$

Let P_{ref}^0 denote an initial guess of the reference EV power demand, which can be safely assumed to be the midpoint of the minimum non-EV power demand ($P_{\text{base}}^{\min}$) and the maximum non-EV power demand ($P_{\text{base}}^{\max}$), that is,

$$P_{\text{ref}}^0 = \left(P_{\min}^0 + P_{\max}^0\right)/2, \tag{5.9}$$

where $P_{\min}^0 = P_{\text{base}}^{\min}$ and $P_{\max}^0 = P_{\text{base}}^{\max}$, since EV power demand is most likely to lie between them. From the initial guess for the EV power demand, the number of charging packets available in a time slot t can be estimated as

$$\hat{k}(t) = \left\lceil \frac{P_a(t)}{r_{\max}} \right\rceil = \left\lceil \frac{P_{\text{ref}}^0 - P_{\text{base}}(t)}{r_{\max}} \right\rceil. \tag{5.10}$$

If

$$\hat{K} = \sum_{t=1}^{T_{\text{plugout}}} \hat{k}(t) \geq K, \tag{5.11}$$

then P_{ref}^0 is assigned to $P_{\max}^1$; otherwise, P_{ref}^0 is assigned to $P_{\min}^1$. Then, P_{ref} is updated as follows:

$$P_{\text{ref}}^1 = \left(P_{\min}^1 + P_{\max}^1\right)/2. \tag{5.12}$$

This process is repeated until the iteration reaches at the maximum number of iterations or $|K - \hat{K}| < \epsilon$, $\epsilon > 0$. The pseudocode of the reference EV power demand estimation is listed in Algorithm 4.

As can be seen in Figure 77(b), however, both of the end parts of the estimated reference EV power demand might not be smooth, in other words, the estimated reference EV power demand might not be a C^1-continuous curve[1], resulting in abrupt

[1] A C^1-continuous curve is a curve of which first derivatives are continuous.

Algorithm 4 Pseudocode of the reference EV power demand estimation.

initialize $P_{\min}$ and $P_{\max}$
for $n = 1$ to N **do**
    $E_n \leftarrow (s_{\text{plugout}}(n) - s_{\text{plugin}}(n)) \times \beta_n$
    $k(n) \leftarrow \lceil (E_n/(\eta_n r_{\max}(n)\Delta t) \rceil$
end for
for $i = 0$ to $I_{\max}$ **do**
    $P^i_{\text{ref}} \leftarrow (P^i_{\min} + P^i_{\max})/2$
    for $t = 1$ to T_{plugout} **do**
        $\hat{k}(t) \leftarrow \lceil (P^i_{\text{ref}} - P_{\text{base}}(t))/r_{\max} \rceil$
        if $\hat{k}(t) < 0$ **then**
            $\hat{k}(t) \leftarrow 0$
        end if
    end for
    if $\sum_t \hat{k}(t) > \sum_n k(n)$ **then**
        $P^{i+1}_{\max} \leftarrow P^i_{\text{ref}}$
    else
        $P^{i+1}_{\min} \leftarrow P^i_{\text{ref}}$
    end if
    if $|\sum_t \hat{k}(t) - \sum_n k(n)| < \epsilon$ **then**
        goto end-loop
    end if
    :end-loop
end for

changes in power consumption, which might cause higher ramping costs of generation plants. In consequence, it is desirable to make the reference EV power demand as smooth as possible to minimize the ramping costs of generation plants. In order to make the reference EV power demand smooth, the method for constructing a quadratic Bézier curve[2] is introduced. The method for constructing a quadratic Bézier curve is illustrated in Figure 79. Let's assume that there are three points P_0, P_1, P_2 that need to be connected by a quadratic Bézier curve, and let (x_0, y_0), (x_1, y_1), and (x_2, y_2) denote their coordinates, respectively. Let Q_0 denote a point that moves along the straight line from P_0 to P_1, and let Q_1 denote a point moving along the straight line from P_1 to P_2. Also, let's assume that points Q_0 and Q_1 start moving at $t = 0$ and stops at $t = 1$. Then, the coordinates of the points can be expressed as

$$Q_0 : \ (x_{q_0}, y_{q_0}) = ((x_1 - x_0)t + x_0, (y_1 - y_0)t + y_0) \tag{5.13a}$$

$$Q_1 : \ (x_{q_1}, y_{q_1}) = ((x_2 - x_1)t + x_1, (y_2 - y_1)t + y_1) \tag{5.13b}$$

where $0 \leq t \leq 1$. If another point B moves along the straight line connecting Q_0 and Q_1, starting at $t = 0$ and stopping at $t = 1$, then the locus of point B is given by

$$B : \ (x_B, y_B) = ((x_{q_1} - x_{q_0})t + x_{q_0}, (y_{q_1} - y_{q_0})t + y_{q_0}), \tag{5.14}$$

leading to a quadratic Bézier curve. Figure 80 shows the estimation results of reference EV power demand using linear Bézier and quadratic Bézier curves.

In this subsection, it is explained how to estimate power available for EV charging to calculate the number of available processing queues by estimating energy required, called a *reference EV power demand*. The ODC algorithm proposed in [19] can be used with a few modifications for this purpose, but for taking into account timing constraints as well as for improving simulation efficiency, a new algorithm to estimate

[2]Bézier curves are widely used in computer graphics to model smooth curves.

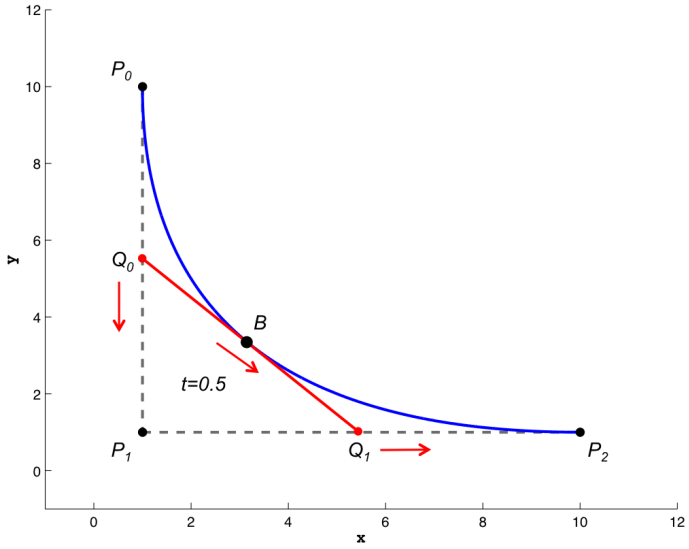

Figure 79: Construction of a quadratic Bézier curve (solid blue line: quadratic Bézier curve, dashed gray line: straight lines connecting P_0, P_1, P_2).

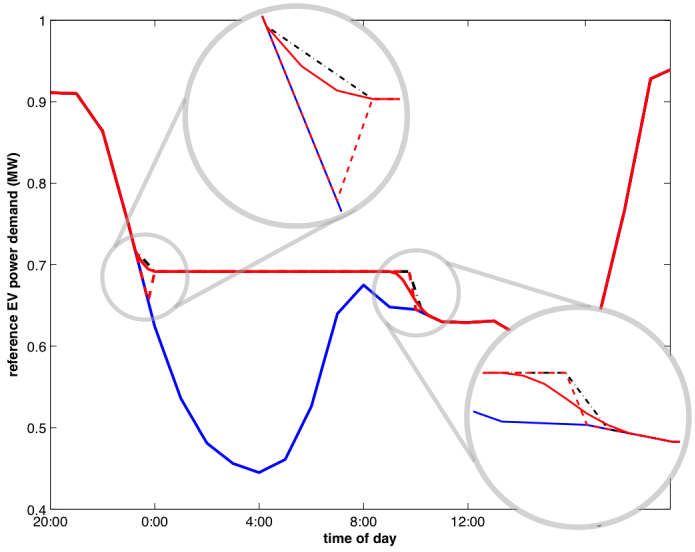

Figure 80: Reference EV power demand estimation using Bézier curve (solid blue line: non-EV power demand, dashed red line: without smoothing, dash-dot black line: linear Bézier, solid red line: quadratic Bézier).

available power is proposed and implemented. In order to find an optimal reference EV power demand, the popular binary search algorithm is utilized. Additionally, to minimize ramping costs of generation plants, a method to smooth out the end parts of the reference EV power demand using the construction method of quadratic Bézier curves is introduced. In the following subsection, it will be explained how to calculate the number of available processing queues based on the estimated reference EV power demand.

5.3.2 Determination of the Number of Processing Queues and Charging Rates

As explained in the previous subsection, it is required to calculate available charging capacity, i.e., the number of available processing queues (n_{PQ}) before an actual charging schedule is generated. The determination of the number of processing queues can be divided into two cases, depending on the homogeneity of charging stations in the system. For homogenous cases, where all charging stations have the same power ratings, especially maximum allowable charging rate, the number of available processing queues can be calculated using Equation (5.1). However, for heterogeneous cases, the maximum charging rate ($r_{\max}$) cannot be used to calculate the number of available processing queues any longer since all charging stations have different power ratings. Thus, Equation (5.1) needs to be reformulated in a different way.

First, let's take a look at how the charging rates for homogeneous cases are determined. Since, for simplicity, all EVs can be charged only at the maximum charging rate for homogeneous cases, the charging rates for n EVs in the processing queue at time t are simply given by

$$\bar{r}(t) = \left\{r_1,\, r_2,\, \ldots,\, r_{n(t)}\right\} = \{\underbrace{r_{\max},\, r_{\max},\, \ldots, r_{\max}}_{n(t)}\}, \tag{5.15}$$

where $n(t) \leq n_{\mathrm{PQ}}(t)$, if $P_{\mathrm{a}}(t)$ is a multiple of $r_{\max}$, i.e., $P_a(t) - n_{\mathrm{PQ}}(t) r_{\max} = 0$, $n_{\mathrm{PQ}}(t) = \lceil P_a(t)/r_{\max} \rceil$, as illustrated in Figure 81(a). However, if $P_{\mathrm{a}}(t)$ is not a

multiple of $r_{\max}$ and the processing queues are fully utilized, i.e., $n(t) = n_{\text{PQ}}(t)$, then $P_a(t)$ becomes less than $n_{\text{PQ}}(t)r_{\max}$, i.e., $P_a(t) - n_{\text{PQ}}(t)r_{\max} < 0$, and, as a consequence, charging the EV, assigned to the n_{PQ}-th processing queue, at the maximum charging rate $r_{\max}$ will cause energy to be overutilized, which would, in turn, aggravate the flatness of load curves. In order to avoid this undesirable situation, the EV assigned to the n_{PQ}-th processing queue might need to be charged at a fraction of the maximum charging rate rather than the maximum charging rate. Therefore, in this case, the charging rates need to be modified as

$$\bar{r}(t) = \{\underbrace{r_{\max},\, r_{\max},\, \ldots,\, r_{\max},\, [P_a(t) - (n_{\text{PQ}}(t) - 1)r_{\max}]}_{n_{\text{PQ}}(t)}\}, \tag{5.16}$$

which is illustrated in Figure 81(b).

A similar situation can take place when the energy queue length of an EV is less than the maximum charging rate, which, in contrast, might result in energy

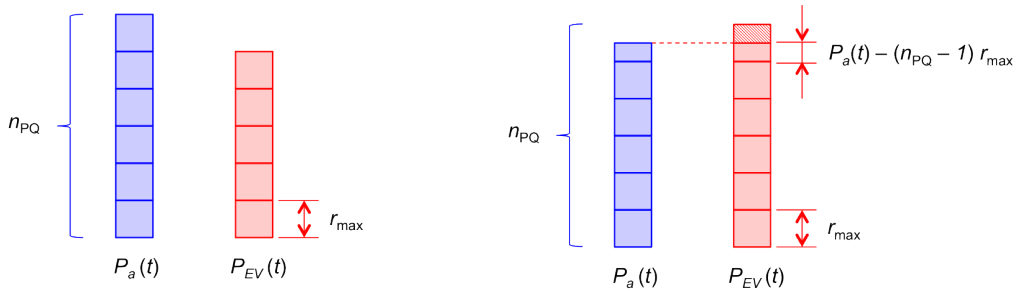

(a) $P_a(t)$ is a multiple of $r_{\max}$ (b) $P_a(t)$ is **not** a multiple of $r_{\max}$

Figure 81: Energy overutilization resulting from being charged at the maximum charging rate.

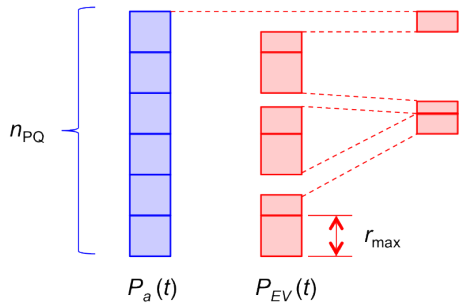

Figure 82: Energy underutilization due to energy queue length.

underutilization. Since it is assumed to be charged only at the maximum charging rate, an EV might be allocated maximum allowable energy even though it requires only a smaller amount of energy to be fully charged as illustrated in Figure 82. In order to avoid this situation, the charging rates given by Equation (5.16) is reformulated as follows:

Find $n(t)$ such that

$$\sum_{i=1}^{n(t)-1} r_i(t) \leq P_a(t) < \sum_{i=1}^{n(t)} r_i(t) \tag{5.17}$$

where

$$r_i(t) = \min\left\{r_{\max},\ E_i(t)/(\eta_i \Delta t)\right\}, \quad i = 1, \ldots, n(t). \tag{5.18}$$

As a result, the charging rate is given by

$$\bar{r}(t) = \{r_1, r_2, \ldots, r_{n(t)}\}, \quad 0 \leq n(t) \leq n_{\mathrm{PQ}}(t) \tag{5.19}$$

where

$$r_i(t) = \begin{cases} \min\{r_{\max},\ E_i(t)/(\eta_i \Delta t)\} & i = 1, \ldots, (n(t)-1) \\ P_a(t) - \sum_{i=1}^{n(t)-1} r_i(t) & i = n(t) \end{cases}. \tag{5.20}$$

The pseudocode of determining charging rates for homogeneous cases is listed in Algorithm 5.

Now let's consider the determination of the number of available processing queues and charging rates for heterogeneous cases. Different from homogeneous cases, the number of available processing queues cannot be calculated using Equation (5.1) for heterogeneous cases. Therefore, another approach needs to be come up with. For heterogeneous cases, rather than being assigned by means of charging packets, available power is directly allocated to active charging stations as follows. First, let's assume that all charging stations need to be registered to the controlling authority

Algorithm 5 Pseudocode of determining charging rates for homogeneous cases.

$P_a(t) \leftarrow P_{\text{ref}}(t) - P_{\text{base}}(t)$
for $i = 1$ to $n_{\text{PQ}}(t)$ **do**
    if $E_i(t)/(\eta_i \Delta t) \geq r_{\max}$ **then**
        $r_i(t) \leftarrow r_{\max}$
    else
        $r_i(t) \leftarrow (E_i(t)/(\eta_i \Delta t)$
    end if
    if $P_a(t) - r_i(t) \geq 0$ **then**
        $P_a(t) \leftarrow P_a(t) - r_i(t)$
    else
        $r_i(t) \leftarrow P_a(t)$
        break
    end if
end for

when installed, meaning the controlling authority have all power rating information of charging stations at hand. Then, if all EVs in the system can be arranged according to their priorities, for instance, $(\text{EV}_1, \text{EV}_2, \ldots, \text{EV}_N)$, where N is the total number of EVs in the system and, without loss of generality, EV_1 has the highest priority and EV_N has the lowest priority, then the number of EVs that can be charged simultaneously at time t, $n(t)$, can be obtained so as to maximize energy utilization as

$$\underset{n(t)}{\text{minimize}} \left\{ P_a(t) - \sum_{i=1}^{n(t)} r_i(t) \right\}^2, \quad t = 1, \ldots, T, \tag{5.21}$$

where

$$0 \leq r_i(t) \leq \min\{r_{\max}(i),\, E_i(t)/(\eta_i \Delta t)\} \quad \text{and} \quad 0 \leq n(t) \leq N. \tag{5.22}$$

Since it is assumed that the N EVs are sorted out with respect to their priorities, the optimization problem in Equation (5.21) can be solved as follows:

Find the maximum $n(t)$ such that

$$\sum_{i=1}^{n(t)-1} r_i(t) \leq P_a(t) < \sum_{i=1}^{n(t)} r_i(t), \quad 0 \leq n(t) \leq N, \tag{5.23}$$

where

$$r_i(t) = \begin{cases} \min\{r_{\max}(i),\ E_i(t)/(\eta_i \Delta t)\} & i = 1, \ldots, (n(t)-1) \\ P_a(t) - \sum_{i=1}^{n(t)-1} r_i(t) & i = n(t) \end{cases} . \quad (5.24)$$

Note that Equation (5.24) is the same as Equation (5.20), except that $r_{\max}$ is replaced by $r_{\max}(i)$ since not all EVs have the same maximum charging rate .

In this subsection, the methods to calculate the number of available processing queues both for homogeneous and heterogeneous cases are introduced and the allocation of available power to activated charging stations is also explained. These technical approaches will be evaluated through simulation studies, which will be presented in the next chapter.

5.3.3 Electricity Prices for V2G-based Frequency Regulation and EV Charging

As introduced in Chapter 3, four different charging modes are considered in this research: 1) charge now, 2) charge when power is available, 3) charge when given less expensive electricity price, and 4) charge/supply. In order to make EVs with charging mode 3, electricity price for charging must be made less expensive when there are available spots in the processing queue than when EVs with charging modes 1 and 2 occupy the entire processing queue. In addition, electricity price for V2G-based frequency regulation is set higher than the nominal price for EV charging to encourage EV owners to participate in V2G-based frequency regulation.

One of the objectives of this research is to investigate and characterize the system-level interactions between real-time EV charging and V2G-based frequency regulation, and thus it is not necessary and beyond the scope of this research to establish an accurate model of electricity prices for V2G-based frequency regulation and EV charging. Therefore, electricity price for EV charging when power is available for charging EVs with modes 1 and 2 is assumed to be a nominal price and set to \$1 per megawatt-hour.

When the amount of available power is more than power required to charge EVs with modes 1 and 2, electricity price for charging EVs is made less than the nominal price, \$0.5 per megawatt-hour, to encourage EV owners who select the charging modes 3 and 4 to start charging. On the other hand, for down-regulation, where load exceeds generation, the real-time EV charging system must increase electricity price for EV charging to discourage EVs with charging mode 3 from charging batteries and, at the same time, pay higher price for V2G-based frequency regulation to make EVs with charging mode 4 participate in the service. For this case, the prices for both EV charging and V2G-based frequency regulation are set to \$1.5 per megawatt-hour.

5.3.4 Real-time Scheduling Algorithms and Dynamic Priority

Referred to Figure 65 on page 146, the next step is the determination of priority assignment policies, followed by the implementation of real-time scheduling algorithms, introduced in §3.1.2. Since priority assignment is closely related to type of scheduling algorithms, which are applied to a problem of interest, two topics are dealt with together in this subsection. Basically, in this research, two perspectives are considered when priority assignment policies are designed: 1) *when EV owners want their cars to be charged* (i.e., charging mode) and 2) *how quickly EVs need to be recharged to meet their timing constraints*. Hence, a priority assignment policy is implemented such that a priority is dynamically assigned to each charging station where an EV is plugged in and updated every 15 minutes, based on 1) the *charging mode of the EV* and 2) the *amount of time required to refill the battery*. For this purpose, a parameter, called "*urgency*", taking account to the time required to refill the battery, is introduced and calculated as:

$$\gamma_n(t) = \frac{E_n(t)}{t_{\text{plugout}}(n) - t} \qquad \text{for } n = 1, \ldots, N, \quad t = 1, \ldots, T \tag{5.25}$$

where γ_n is the dynamic urgency of the n-th EV, $t_{\text{plugout}}(n)$, the plug-out time of the n-th EV, and t, the index of the current time slot, and E_n is the energy queue

length, i.e., energy necessary for the n-th EV to be fully charged, defined as $E_n = (s_{\text{plugout}}(n) - s_n(t)) \times \beta_n$, where β_n is the battery capacity, $s_{\text{plugout}}(n)$, the plug-out SOC, $s_n(t)$, the current SOC, and η_n, charging efficiency of the n-th EV, respectively. Combined with its charging mode, an EV with larger necessary energy (E_n) and shorter time-to-complete-charging ($t_{\text{plugout}} - t$) will have a higher priority.

As a proof of concept, a global EDF algorithm is first implemented, and its two variants with different priority assignment policies are also implemented to see the effects of the priority assignment on the performance of real-time EV charging. In order to apply the global EDF to EV charging control, the multiprocessor system model as illustrated in Figure 66(b) on page 147 is used. For the original global EDF algorithm, the priorities of EVs are determined by the *closeness to their absolute deadline*, i.e., $t_{\text{plugout}} - t$, where t is the current time; the EV with the shorter time to plug-out always has the highest priority. However, the n highest-priority EVs are being charged by the n processing queues in every time slot, where $n(t)$ is the number of unoccupied processing queues at a time instant, calculated as

$$n(t) = n_{\text{PQ}}(t) - n_{\text{EVsInPQ}}(t), \tag{5.26}$$

where n_{PQ} is the number of available processing queues, and n_{EVsInPQ} is the number of EVs occupying processing queues, respectively. With global EDF, EVs that are plugged in and ready to charge are placed in the waiting queue and sorted in a non-decreasing order with respect to their closeness to absolute deadlines, from which the first n EVs with higher priorities are assigned to the n available processing queues, if any. The pseudocode of the real-time EV charging scheduling algorithm is listed in Algorithm 6.

Figure 83 illustrates the process of investigating the applicability of the existing real-time scheduling algorithms to real-time EV charging control. In order to test the Hypotheses I-1 and I-2, real-time scheduling algorithms are first surveyed and qualitatively evaluated based on the characteristics of the problem. Scheduling algorithms

Algorithm 6 Pseudocode of the global EDF algorithm for real-time EV charging.

estimate P_{ref}
initialize w and p ▷ w (p): pointer for waiting (processing) queue
for $t = 1$ to T **do**
  $n_{\text{PQ}}(t) \leftarrow (P_{\text{ref}}(t) - P_{\text{base}}(t))/r_{\max}(t)$ ▷ $r_{\max}$: maximum charging rate
  for $n = 1$ to N **do**
    $E_n(t) \leftarrow (s_{\text{plugout}}(n) - s_n(t)) \times \beta_n$
  end for
  $\mathbf{W}(w : w + m) \leftarrow \mathbf{EV}(1 : m)$ ▷ $\mathbf{W}$: waiting queue
  $w \leftarrow w + m$ ▷ m: number of EVs plugged in
  if $(t_{\text{plugout}}(i) - t) < (t_{\text{plugout}}(j) - t)$ **then**
    $\mathbf{W}(j) \leftarrow \mathbf{W}(i)$, $\mathbf{W}(i) \leftarrow \mathbf{W}(j)$ ▷ sort waiting queue
    $\mathbf{P}(j) \leftarrow \mathbf{W}(i)$, $\mathbf{W}(i) \leftarrow \mathbf{P}(j)$ ▷ preemption
  end if
  if $n_{\text{PQ}}(t) - n_{\text{EVsInPQ}}(t) > m$ **then**
    $k \leftarrow m$ ▷ k: number of available processing queues
  else
    $k \leftarrow n_{\text{PQ}}(t) - n_{\text{EVsInPQ}}(t)$
  end if
  if $k > 0$ **then**
    $\mathbf{P}(p : p + k - 1) \leftarrow \mathbf{W}(1 : k)$ ▷ $\mathbf{P}$: processing queue
    $\mathbf{W}(1 : w - k - 1) \leftarrow \mathbf{W}(k + 1 : w - 1)$
    $p \leftarrow p + k$
    $w \leftarrow w - k$
  end if
  if $(t_{\text{plugout}}(i) - t) < (t_{\text{plugout}}(j) - t)$ **then**
    $\mathbf{P}(j) \leftarrow \mathbf{P}(i)$, $\mathbf{P}(i) \leftarrow \mathbf{P}(j)$ ▷ sort processing queue
  end if
  for $n = 1$ to N **do**
    $s_n(t + 1) \leftarrow 1 - (E_n(t) - \eta_n r(t) \Delta t)/\beta_n$ ▷ update state-of-charge (SOC)
  end for
end for

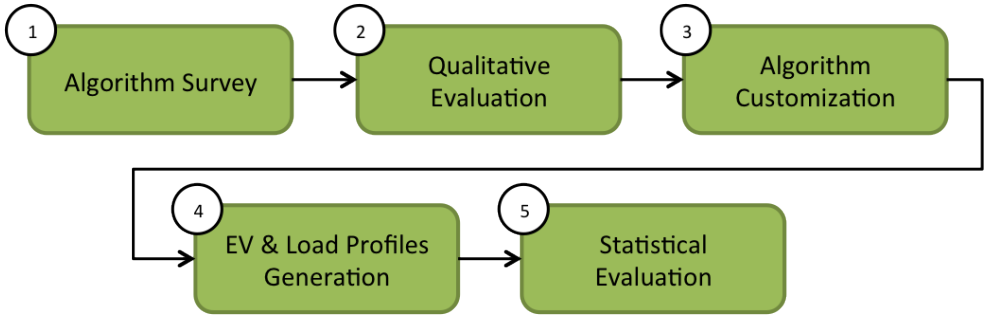

Figure 83: Investigation process of real-time scheduling algorithms.

that can be applied to the problem are tailored and quantitatively evaluated with a number of random EV charging profiles and load profiles in terms of the performance metrics such as guarantee ratio, averaged plug-out SOC, and total load variance.

5.3.5 Effects of Charging Rates Control on Real-time EV Charging Control

As mentioned in §3.1.3, it is observed from the proof-of-concept simulation, which will be presented in §6.2.1, that all EVs, especially EVs with charging modes 3 and 4, are not fully charged even though the day-ahead generation is planned based on the total energy required for all the EVs to be fully charged. In order to increase the number of EVs with modes 3 and 4 that are fully charged, formulated was the following hypothesis: if charging rates are controlled based on both the energy utilization and the number of EVs that are charging simultaneously for a given time slot, then the guarantee ratio, defined as the ratio of fully charged EVs meeting their deadlines to the total number of EVs in the system, will be improved (Hypothesis I-3). In addition, it was mathematically proved that charging rates need to be determined to maximize the energy utilization by charging batteries at the maximum charging rate while maximizing the number of EVs that can be charged simultaneously by making charging rates as low as possible, and thus an optimization problem for charging rates was formulated.

In this research, rather than solved with some optimization problem solving techniques, the optimization problem, given by Equation (3.17) on page 98, is solved in a heuristic approach. Figure 84 illustrates the experimental setting for testing Hypothesis I-3. To test the first part of the hypothesis, the charging rate will be swept by the unit of 0.1 C-rate (1 C-rate charging fills up the SOC as much as 100% in an hour) in the allowable range to see if the change in charging rates affects the performance of the proposed EV charging system. It is expected that, at the very beginning of

charging process where available power is relatively small and the number of EVs required to be charged is relatively large, a smaller charging rate will provide the better performance because it can allow more EVs to start charging. However, for time slots where available power is relatively large, a higher charging rate will provide better performance because the number of EVs to be charged is relatively small, compared with available energy, and smaller charging rates might result in lower energy utilization, resulting in the degradation of the optimality. Once the effects of charging rates on the performance of the real-time EV charging system is confirmed, the charging rate will be optimized with heuristics and evaluated through statistical simulations, in which the real-time EV charging system will be exposed to a variety of pseudorandom EV charging profiles and load profiles, in order to test the second part of the hypothesis.

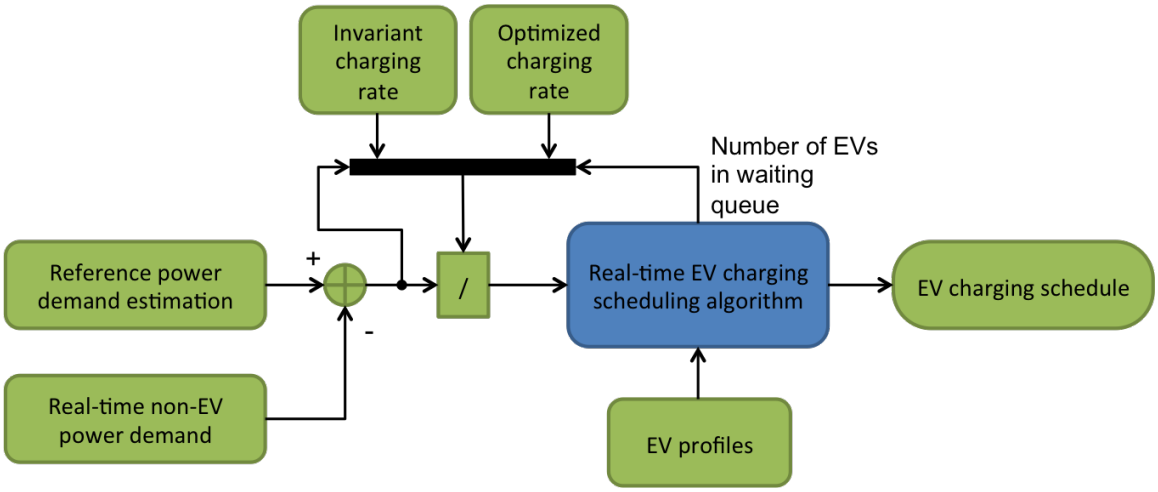

Figure 84: Experimental setting for testing Hypothesis I-3.

5.4 Real-time EV Charging Scheduling in Support of V2G-based Frequency Regulation

5.4.1 V2G-based Frequency Regulation within Real-time EV Charging Control

Figure 85 overviews the verification process of the incorporation of V2G-based frequency regulation into the real-time EV charging system. First, in order to verify the capability of the proposed real-time EV Charging control strategy to provide V2G-based frequency regulation, it is necessary to make non-EV demand fluctuating around the baseload profile. According to an ORNL's technical report, "Regulation is a zero-energy service, making it an ideal candidate for supply by storage" [37]. To validate this assertion, a set of real frequency regulation data is acquired from California ISO, as shown in Figure 86. The average of the data is 9.77% of peak loads; however, the net sum is -5.88×10^{-13}. Therefore, it is safely assumed that frequency deviation can be modeled as an *additive White Gaussian noise* (AWGN) with zero mean and σ^2-variance. Then, the following question arises: how can we determine the magnitude of frequency deviation, σ? FERC requirements for frequency regulation

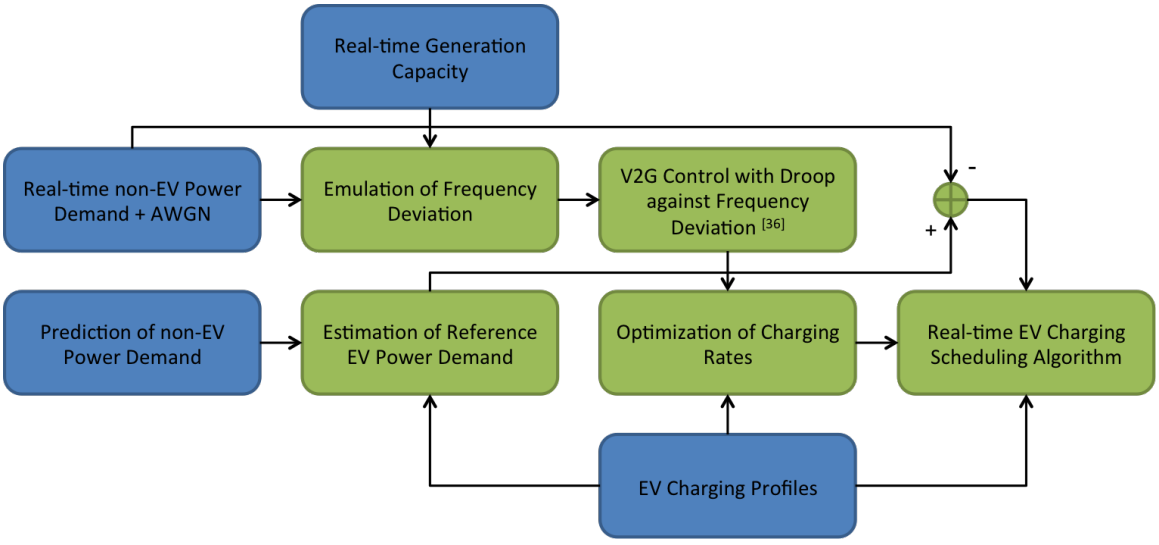

Figure 85: Overview of verification of V2G-based frequency regulation (blue: external data, green: algorithms).

is that frequency deviation must be less than 1% of peak load, and the maximum percentage of frequency deviation per 5-minute interval is no greater 10% as depicted in Figure 86. So, for the proof of the support of V2G-based frequency regulation as a by-product by applying real-time scheduling techniques to EV charging, 10% frequency deviation, that is, an AWGN with zero-mean and 10%-variance is applied to the baseload profile (non-EV power demand), and the following equation is used to calculate the frequency deviation from the nominal frequency:

$$-\frac{d\Delta f}{dt} = \Delta P(t) = P_{\text{gen}}(t) - P_{\text{demand}}(t) \tag{5.27}$$

For V2G-based frequency regulation, the V2G control methodology proposed in [62] will be used, and the proposed optimization algorithm for charging rates control will be utilized for scheduled charging. The number of available processing queues for the real-time scheduling will be calculated based on measurements of the real-time non-EV power demand and the reference EV power demand estimation. Through the process, it will be verified that the impacts of V2G-based frequency regulation on the real-time EV charging scheduling can be minimized if the interaction between V2G-based regulation and real-time scheduling is considered when designing a real-time EV

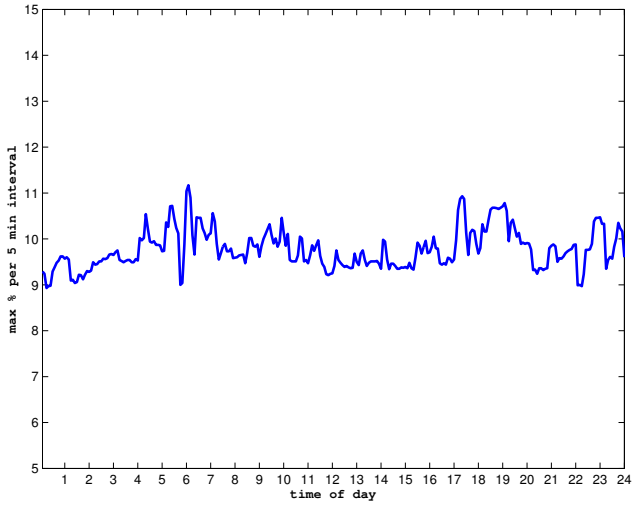

Figure 86: Frequency regulation in CAISO (Source: California ISO Open Access Same-time Information System (OASIS) [4]).

charging system. In addition, the relationship between EVs' SOCs and desirability for participation in V2G-based frequency regulation as illustrated in Figure 87, is used. The figure indicates that EVs with higher SOC are more desirable for up-regulation, while EVs with lower SOC are more suitable for down-regulation.

5.4.2 Effects of V2G-based Frequency Regulation on Real-time EV Charging Control

It is claimed in §3.2.2 that the incorporation of V2G-based frequency regulation may degrade the performance, esp. guarantee ratio, of the real-time EV charging system since EV charging possibly keep interrupted by the frequency regulation, which causes EVs to take longer time to complete their scheduled charging. In order to avoid this performance degradation, it is hypothesized that *if the statistics of EV charging profiles (and/or frequency regulation) is taken into account in generating charging schedules, then the real-time EV charging system can satisfy timing constraints while providing V2G-based frequency regulation* (Hypothesis II-2), and the concept of "*timing buffer*", in which the statistics of EV charging profiles are reflected, is introduced to avoid this undesirable situation. It is expected that the timing buffer will allow

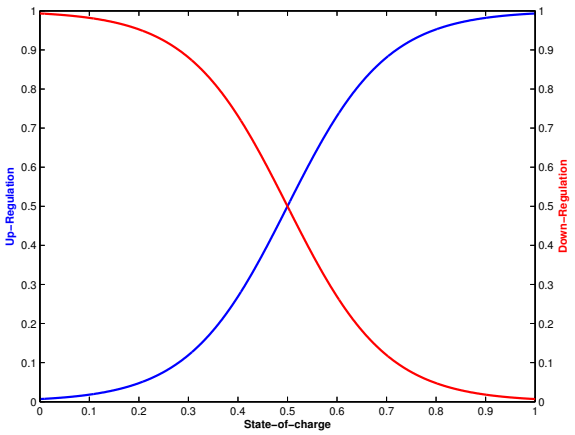

Figure 87: Desirability for frequency regulation against SOC (blue: up-regulation, red: down-regulation).

extra energy for V2G-based frequency regulation besides EV charging, and also expedite the charging process by encouraging EVs to complete refilling their batteries earlier than their plug-out times. A timing buffer is calculated based on the statistics of EV charging profiles on a specific day of the week, and included in each EV's timing constraint.

Figure 88 illustrates the consolidation of the concept of timing buffer in the estimation process for statistical reference EV power demand and the real-time EV charging scheduling, and overviews the process for testing Hypothesis II-2. Since it is not known whether or not V2G-based frequency regulation affects the performance of real-time EV charging control, the scheduling algorithm will be first exposed to a set of baseload profiles that are corrupted by an AWGN to confirm the effects of V2G-based frequency regulation on real-time EV charging. Once the effects are confirmed, it will be ensured that the concept of timing buffer is able to improve the performance of the real-time EV charging control strategy even when it provides V2G-based ancillary service while charging EVs. The statistics of EV charging profiles, such as means and standard deviations of plug-in/-out times and plug-in/-out SOCs, are calculated

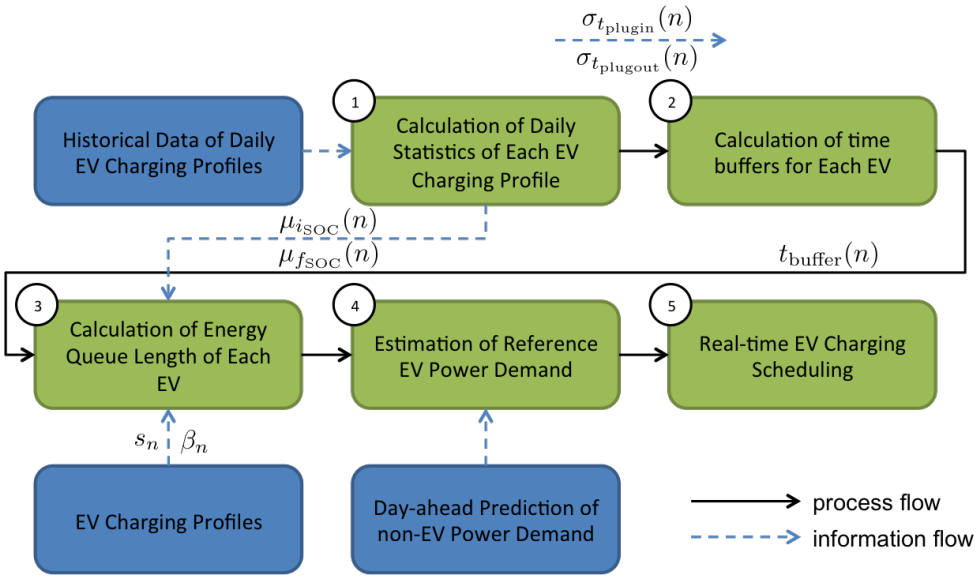

Figure 88: Schematic overview of testing Hypothesis II-2 (blue: external data, green: algorithms).

based upon historical data of daily EV charging profiles; however, it is not possible to collect such historical data because EVs are not widely commercialized and it is not confirmed that such charging stations that can accept user-specified charging profiles have been released. Therefore, a set of fictitious EV charging profiles, which can represent charging profiles on day of the week, will be generated instead. Once the statistics of EV charging profiles have been calculated, a day-ahead reference EV power demand will be optimized based on the statistics and a day-ahead prediction of non-EV power demand. Finally, the statistically estimated day-ahead reference EV power demand will be applied to the real-time EV charging scheduling algorithm, of which performance will be, in turn, evaluated to test Hypothesis II-2.

5.5 Simulation Framework for Real-time EV Charging Control

A simulation framework for evaluating the real-time EV charging scheduling algorithm is implemented using MATLAB Graphical User Interface Development Environment (GUIDE). It has the following features:

- It provides several representative EV and baseload (non-EV demand) profiles.
- It allows a user to create or specify one's own profiles.
- It provides statistics information of EV and load profiles in a graphical way.
- It offers a simulation environment for different scheduling policies, timing constraints, etc.
- It lets a user to simulate and characterize real-time EV charging with V2G-based frequency regulation.

Figure 89(a) is the first window that appears when the program is run. It contains a set of instructions for setting up parameters and running a simulation. On the window in Figure 89(b), a user can select an EV profile or generate EV profiles. It provides users with a default profile and several existing profiles, and also allows

a user to create one's own profiles with different statistics. In addition, it provides statistics information and graphical interpretation of the selected EV profile. A user can save the profile figures for later use. The window in Figure 89(c) offers an interface for selecting a load profile. It provides a default baseload profile and several representative profiles for typical winter and summer days. It also provides an environment and a guideline for a user to create one's own baseload profiles. A user can save the profile figure for later use. The window in Figure 89(d) enables a user to run simulations for the chosen profiles. For comparing with the valley-filling strategy, it allows a user to run a simulation on the valley-filling strategy, too. It provides a variety of simulation parameters for case studies such as no timing constraints, load fluctuation, V2G-based frequency regulation, and various scheduling policies. A user can also run Monte Carlo simulations on a set of different EV profiles or baseload profiles.

(a) Main window

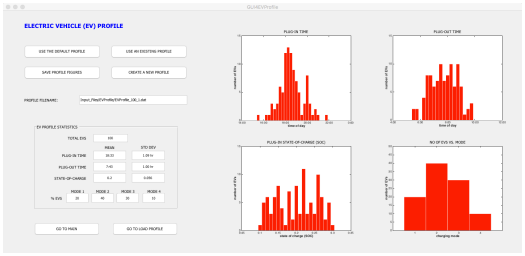

(b) Window for EV profile selection

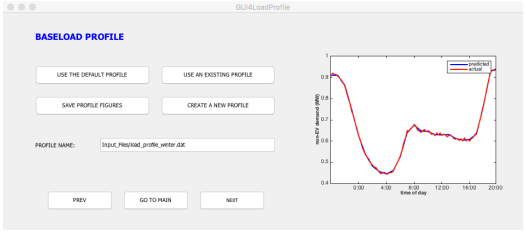

(c) Window for baseload profile selection

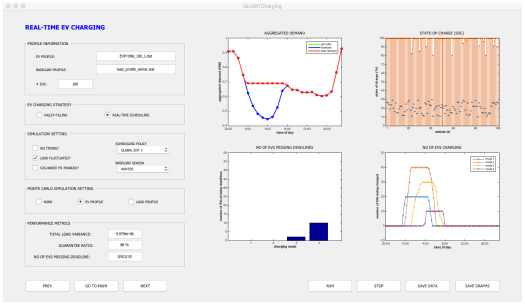

(d) Window for simulation running

Figure 89: Front-end graphical user interface of simulation framework.

CHAPTER VI

SIMULATION STUDIES

The purpose of simulation studies is to test the hypotheses presented in Chapter 3. First, the preparation of a dataset such as baseload profiles and EV charging profiles and the implementation of a benchmark system, i.e. the valley-filling charging strategy, are explained, and then the technical gaps of the benchmark system are substantiated. After the dataset and the benchmark system are prepared, the applicability of real-time scheduling techniques to EV charging control and various real-time scheduling algorithms is examined, and then the effects of charging rates control on the performance of the proposed EV charging strategy is tested. Once the applicability of real-time scheduling techniques to EV charging is confirmed, the proposed real-time EV charging control strategy is proved to fill the technical limitations of the valley-filling EV charging strategy. Finally, the capability of the proposed EV charging concept to provide V2G-based frequency regulation within the same framework is demonstrated.

6.1 Preparation of Dataset and Benchmark System

The first step for simulation studies is to generate a set of input data such as EV charging profiles and baseload profiles for simulations, and to develop a benchmark system, with which the proposed real-time EV charging scheme can be compared. This section articulates how to generate a dataset for demonstrating the applicability of real-time scheduling techniques to EV charging control, followed by the explanation on the implementation of a benchmark system.

6.1.1 Baseload Profiles and EV Charging Profiles

A variety of load profiles are available from the websites of almost all Independent Service Operators (ISOs), and, for this study, data from California ISO is utilized to investigate the proposed real-time EV charging scheme. In order to compare the proposed real-time EV charging strategy with the "valley-filling" control strategy proposed in [19], the same load profile used in [19], the average residential load profile in a service area of Southern California Edison (SCE) from 20:00 on February 13th, 2011 to 19:00 on February 14th, 2011, is selected as a non-EV base demand profile and scaled down to represent 20% penetration level of EVs, as shown in Figure 90.

The EV charging parameters for simulation studies are summarized in Table 23. According to the typical charging characteristics of EVs in [30], it is assumed that the battery capacity is 16 kWh, the maximum charging rate is 3.3 kW, and the charging efficiency is 0.95. The maximum charging rate of 3.3 kW is limited by the on-board charger of an EV, although a single-phased, Level 2 charger supplies 240V/30A and allows for a wide range of charging speeds, all the way up to 19.2 kW. Note that simulations are first performed on a set of homogenous fleet of EVs, that

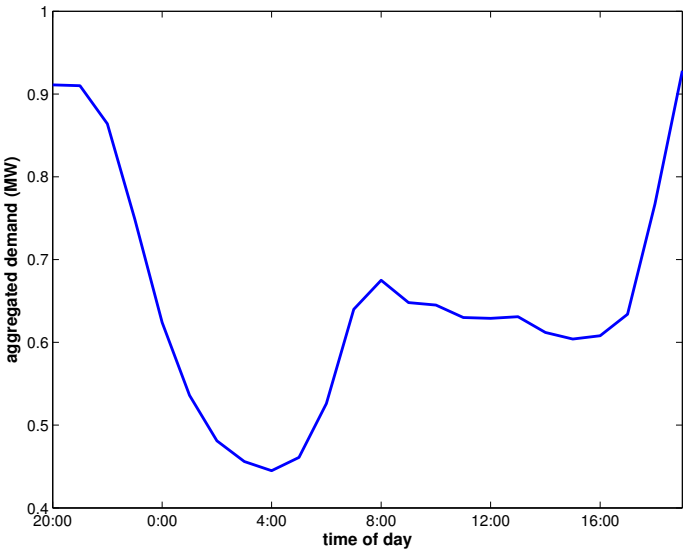

Figure 90: Baseload profile (Source: Southern California Edison [76]).

Table 23: EV charging parameter settings for simulation studies.

Parameter	Value
Number of EVs	100
Battery capacity	16 kWh
Max. charging rate	3.3 kW
Charging efficiency	0.95
Charging window	0:00 – 17:00

is, the aforementioned characteristics are assumed to be identical for all EVs, and, later, this restriction is relaxed for more realistic simulation studies. The scheduling horizon, typically 24 hours, is divided into 96 time slots, each of 15 minutes, during which the charging rate of each EV is assumed to be not changed. Based on the averaged non-EV power consumption, the number of EVs is assumed to be 100, representing 20% penetration level[1], according to which the non-EV base demand profile is appropriately scaled. In addition, the charging window is assumed to be 12:00 am to 5:00 pm to achieve the flattened load shape of the"valley-filling" charging scheme.

In order to take account of EV owners' charging preferences including timing constraints for charging, a variety of sets of EV charging profiles such as plug-in time, plug-out time, plug-in SOC, and plug-out SOC are generated in a random fashion and an example is shown in Figure 91. The plug-in time is assumed to be normally distributed around 6:00 pm with standard deviation of 2 hours. Similarly, it is assumed that the plug-out time has a normal distribution with mean of 7:00 am and standard deviation of 2 hours. The initial plug-in SOC is uniformly distributed between 10% and 30%, and the plug-out SOC is assumed to be 1. The charging modes

[1] "In 2010, the average annual electricity consumption for a U.S. residential utility customer was 11,496 kWh, an average of 958 kWh per month, and an average of 32 kWh per day" [81].

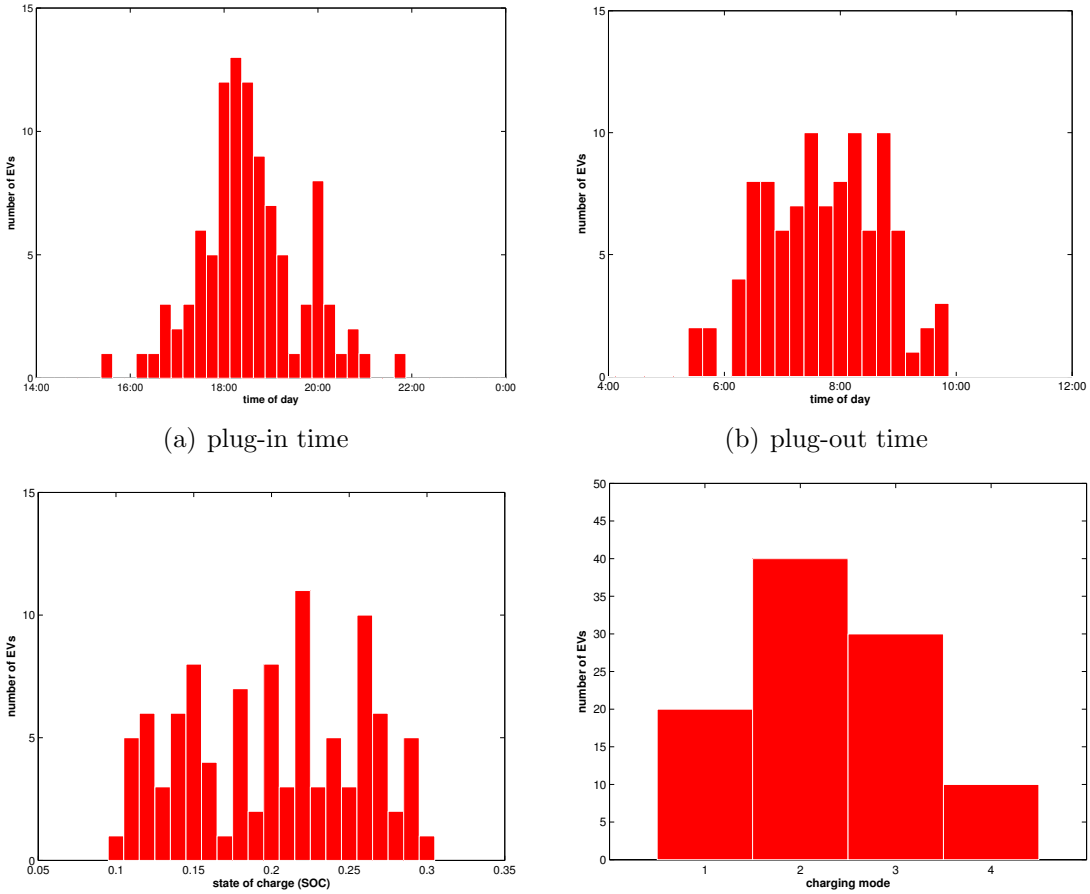

(a) plug-in time

(b) plug-out time

(c) initial state-of-charge (SOC)

(d) charging modes

Figure 91: An example of EV charging profiles.

as summarized in Table 7 are assigned to each EV based on its urgency measure, γ, defined as

$$\gamma_n(t) = \frac{E_n(t)}{t_{\text{plugout}} - t} \tag{6.1}$$

where $\gamma_n(t)$ is the urgency of the n-th EV at time t, t_{plugout}, plug-out time, E_n, the energy queue length, given as $E_n(t) = (s_{\text{plugout}}(n) - s_n(t)) \times (\beta_n/\eta_n)$, β_n, battery capacity, and η_n, charging efficiency. Equation (6.1) can be interpreted as follows: the energy queue length is the amount of energy required to refill the battery, and $(t_{\text{plugout}} - t)$ can be viewed as the time required to be fully recharged; therefore, the more the energy required to refill is and the shorter the time to full charge is, the greater the urgency is, that is, the more likely an EV owner prefers a charging mode with higher priority in order to refill the battery by the time he/she wants to drive off. The fleet mix is assumed to have, in descending order of the urgency, 20% of EVs for charging mode 1, 40% for charging mode 2, 30% for charging 3, and 10% for charging mode 4, the lowest priority(for V2G-based frequency regulation), respectively.

Figure 92 shows how many EVs are plugged in to the system with respect to time of day (see Figure 92(a)) and the distribution of averaged duration for which EVs are plugged in (see Figure 92(b)) for the exemplary EV charing profile presented in

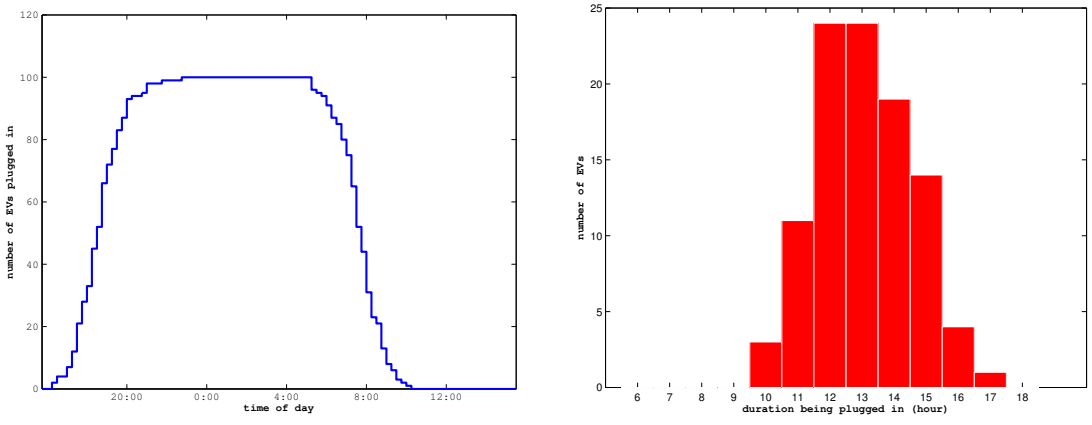

(a) number of EVs plugged in (b) duration being plugged in

Figure 92: Timing characteristics of the exemplary EV profile.

Figure 91. Based on Table 23, it takes approximately 5 hours, that is, 20 consecutive time slots, for an EV to be fully recharged, and, as shown in Figure 92(b), EVs have been plugged in for about 13 hours on average, which is plenty of time for EVs to refill their batteries unless available power is considered. The dataset, necessary to verify the benchmark system and the proposed real-time EV charging system and to compare with each other, is ready, and then the next step is to implement and verify the benchmark system, and substantiate its technical gaps before the proposed real-time EV charging scheme is verified and investigated.

6.1.2 Implementation of a Benchmark System and Substantiation of Its Technical Gaps

As addressed in §2.3.2, the decentralized "valley-filling" charging scheme has a number of technical limitations from the practical point of view, which are re-summarized as follows:

1. It only deals with day-ahead negotiation of charging profiles.
2. The prediction of non-EV power demand must be accurate.
3. All EVs must participate in the negotiation simultaneously.
4. Energy demand of EVs must be known to utilities beforehand.
5. The charging requirements of EVs must not change to guarantee the optimality.
6. The scheme does not take into account EV owners' timing constraints.

The first, third and fourth limitations are too obvious to substantiate because the algorithm is derived based on the assumption that the scheduler, i.e., a utility, can predict load profile quite precisely and knows charging requirements of EV owners beforehand. The second limitation can be justified by introducing some uncertainty to the baseload profile or an abrupt change in the baseload profile. In the similar manner, the last two limitations can be shown by applying EV charging profiles with timing constraints and then introducing some discrepancies to the EV charging profile

that is used for the day-ahead charging schedule.

In order to substantiate the technical gaps of the benchmark system, the valley-filling EV charging strategy proposed in [19] is implemented. Basically, the charging profile generated by their valley-filling charging scheme is a Nash equilibrium that is converged through the day-ahead negotiation process, which is identical for all EVs, and, hence, the scheme allocates available power equally to all EVs. Therefore, the charging profile of the benchmark system can be approximately derived by dividing available power by the total number of EVs to be charged, and it can be obtained by applying the algorithm for estimating the reference EV demand explained in §5.3.1. For case studies, Gan *et al.* chose "the average residential load profile in the service area of Southern California Edison (SCE) from 20:00 on February 13th, 2011 to 19:00 on February 14th, 2011 as the normalized base demand profile" as mentioned in §6.1.1 [19]. All EVs are assumed to plug in at 20:00 and have deadline 19:00 the next day, and the maximum charging rate is set to 3.3 kW.

Figure 93 shows the aggregated demand profile of the implemented benchmark system for the case described in the previous paragraph, and compares with the one presented in Gan *et al.*'s study. In the ideal case where no EV owners' timing con-

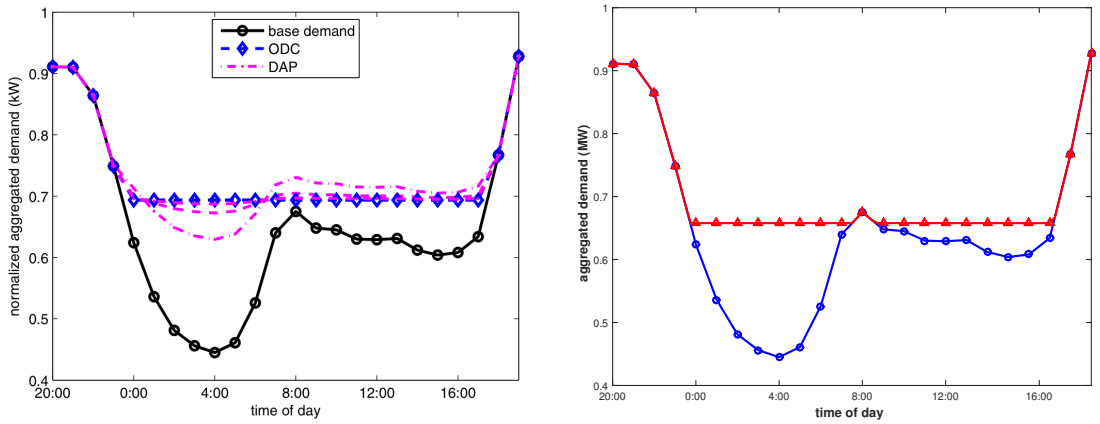

(a) aggregated demand presented in Gan *et al.*'s study [19]

(b) aggregated demand by Implemented benchmark

Figure 93: Verification of the implemented benchmark system.

straints (i.e., plug-in/-out time) are taken into account and all charging requirements (i.e., plug-out SOC) are assumed to be known to the utility beforehand, the implemented benchmark system achieves the same flat load curve as illustrated in Figure 93(b), albeit the amplitude of the load curve is a little smaller than the one presented in Figure 93(a), resulting from the fact that the EV charging profiles used to estimate the reference EV demand doest not exactly match the ones for Gan *et al.*'s case study and are normalized on a different scale.

Even though the effect of load variations on the valley-filling charging scheme is obvious, the implemented benchmark valley-filling scheme is applied to the SCE's baseload profile corrupted with an additive White Gaussian noise (AWGN) to justify the claim that the valley-filling EV charging scheme is sensitive to the change in load/generation capacity, i.e., the second claim in the very first paragraph of this subsection. First, a load fluctuation, modeled as an AWGN, as explained in §5.4.1, is applied to the baseload profile and simulations are run to capture the effects of load fluctuations on the valley-filling charging scheme. It is assumed that generation adheres to its day-ahead plan and there is no failure of generation. As seen in Figure

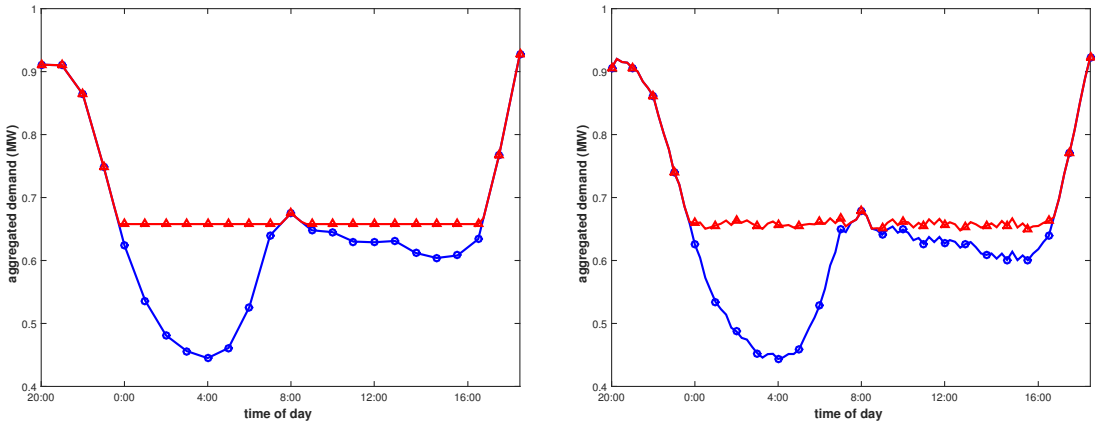

(a) planned (**no** load fluctuation) (b) actual (**with** load fluctuation)

Figure 94: Load profile of valley-filling strategy with load fluctuation (blue circle: base, red triangle: base + EV).

94(b), although the load profile is fluctuating, all EVs charge their batteries in accordance with the day-ahead charging plan, regardless of the actual load profile, and, thus, the scheme does not provide a flat load profile any longer, reflecting the exact load fluctuation on the load profile; in other words, it is literally not "valley-filling" any longer (see Figure 94(a) for the predicted load profile based on the day-ahead charging plan). As illustrated in Figure 95, no matter whether instantaneous power consumption increases or decreases, all EVs are recharging their batteries in accordance with their day-ahead charging schedules, sharing all available power, if any, and, therefore, it still provides the same plug-out SOCs (Figure 96(b)) as the ones without load fluctuation (Figure 96(a)).

In order to justify the fifth and sixth claims on the technical limitations of the valley-filling strategy, a set of EV charging profiles, introduced in §6.1.1, is applied to the valley-filling charging scheme. First, the fifth claim is verified by applying two EV profiles to the valley-filling scheme. A set of EV charging profiles is used to generate a charging plan, and then another set of EV profiles, which is slightly different from the one used for planning, is used when actual charging takes place. As claimed, Figure 97(a) shows a load profile that is not flat any longer, and none of EVs satisfies

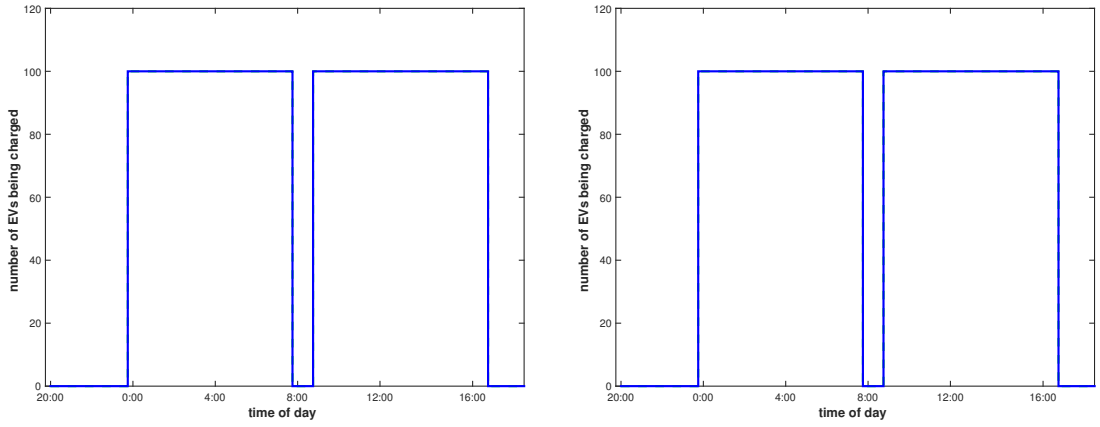

(a) planned (**no** load fluctuation) (b) actual (**with** load fluctuation)

Figure 95: Number of EVs being charged of valley-filling strategy with load fluctuation.

its timing constraints, as illustrated in Figure 97(e). To justify the sixth claim that, if EV owners' timing constraints are considered, the valley-filling scheme would not guarantee the flat load curve, let alone the satisfaction of the timing constraints, a charging schedule is generated based only upon energy required to fill the batteries of all EVs, which is directly related to the initial and departure SOCs, and then EVs are made stop recharging on the plug-out times that EV owners would specify when they plugged in their vehicles. As illustrated in Figure 97(b), if timing constraints are taken into account, then the valley-filling scheme does not guarantee its optimality, that is, the load curve is not flat any more. Since the optimal charging profiles are generated one day before the actual charging takes place such that the shape of the load profile is flattened out all over the charging window and all EVs share available power at the same time, all EVs start charging simultaneously at the beginning of the charging window, i.e., 12:00 am, and finish charging at the end of the charging window, i.e., 5:00 pm. Therefore, if many EVs are plugged out from charging stations earlier than the schedule generated the day before actual charging as illustrated in Figure 97(d), then its optimality is no longer guaranteed, not to mention ending up with not fully charged batteries, as illustrated in Figure 97(f), which looks a little worse compared to

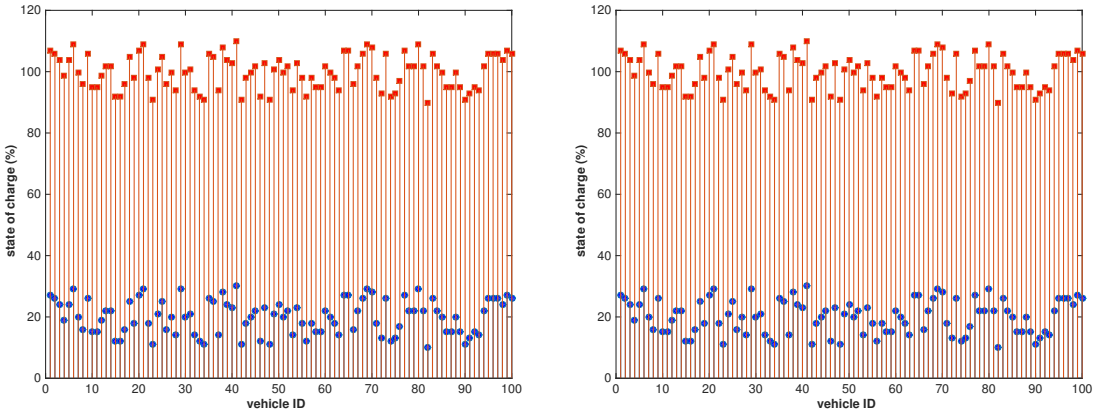

(a) planned (**no** load fluctuation) (b) actual (**with** load fluctuation)

Figure 96: State-of-charge (SOC) of valley-filling strategy with load fluctuation (blue circle: plug-in SOC, red rectangle: plug-out SOC).

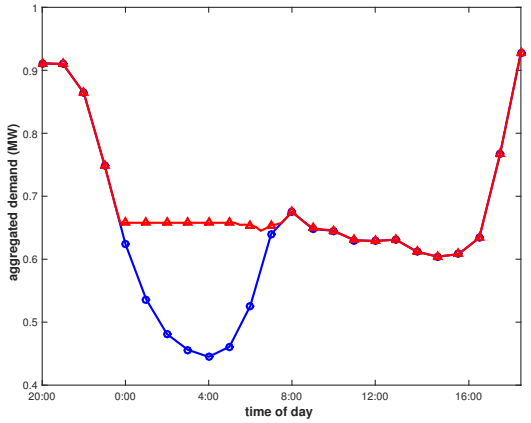

(a) load profile (blue circle: base, red triangle: base + EV)

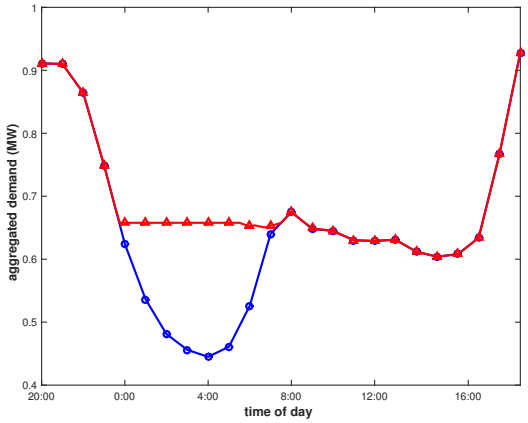

(b) load profile (blue circle: base, red triangle: base + EV)

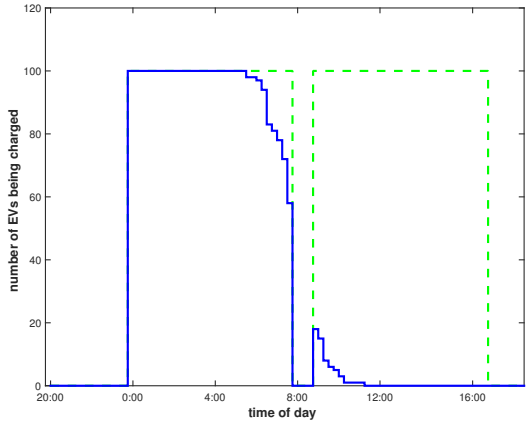

(c) number of EVs being charged (solid blue: actual, dashed green: scheduled)

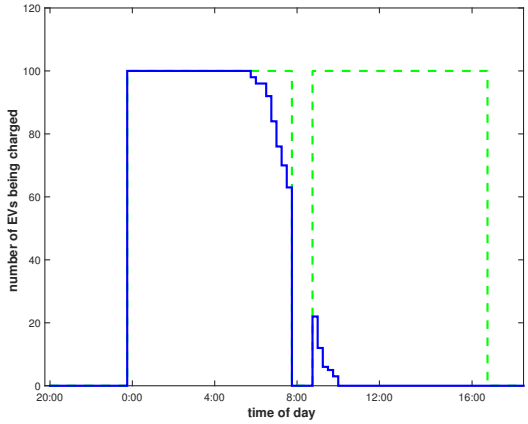

(d) number of EVs being charged (solid blue: actual, dashed green: scheduled)

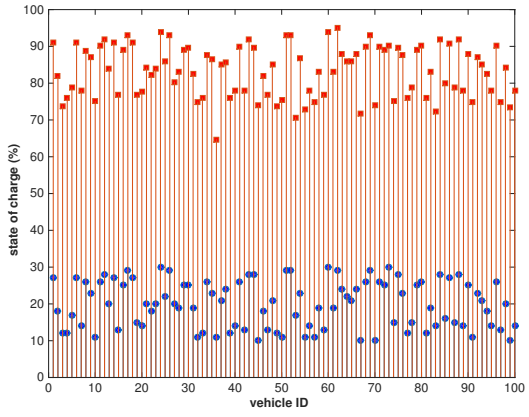

(e) state-of-charge (blue circle: plug-in SOC, red rectangle: plug-out SOC)

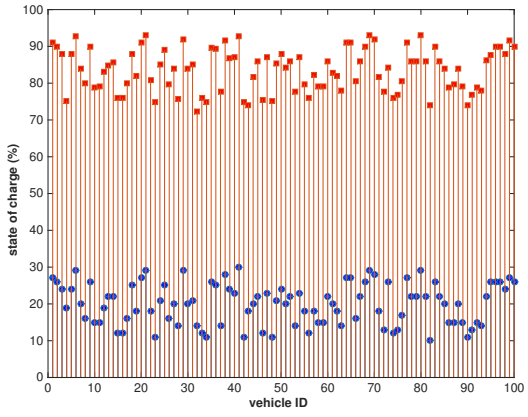

(f) state-of-charge (blue circle: plug-in SOC, red rectangle: plug-out SOC)

Figure 97: Valley-filling strategy with different EV profiles and timing constraints (left figures: with different EV profiles, right figures: with timing constraints).

Figure 96(a). Through simulations are substantiated the technical gaps of the valley-filling EV charging scheme that it is very sensitive to changes in load/generation and does not guarantee the social optimality if EV owners' timing constraints are taken into account. Next section will verify the applicability of real-time scheduling techniques to EV charging control and compare the proposed real-time EV charging scheme with the valley-filling scheme.

6.2 Applicability of Real-time Scheduling Techniques to EV Charging Control

In the previous section, the preparation of a dataset for simulation studies is explained, a benchmark system is implemented and verified, and its technical gaps are substantiated. As expected, the benchmark system, i.e., the valley-filling EV charging strategy, does not guarantee its social optimality if non-EV power demand fluctuates or EV charging requirements are different from the ones used for the day-ahead negotiation process for generating EV charging profiles, not to mention that it does not satisfy EV owners' timing constraints at all. In this section, the implemented real-time EV charging control in accordance with the technical approaches described in the previous chapter is verified and compared with the valley-filling charging scheme in order to see if it could be another approach for charging EVs to mitigate its impacts on the power grid and how well it fills the technical gaps of the valley-filling scheme.

6.2.1 (HYP I-1) Verification of Real-time EV Charging Control

As demonstrated in the previous section, the day-ahead valley-filling EV charging scheme cannot guarantee a flat load curve, let alone the satisfaction of EV owners' charging requirements, if EV owners' timing constraints are considered when EV charging is scheduled. Also, it is demonstrated that the valley-filling charging scheme is very sensitive to change in load, and, furthermore, it can be expected that its

optimality will severely depend on change in generation capacity, too.

To verify the implemented real-time EV charging scheme, simulations are run on the real-time scheduler with global EDF. In order to verify that the proposed control scheme works identically with the valley-filling scheme, out of the timing constraints, only the plug-out time constraints are relaxed and simulations are run since the charging window starts at 12:00 am after all EVs have been plugged in to the system and, thus, the plug-in time does not affect the charging scheduling. If the plug-out time constraints are relaxed, then the real-time charging scheme achieves exactly the same load profile as the one of the valley-filling scheme as shown in Figure 98; however, from Figure 99, it can be seen that all EVs are charging simultaneously at the charging rate varying over time in the valley-filling case while the proposed real-time charging scheme adjusts the number of EVs being charged simultaneously with the fixed charging rate, i.e., maximum charging rate, based on instantaneous power consumption. Therefore, it can be concluded from the both figures that the real-time charging scheme does the same job in a different way.

Now, plug-out time constraints are applied to the charging scheme in order to see the effects of timing constraints on EV charging scheduling. Note that the global

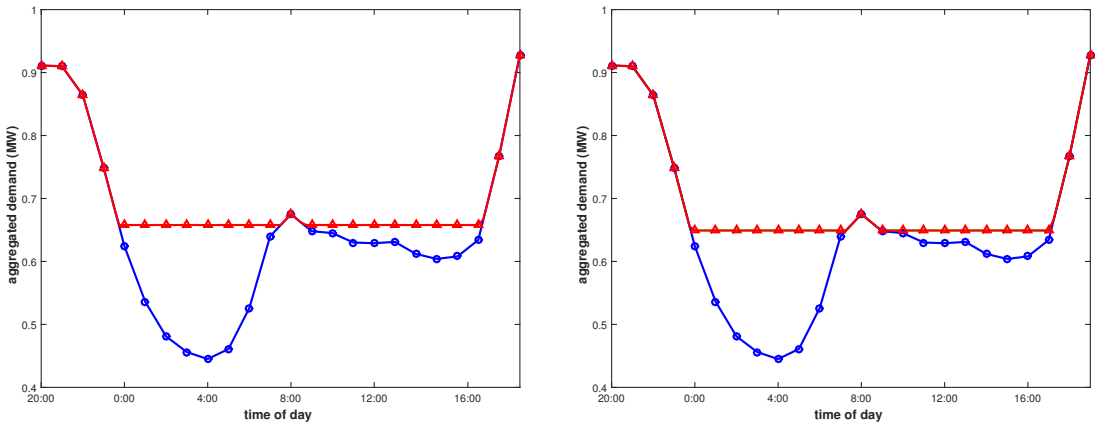

(a) valley-filling charging scheme (b) real-time charging by global EDF

Figure 98: Load profiles of valley-filling and real-time charging by global EDF with **no** timing constraints (blue circle: base, red triangle: base + EV).

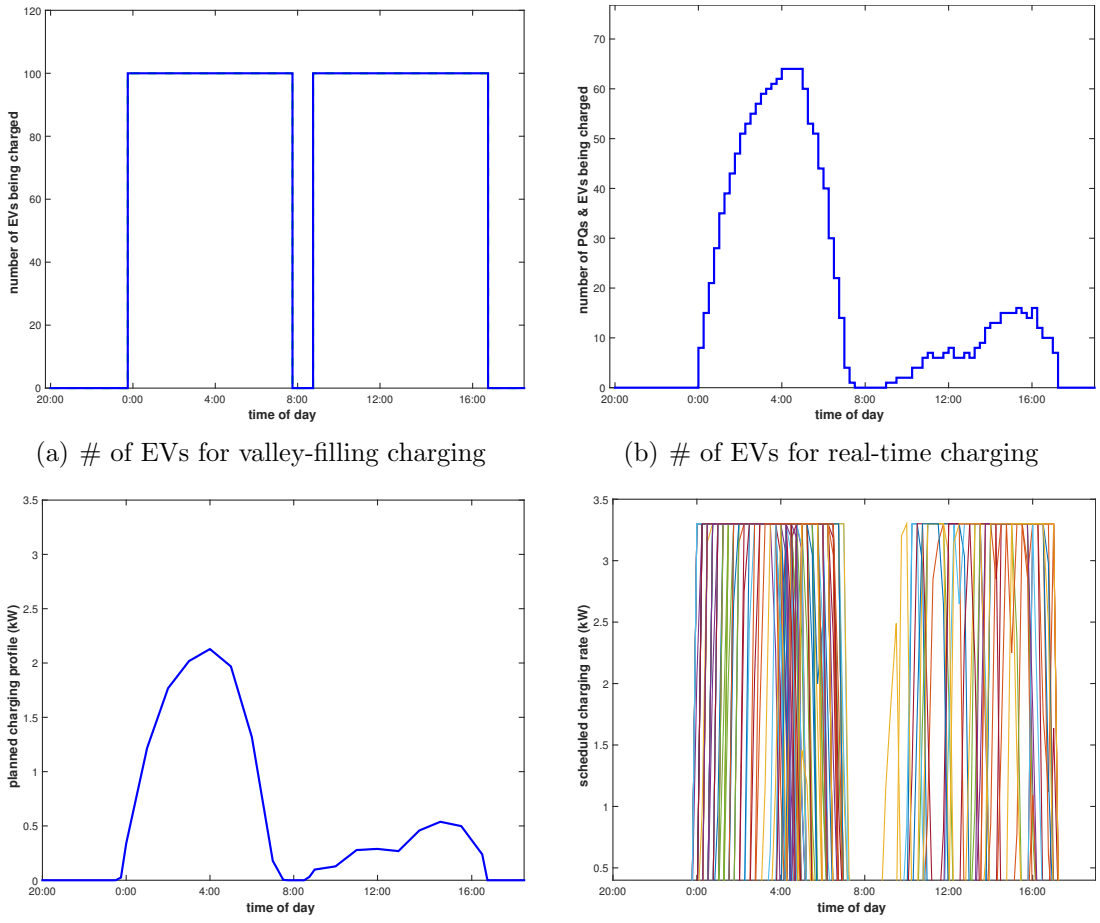

(a) # of EVs for valley-filling charging

(b) # of EVs for real-time charging

(c) charging profile for valley-filling charging

(d) charging profile for real-time charging

Figure 99: Number of EVs being charged and charging rate of valley-filling and real-time charging by global EDF with **no** timing constraints.

EDF with preemption – will be explained later in this subsection – allowed is used for real-time EV charging control and the charging window is assumed to be 12:00 am to 5:00 pm. As illustrated in Figure 100, both charging schemes do not make the load curve flat since many EVs are plugged out based on EV owners' timing constraints much before the charging window ends at 5:00 pm. It can also be seen that the real-time charging scheme consumes more power early in the morning to charge as many EVs as possible. The difference between the valley-filling and real-time EV charging schemes can be seen more obviously in Figure 101. The valley-filling scheme adjusts charging rates, which is the same for all EVs, while the number of EVs being charged simultaneously at the maximum rate is controlled in the real-time charging scheme. In case of the valley-filling scheme, all of the 100 EVs start charging at the same time at a non-maximum charging rate to achieve a flat load curve, and the number of EVs being charged simultaneously decreases as EVs are plugged out from wall outlets, compared with Figure 99(a). On the other hand, the real-time charging scheme varies the number of EVs being charged simultaneously at the maximum charging rate along with available power over charging period and allows the EVs with higher charging

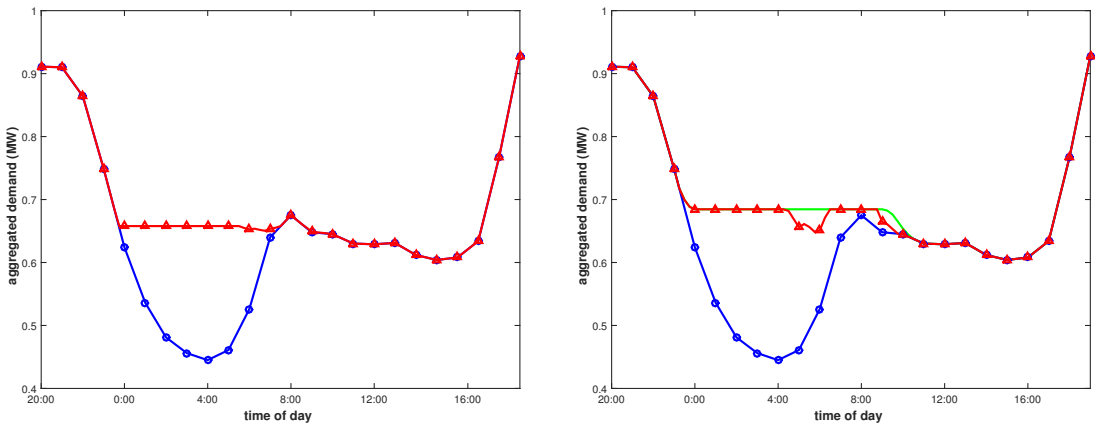

(a) valley-filling charging scheme

(b) real-time charging by global EDF

Figure 100: Load profile of valley-filling and real-time charging by global EDF **with** timing constraints (blue circle: base, red triangle: base + EV, green: generation plan).

modes and shorter time-to-complete-charging to be charged earlier.

Figure 102 illustrates how well the real-time EV charging strategy satisfies EV owners' timing constraints as well as a utility's requirement, that is, a flat load curve, compared with the day-ahead valley-filling scheme. For the valley-filling case (Figure 102(a)), since all EVs are charging simultaneously at the same charging rate, none of EVs are fully charged to their desired departure SOCs when they are plugged out; however, all EVs are evenly charged compared with the real-time case (Figure 102(b)).

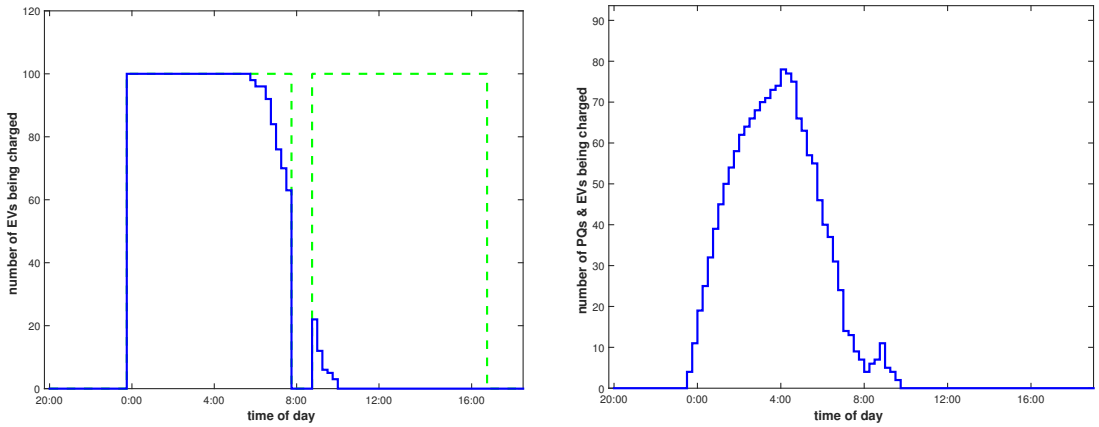

(a) valley-filling charging scheme (b) real-time charging by global EDF

Figure 101: Number of EVs being charged of valley-filling and real-time charging by global EDF with timing constraints (dashed green: day-ahead schedule for valley-filling).

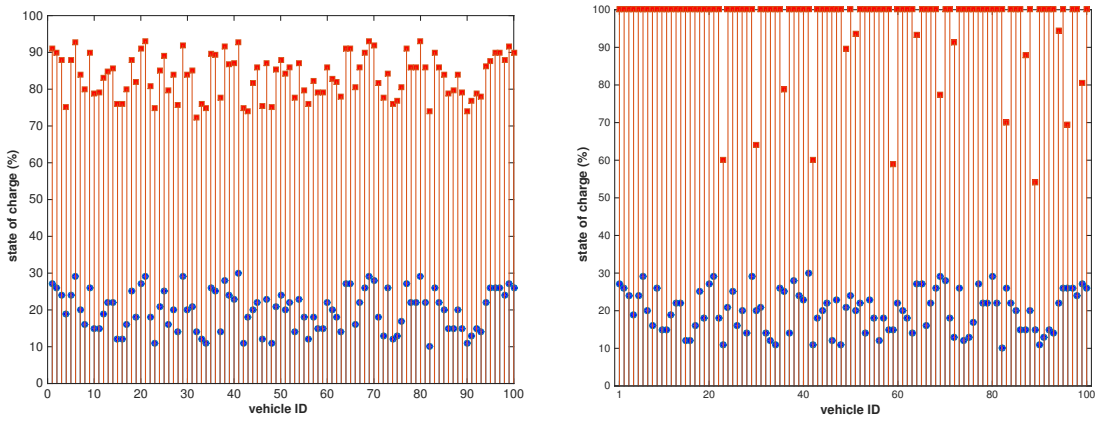

(a) valley-filling charging scheme (b) real-time charging by global EDF

Figure 102: State-of-charge (SOC) of valley-filling and real-time charging by global EDF with timing constraints (blue circle: plug-in SOC, red rectangle: plug-out SOC).

On the other hand, the real-time charging scheme fully charges the batteries of EVs with higher charging modes (1: highest, 4: lowest) and shorter time to full charge while many EVs with lower charging modes and longer time to full charge miss their deadlines, in other words, are not fully charged when plugged out, as illustrated in Figure 103. Out of 100 EVs, 16 EVs missed their deadlines, 6 of which are of charging mode of 3, and 10 of which have charging mode 4, the lowest charging mode.

For the previous simulation studies, the global EDF with priority assigned based both on charging mode and the closeness to absolute deadline, i.e., plug-out time, is used, and the concept of "preemption" is also allowed. In this study, the preemption means that EVs with higher priorities can interrupt the charging of EVs with lower priorities: in other words, higher-priority EVs are allowed to preempt slots of the processing queue that are occupied by EVs with lower priorities. The effect of allowing the preemption for scheduling real-time EV charging can be obviously seen by comparing Figures 104 and 105. In Figure 104, EVs with higher priorities, i.e., higher charging modes (1 or 2) and shorter time to deadlines, start charging earlier than others with lower priorities. Once they start charging, the charging process cannot be interrupted except when power is not available for EV charging. Even when power

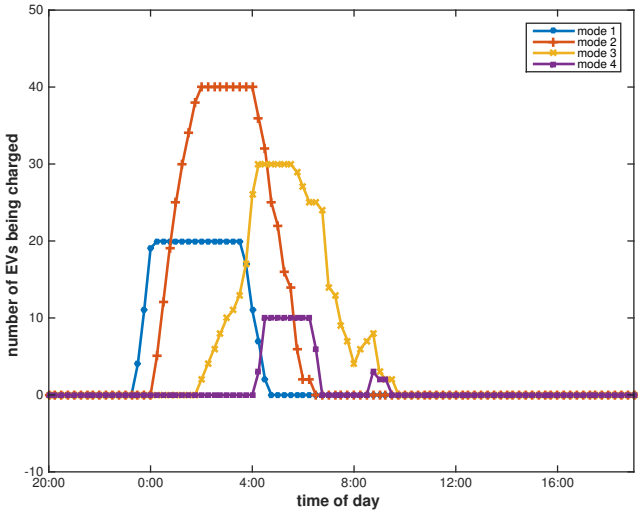

Figure 103: Number of EVs being charged (global EDF).

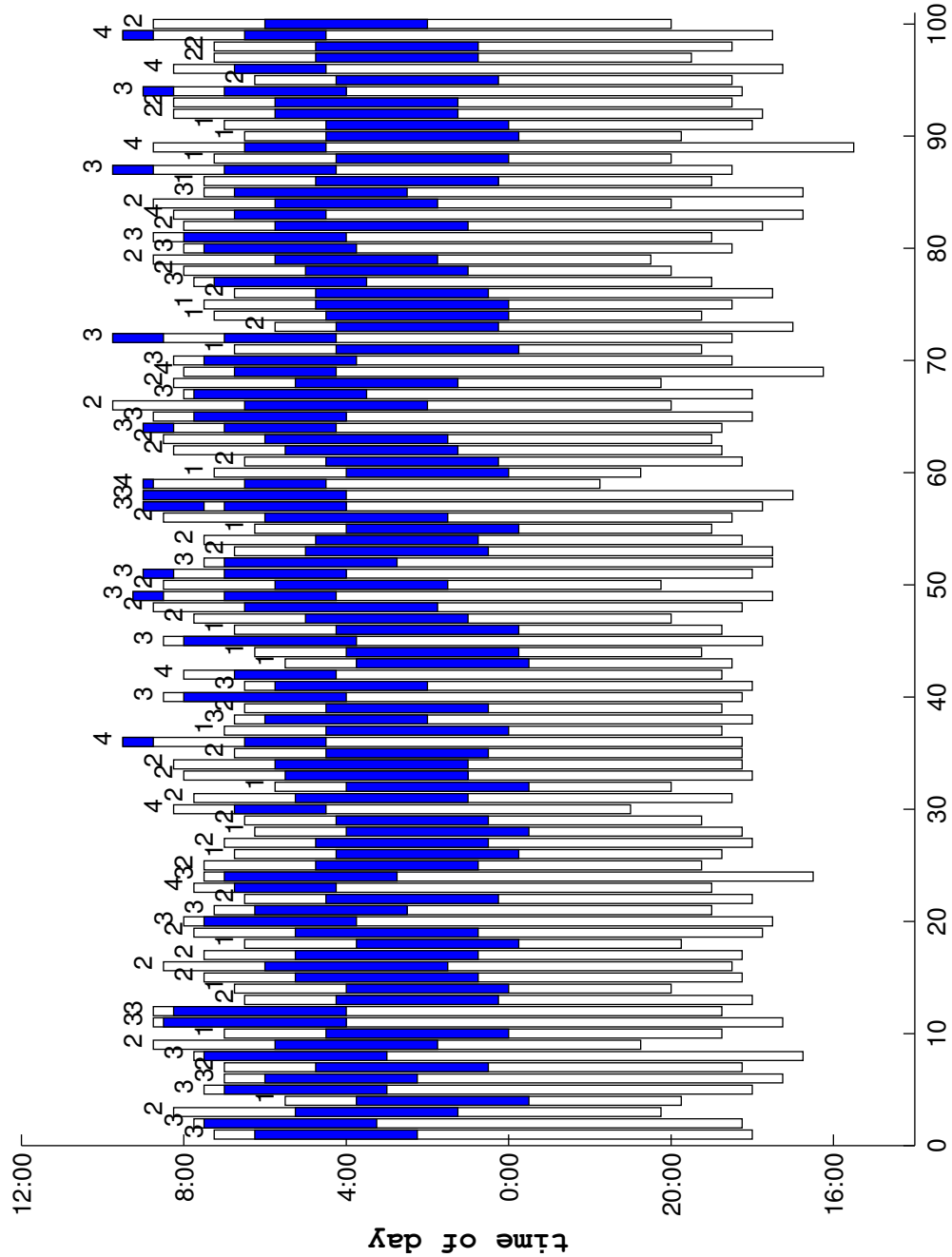

Figure 104: Duration plugged in vs. duration being charged **without** preemption.

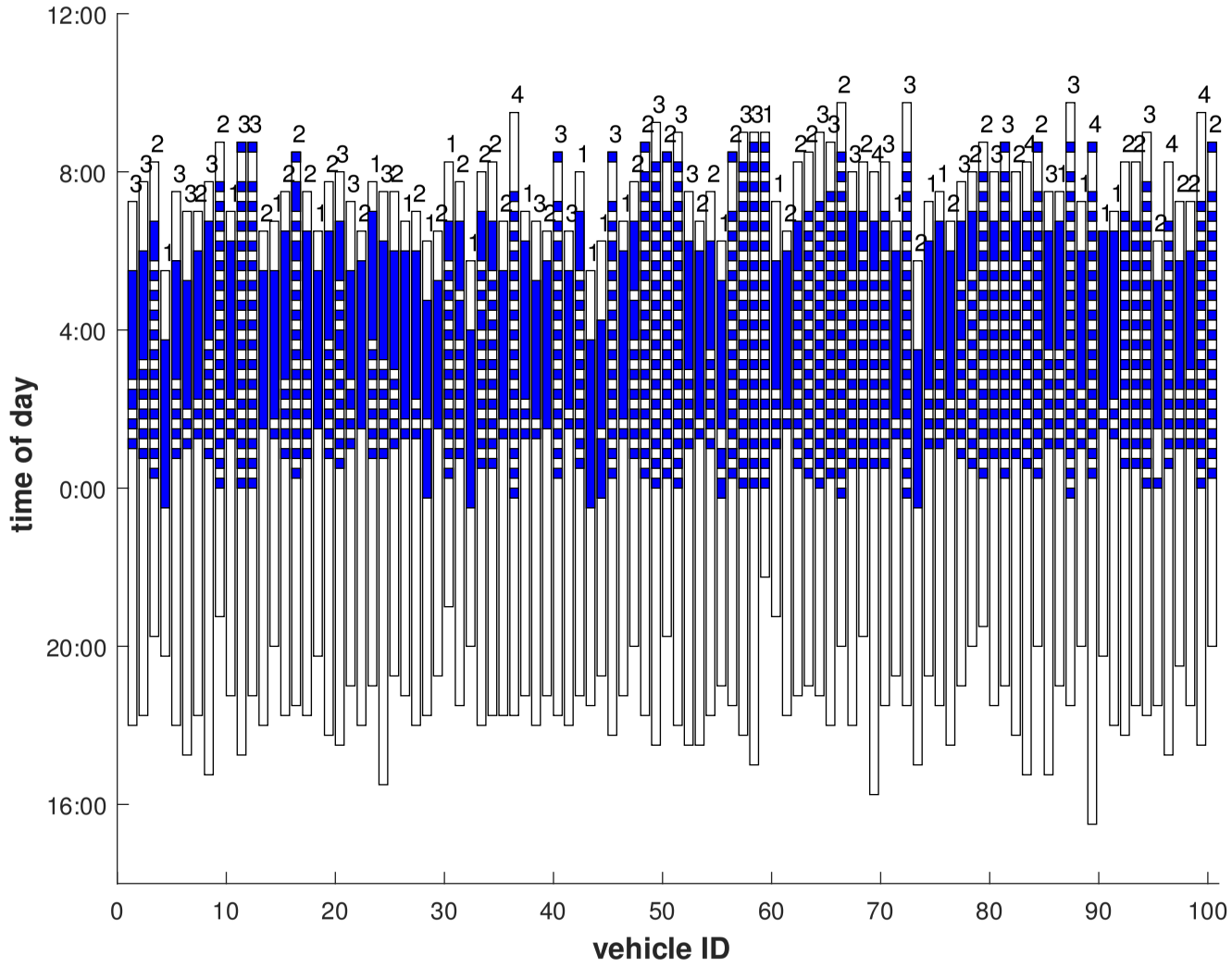

Figure 105: Duration plugged in vs. duration being charged **with** preemption.

is not available, the charging of EVs with lower priorities is interrupted, and EVs with higher priorities are seldom interrupted, as seen in Figure 104, where the numbers above vertical bars denote the charging mode for each vehicle, white rectangles represent plug-in but idle periods, and blue rectangles indicate charging periods. On the other hand, if the preemption is allowed, the charging of EVs, even EVs with charing mode 1, is interrupted frequently, as illustrated in Figure 105, in accordance with the dynamic priority assignment policy that updates the priorities of EVs based on required energy and time to deadline, also depending on available power for EV charging.

In this subsection, the applicability of real-time scheduling techniques to the EV charging control problem is experimentally shown. Based upon the case studies presented in this subsection, it can be concluded that even when EV owners' charging requirements, esp. timing constraints, are considered, the proposed real-time EV charging scheme can fill the technical gaps of the existing valley-filling scheme in that it can achieve a flat load curve (less total load variance) with higher satisfaction of EV owners' charging requirements (higher guarantee ratio).

6.2.2 (HYP I-2) Evaluation of Real-time Scheduling Algorithms for EV Charging

Various real-time scheduling algorithms are reviewed in §4.2.3 and §4.2.4. Among those algorithms, the global EDF is selected, and two variants of the global EDF with different priority assignment policies are considered for simulation studies. One have a priority assignment policy that assigns EVs with priority based on charging mode and urgency, introduced in §5.3.4. The other assigns priorities to EVs based only on their urgency, to see the effects of charging mode on the performance of the proposed real-time EV charging strategy. In addition to the global EDF family, two additional algorithms are investigated: max EVs and first come, first served (FCFS).

Table 24: Quantitative comparison of real-time scheduling algorithms.

Algorithms	Performance Measures			
	Load variance	Guarantee ratio	Average final SOC	# Missed EVs (mode 1/2/3/4)
Max EVs	2.0862e-04	29%	94.97%	20/31/15/5
FCFS	2.4856e-04	80%	95.55%	0/0/10/10
Global EDF	2.0879e-04	84%	96.24%	0/0/6/10
Global EDF variant 1	2.3714e-04	74%	95.95%	0/0/16/10
Global EDF variant 2	2.3714e-04	74%	95.95%	0/0/16/10

In the max EVs algorithm, a charging schedule is generated to allow the maximum number of EVs to charge their batteries for a given time slot like the valley-filling strategy. In the FCFS algorithm, as the name implies, EVs are assigned to the processing queue according to their order of being plugged in to the charging station and sending a request signal to the real-time dispatch scheduler. The five algorithms are applied to a set of EV profiles with the baseload profile of SCE, and simulation results are summarized in Table 24.

The Max EVs algorithm yields the worst results since it tries to allow as many EVs as possible to charge no matter how urgently an EV need to charge its battery by the plug-out time, similarly to the valley-filling strategy. However, it shows the least total load variance among the algorithms, indicating that its load profile is the flattest, i.e., fills the valley the best. For the FCFS case, the guarantee ratio and the averaged plug-out SOC are improved, compared with the Max EVs case, and EVs with charging modes 1 and 2 do satisfy their timing constraints since the charging mode is also considered when a priority is assigned. Unlike the expectation that the concept of "urgency" would provide better performance as a factor for priority

assignment policy, among the global EDF family, the original version shows better performance than the other variants. The priority assignment policy for the original version of global EDF is to assign priorities based on 1) charging mode, 2) closeness to deadline, and 3) current SOC, while the other variants assigns priorities based on both on charging mode and urgency or only urgency, respectively. Since the original version of global EDF shows better results, it is used for the following simulation studies.

6.2.3 (HYP I-3) Effects of Charging Rates Control on Real-time EV Charging

From the previous simulation studies, it is observed that the real-time EV charging algorithm does not utilize a small chunk of energy around 5:00 am (see Figure 100(b) on page 204), due to the fact that at that time there are not enough EVs to use the energy and EVs are charged only at the maximum rate. Therefore, in §3.1.3, it is hypothesized that if charging rates are controlled based on both the energy utilization and the number of EVs that are charging simultaneously for a given time slot, then the performance of the real-time EV charging algorithm will be improved. Additionally, it is mathematically proved that the charging rate should be maximized to fully utilize available energy in the valley(s) and, to increase the probability that EVs are fully charged as well as satisfy their deadlines, it is advantageous to make the charging rate as low as possible (refer to Equation (3.17) on page 98). To see the effects of charging rates on the performance of the proposed charging scheme, the following experiment is conducted. The charging rate is increased from 10% to 100% of the maximum rate by 10%, and the weighting factors ω_1 and ω_2 in Equation (3.17) are set to 0.5. Simulations with the global EDF algorithm are run, and the results are summarized in Table 25.

It can be seen that the total load variance decreases as the charging rate increases,

Table 25: Performance measures for different charging rates.

	Performance Measures		
Charging rate (% of max rate)	Total load variance	Averaged plug-out SOC	# Missed EVs for modes
10	2.0145e-04	97.06%	19/20/2/2
20	2.0145e-04	97.22%	19/20/2/2
30	2.0145e-04	97.44%	19/21/3/2
40	1.8832e-04	97.63%	16/23/5/4
50	1.6544e-04	98.05%	15/19/11/8
60	1.6544e-04	98.15%	5/8/18/8
70	1.3990e-04	98.08%	2/0/16/8
80	1.3990e-04	97.43%	0/0/4/8
90	1.3990e-04	97.40%	2/0/16/8
100	1.3990e-04	97.48%	0/0/20/8

which confirms the mathematical proof in §3.1.3. On the other hand, the averaged plug-out SOC is the highest when the charging rate is 60% as high as the maximum rate, and the number of EVs missing deadlines is the smallest when the charging rate is 80% of the maximum rate. This contradicts the claim that the charging rate is made as small as possible in order to increase the number of EVs satisfying their timing constraints. Simulations are run on 100 EVs, and charging those EVs simultaneously won't use up available energy since eventually the number of EVs being charged times the charging rate is equal to utilized energy. Therefore, if there are enough EVs in the system, then decreasing the charging rate will improve the guarantee ratio to some extent, but, if not, it is not helpful for the real-time EV charging algorithm. Also, it is observed that the total load variance does not change for charging rates within some range: for instance, the total load variance is the same for charging rate greater than 70% of the maximum rate no matter how high the charging rate is. Contrarily, the averaged plug-out SOC and the number of EV missing deadlines show the highest value for a specific value of charging rates. Figure 106 shows the effect of near-optimal charging rate on the load profile. Through a heuristic approach, the charging rate of 82% is proved to offer the best guarantee ratio, and is chosen to calculate the

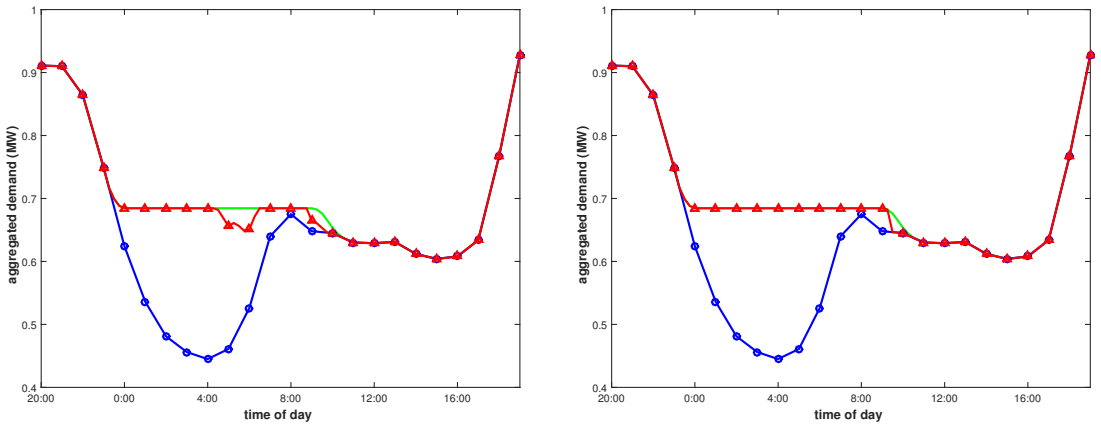

(a) charging at **maximum** rate

(b) charging at **near-optimal** rate

Figure 106: Effects of charging rate on load profile with global EDF (blue circle: base, red triangle: base + EV, green: generation plan).

number of processing queue to see the change in the load profile. Compared with Figure 106(a), the unused chunk of energy at 5:00 am is utilized and the load profile becomes flat like the ideal valley-filling case as depicted in Figure 106(b). In addition, it can be seen that the performance in terms of averaged plug-out SOC is improved as illustrated in Figure 107; however, the guarantee ratio, defined as the ratio of the number of EVs satisfying their desired plug-out SOCs to the total number of EVs in the system, is degraded compared with the case of the maximum rate charging.

From the simulation studies described in this subsection, the effects of charging rates on the real-time EV charging is investigated, and Hypothesis I-3 is tested. It is proved that the performance of the real-time EV charging algorithm is affected by the charging rate, and it is confirmed that charging EVs at the maximum rate maximizes the energy utilization, that is, minimizes the total load variance. However, the claim that as the charging rate gets smaller, the guarantee ratio will increase is proved to be wrong. Since EVs have a limited time to be plugged in and also have the amount of energy required to refill their batteries, the claim does not make sense in reality,

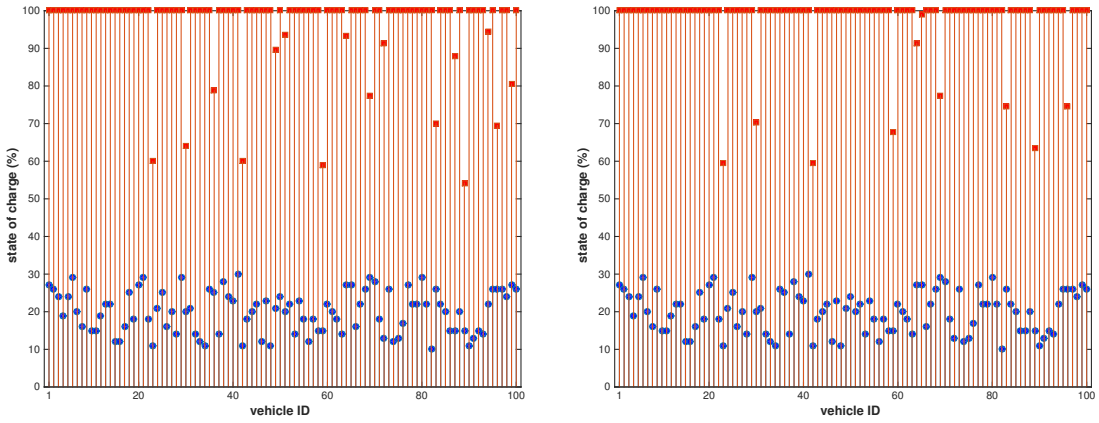

(a) charging at **maximum** rate (b) charging at **near-optimal** rate

Figure 107: Effects of charging rate on state-of-charge (SOC) with global EDF (blue circle: plug-in SOC, red rectangle: plug-out SOC).

or the mathematical formulation in §3.1.3 is wrong in that the energy constraint

$$\sum_{t=0}^{T-1} r_n(t) = \frac{(s(T) - s(0))\beta_n}{\eta \Delta t}, \tag{6.2}$$

where r_n is the charging rate, $s(0)$ and $s(T)$ are plug-in and plug-out SOCs, respectively, β_n is the battery capacity, η_n is the charging efficiency, and Δt is the period of the time slot, must be included when the optimization problem is established to guarantee the satisfaction of timing constraints with batteries fully charged.

6.2.4 (HYP I) Real-time Charging Control Strategy vs. Valley-filling Control Strategy

In §6.2.1, it is verified that the proposed real-time EV charging algorithm somewhat, not perfectly, satisfies EV owners' timing constraints while providing an almost flat load profile. It is also observed that the real-time EV charging algorithm does the same job as the valley-filling strategy in a slightly different way in that it adjusts the number of EVs being charged simultaneously with a fixed charging rate in real time; on the other hand, the valley-filling strategy generates a charging schedule by adjusting charging rate through a day-ahead negotiation process with EVs and let all EVs charge at the same time.

As the next step, the effects of load fluctuations on the real-time EV charging strategy is investigated. In order to verify that it can still provide a flat load curve even in the existence of load fluctuation and satisfy EV owners' charging preferences/requirements, the same baseload profile corrupted with an AWGN, described in §6.1.2, is applied to the real-time EV charging algorithm, and simulation results are presented in Figures 108, 109, and 110. As can be seen in Figure 108, the real-time EV charging still provides a flat load curve even with fluctuating load by adjusting the number of EVs being charged in real time, i.e., when actual charging takes place. This fact can be confirmed by the later part of the load curve where all EVs are plugged out and thus the load fluctuation cannot be compensated for and is directly

reflected in the load profile. From Figure 109(b), it can also be seen that the number of EVs being charged keep changing, depending on real-time measurements of available energy for EV charging, while the valley-filling strategy cannot adjust charging rates since it determines the charging rate through the day-ahead negotiation with EVs. Figure 110 shows that the proposed real-time EV charging scheme makes more EVs satisfy their deadlines with fully charged battery than the valley-filling scheme does; however, the uniformity of plug-out SOCs of the valley-filling scheme is still better although it does not fully charge any of EVs by their plug-out times.

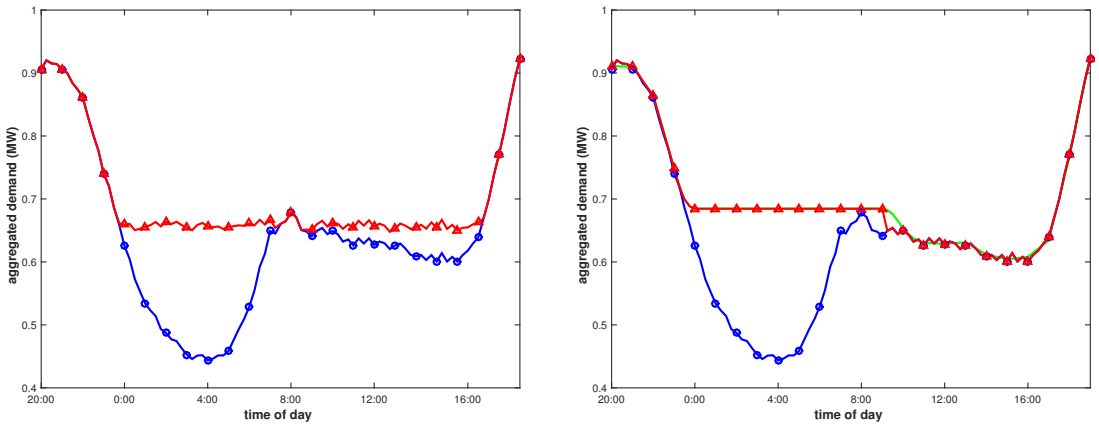

(a) valley-filling strategy (b) real-time charging

Figure 108: Load profiles of valley-filling and real-time with load fluctuation (blue circle: base, red triangle: base + EV, green: generation plan).

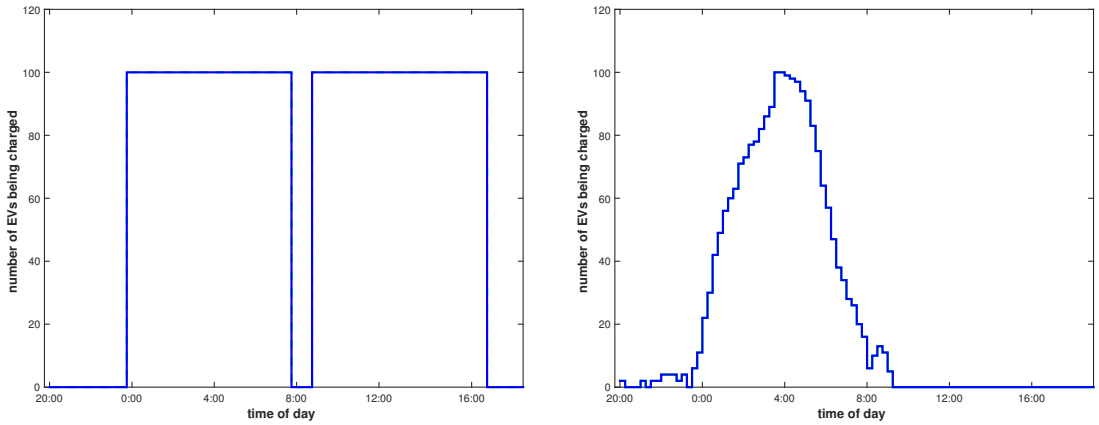

(a) valley-filling strategy (b) real-time charging

Figure 109: Number of EVs being charged of valley-filling and real-time with load fluctuation.

To see the effects of fluctuating load on the scheduling algorithm in more detail, the simulation results of the case with load fluctuation are compared with the one without load fluctuation. It can be seen in Figure 111 that the aggregated demand (base + EV demand), i.e., the load profile, of the case with load fluctuation is the same as the one of the without-load-fluctuation case. The tail of the flat curve part of the load profile results from the fact that all EVs are plugged out around 9:00 am and thus there is no available EVs to use up the available energy, i.e., the difference between generation plan (green curve) and non-EV demand (blue curve).

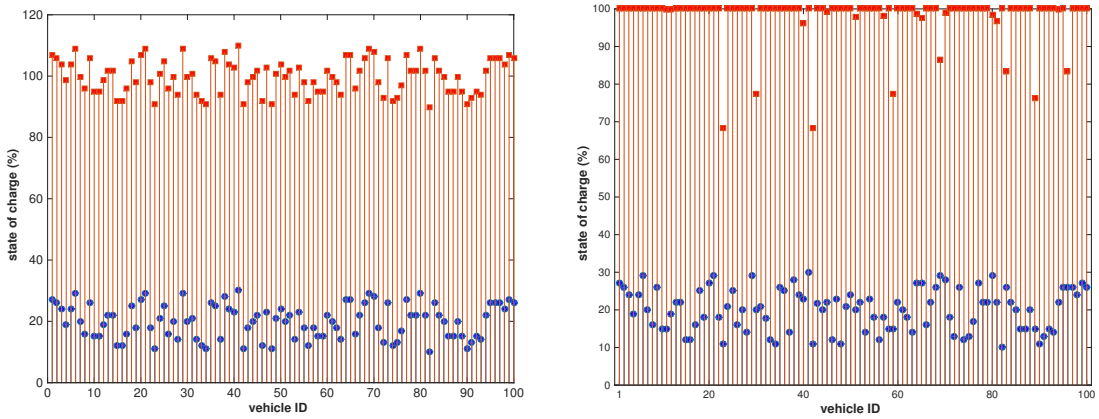

(a) valley-filling strategy (b) real-time charging

Figure 110: State-of-charge (SOC) of valley-filling and real-time with load fluctuation (blue circle: plug-in SOC, red rectangle: plug-out SOC).

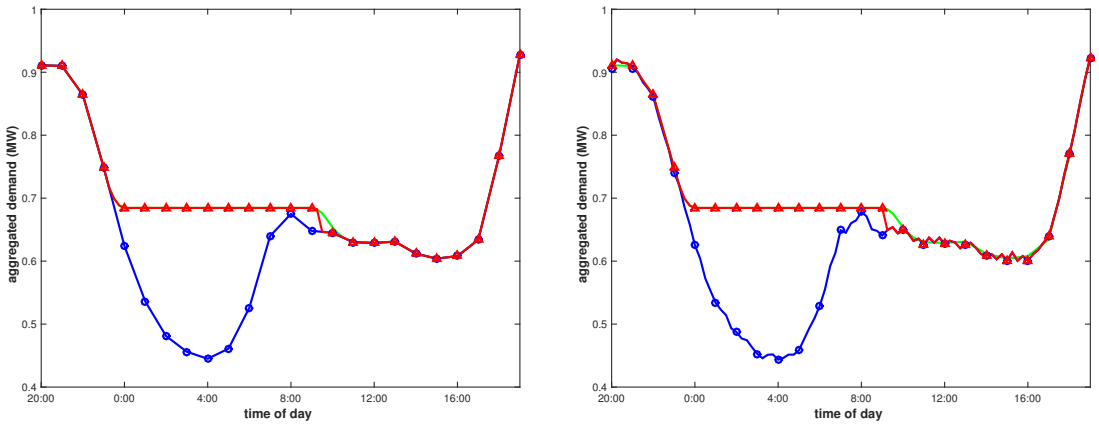

(a) **without** load fluctuation (b) **with** load fluctuation

Figure 111: Load profile of real-time charging scheme with load fluctuation (blue circle: base, red triangle: base + EV, green: generation plan).

The performance of the proposed charging scheme is not affected by load fluctuation, or inaccurate prediction of non-EV demand, since it keeps adjusting the number of EVs being charged at the same time and charging rates as well, based upon real-time measurements of non-EV demand and communications with EVs in the system as illustrated in Figure 112. In addition, it is observed that the load fluctuation has sometimes a positive effect on EV charging since energy available for charging EVs might increase if load fluctuates in the direction of getting less than the day-ahead prediction as shown in Figure 113. Negative values of demand prediction error n Figure 113(a) represent that power is consumed less than the day-ahead prediction and the underutilized power can be used for charging EVs. Figure 113(b) shows that, from time to time, available power for EV charging increases due to load fluctuation, compared to one of the case without load fluctuation. For instance, there are some EVs charging from 20:00 to 0:00 as illustrated in Figure 112(b) while there are no EVs charging during that time period in the case without load fluctuation (see Figure 112(a)).

From the perspective of the satisfaction of timing constraints, the number of EVs missing their deadlines is slightly increased – totally 10 EVs to 20 EVs, especially

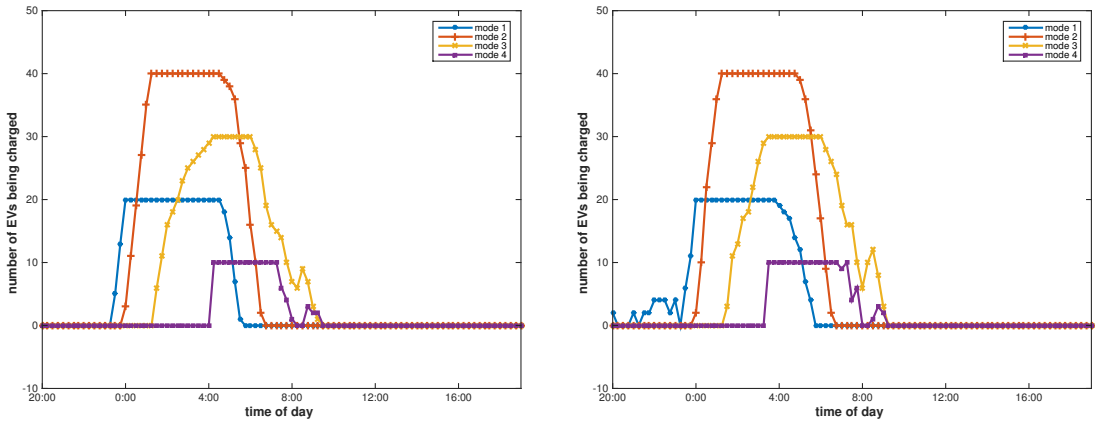

(a) **without** load fluctuation (b) **with** load fluctuation

Figure 112: Number of EVs per mode without and with load fluctuation.

EVs with mode 3 increases by 10, as shown in Figure 114, but the averaged plug-out SOC is improved by about 1%. However, in the case without load fluctuation, total power available for EV charging is 5.4081 MW, while power of 5.5130 MW is available and slightly greater in the case with load fluctuation. As can be seen in Figure 115, the 8 EVs with mode 4, of which plug-out SOCs are far below the desired plug-out SOCs, that is, 100%, for both the cases, get charged more in the case with load fluctuation than the case without fluctuation, and the 12 EVs with mode 3 are almost fully charged. In consequence, the performance of the proposed real-time EV

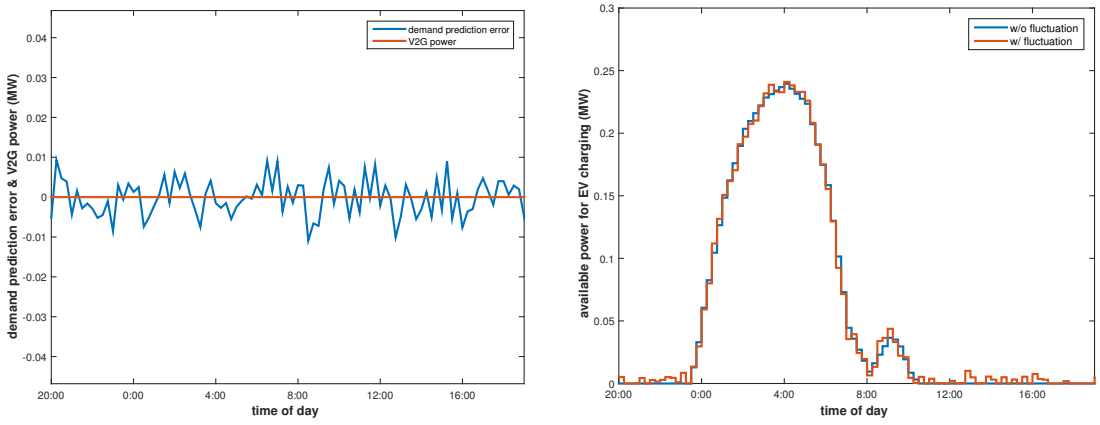

(a) load prediction error (b) available power for EV charging

Figure 113: Load prediction error (positive: actual > predicted, negative: actual < predicted) and available power for EV charging with load fluctuation.

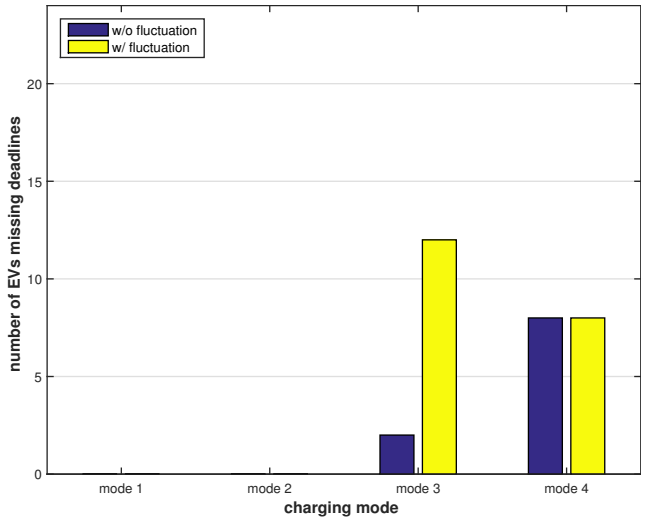

Figure 114: Number of EVs missing deadlines without and with load fluctuation.

Table 26: Summary of real-time charging scheme performance with load fluctuation.

	without fluctuation	**with** fluctuation
# of EVs missing deadlines	0/0/2/8	0/0/12/8
Sample variance of total load	1.3990e-04	7.0445e-03
Guarantee ratio	90%	80%
Averaged plug-out SOC	97.37%	98.03%

charging algorithm gets improved in spite of load fluctuation, which is modeled as an AWGN and could represent the prediction error of or continuous changes in non-EV demand. Simulation results for both the cases, in terms of the performance metrics, are summarized in Table 26.

Since simulation results on a specific set of EV profiles are presented previously, Monte Carlo simulations are run on 100 sets of baseload profiles, which are generated by applying 100 sets of an AWGN to the SCE's typical winter baseload profile, to see the effects of load fluctuation thoroughly on the proposed scheduling algorithm, and the results are summarized in Table 27 and the number of EVs missing deadlines

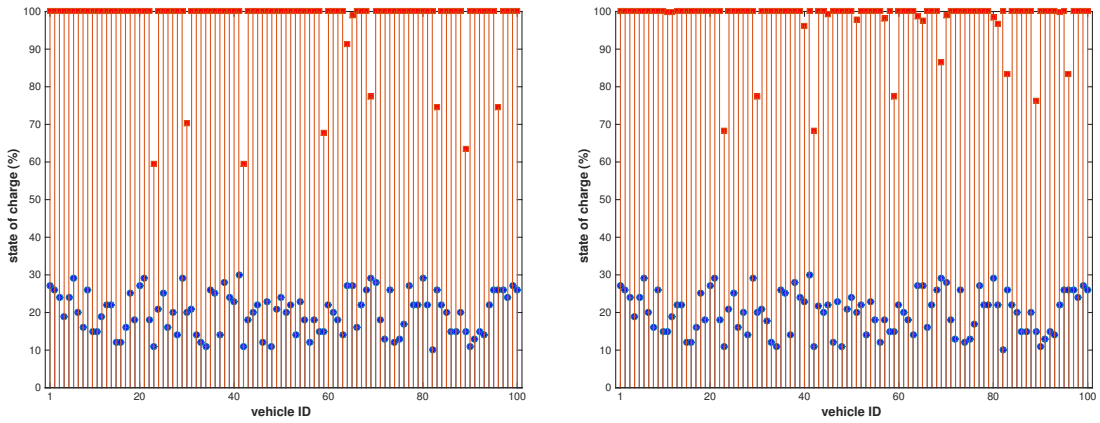

(a) **without** load fluctuation (b) **with** load fluctuation

Figure 115: State-of-charge (SOC) of real-time charging scheme with load fluctuation (blue circle: plug-in SOC, red rectangle: plug-out SOC).

Table 27: Summary of Monte Carlo simulation on effects of load fluctuation.

	without fluctuation	**with** fluctuation
Averaged # of EVs missing deadlines	17.6	20.4
Sample variance of total load	9.88×10^{-6}	3.26×10^{-4}
Averaged guarantee ratio	82.4%	79.6%
Averaged plug-out SOC	96.3%	96.4%

for the 100 cases is presented in Figure 116. In average, smaller number of EVs miss their deadlines in the case without load fluctuation, but there is no case where all EVs satisfy their timing constraints. On the other hand, the number of EVs missing deadlines of the case with load fluctuation is relatively large, but quite a few cases meet EV owners' charging preferences/requirements.

From this case study, it can be concluded that the proposed real-time EV charging algorithm can provide a near-optimality, i.e., almost minimize total load variance, and fill the valley of the load profile while satisfying EV owners' timing constraints regardless of whether load fluctuates or not. However, the performance of the strategy,

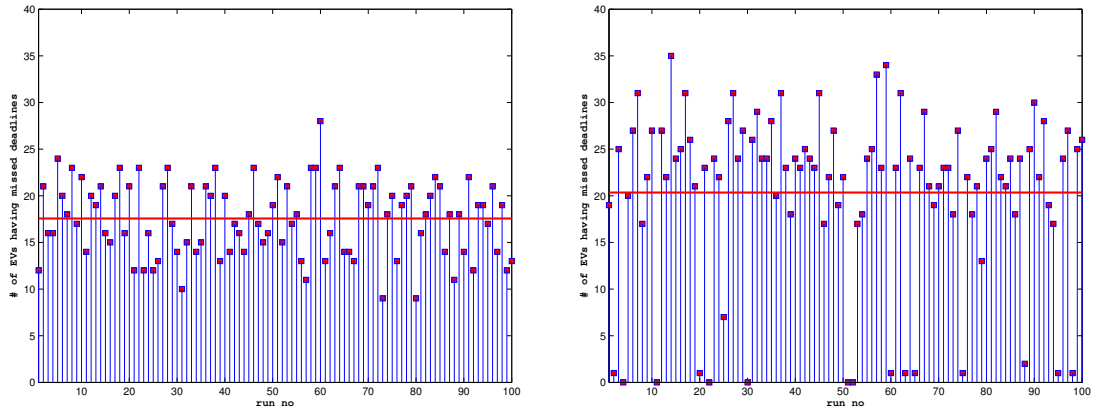

(a) **without** load fluctuation (b) **with** load fluctuation

Figure 116: Monte Carlo simulation of number of EVs missing deadlines with load fluctuation (red rectangle: number of EVs, orange horizontal straight line: average).

especially in terms of guarantee ratio, is somehow affected by the changing patterns and degree of load fluctuation.

For the last step to compare the proposed scheme with the existing valley-filling scheme, since the superiority of the proposed real-time EV charging control scheme is demonstrated only for a specific set of EV charging profiles and a specific load profile previously, it is necessary to show that the real-time EV charging scheme outperforms the valley-filling charging scheme for comprehensive sets of EV charging profiles and load profiles. Therefore, as shown in Figure 117, Monte Carlo simulations with various sets of EV charging profiles and baseload profiles are also run. A number of EV charging profiles, randomly generated in the similar way as described in §6.1.1, are used to take into account the random charging behaviors/patterns of EV owners. Baseload profiles are also generated by applying a set of AWGN with the same mean and variance, that is, zero mean and the variance of 1% of peak load. The statistics of performance metrics such as the number of EVs missing their deadlines, sample total load variances for optimality measure, and guarantee ratios of the valley-filling and real-time charging schemes, defined as the ratio of the number of EVs satisfying their deadlines to the total number of EVs are summarized in Tables 28 and 29.

As can be seen in the tables above, the valley-filling strategy does not satisfy timing constraints of any of the cases, but the real-time charging provides much better performance in terms of the satisfaction of timing constraints, even if it does not

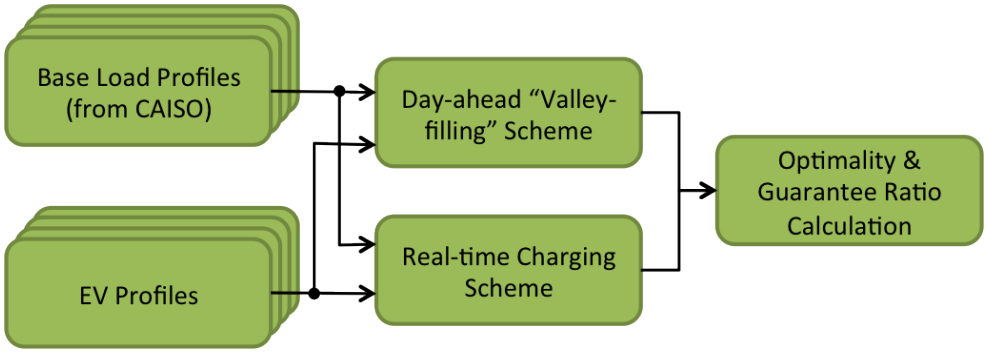

Figure 117: Overview of sensitivity analysis.

Table 28: Summary of Monte Carlo simulation runs on a set of load profiles.

	Valley-filling	Real-time
Averaged # of EVs missing deadlines	100	12.8
Sample variance of total load	2.43×10^{-5}	9.54×10^{-6}
Average guarantee ratio	0%	87.2%
Averaged plug-out SOC	82.9%	98.66%

Table 29: Summary of Monte Carlo simulation runs on a set of EV profiles.

	Valley-filling	Real-time
Averaged # of EVs missing deadlines	100	15.1
Sample variance of total load	1.04×10^{-5}	9.98×10^{-6}
Average guarantee ratio	0%	84.9%
Averaged plug-out SOC	83.7%	97.46%

satisfy the charging requirements of all EVs in every case perfectly. In addition, the real-time charging strategy yields improved total load variance since the valley-filling strategy generates a charging schedule through the day-ahead negotiation based on the prediction of load and thus can't compensate for the changes in load or generation capacity when EVs charge their batteries. However, in terms of the uniformity of plug-out SOCs, the valley-filling strategy performs better, and it is necessary to improve the real-time scheduling algorithm so that it allocates available energy to every EV uniformly while maintaining its guarantee ratio and averaged plug-out SOCs.

6.3 Real-time EV Charging Control Strategy in Support of V2G-based Frequency Regulation

As discussed in §1.1.1, one of the most promising benefits that an aggregated network of EVs can provide is that it can be used as electric energy storage (EES) so that it can mitigate the intermittency of renewable energy sources (RES) such as wind and solar, and thus stabilize the system frequency. According to many studies, the most valuable V2G-based service is frequency regulation; however, it is highly likely that V2G-based frequency regulation will degrade the performance of the proposed real-time EV charging system if they are designed independently of each other. To cope with this technical challenge, it is claimed that if V2G-based frequency regulation can be incorporated into the real-time EV charging system, then the real-time scheduling can be done without any performance degradation. For this reason, in §3.2.1, it is hypothesized that *the introduction of different charging modes and the control of charging rates of EVs that opt to participate in V2G-based frequency regulation will enable V2G-based frequency regulation to be incorporated in the real-time EV charging system* (Hypothesis II-1), and a methodology for incorporating V2G-based frequency regulation into the real-time EV charging system is introduced. In this section, the functionality of the V2G-based frequency regulation that is incorporated into the real-time charging algorithm is examined, its effects on the performance of the real-time charging strategy are investigated, and the relevant hypotheses are tested.

6.3.1 (HYP II-1) Incorporation of V2G-based Frequency Regulation into Real-time EV Charging

For the V2G-based frequency regulation, the algorithm encourages EVs with charging mode 4 to provide power to the grid after plugged in, rather than adjusts the number of EVs being charged simultaneously, when actual aggregated demand is greater than generation plan. No lower limit for SOC is considered in verifying the functionality of

V2G-based frequency regulation incorporated in the real-time EV charging algorithm. EVs with mode 4 sell electricity stored in their batteries when EVs with other modes are required to charge but power is not available for charging EVs. For the purpose of verification, the same EV profiles and baseload profile are used.

The load profile for the case with V2G-based frequency regulation implemented is given in Figure 118 along with the one of the case without V2G-based frequency regulation in order to see the effects of V2G-based frequency regulation. As can be seen in Figure 118(b), the V2G-based frequency regulation makes the load profile get worse, compared with the one that does not have V2G-based frequency regulation implemented, and consequently EVs do not fully utilize available power. Without V2G-based frequency regulation, the real-time scheduling algorithm tries to fully utilize available power and compensate for load fluctuation by adjusting the number of EVs that can be charged simultaneously; however, the V2G-based frequency regulation makes up for load fluctuation by encouraging EVs with mode 4 to sell their power to the grid in order to fill the batteries of EVs with other modes. Accordingly, EVs with modes 1 and 2 can be fully charged by their deadlines, but the SOCs of EVs with modes 3 and 4 are significantly decreased. The total number of EVs being

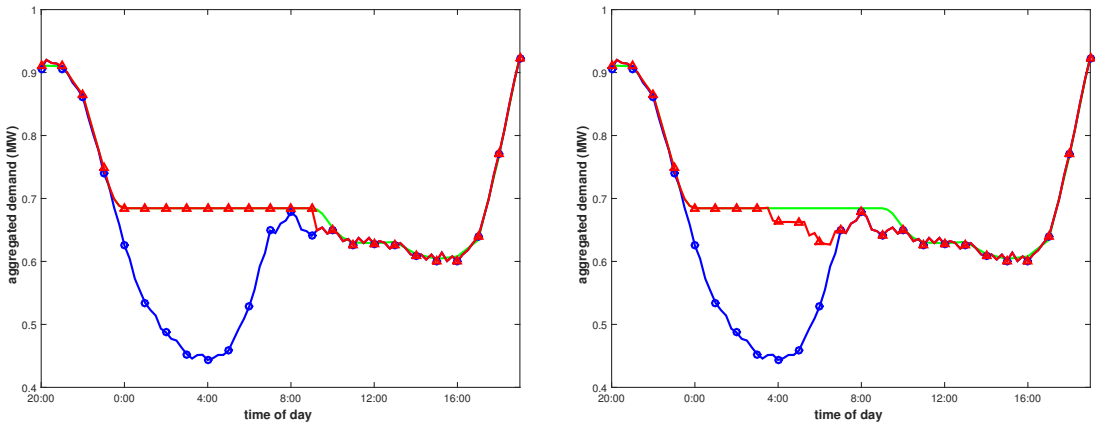

(a) **without** V2G-based FR (b) **with** V2G-based FR

Figure 118: Load profiles without and with V2G-based FR (blue circle: base, red triangle: base + EV, green: generation plan).

charged, which reflects the available power at a time slot, is similar to the one without V2G-based frequency regulation, but, after 7:00 am, the real-time charging algorithm with V2G-based frequency regulation does not utilize the available processing queues, depicted with the green curve in Figure 119(b), since many EVs are plugged out at that time even though there is power available, and EVs with mode 4 don't have enough time to fill their batteries since they sell their power to the grid to charge EVs with other modes while they are plugged in. As expected, the average of plug-out SOCs gets lowered and the number of EVs missing their deadlines increases, as illustrated in Figure 120(b). The reason generation capacity (green curve in Figure 118(b)), which is planned based on the information EVs provide when plugged in, is not fully utilized can be obviously seen in Figure 121. First, EVs with mode 1 start charging earlier in the evening when actual demand is less than the predicted demand, although the real-time dispatch scheduler does not start scheduling – it starts at 0:00 am, and the number of them decreases around 7:00 am next day. Similarly, EVs with mode 2 charge their batteries as soon as power is available, and the maximum number of them are charging around 1:00 am. EVs with those two modes charge in the same way as the one without V2G-based frequency regulation, as illustrated in

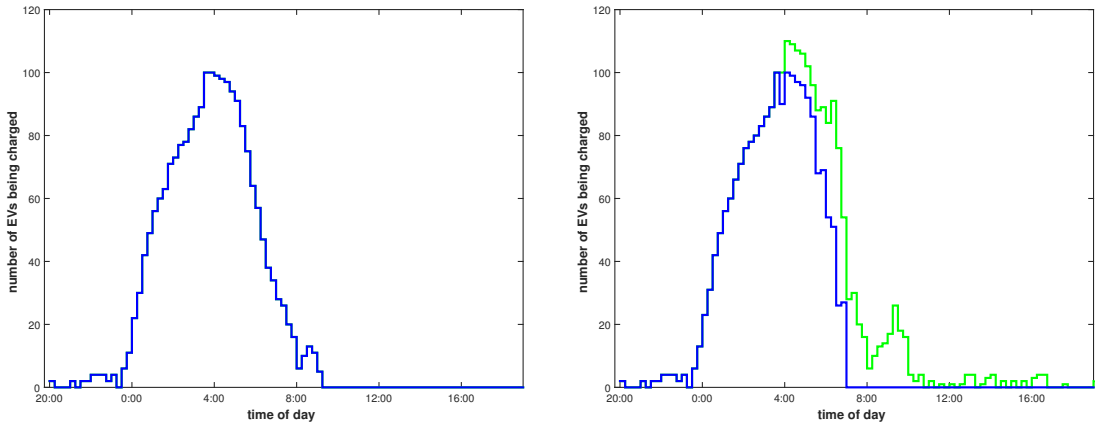

(a) **without** V2G-based FR (b) **with** V2G-based FR

Figure 119: Total number of EVs being charged without and with V2G-based FR (blue: # of EVs being charged, green: # of available processing queues).

Figure 121(a). However, EVs with mode 4 sell their electricity when actual demand is greater than the predicted demand and EVs with higher modes need to be charged. From Figure 121(b), where the negative numbers of EVs represent the number of EVs selling power to the grid, it can be seen that all EVs with mode 4, of which number is assumed to be 10% of total EVs in the system, participate in V2G-based frequency regulation when up-regulation is necessary. Figure 122 shows V2G power for the two cases. Right after the charging scheduling starts, EVs with mode 4 start selling power to the grid, and, around 4:00 am, and the number of EVs with mode

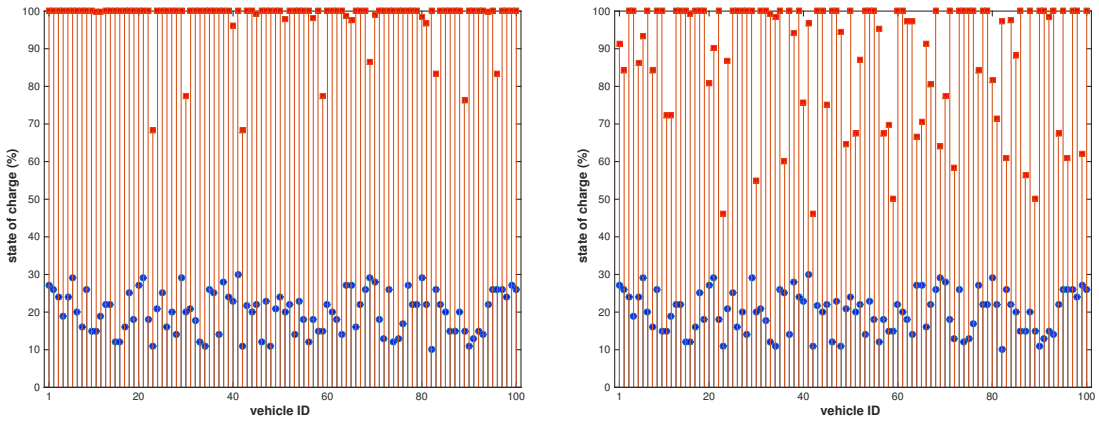

(a) **without** V2G-based FR (b) **with** V2G-based FR

Figure 120: State-of-charge (SOC) without and with V2G-based FR (blue circle: plug-in SOC, red rectangle: plug-out SOC).

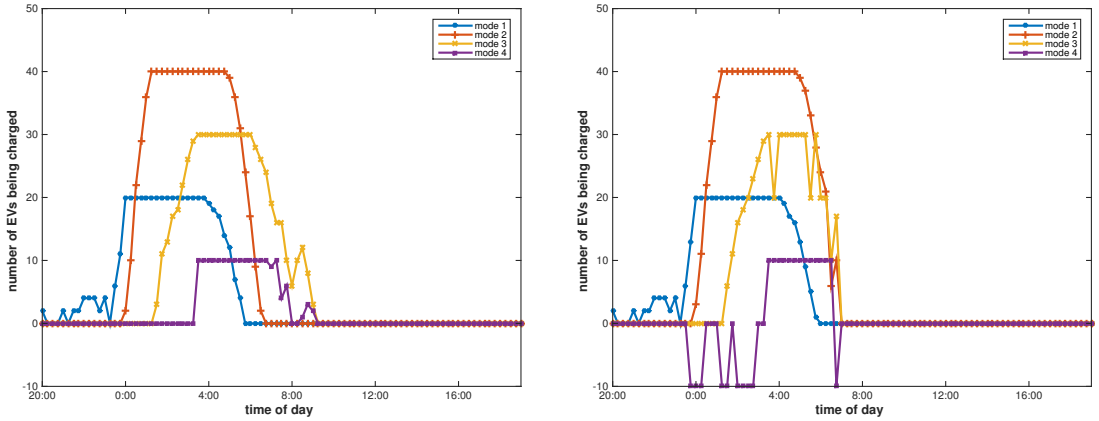

(a) **without** V2G-based FR (b) **with** V2G-based FR

Figure 121: Number of EVs per mode without and with V2G-based FR.

3 decreases momentarily in order to pull up the SOCs of EVs with mode 4 to the pre-specified levels. The SOCs of EVs with mode 4 for both the cases are illustrated in Figure 123. In the case without V2G-based frequency regulation, the SOCs of the EVs keep increasing after they start charging, and one of them reaches the desired SOC of 100%. However, the SOCs of the EVs in the case with V2G-based frequency regulation start decreasing when the real-time dispatch scheduler starts scheduling, and they start recharging their batteries around 4:00 am and manage to reach a certain level of SOC, resulting in the dissatisfaction of timing constraints.

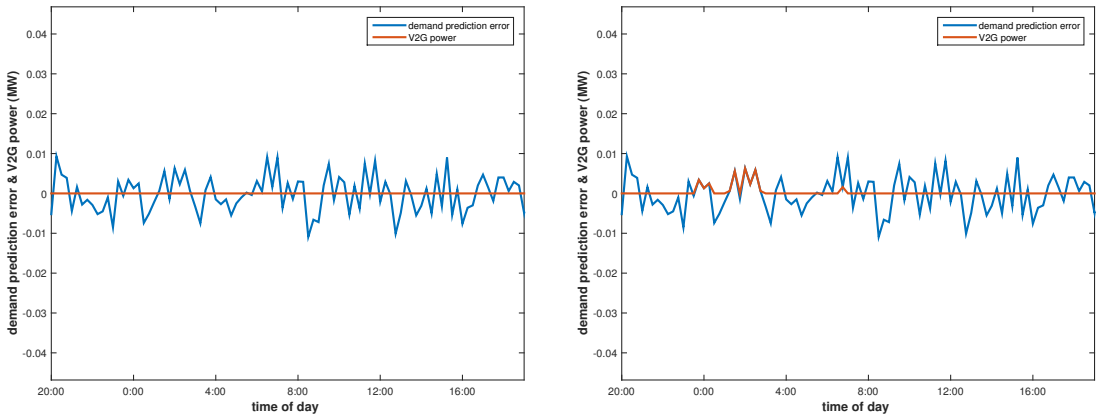

(a) **without** V2G-based FR (b) **with** V2G-based FR

Figure 122: V2G power without and with V2G-based FR (positive: actual > predicted, negative: actual < predicted).

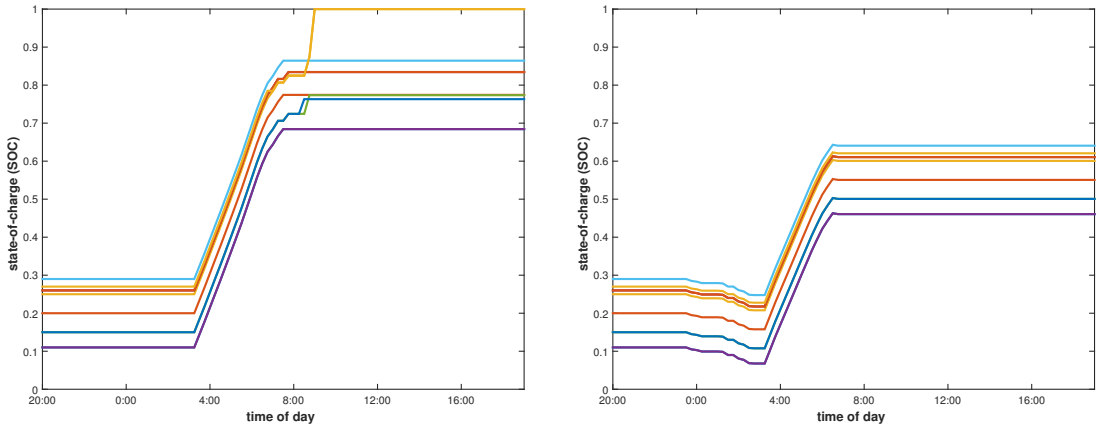

(a) **without** V2G-based FR (b) **with** V2G-based FR

Figure 123: State-of-charge (SOC) of EVs with mode 4 without and with V2G-based FR (blue circle: plug-in SOC, red rectangle: plug-out SOC).

In this subsection, the functionality of the real-time EV charging algorithm to provide V2G-based frequency regulation is investigated through simulations. It is demonstrated that the real-time charging algorithm can provide the service by encouraging EVs with charging mode 4 to sell electricity stored in their batteries to the grid to match generation with demand. However, as expected, the performance of the charging strategy is degraded due to the provision of V2G-based frequency regulation since some EVs need to participate in frequency regulation, not charging their batteries during the given charging period. In the next subsection, the impacts of V2G-based frequency regulation on the real-time charging strategy are investigated for a variety of scenarios, and the hypothesis formulated in §3.2.2 is examined.

6.3.2 (HYP II-2) Evaluation of the Impacts of V2G-based FR on Real-time EV Charging

In the previous subsection, the impacts of V2G-based frequency regulation on real-time EV charging are investigated for a specific set of baseload profile and EV profiles. As expected, the performance, in terms of total load variance and guarantee ratio, of the charging scheme is degraded, because EVs with mode 4, which are supposed to provide V2G power to the grid, do not have enough time to charge their batteries, selling power with which EVs with other modes can be charged and the mismatch between generation and demand can be balanced out. In order to verify that the degradation is really due to V2G-based frequency regulation or it happens only for the specific set of profiles, 100 sets of EV profiles and 100 sets of baseload profiles are applied to the real-time EV charging algorithm with V2G-based frequency regulation incorporated.

Figures 124 and 125 show the Monte Carlo simulation results of the case with 100 sets of baseload profiles. For easy comparison, the results of the case without V2G-based frequency regulation are presented together. It can be seen from Figure

124 that the number of EVs missing deadlines is noticeably increased when V2G-based frequency regulation is incorporated into the real-time EV charging scheme. The reason is that EVs with mode 4 are frequently preempted by other EVs with higher modes and, to make things even worse, they provide power to the grid so that it can charge other EVs and make up for the change in non-EV demand. Also, the extent to which the scheme is affected by the provision of V2G-based frequency regulation depends on the changing patterns and the amount of energy for up- and down-regulation requested by the real-time dispatch scheduler. The deterioration

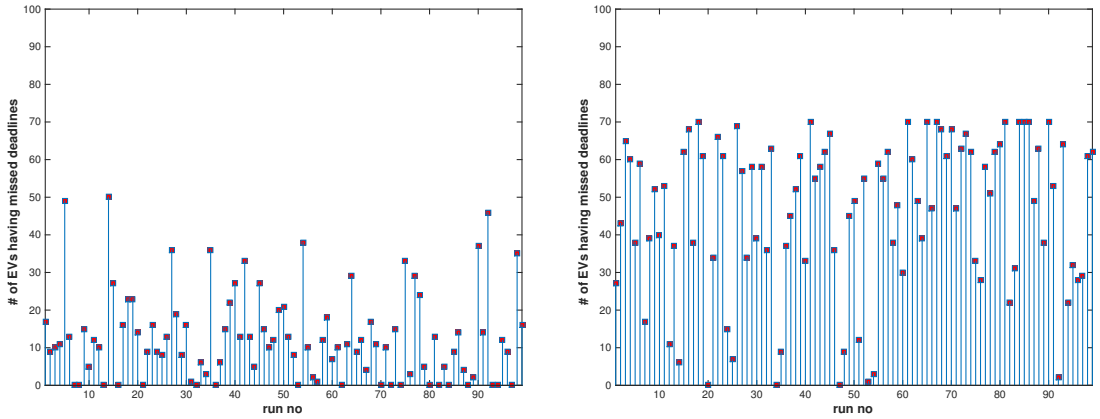

(a) **without** V2G-based FR (b) **with** V2G-based FR

Figure 124: Monte Carlo simulations on the number of EVs missing deadlines with 100 sets of load profiles.

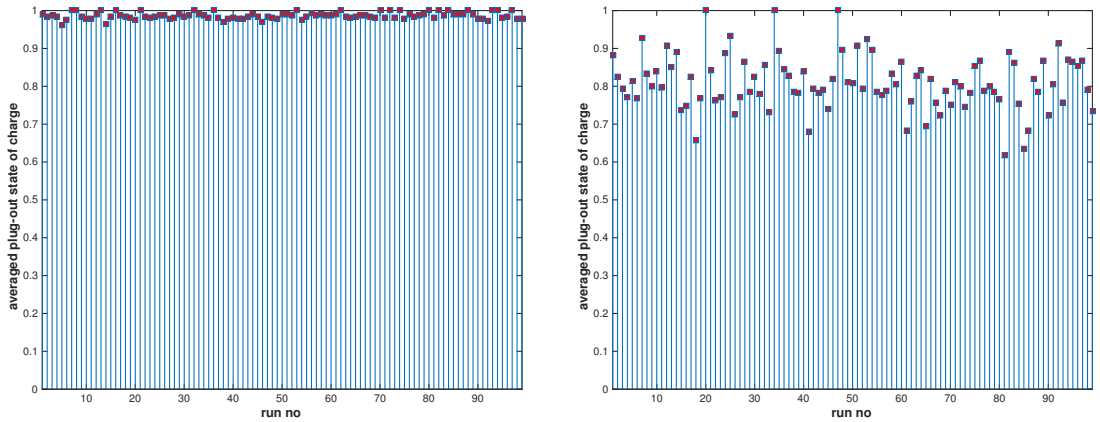

(a) **without** V2G-based FR (b) **with** V2G-based FR

Figure 125: Monte Carlo simulations on averaged plug-out SOC with 100 sets of load profiles.

in the number of EVs missing deadlines can be also found in plug-out SOCs, as illustrated in Figure 125. There are a few cases where all EVs are fully charged, but, compared with the case without V2G-based frequency regulation, the performance in terms of plug-out SOC is significantly affected by the ancillary service.

Figures 126 and 127 show the results on 100 sets of EV profiles. Both the cases provide better results on the number of EVs missing deadlines and the averaged plug-out SOC than the simulations with sets of load profiles. The number of EVs missing deadlines for every simulation run is evenly distributed, compared with the simulation

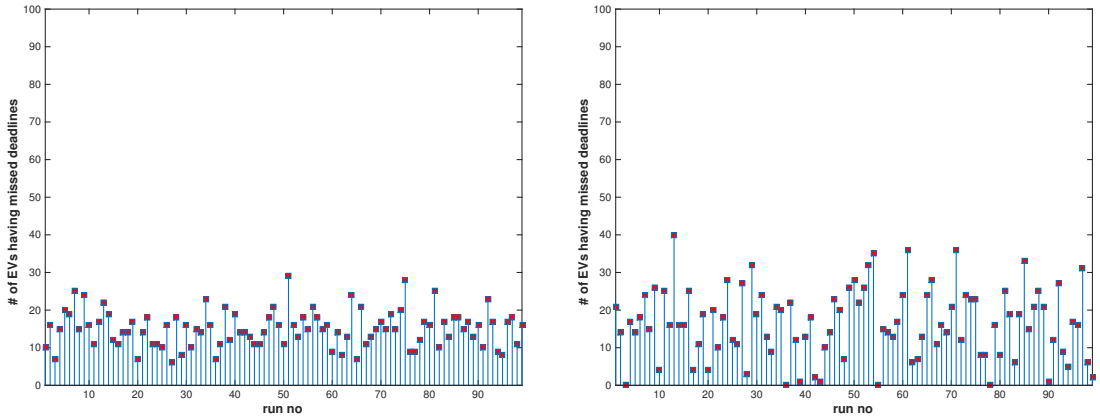

(a) **without** V2G-based FR (b) **with** V2G-based FR

Figure 126: Monte Carlo simulations on the number of EVs missing deadlines with 100 sets of EV profiles.

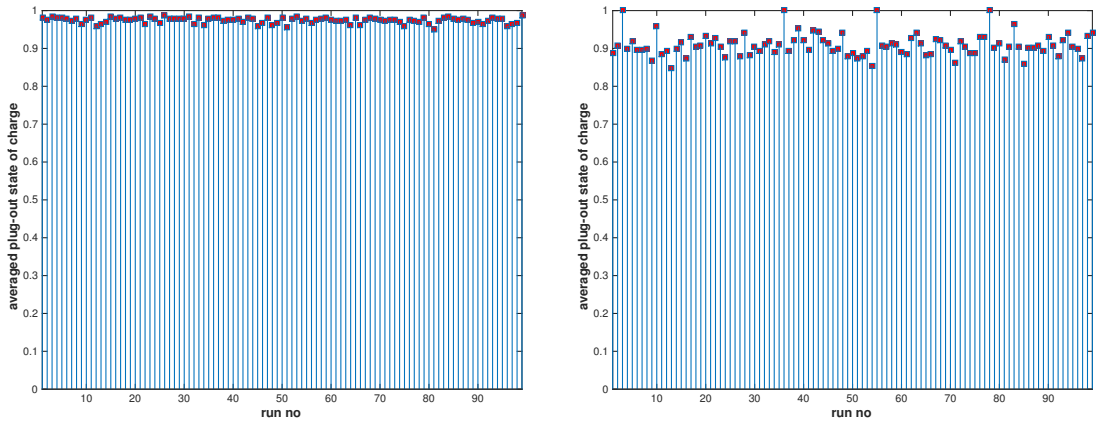

(a) **without** V2G-based FR (b) **with** V2G-based FR

Figure 127: Monte Carlo simulations on averaged plug-out SOC with 100 sets of EV profiles.

case on load profiles, and, likewise, there are a few runs where all EVs satisfy their timing requirements. From these simulation studies, it is observed that load profiles are more likely to affect the performance of the proposed charging algorithm than EV profiles. A set of EV profiles is generated under the assumption that EV owners would plug in their vehicles at a similar time every day with a slight change and drive off their cars for work at a certain time in the morning. In addition, the reference EV demand, introduced in §5.3.1 and used to calculate the number of processing queues, is estimated based on the information such as plug-in times, plug-out times, and desired plug-out SOCs, provided by EV owners, that is, EV profiles. Therefore, the performance of the proposed charging scheme is less affected by EV profiles. On the other hand, the scheme must cope with the instantaneous change in non-EV demand, i.e., load profile, and hence its performance heavily depends on load profiles. Also, if an EV doesn't come up to the target SOC, even by less than 1%, it is considered to fail to satisfy the timing requirement and, in consequence, the performance metric, the number of EVs missing deadlines, looks worse, even though the averaged plug-out SOC are sufficiently high. The numeric results of the Monte Carlo simulations on load profiles and EV profiles are compiled in Table 30.

So far, the impacts of the provision of V2G-based frequency regulation on the performance of the proposed charging scheme have been examined through simulation studies, and it can be concluded that the performance of the scheme is greatly influenced by the V2G-based ancillary service as well as circumstances such as non-EV demand patterns and EV owners' preferences/requirements, and it is necessary to come up with an idea to mitigate the impacts.

Table 30: Summary of Monte Carlo simulation runs on V2G-based FR **without** timing buffer.

Profile set	Statistics	**without** V2G-based FR		**with** V2G-based FR	
		averaged # of EVs missing deadlines	averaged plug-out SOC	averaged # of EVs missing deadlines	averaged plug-out SOC
Monte Carlo on load profiles	Mean	12.8283	98.66%	45.8283	81.01%
	Std dev	11.8632	0.84%	20.7561	7.21%
Monte Carlo on EV profiles	Mean	15.0909	97.46%	16.5152	90.93%
	Std dev	4.7896	0.77%	9.3856	2.96%

Now, Hypothesis II-2, regarding the mitigation of the impacts of V2G-based frequency regulation, is tested. Since the sets of EV profiles are generated in quite a random way such that charging requirements for an EV from a set have nothing to do with ones for the EV from other sets, it does not make sense to calculate the means and standard deviations of plug-in and plug-out times for each EV from the sets of EV profiles and use them as a timing buffer, of which concept is described in §3.2.2. Therefore, an arbitrary number is used for all EVs as the timing buffer to see if the concept can mitigate the impacts of V2G-based frequency regulation on real-time EV charging. For this purpose, the timing buffer of 2 hours is applied to calculate the reference EV demand estimation for the real-time scheduling algorithm with V2G-based frequency regulation, and a simulation is run on the same set of EV profile and baseload profile that are used for the simulations in §6.3.1.

Figure 128 shows one of the simulation results, aggregated demand profile. It can be seen that the load profile becomes flat again during the charging window, from 0:00 am until 2 hours before the latest plug-out time, by introducing the timing buffer. It can also be observed that the timing buffer leads to an increase in the reference EV demand estimation, which is now slightly greater than the day-ahead generation plan,

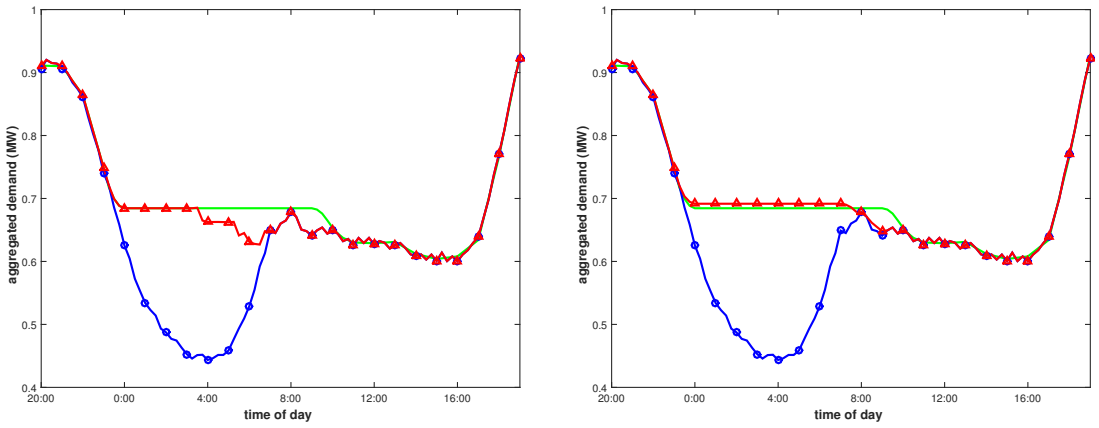

(a) **without** timing buffer (b) **with** timing buffer

Figure 128: Load profiles without and with timing buffer for V2G-based FR (blue circle: base, red triangle: base + EV, green: generation plan).

depicted in green curve. The timing buffer has the effect of encouraging EVs to complete charging 2 hours ahead of their plug-out times and, instead, increasing energy required for charging EVs. The effects can be seen in plug-out SOCs of the EVs, as illustrated in Figure 129. Introducing the concept of timing buffer moves the average of plug-out SOC's back to the level of the algorithm without V2G-based frequency regulation. Although the algorithm still does not satisfy the charging requirements of all EVs, the plug-out SOCs of EVs with mode 4 are significantly improved, compared with the one without timing buffer, and are even better than the one without V2G-based frequency regulation. In addition, EVs with the other modes complete recharging, 100%, before they are plugged out.

Like the previous case, in order to verify the effects of timing buffer on the performance of the real-time EV charging algorithm with V2G-based FR thoroughly, Monte Carlo simulations with 100 sets of load profiles and 100 sets of EV profiles are run. Figure 130 shows the simulation results on the number of EVs missing deadlines with 100 sets of load profiles, which are corrupted with AWGN to represent a situation where load is fluctuating by 1% of the peak load early in the evening. In overall, the performance in terms of the number of EVs missing deadlines is improved, compared

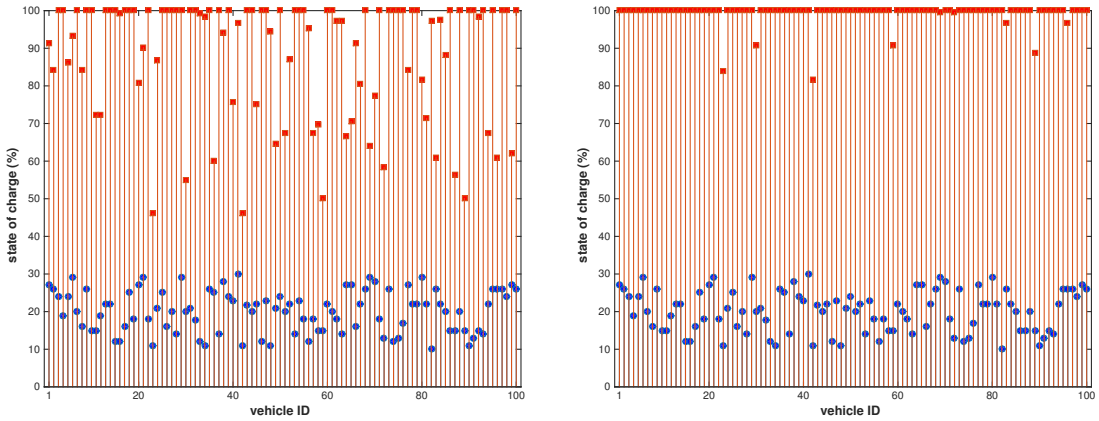

(a) **without** timing buffer (b) **with** timing buffer

Figure 129: State-of-charge (SOC) without and with timing buffer for V2G-based FR (blue circle: plug-in SOC, red rectangle: plug-out SOC).

with the case without timing buffer, but there are still the cases where almost 70% EVs don't satisfy their timing constraints although the timing buffer is introduced. However, scrutinizing the averaged plug-out SOC in Figure 131(b) reveals that most of the EVs are plugged out with SOCs close to their desired departure SOCs, but not perfectly 100%, making the number of EVs missing deadlines look worse than it really is. The number of EVs missing deadlines, averaged out over the 100 sets of load profiles, is 31.8, and its standard deviation is 13.3, indicating that the performance of the real-time EV charging algorithm is severely affected by fluctuating patterns in

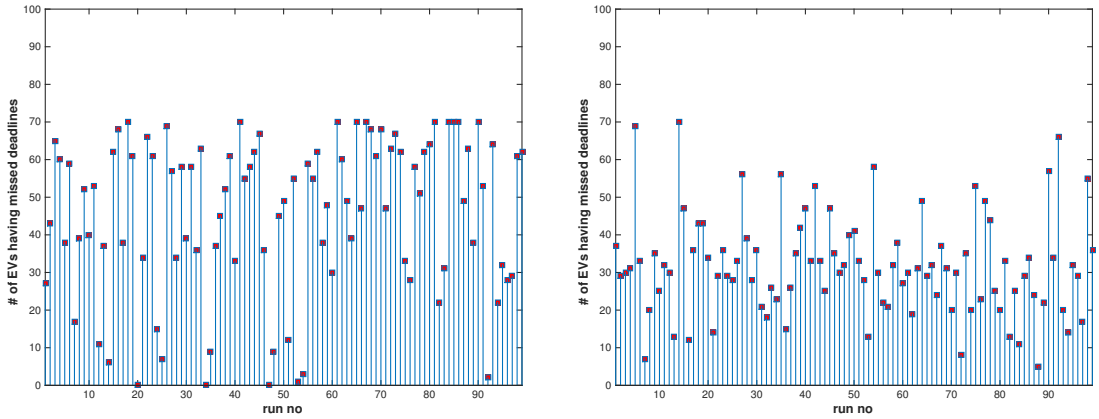

(a) **without** timing buffer (b) **with** timing buffer

Figure 130: Monte Carlo simulations on the number of EVs missing deadlines for timing buffered V2G-based FR with 100 sets of load profiles.

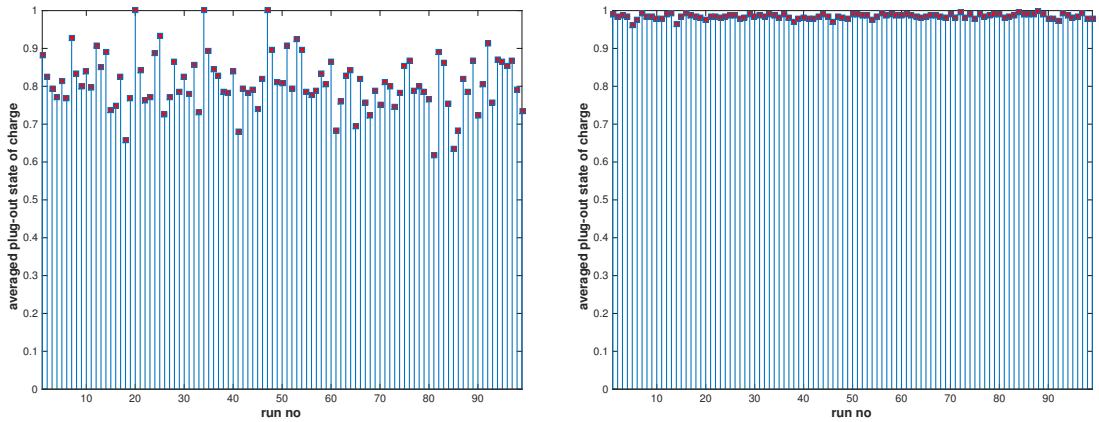

(a) **without** timing buffer (b) **with** timing buffer

Figure 131: Monte Carlo simulations on averaged plug-out SOC for timing buffered V2G-based FR with 100 sets of load profiles.

load profiles because the sets of load profiles are generated by corrupting the load profile from the CAISO database with a variety of random noise.

Now, let's take a look at the simulation results on EV profiles, presented in Figures 132 and 133. Unlike the case with load profiles, the number of EVs missing deadlines increases rather than decreases, and there is no case in which all EVs satisfy their deadlines, even though energy for EV charging is increased by introducing the timing buffer. The average of the number of EVs missing deadlines for the case without timing buffer is 16.5, whereas the average for the case with timing buffer is 25.1,

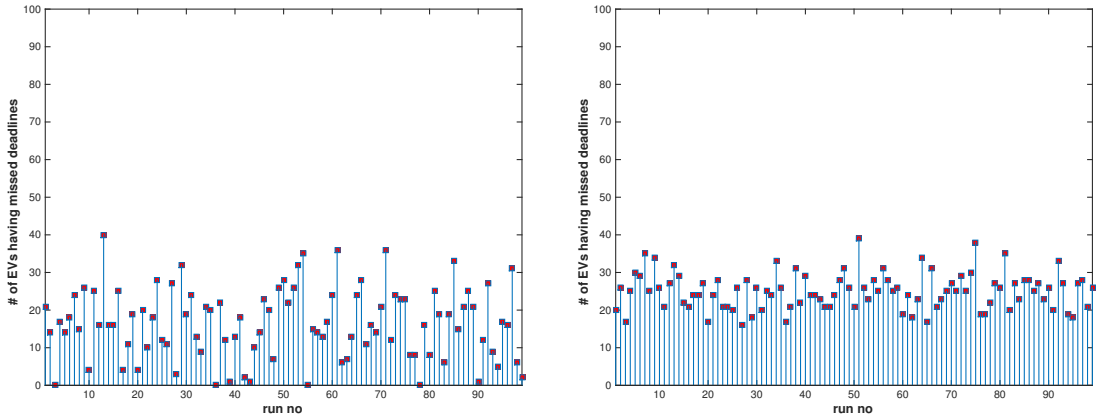

(a) **without** timing buffer (b) **with** timing buffer

Figure 132: Monte Carlo simulations on the number of EVs missing deadlines for timing buffered V2G-based FR with 100 sets of EV profiles.

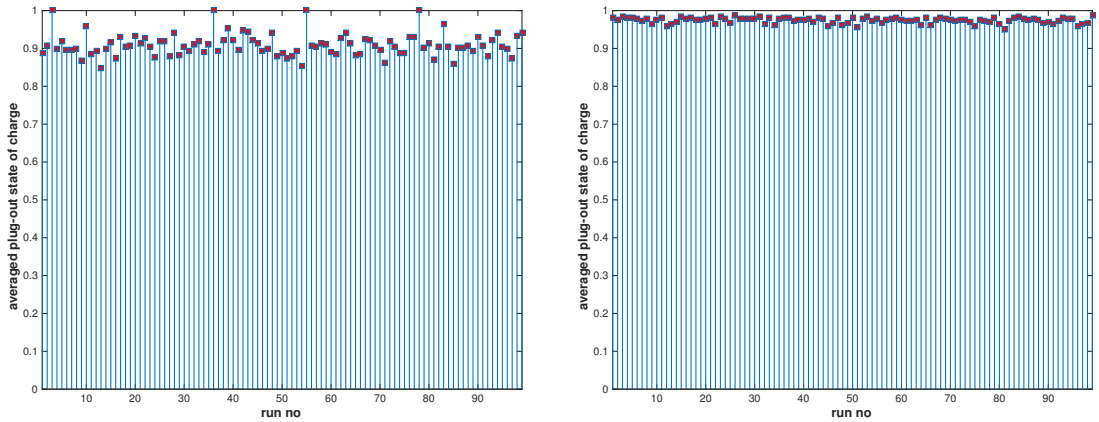

(a) **without** timing buffer (b) **with** timing buffer

Figure 133: Monte Carlo simulations on averaged plug-out SOC for timing buffered V2G-based FR with 100 sets of EV profiles.

increasing by 52%. However, Figure 133 explains why the number of EVs missing deadlines increases. For the same reason as the simulation case on load profiles, the averaged plug-out SOC for each case is increased, almost up to 100%, and, based on the standard deviation of 0.77%, their uniformity is improved – by 7%, compared with the case without timing buffer. The summary of Monte Carlo simulations on timing buffer are compiled in Table 31.

In this subsection, the impacts of V2G-based frequency regulation on the real-time EV charging algorithm are addressed. By introducing the different charging modes and modifying the real-time EV charging algorithm such that charging rates are adjusted based on both the current SOCs and whether or not they participate in the service, V2G-based frequency regulation can be provided within the real-time EV charging framework. V2G-based ancillary services are required to be provided while EVs are plugged in, implying that the services will have an influence on the performance of the proposed real-time scheduling algorithm. In order to investigate the impacts, a various types of simulations are performed on a variety of EV and load profile sets, which take account of random characteristics of load profiles and EV owners' charging preferences. It is verified through simulation studies that V2G-based frequency regulation affects real-time EV charging: it tends to decrease the number of EVs satisfying their deadlines, especially EVs with mode 4, and makes plug-out SOCs deviated more from the desired plug-out SOCs, in contrast to the real-time EV charging algorithm without V2G-based frequency regulation. However, introducing the concept of timing buffer is shown to mitigate the impacts of V2G-based frequency regulation on the real-time EV charging, and restores the performance of the algorithm to its previous state without consideration of V2G-based frequency regulation.

Table 32 summarizes all of the hypotheses testing activities and findings from those activities addressed in this chapter.

Table 31: Summary of Monte Carlo simulation runs on V2G-based FR **with** timing buffer.

Profile set	Statistics	V2G-based FR **without** timing buffer		V2G-based FR **with** timing buffer	
		averaged # of EVs missing deadlines	averaged plug-out SOC	averaged # of EVs missing deadlines	averaged plug-out SOC
Monte Carlo on load profiles	Mean	45.8283	81.01%	31.8081	98.47%
	Std dev	20.7561	7.21%	13.2562	0.61%
Monte Carlo on EV profiles	Mean	16.5152	90.93%	25.0909	97.46%
	Std dev	9.3856	2.96%	4.7896	0.77%

Table 32: Summary of hypotheses testing and findings.

Thesis section	Hypotheses testing	Findings
6.1.2	(Hypothesis Ia) Substantiation of the technical gaps of the valley-filling EV charging strategy	- The strategy won't guarantee its social optimality when: 1) the prediction of load profile is inaccurate or the actual non-EV demand is fluctuating, and 2) EV profiles are different from the ones used for the day-ahead negotiation. - It does NOT satisfy any timing constraints EV owners specified when plugging in their vehicles.
6.2.1	(Hypothesis I-1) Verification of real-time EV charging control	- The EV charging system can be modeled as a real-time system so that real-time scheduling techniques are applicable to EV charging control. - The real-time EV charging control does the same job as the valley-filling strategy does in a different way in terms of the social optimality. - The real-time EV charging strategy satisfies EV owners' timing contraints, but not perfectly 100%. - EVs with charging mode 4 do not have enough chances to charge their batteries due to their lower priorities, leading to non-flat load profiles.
6.2.2	(Hypothesis I-2) Evaluation of real-time scheduling algorithms for EV charging	- The EV charging system can be viewed as a uniprocessor system or a multiprocessor system, depending on how available power is interpreted. - A variety of real-time scheduling algorithms can be tailored to be applied to EV charging control. - The performance measures such as guarantee ratio and total load variance are affected by type of real-time scheduling algorithms and priority assignment policy.
6.2.3	(Hypothesis I-3) Effects of charging rates control on real-time EV charging	- Charging rates have an influence on the performance of EV charging control. - Charging EVs at the maximum rate maximizes the energy utilization, that is, minimizes the total load variance. - The guarantee ratio won't be improved by minimizing the charging rate since EVs have a limited time to be plugged in and also have the amount of energy required to refill their batteries. Therefore, the energy constraint must be considered when the charging rate is optimized.
6.2.4	(Hypothesis Ib) Real-time charging control vs. valley-filling strategy	- The real-time EV charging strategy will guarantee the social optimality as well as the satisfaction of EV owners' charging preferences better than the valley-filling strategy even when non-EV demand is fluctuating. - The valley-filling strategy provides a better uniformity on plug-out state-of-charge (SOC), but the real-time charging strategy is the better in terms of averaged plug-out SOC.

Table 32 (continued).

Thesis section	Hypotheses testing	Findings
6.2.4	(*cont'd*)	- The performance of the strategy, especially guarantee ratio, is somehow affected by the changing patterns and degree of load fluctuation.
6.3.1	(Hypothesis II-1) Incorporation of vehicle-to-grid (V2G)-based frequency regulation (FR) into real-time EV charging	- The functionality of the real-time EV charging algorithm to provide V2G-based FR by introducing different charging modes and at the same time controlling charging rates of EVs that opt to participate in the ancillary service is verified. - The performance of the charging strategy is degraded due to the provision of V2G-based FR since some EVs need to participate in the service, not charging their batteries during the given charging period, and consequently EVs do not fully utilize available power.
6.3.2	(Hypothesis II-2) Evaluation of the impacts of V2G-based FR on real-time EV charging	- The number of EVs missing their deadlines is noticeably increased when V2G-based FR is incorporated. - The extent to which the scheme is affected by the provision of V2G-based FR depends on the changing patterns and the amount of energy for up- and down-regulation requested by the real-time dispatch scheduler. - It is observed that load profiles are more likely to affect the performance of the algorithm than EV profiles. - The concept of "timing buffer" can mitigate the impacts of V2G-based FR on the real-time EV charging algorithm by increasing the reference EV demand estimation and encouraging EVs to complete charging ahead of their plug-out times. - Most of EVs from the fictitious dataset are plugged out with SOCs close to their desired departure SOCs, but not perfectly 100%, making the number of EVs missing deadlines look worse than it really is.

CHAPTER VII

CONCLUSION

7.1 Recapitulation of the Thesis

Electric vehicles (EVs) are believed to provide "significant potential for increasing energy efficiency, reducing greenhouse gas emissions, and relieving reliance on foreign oil for transportation" [19]. In addition to these economical and environmental benefits, the large-scale adoption of EVs is expected to present an opportunity to provide electric energy storage (EES)-based ancillary services for ensuring grid-wide frequency stability by smoothing the natural intermittency of large-scale renewable energy sources (RES) [62]. However, the integration of a large population of EVs into the electric grid is expected to "come with a multitude of challenges, especially those in the integration into the electric power grid" [19]. Since EVs consume a large amount of electrical energy, the charging of a large population of EVs will have many undesirable impacts on the distribution grid.

"Many simulation-based studies have suggested that adopting a smart charging strategy for the high penetration of EVs can alleviate some of the integration challenges and defer infrastructure investment needed otherwise" [19]. This research was motivated by the suggestion, and focused on the development of a smart EV charging strategy such that it can minimize the impacts of charging EVs on the grid as well as leverage the technical benefits as an EES-based ancillary service provider. Reviewing the literature on the EV charging strategies revealed that the existing strategies have technical limitations: when generating a charging schedule, those strategies don't consider EV owners' charging preferences, esp. timing constraints, which might be much more important than the minimization of the impacts of EV charging on the

grid since a utility will not have the control authority over EV charging; and they require the perfect knowledge on non-EV demand profile and EV charging profiles to schedule EV charging; and they are very sensitive to the prediction accuracy and fluctuation of load profiles.

The real-time scheduling technique was identified as a promising option for a smart EV charging control strategy, based on the observation of the similarity between a real-time system and an EV charging system. In response to this finding, the research questions and hypotheses were formulated to develop and evaluate a real-time EV charging control strategy. The theoretical foundations on which the formulated hypotheses can be tested was laid in Chapter 4. The EV charging problem was briefly introduced, and real-time scheduling algorithms were discussed in detail as these algorithms provide a main building block to develop and investigate the proposed real-time charging strategy. The basic concepts of frequency regulation and vehicle-to-grid (V2G) were reviewed, and a few technical approaches to V2G-based frequency regulation were introduced. Given the theoretical foundations, an object-oriented programming (OOP) model for an EV charging system was implemented to capture the behavioral characteristics of the system, and the development process for a real-time scheduling algorithm based on global scheduling algorithm was elaborated in Chapter 5. Also, a simple V2G-based frequency regulation was implemented by introducing different charging modes to allow EVs to sell electricity to the grid.

For simulation studies, a typical winter day load profile in a residential area from the CAISO database was corrupted with additive White Gaussian noises to generate a set of baseload profiles, representing the inaccurate prediction of load profiles and non-EV demand fluctuation. In a similar approach, a set of EV profiles was generated to investigate the system behaviors of the proposed charging strategy thoroughly. A benchmark system was developed to substantiate the technical gaps of the existing valley-filling strategy, and the performance of the proposed strategy was compared

with the benchmark system. Once the feasibility of the real-time EV charging algorithm was verified, the hypotheses regarding the algorithm itself were tested, and the results were given in Chapter 6, followed by the hypothesis testings related to the capability of the real-time EV charging algorithm for the provision of the V2G-based frequency regulation.

In order to help readers understand this research, a list of bread-and-butter references is presented in Table 32.

7.2 Contributions and Recommendations

The most important contribution of this research is that it proposes and verifies a novel EV charging control strategy based on real-time scheduling techniques, which is the first attempt to apply the techniques to the EV charging control problem. It is meaningful in that a design methodology for an EV charging system, which is a problem in Electrical Engineering (EE) and Systems Engineering (SE) domains, is developed by leveraging real-time scheduling techniques that are widely utilized in Computer Science (CS) and Industrial & Systems Engineering (ISyE) domains. The proposed real-time EV charging strategy is verified to satisfy EV owners' charging requirements, esp. timing constraints, which is one of the technical limitations of the existing charging strategies, and also minimize the impacts of charging EVs on the grid so that a large scale of EV population can be deployed with the undesirable impact on the grid minimized.

Another contribution is that a method to model an EV charging system as a real-time system is proposed, based on its analogy with a real-time system in order to apply real-time scheduling techniques to EV charging control. There have been a few attempts at modeling household appliances to curtail power usage for demand response, but modeling an EV charging system using real-time system parameters is the first attempt, which establishes a theoretical foundation for further studies

Table 32: List of bread-and-butter references.

AREA	REFERENCES
Operational management and control strategies for EV charging	Ma, Z., Callaway, D., and Hiskens, I.,"Decentralized Charging Control for Large Populations of Plug-in Electric Vehicles: Application of Nash Certainty Equivalence Principle," in *2010 IEEE International Conference on Control Applications*, pp.191-195, September 2010. Gan, L., Topcu, U., and Low, S. H., "Optimal Decentralized Protocol for Electric Vehicle Charging," in *IEEE Transactions on Power Systems*, vol.28, pp.940-951, May 2013.
Real-time scheduling techniques for electric power systems	Facchinetti, T., Bini, E., and Bertogna, M., "Reducing the Peak Power through Real-time Scheduling Techniques in Cyber-Physical Energy Systems," in *Proceedings of the First International Workshop on Energy Aware Design and Analysis of Cyber Physical Systems (WEA-CPS)*, 2010. Vedova, M. D., Palma, E. D., and Facchinetti, T., "Electric Loads as Real-time Tasks: An Application of Real-time Physical Systems," in *Wireless Communications and Mobile Computing Conference (IWCMC)*, pp.1117-1123, July 2011.
Real-time systems & real-time scheduling algorithms	Laplante, *Real-time Systems Design and Analysis*, John Wiley & Sons, 3rd Ed., April 2004. Krishna, C. M. and Shin, K. G., *Real-time Systems*, MIT Press and McGraw-Hill Company, 1997. Mohammadi, A. and Akl, S. G., "Scheduling Algorithms for Real-time Systems," Technical Report No. 2005-499, School of Computing, Queen's University, July 2005. Srinivasan, A. and Baruah, S., "Deadline-based Scheduling of Periodic Task Systems on Multiprocessors," *Information Processing Letters*, 84, pp.93-98, 2002.
Ancillary services & frequency regulation	Kempton, W. and Tomić, "Vehicle-to-grid Power Fundamentals: Calculating Capacity and Net Revenue," *Journal of Power Sources*, vol.144, pp.268-279, June 2005. Kirby, B. J., "Frequency Regulation Basics and Trends," Technical Report ONRL/TM-2004/291, Oak Ridge National Laboratory, December 2004.
Vehicle-to-grid (V2G) technologies	Kempton, W. and Tomić, J., "Vehicle-to-grid Power Fundamentals: Calculating Capacity and Net Revenue," *Journal of Power Sources*, vol.144, pp.268-279, June 2005. Kempton, W. and Tomić, J., "Vehicle-to-grid Power Implementation: From Stabilizing the Grid to Supporting Large-scale Renewable Energy," *Journal of Power Sources*, vol.144, pp.280-294, June 2005. Kirby, B. J., "Frequency Regulation Basics and Trends," Technical Report ONRL/TM-2004/291, Oak Ridge National Laboratory, December 2004.
Object-oriented programming	MathWorks, "Object-oriented Programming with MATLAB." http://www.mathworks.com/discovery/object-oriented-programming.html

on real-time EV charging control. In addition, to develop the charging strategy, a variety of real-time scheduling algorithms that are applicable to EV charging control and priority assignment policies are reviewed and evaluated.

Most of studies regarding the concept of vehicle-to-grid (V2G) have addressed either the economic viability of the concept or a methodology for the provision of V2G-based ancillary services, especially frequency regulation. Some researches considered the EV charging problem along with V2G-based frequency regulation, based on a simple relationship between V2G-based frequency regulation and the states-of-charge (SOCs) of EVs; however, no research with consideration of EV owners' charging preferences have been found. In this research, V2G-based frequency regulation is incorporated within the EV charging control framework, which enables the characterization of the interactions between EV charging and V2G-based frequency regulation, and also indicates a possibility to expand the capability of the algorithm for further investigation with other power systems, such as home energy management system (HEMS).

Following research topics are recommended for further researches using the developed algorithm and simulation framework:

- Expansion of the simulation model to a "decentralized", real-time EV charging control: The proposed real-time scheduling algorithm controls EV charging in a centralized way in that the real-time dispatch scheduler determines when and which EVs can start charging, based on the information EVs provide. The current simulation model is implemented using the object-oriented programming (OOP) technique offered by MathWorks® Matlab, which can be easily expanded to agent-based modeling and simulation (ABM&S). The expansion will allow the real-time scheduling algorithm to control EV charging in a decentralized way so that each EV determines its own charging schedule based on the electricity price information provided by the dispatch scheduler. I believe

that the ABM&S with timing constraints considered probably will be a novel approach for Systems Engineering (SE).

- Investigation of the interactions with HEMS: In addition to V2G-based ancillary services, a HEMS is expected to directly interact with an EV charging system, since the EV charging system will be the part of the HEMS, as illustrated in Figure 134, and the HEMS will control EV charging in order to manage household electricity usage, independently of the real-time dispatch scheduler. Accordingly, the HEMS will influence the performance of the real-time EV charging algorithm, thus its impacts should be investigated, and the algorithm needs to be augmented, if necessary. I believe that the expansion of the simulation model to ABM&S will allow for the investigation of the interactions of the real-time EV charging system with HEMS.

- Relaxation of the assumptions on the problem: In this research, an EV charging control strategy over private chargers, to which EVs are assumed to be plugged in and charged at night, is only considered. However, EVs can be charged at publicly available chargers at work or at a big shopping mall, anytime during a day. In addition, a real-time dispatch scheduler might need to control the

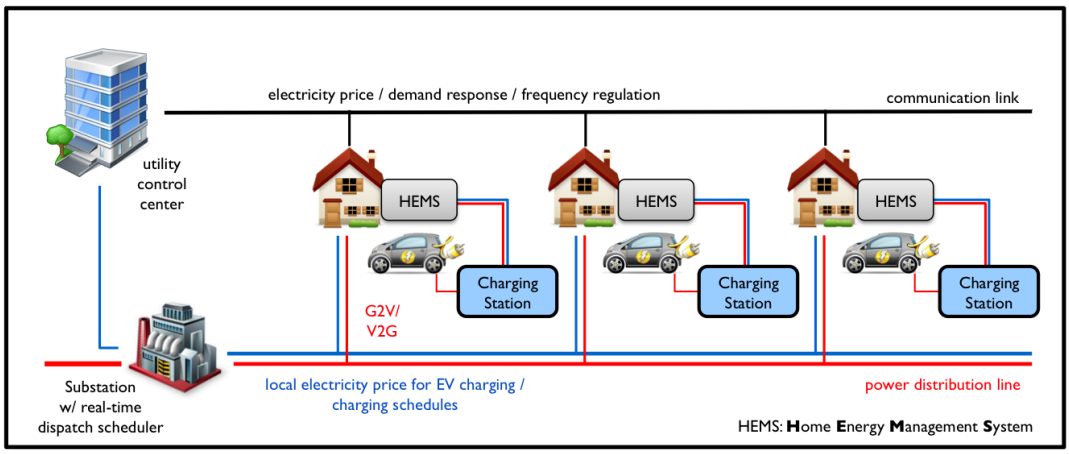

Figure 134: Schematic overview of EV charging system with HEMS.

charging of other vehicles, such as cabs, school buses, forklifts and service vans at a mall, or a mixture of various types of vehicles, as well as personal EVs. Therefore, in order to capture and investigate the reality more accurately, further studies on the problem with the aforementioned assumptions relaxed need to be conducted. Furthermore, a study on the impacts of a mixture of Level 1/Level 2/Fast DC chargers on the proposed scheduling algorithm would be worthwhile.

- Incorporation of renewable energy source (RES), esp. solar energy: One of the technical benefits a large population of EVs can provide is that they can be utilized to smooth the natural intermittency of RES for ensuring grid-wide frequency stability. The number of houses equipped with solar panels increases, and thus their effects need to be investigated. There are four technical challenges regarding a large-scale deployment of EVs identified in Chapter 1, of which the third one is not addressed in this research, and RES's can be preferentially used for charging EVs. Therefore, the research can be further carried out by evaluating the capability of the real-time EV scheduling algorithm to smooth out the intermittency of solar energy.

7.3 Q & A from the Thesis Defense

In this section, the questions/comments given by the Final Doctoral Examination Committee during the thesis defense and the responses to those questions/comments are summarized.

Question 1: *What are the implications of real world constraints on an electricity distribution network (e.g., congestion) that might occur in neighborhoods with more vehicles charging?* (Mr. Caird)

Answer 1: It's outside of the scope of what I am looking at, i.e., I assume the system can handle the loads; I'm just proposing how to better stage them. Now, on the other hand, my system could help congestion by taking into account more granular constraints, e.g., translating distribution capacity limitations in the local neighborhood of different charging vehicles. But that seems to be a different layer of modeling from what is considered directly by my algorithms. But the outputs of that modeling layer (i.e., some additional constraints to take into account) could be something that could be considered. However, trying to do that is not compatible at all with how my algorithms are currently formulated.

Question 2: *What would be the impact on your scheduler (and, the grid performance metrics) if all EV owners suddenly wanted their charging done as fast as possible, e.g., to head to the Braves game, or evacuate?* (Mr. Caird)

Answer 2: In the proposed scheduling algorithm, the order of EVs to start charging depends on real-time electricity price and the urgency based on both the amount of energy to refill the battery and the closeness to deadline, i.e., plug-out time. When an EV owner plugs in his/her car to the charger, the owner specifies the charging mode, reflecting the urgency, and sets the price that he/she is willing to pay for charging or to be paid for selling electricity to the grid. The algorithm dynamically adjusts the electricity price for EV charging based on the available power (supply) and the number of EVs being charged simultaneously (demand). For example, when many EVs are charging and there is not enough power, the algorithm increases electricity price to keep EVs from charging; on the other hand, if there is a lot of power underutilized, then the algorithm reduces electricity price to encourage more EVs to start charging. If all EV owners suddenly want their charging done as fast as possible, e.g., all EVs have charging mode 1 ("charge now"), the algorithm first tries to assign priorities to EVs with respect to their urgencies and apply the dynamic pricing based on demand

and supply to maximize the satisfaction of EV owners. However, the satisfaction of EV owners' preferences would eventually decrease as the number of EV owners willing to pay higher electricity price to get their charging done quickly increases.

Question 3: *Is there some way to incorporate priority for renewable energy sources?* (Mr. Caird)

Answer 3: Seen by the real-time dispatch scheduler, the fluctuations of generation due to the natural intermittency of renewable energy sources can be thought of as fluctuating non-EV demand since the algorithm generates a schedule based on the difference between generation and real-time non-EV demand measurements, and it does not care from which the fluctuations result; the amount of power available for EV charging only matters. If generation fluctuates, i.e., the available power for EV charging changes, then the algorithm will smooth out the intermittency by adjusting the number of EVs being charged and thus reducing the power consumption for EV charging. Therefore, it is not necessary to incorporate priority for renewable energy sources to the current structure of the algorithm, and the incorporation of renewable energy sources into the algorithm has already been identified for future work in the thesis.

Question 4: *Your choice of scheduling algorithms seemed to be in part a heuristic. Is there some more rigorous way to select optimal scheduling schemes if you had more time?* (Mr. Caird)

Answer 4: Extensive search for literature regarding the selection of optimal scheduling algorithms revealed that there is no explicit way to identify an optimal algorithm as stated in §3.1.2. As far as I know, the approach based on heuristics or through comparative studies is the best option to select an algorithm. For future work, more algorithms, not presented in this thesis, could be implemented and compared with

each other to identify the better one, but it does not seem possible to establish a methodology to select optimal scheduling schemes.

Question 5: *How does the charging scheme implied by your scheduling algorithm drive requirements for communications networks? And, are there communications standards already that would enable your scheme?* (Mr. Caird)

Answer 5: The message protocols proposed in this thesis requires 43 bits for a message from each EV to the real-time dispatch scheduler and 30 bits for a message from the scheduler to EVs. At every 15 minute, EVs and the scheduler communicate with each other, and data of 7,300 bits (100 EVs $\times$ 73 bits per communication between an EV and the scheduler), i.e., less than 1 kByte, need to be transmitted, indicating that the scheduling algorithm does not require a communication network with broad bandwidth for EV charging control. Even though the channel capacity required for scheduling EV charging will increase proportionally as the number of EVs in the system increases, it is not likely that EV charging would impose a restriction on communications systems. For instance, Ethernet can support a maximum data rate of 100 Mbps, i.e., about 0.1 billion bits per second, which can support the communications of 1 million EVs in an area controlled by a dispatch scheduler in a distribution substation. Power line communication (PLC), one of the standards proposed for the communications between vehicles, off-board charging stations, and the grid, can support up to 30 Mbits/s. Therefore, data rates that can be provided by the candidate standards for communications is big enough for the proposed scheduling algorithms to be implemented. In addition, no standard for message protocols has been established yet.

Question 6: *What is the scalability of your technical work?* (Dr. Mavris)

Answer 6: The simulation environment was verified with 100 EVs, representing 20%

penetration level of EVs in a service area. It is believed to handle more than 100 EVs since the number of EVs in the system is used as a simulation variable, which, however, needs to be proved by applying more than 100 EV charging profiles.

Question 7: *What methodology do you follow that yielded the simulation environment you created?* (Dr. Mavris)

Answer 7: Figure 135 presents the proposed real-time scheduling algorithm for EV charging with the numbers representing the steps followed to implement the simulation framework. In a typical real-time computing system, the number of processors or the amount of computing resources is known before an actual scheduling process is performed. As well for the real-time EV charging system, it is important to know the charging capability of the system, and the first step is to estimate the reference EV power demand based on the prediction of non-EV power demand and EV charging profiles informed by EV owners. Next, the number of available processing queues is initially calculated by dividing the reference EV power demand by the maximum

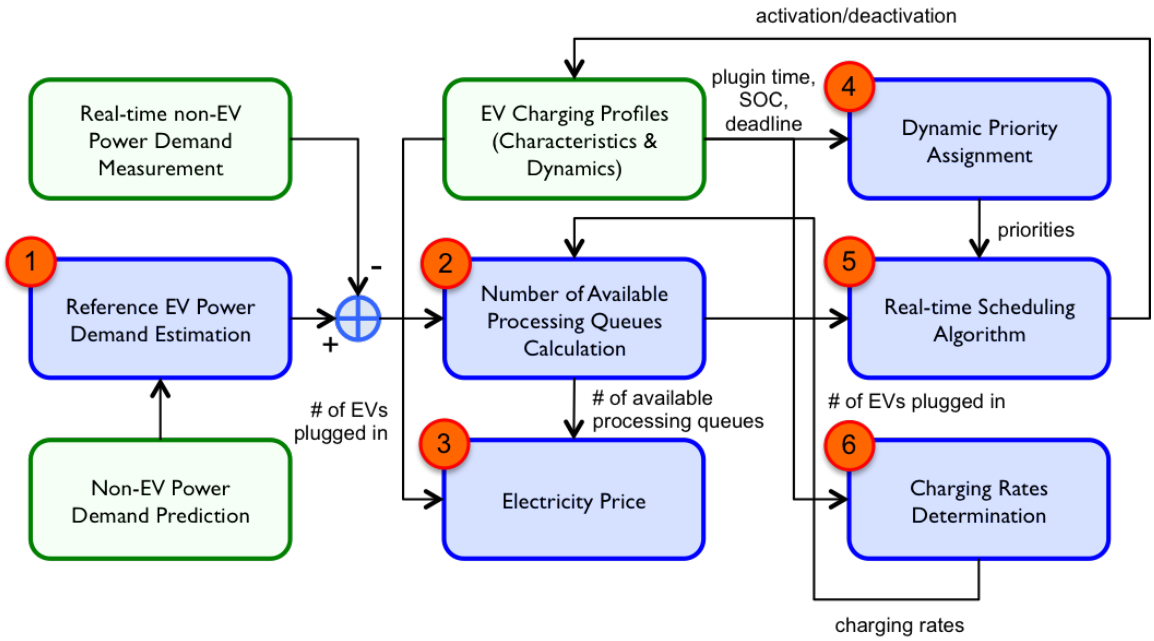

Figure 135: Proposed real-time scheduling algorithm for EV charging.

charging rate. And then the electricity price is determined based on the number of EVs that want to start charging and the amount of energy for EV charging at a time instant. For this purpose, a simple dynamic pricing model based on demand and supply is implemented. The essence of the proposed real-time scheduling algorithm for EV charging control is to design a dynamic priority assignment policy and select an existing real-time scheduling algorithm. For dynamic priority assignment, the concept of "urgency" based on the closeness to plug-out time and the amount of energy required for full charge is introduced, and through comparative studies, the best option for real-time scheduling algorithm is chosen and tailored to be applicable to the problem. In order to achieve the social optimality, i.e., a flat load profile, by maximizing the energy utilization, the charging rate is optimized and re-applied to calculate the number of processing queues. Finally, in order to incorporate V2G-based frequency regulation, different charging modes are introduced, charging rates are allowed to be negative, and the scheduling algorithm is modified to compensate for the changes in available power due to load fluctuations and/or the intermittency of renewable energy sources.

Comment 8: *The total charging times achieved by your scheduling method imply that the cars are charged at a rate faster than what typical U.S. electric plug outlets can provide; therefore, it is implied that the vehicles participating would need to have 220V charging hardware installed into their homes. This does not invalidate your method, but this hidden assumption should be mentioned.* (Dr. Schrage)

Response 8: Based on the parameter settings for the simulation studies, it takes about 5 hours to refill the battery with capacity of 16 kWh from 0% to full charge if an EV is assumed to charge at the maximum charging rate, 3.3 kW, which can be provided by a single-phase, Level 2 charger that supplies 240V/30A, like what an electric dryer or oven uses, and allows for a wide range of charging speeds, all

the way up to 19.2 kW. The same simulation settings as in Gan *et al.*'s work on "valley-filling" strategy, a benchmark system, were used for easy comparison and verification. Another reason that the maximum charging rate is assumed to be 3.3 kW is as follows. Typically, the maximum charging rate is limited by the on-board charging electronics. For instance, the first model-year Leafs can only use 3.3 kW, about 12 miles of range per hour, or about 8 hours for a full charge from empty, meaning that it takes about 22 hours for a full charge if a Level 1 charger is used. The Chevy Volt's on-board charger is also limited to 3.3 kW, although its smaller battery pack gets full sooner. Longer charging periods would complicate the problem much further, and hence it is assumed that EVs can fully utilize their on-board electronics to narrow down the scope of work in this research since the maximum charging rate and battery capacity will obviously increase as battery technologies and on-board electronics have advanced. However, a further study on the effects of charger mix on the proposed algorithm is added to the second recommendation for future work.

Question 9: *Please comment on the implications of emergency plug-out, i.e., if people have to withdraw early from the scheduling scheme.* (Dr. Schrage)

Answer 9: For the simulation studies, it is assumed that all EVs are plugged out at the pre-specified time. The algorithm generates a charging schedule every 15 minute based on the messages sent by EVs that contain the information such as plug-in status, state-of-charge (SOC), and plug-out time and those pieces of information are updated every 15 minute. If an EV is plugged out earlier than its pre-specified plug-out time, the algorithm tries to maintain the flatness of the load profile by charging the EV with highest priority in the waiting queue. However, the performance of the proposed scheduling algorithm will be degraded as the number of EVs that are plugged out earlier increases. Therefore, the impacts of EVs that are plugged out earlier than their pre-specified plug-out times on the performance of the proposed

scheduling algorithm need to be investigated.

Question 10: *How might pricing be considered, especially for V2G? For instance, is it possible for the EV owners to safeguard against selling back (to the grid) electricity at price rates lower than what they bought it for (from the grid)?* (Dr. Schrage)
Answer 10: In the thesis, a simple scheme for electricity pricing is introduced to encourage EVs with mode 3 to start charging and EVs with mode 4 to sell their electricity to the grid, which is described in §5.3.3. For example, if the electricity price is less expensive than the set price EV owners notified the dispatch scheduler when plugging in their cars, then their EVs with mode 3 are activated to start charging. The same goes for EVs with mode 4. The dispatch scheduler must adjust the electricity price for V2G power to encourage EVs with more 4 to sell their power to the grid. The simple mechanism for pricing described above is implemented in the simulation framework, making possible to conduct trade studies on electricity pricing policies over EV charging control and V2G-based applications.

Question 11: *Would the consideration be different for fleets than it would be for individual owners? How would that drive requirements of your system?* (Dr. Jagoda)
Answer 11: To determine a charging schedule for any fleet EVs, the following must be considered [75]:

- the number of vehicles expected to charge, their all-electric ranges, lengths of their routes and frequency of expected use
- charging-location options (with areas closer to electrical service preferable to minimize installation costs)
- expected charging time periods
- speed of charging equipment

The considerations for fleet charging are quite similar to those for individual EVs

except how an optimal charging schedule for the fleet is obtained and how to specify charging requirements for each EV in the fleet. According to some studies [28, 72], in order to obtain a charging schedule for an EV fleet, an optimal charging of each individual vehicle within the fleet is first obtained separately, and then an optimized schedule on the fleet level is obtained by posing an upper constraint on the grid power used for charging and coupling together the individual charging optimizations. The upper constraint on power required for EV fleet charging can be thought of as a reference EV power demand in the proposed real-time scheduling algorithm for EV charging, and, therefore, I believe that the proposed real-time scheduling algorithm in this thesis can be extended to the EV fleet with the considerations enumerated above and by identifying how to specify charging requirements for individual EVs within the fleet.

7.4 Concluding Remarks

I believe that the proposed real-time scheduling algorithm for EV charging and the simulation framework for evaluating the algorithm lay the groundwork for applying real-time scheduling techniques to EV charging control. As a proof-of-concept, the algorithm is implemented and verified over a variety of EV and load profiles. It was verified that the algorithm does not only provide the social optimality – minimize the impacts of EV charging on the grid and a utility's operating costs as well – but also satisfies EV owners' charging preferences. However, it was shown through simulation studies that the algorithm does not satisfy EV owners' preferences perfectly in terms of plug-out SOC and the uniformity of plug-out SOCs is not as good as the one obtained by applying the valley-filling strategy, meaning that the guarantee ratio, defined as the ratio of the number of EVs satisfying their requirements to the total number of EVs in the system, is increased at the expense of some EV owners' inconvenience.

Therefore, in addition to the recommendations for future work, these limitations can be resolved hopefully. Also, I hope that readers, especially electric power systems engineers or researchers, who need a simulation environment 1) to investigate the impacts of EV charging on the grid more realistically, 2) to design and evaluate their charging strategies based on real-time scheduling techniques, or 3) to evaluate the communications network capacity for a large-scale deployment of EVs take this work further.

In 2015, the world-wide sales of EVs, limited to battery electric vehicles (BEVs) and plug-in hybrid electric vehicle (PHEVs), exceeded 1 million, setting a milestone in the market. EV sales are expected to continuously increase as major automakers introduce new EV models to the market and offer sales promotions so that a larger number of models are readily available. After the Dieselgate scandal, Volkswagen decided to make investments to roll out 20 new models by 2020 and sell 3 million EVs by 2025, and Hyundai-Kia also plans to develop 8 EV models by 2020 [90]. At the same time, "the total number of electric vehicle supply equipment (EVSE) outlets reached 1.45 million in 2015, up from 0.82 million in 2014 and only roughly 20,000 in 2010" [10].

As the sales of EVs and the number of EVSE outlets increase, the importance of operational management and control strategies over the large-scale deployment of EVs will be on the rise more and more. However, the electric power system is one of the most complex system of systems (SoS) so that it is almost impossible to be modeled completely and its system behaviors are hard to capture. Therefore, more research to fill the various technical gaps regarding the integration of EVs to the grid is still needed. I hope again that the reader will find many motivating ideas from the proposed methodology and the real-time EV charging control algorithm and gain an insight into the understanding of the issues and the development of new technologies for EV integration from this dissertation.

REFERENCES

[1] Adiga, R., "Selecting the right RTOS scheduling algorithms using system modeling." https://www.design-reuse.com/articles/32732/rtos-scheduling-algorithms-selection.html, August 2013.

[2] Becker, T. A., Sidhu, I., and Tenderich, B., "Electric Vehicles in the United States: A New Model with Forecasts to 2030," tech. rep., Center for Entrepreneurship & Technology, University of California, Berkeley, August 2009.

[3] Brandenburg, B. B., Calandrino, J. M., and Anderson, J. H., "On the Scalability of Real-time Scheduling Algorithms on Multicore Platforms: A Case Study," *IEEE Real-Time Systems Symposium*, pp. 157–169, 2008.

[4] California ISO, "California ISO Open Access Same-time Information System (OASIS)." [online] - Available: http://oasis.caiso.com, 2012.

[5] Clement, K., Haesen, E., and Driesen, J., "Coordinated Charging of Multiple Plug-in Hybrid Electric Vehicles in Residential Distribution Grids," in *Proc. Power Systems Conference and Exposition 2009 (PSCE '09), IEEE/PES*, pp. 1–7, March 2009.

[6] Clement-Nyns, K., Haesen, E., and Driesen, J., "The Impact of Charging Plug-in Hybrid Electric Vehicles on a Residential Distribution Grid," *Power Systems, IEEE Transactions on*, vol. 25, pp. 371–380, February 2010.

[7] DeForest, N., Funk, J., Lorimer, A., Ur, B., Sidhu, I., Kaminsky, P., and Tenderich, B., "Impact of Widespread Electric Vehicle Adoption on the Electrical Utility Business - Threats and Opportunities," tech. rep., Center for Entrepreneurship & Technology (CET), University of California, Berkeley, August 2009.

[8] Deilami, S., Masoum, A. S., Moses, P. S., and Masoum, M. A. S., "Real-time Coordination of Plug-in Electric Vehicle Charging in Smart Grids to Minimize Power Losses and Improve Voltage Profile," in *IEEE Transactions on Smart Grid*, vol. 2, pp. 456–467, September 2011.

[9] Denholm, P. and Short, W., "An Evaluation of Utility System Impacts and Benefits of Optimality Dispatched Plug-in Hybrid Vehicles," Tech. Rep. NREL/TP-620-40293, National Renewable Energy Laboratory, October 2006.

[10] Directorate of Sustainability, Technology and Outlooks (STO), "Global EV Outlook 2016: Beyond One Million Electric Cars," tech. rep., International Energy Agency, 2016.

[11] Edward G. Coffman, J., Galambos, G., Martello, S., and Vigo, D., *Bin Packing Approximation Algorithms: Combinatorial Analysis*. Handbook of Combinatorial Optimization, Kluwer Academic Publishers, 1998.

[12] Electric Power Research Institute, "Environmental Assessment of Plug-in Hybrid Electric Vehicles - Volume 1: Nationwide Greenhouse Gas Emissions," 2007.

[13] Electric Power Research Institute, "Environmental Assessment of Plug-in Hybrid Electric Vehicles Vol. 1: Nationwide Greenhouse Gas Emissions." http://my.epri.com/portal/server.pt?open=512&objID=243&PageID=223132&cached=true&mode=2, 2007.

[14] Facchinetti, T., Bini, E., and Bertogna, M., "Reducing the Peak Power through Real-time Scheduling Techniques in Cyber-Physical Energy Systems," in *Proceedings of the First International Workshop on Energy Aware Design and Analysis of Cyber Physical Systems (WEA-CPS)*, 2010.

[15] Federal Energy Regulatory Commission, "FERC: Guide to Market Oversight - Glossary." https://www.ferc.gov/market-oversight/guide/glossary.asp, March 2016.

[16] Fluhr, J., "A Stochastic Model for Simulating the Availability of Electric Vehicles for Services to the Power Grid," in *43rd International Conference on Science Systems*, 2010.

[17] Ford, A., "The Impacts of Large Scale Use of Electric Vehicles in Southern California," in *Energy and Buildings*, vol. 22, pp. 207–218, August 1995.

[18] Funk, S., Goossens, J., and Baruah, S., "On-line Scheduling on Uniform Multiprocessors," in *Real-Time Systems Symposium, 2001. (RTSS 2001). Proceedings. 22nd IEEE*, pp. 183–192, December 2001.

[19] Gan, L., Topcu, U., and Low, S., "Optimal Decentralized Protocol for Electric Vehicle Charging," in *Decision and Control and European Control Conference (CDC-ECC), 2011 50th IEEE Conference on*, pp. 5798 –5804, December 2011.

[20] Gan, L., Topcu, U., and Low, S. H., "Optimal Decentralized Protocol for Electric Vehicle Charging," in *IEEE Transactions on Power Systems*, vol. 28, pp. 940–951, May 2013.

[21] Gardiner, A., "Texas Reliability Entity^{TM}: Frequency Control." http://www.texasre.org/CPDL/Frequency Control_operations seminar (2).pdf.

[22] Garey, M. and Johnson, D., "Complexity Results for Multiprocessor Scheduling under Resource Constraints," in *SICOMP*, vol. 4, pp. 397–411, 1975.

[23] Garey, M. R. and Johnson, D. S., *Computers and Intractability: A Guide to the Theory of NP-Completeness*. W. H. Freeman, 1st ed., January 1979.

[24] Hadley, S. W. and Tsvetkova, A., "Potential Impacts of Plug-in Hybrid Electric Vehicles on Regional Power Generation," Tech. Rep. ORNL/TM-2007/150, Oak Ridge National Laboratory, Oak Ridge, TN, USA, January 2008.

[25] Han, S., Han, S., and Sezaki, K., "Optimal Control of the Plug-in Electric Vehicles for V2G Frequency Regulation using Quadratic Programming," in *Innovative Smart Grid Technologies (ISGT), 2011 IEEE PES*, pp. 1–6, January 2011.

[26] Han, S., Han, S., and Sezaki, K., "Development of an Optimal Vehicle-to-Grid Aggregator for Frequency Regulation," *IEEE Transactions on Smart Grid*, vol. 1, pp. 65–72, June 2010.

[27] Hemphill, M., "Electricity Distribution System Planning for an Increasing Penetration of Plug-in Electric Vehicles in New South Wales," in *22nd Australasian Universities Power Engineering Conference (AUPEC)*, September 2012.

[28] Hu, J., stergaard, J. O., Lind, M., and Wu, Q., "Optimal Charging Schedule of an Electric Vehicle Fleet," in *46th International Universities Power Engineering Conference*, pp. 1–6, 2011.

[29] Hybridcars.com, "Electric Cars: A Definitive Guide to Electric Vehicles." http://www.hybridcars.com/electric-car.

[30] Ipakchi, A. and Albuyen, F., "Grid of the Future," in *IEEE Power and Energy Magazine*, vol. 7, pp. 52–62, 2009.

[31] Joseph, M., *Real-time Systems: Specification, Verification and Analysis*. Prentice Hall, 1996.

[32] Juul, F., Negrete-Pincetic, M., MacDonald, J., and Callaway, D., "Real-time Scheduling of Electric Vehicles for Ancillary Services," in *Power & Energy Society General Meeting, 2015 IEEE*, pp. 1–5, July 2015.

[33] Kempton, W. and Tomić, J., "Vehicle-to-grid power fundamentals: Calculating capacity and net revenue," *Journal of Power Sources*, vol. 144, pp. 268–279, June 2005.

[34] Kempton, W. and Tomić, J., "Vehicle-to-grid power implementation: From stabilizing the grid to supporting large-scale renewable energy," *Journal of Power Sources*, vol. 144, pp. 280–294, June 2005.

[35] Kempton, W., Udo, V., Huber, K., Komara, K., Letendre, S., Baker, S., Brunner, D., and Pearre, N., "A Test of Vehicle-to-Grid (V2G) for Energy Storage and Frequency Regulation in the PJM System," tech. rep., University of Delaware, November 2008.

[36] Kinter-Meyer, M., Schneider, K., and Pratt, R., "Impacts Assessment of Plug-In Hybrid Electric Vehicles on Electric Utilities and Regional U.S. Power Grids, Part 1: Technical Analysis," *Journal of Energy, Utility & Environment Conference (EUEC)*, vol. 1, 2007.

[37] Kirby, B. J., "Frequency Regulation Basics and Trends," Tech. Rep. ORNL/TM-2004/291, Oak Ridge National Laboratory, December 2004.

[38] Krishna, C. M. and Shin, K. G., *Real-time Systems*. MIT Press and McGraw-Hill Company, 1997.

[39] Kromer, M. A. and Heywood, J. B., "Electric Powertrains: Opportunities and Challenges in the U.S. Light-Duty Vehicle Fleet," tech. rep., MIT Laboratory for Energy and the Environment, Cambridge, Massachusetts, 2007.

[40] Lan, T., Hu, J., Wu, G., You, S., Wang, L., and Wu, Q., "Optimal Charge Control of Electric Vehicles in Electricity Markets," in *46th International Universities Power Engineering Conference*, (Soest, Germanry), September 2011.

[41] Laplante, P. A., *Real-time Systems Design and Analysis*. John Wiley & Sons, 3rd ed., April 2004.

[42] Lee, I., "OS Overview - Real-Time Scheduling." Lecture Notes for CIS 505: Software Systems, 2007.

[43] Lemoine, D. M., Kammen, D. M., and Farrell, A. E., "An Innovation and Policy Agenda for Commercially Competitive Plug-in Hybrid Electric Vehicles," in *Environmental Research Letters*, vol. 3, February 2008.

[44] Leo, M., Kavi, K., Anders, H., and Moss, B., "Ancillary Service Revenue Opportunities from Electric Vehicles via Demand Response," Master's thesis, School of Natural Resources and Environment, University of Michigan, April 2011.

[45] Letendre, S. and Watts, R. A., "Effects of Plug-in Hybrid Electric Vehicles on the Vermont Electric Transmission System," in *in Transportation Research Board Annual Meeting*, pp. 11–15, January 2009.

[46] Leung, J. and Whitehead, J., "On the Complexity of Fixed Priority Scheduling of Periodic Real-time Tasks," in *Performance Evaluation*, vol. 2, pp. 237–250, 1982.

[47] Li, C., Srinivasan, D., and Reindl, T., "Real-time Scheduling of Time-shiftable Loads in Smart Grid with Dynamic Pricing and Photovoltaic Power Generation," in *2015 IEEE Innovative Smart Grid Technologies - Asia (ISGT ASIA)*, pp. 1–6, November 2015.

[48] Liang, H., "Ancillary Services in Vehicle-to-Grid (V2G)." BBCR Smart Grid Subgroup Meeting, University of Waterloo, January 2012.

[49] Liu, C. L. and Layland, J. W., "Scheduling Algorithms for Multiprogramming in a Hard-real-time Environment," *Journal of the Association for Computing Machinery*, vol. 20, pp. 46–61, January 1973.

[50] Liu, J., *Real-time Systems*. Prentice Hall, 2000.

[51] Lopes, J. A. P., Almeida, P. M. R., and da Silva, A. M. M., "Smart Charging Strategies for Electric Vehicles: Enhancing Grid Performance and Maximizing the Use of Variable Renewable Energy Sources," in *Proc. International Battery, Hybrid and Fuel Cell Electric Vehicle Symposium and Exhibition*, pp. 1–11, 2009.

[52] Lopes, J. A. P., Soares, F. J., and Almeida, P. M. R., "Integration of Electric Vehicles in the Electric Power System," in *Proceedings of the IEEE*, vol. 99, pp. 168–183, January 2011.

[53] Lopes, J. A. P., Soares, F. J., and Almeida, P. M. R., "Identifying Management Procedures to Deal with Connection of Electric Vehicles in the Grid," in *PowerTech, 2009 IEEE Bucharest*, pp. 1–8, July 2009.

[54] Ma, Z., Callaway, D., and Hiskens, I., "Decentralized Charging Control for Large Populations of Plug-in Electric Vehicles," in *49th IEEE Conference on Decision and Control (CDC)*, pp. 206 –212, December 2010.

[55] Ma, Z., Callaway, D., and Hiskens, I., "Decentralized Charging Control for Large Populations of Plug-in Electric Vehicles: Application of Nash Certainty Equivalence Principle," in *2010 IEEE International Conference on Control Applications, Part of 2010 IEEE Multi-Conference on Systems and Control*, pp. 191–195, September 2010.

[56] MathWorks, "Object-Oriented Programming with MATLAB." http://www.mathworks.com/discovery/object-oriented-programming.html.

[57] Mohammadi, A. and Akl, S. G., "Scheduling Algorithms for Real-time Systems," Tech. Rep. No. 2005-499, School of Computing, Queen's University, July 2005.

[58] Mok, A. K., *Fundamental Design Problems of Distributed Systems for the Hard Real-time Environment*. PhD thesis, Department of Electrical Engineering and Computer Science, Massachuetts Institute of Technology, Cambridge MA, May 1983.

[59] Mullen, S. K., *Plug-in Hybrid Electric Vehicles as a Source of Distributed Frequency Regulation*. PhD thesis, University of Minnesota, September 2009.

[60] Oh, Y. and Son, S., "Allocating Fixed-Priority Periodic Tasks on Multiprocessor Systems," in *Real-Time Systems*, vol. 9, pp. 207–239, 1995.

[61] Oracle, "Java™ Tutorials: Object-Oriented Programming Concepts." http://docs.oracle.com/javase/tutorial/java/concepts/index.html.

[62] Ota, Y., Taniguchi, H., Nakajima, T., Liyanage, K. M., Baba, J., and Yokoyama, A., "Autonomous Distributed V2G (Vehicle-to-Grid) Satisfying Scheduled Charging," *IEEE Transactions on Smart Grid*, vol. 3, pp. 559–564, March 2012.

[63] Parks, K., Denholm, P., and Markel, T., "Costs and Emissions Associated with Plug-in Hybrid Electric Vehicle Charging in the Xcel Energy Colorado Service Territory," Tech. Rep. NREL/TP-640-41410, National Renewable Energy Laboratory, May 2007.

[64] Pratt, R., Kintner-Meyer, M., Schneider, K., Scott, M., Elliott, D., and Warwick, M., "Potential Impacts of High Penetration of Plug-in Hybrid Vehicles on the U.S. Power Grid," in *DOE/EERE PHEV Stakeholder Workshop*, (Washington, DC), Pacific Northwest National Laboratory, June 2007.

[65] Putrus, G. A., Suwanapingkari, P., Johnston, D., Bentley, E. C., and Narayana, M., "Impact of Electric Vehicles on Power Distribution Networks," in *Vehicle Power and Propulsiong Conference (VPPC '09), IEEE*, pp. 827–831, September 2009.

[66] Quinn, C., Zimmerle, D., and Bradley, T. H., "The Effect of Communication Architecture on the Availability, Reliability, and Economics of Plug-in Hybrid Electric Vehicle-to-Grid Ancillary Services," *Journal of Power Sources*, vol. 195, pp. 1500–1509, 2010.

[67] Rahman, S. and Shrestha, G. B., "An Investigation into the Impact of Electric Vehicle Load on the Electric Utility Distribution System," in *IEEE Transactions on Power Delivery*, vol. 8, pp. 591–597, April 1993.

[68] Rand Corp., "Imported Oil and U.S. National Security." http://www.rand.org/pubs/monographs/2009/RAND_MG838.pdf, 2009.

[69] Roe, C., Evangelos, F., Meisel, J., Meliopoulos, A. P., and Overbye, T., "Power System Level Impacts of PHEVs," in *Proc. Hawaii International Conference on System Science*, pp. 1–10, 2009.

[70] Shao, S., Zhang, T., Pipattanasomporn, M., and Rahman, S., "Impact of TOU Rates on Distribution Load Shapes in a Smart Grid with PHEV Penetration," in *Transmission and Distribution Conference and Exposition, 2010 IEEE PES*, pp. 1–6, April 2010.

[71] Shao, S., Pipattanasomporn, M., and Rahman, S., "Challenges of PHEV Penetration to the Residential Distribution Network," in *Power & Energy Society General Meeting 2009 (PES '09), IEEE*, pp. 1–8, July 2009.

[72] Skugor, B. and Deur, J., "Dynamic Programming-based Optimization of Electric Vehicle Fleet Charging," in *2014 IEEE International Electric Vehicle Conference (IEVC)*, pp. 1–8, 2014.

[73] Sortomme, E., Hindi, M. M., MacPherson, S. D. J., and Venkata, S. S., "Coordinated Charging of Plug-In Hybrid Electric Vehicles to Minimize Distribution System Losses," *IEEE Transactions on Smart Grid*, vol. 2, pp. 198 –205, March 2011.

[74] Souppouris, A., "Nissan wants you to use its Lead RV like a Tesla Powerwall." https://www.engadget.com/2015/12/09/nissan-enel-vehicle-2-grid-trial/, December 2015.

[75] Southern California Edison, "Fleets: Electric Vehicle Charging." https://www.sce.com/wps/wcm/connect/83cdda38-864b-47db-928f-31edfebe4fb3/PEV_Business_FleetCharging.pdf?MOD=AJPERES.

[76] Southern California Edison, "Southern California Edison Regulatory Information (2011)." http://www.sce.com/005_regul_info/eca/DOMSM11.DLP, 2011.

[77] Srinivasan, A. and Baruah, S., "Deadline-based Scheduling of Periodic Task Systems on Multiprocessors," *Information Processing Letters, 84*, pp. 93–98, 2002.

[78] Subramanian, A., Garcia, M., Dominguez-Garcia, A., Callaway, D., Poolla, K., and Varaiya, P., "Real-time Scheduling of Deferrable Electric Loads," in *2012 American Control Conference (ACC)*, pp. 3643–3650, June 2012.

[79] Tesla Motors, "Energy Efficiency of Tesla Electric Vehicles." http://www.teslamotors.com/goelectric/efficiency.

[80] U.S. Department of Energy, "Energy Efficiency & Renewable Energy." http://www.fueleconomy.gov/feg/evtech.shtml.

[81] U.S. Energy Information Administration. http://www.eia.gov/tools/faqs/faq.cfm?id=97&t=3.

[82] U.S. Energy Information Administration, "International Energy Outlook 2010." http://www.eia.doe.gov/oiaf/ieo/pdf/0484%292010%29.pdf, July 2010.

[83] U.S. Energy Information Administration, "Annual Energy Outlook 2011 with Projections to 2035," Tech. Rep. DOE/EIA-0383(2011), U.S. Energy Information Administration, April 2011.

[84] U.S. Energy Information Administration, "How Dependent Are We on Foreign Oil?." http://www.eia.gov/energy_in_brief/foreign_oil_dependence.cfm, May 2012.

[85] U.S. Environmental Protection Agency, "U.S. Greenhouse Gas Inventory Report." http://www.epa.gov/climatechange/emissions/downloads11/US-GHG-Inventory-2011-Executive-Summary.pdf, 2011.

[86] Valentine, K., Temple, W. G., and Zhang, K. M., "Intelligent Electric Vehicle Charging: Rethinking the Valley-fill," *Journal of Power Sources*, vol. 196, pp. 10717–10726, December 2011.

[87] Vedova, M. D., Palma, E. D., and Facchinetti, T., "Electric Loads as Real-time Tasks: An Application of Real-time Physical Systems," in *Wireless Communications and Mobile Computing Conference (IWCMC)*, pp. 1117–1123, July 2011.

[88] Vuorinen, A., "Frequency Control and Regulating Reserves." http://www.optimalpowersystems.com/stuff/frequency_control_and_regulating_reserves.pdf, 2007.

[89] Wenzel, G., Negrete-Pincetic, M., Olivares, D. E., MacDonald, J., and Callaway, D. S., "Real-time Charging Strategies for an Electric Vehicle Aggregator to Provide Ancillary Services," in *IEEE Transactions on Smart Grid*, pp. 1–11, March 2017.

[90] Yang, Z., "2015 global electric vehicle trends: Which markets are up (the most)." http:www.theicct.org/blogs/staff/2015-global-electric-vehicle-trends, May 2016.

[91] Zapata, O. U. P. and Alvarez, P. M., "EDF and RM Multiprocessor Scheduling Algorithms: Survey and Performance Evaluation," Tech. Rep. CINVESTAV-CS-RTG-02, CINVESTAV-IPN, Sección de Computación, 2005.

VITA

Joosung Kang was born in South Korea. He received a Bachelor of Science degree in Electrical Engineering from Seoul National University, South Korea, in 1999. His professional career started as a research engineer at the R&D Department in Hanwha Corporation, Daejeon Plant, where he was involved in the KOrea Multi-Purpose SATellite (KOMPSAT) 2 Program and developed a vacuum-simulated hot-fire testing facility for 5-20 lbf class mono-propellant thrusters that was the first facility in Korea and the 8th in the world. After completing the development of the facility, he was involved in developing a surface-to-surface missile system as an electrical systems engineer. While working for the company, he earned his Master of Science degree in Electrical Engineering & Computer Science from Seoul National University in 2007, and he specialized in integrated INS/GPS navigation systems. He joined the Aerospace Systems Design Laboratory (ASDL) at the Georgia Institute of Technology in 2007, and earned his Doctor of Philosophy degree in May 2017. Currently, he is team leader of Air-launched Weapon Systems Development Team at the Defense R&D Center of Hanwha Corporation, and is developing a precision-guided munition system launchable from an aircraft.